# ALTERATIONS IN LYMPHOCYTE SIGNALLING PRODUCED BY EXPOSURE TO MERCURY

A Thesis Submitted to the College of

Graduate Studies and Research

in Partial Fulfilment of the Requirements

for the Degree of Doctor of Philosophy

in the Department of Veterinary Biomedical Sciences

University of Saskatchewan

Saskatoon

by

Margaret Jane Yole

## PERMISSION TO USE

In presenting this thesis in partial fulfilment of the requirements for a Postgraduate degree from the University of Saskatchewan, I agree that the Libraries of this University may make it freely available for inspection. I further agree that permission for copying in any manner, in whole or in part, for scholarly purposes may be granted by the professor or professors who supervised my thesis work or, in their absence, by the Head of the Department or the Dean of the College in which my thesis work was completed. It is understood that any copying or publication or use of this thesis or parts thereof for financial gain shall not be allowed without my written permission. It is also understood that due recognition shall be given to me and to the University of Saskatchewan in any scholarly use which may be made of any material in my thesis.

Requests for permission to copy or make use of material in this thesis in whole or in part should be addressed to:

Head of the Department of Veterinary Biomedical Sciences
University of Saskatchewan
Saskatoon, Saskatchewan S7N 5B4

## ABSTRACT

The effects of 1 min – 4 hr exposures to mercuric chloride ($HgCl_2$), methyl mercuric chloride ($CH_3HgCl$), *p*-chloromercuribenzoate (*p*-CMB) and ethylmercurithiosalicylate (TMS) on cell viability and kinetics of cell death, microtubules, F-actin, CD3 receptor expression, protein tyrosine phosphorylation (PTyr-P), intracellular calcium $[Ca^{2+}]_i$ and responses to polarized signals in YAC-1 lymphoma cells were investigated.

We hypothesized that immunotoxic effects of $HgCl_2$ ($Hg^{2+}$) are initiated by global receptor triggering, accompanied by increased protein tyrosine phosphorylation (PTyr-P) and down-regulation of the T-cell receptor (TCR). As a polychloride anion with poor lipid solubility, inorganic $Hg^{2+}$ may produce effects at the outer cell membrane before significant intracellular accumulation, loss of microtubule integrity (a sensitive target) and activation of cell death through apoptotic pathways. The organomercurial compound *p*-CMB is likewise thought to penetrate membranes slowly as a result of ionization.

In contrast, the highly lipid-soluble organomercurial compounds $CH_3HgCl$ and TMS were expected to reduce responses to polarized stimuli only in conjunction with – and not prior to – loss of microtubule integrity and the onset of necrotic cell death.

Two general patterns of effects were observed. In $HgCl_2$-treated YAC-1 cells, inhibition of responses to polarized stimuli preceded loss of microtubules and onset of cell death. Effects on polarized stimuli were preceded by a transient $Ca^{2+}$ signal;

however, this $Ca^{2+}$ signal appeared abortive, accompanied by a paradoxic decrease in PTyr-P and partial down-regulation of CD3 receptors. Responses to polarised stimuli were inhibited prior to extensive loss of microtubule staining, indicating effects preceded cytosolic $Hg^{2+}$ accumulation. $HgCl_2$ exposure was followed rapidly by necrotic cell death.

Similarly, *p*-CMB-treated YAC-1 cells failed to respond to polarized stimuli before effects on microtubules or loss of viability, and proceeded rapidly to late apoptosis; however, a transient $Ca^{2+}$ signal and progressive loss of F-actin preceded effects in all other assays and may account for loss of polarized responses.

In $CH_3HgCl$- and TMS-treated YAC-1 cells, CD3 receptor expression, $[Ca^{2+}]$ and PTyr-P were increased immediately, along with loss of microtubules. These reductions preceded inhibition of polarized signaling responses and seemed to indicate a general loss of cellular homeostasis not seen in $HgCl_2$- and *p*-CMB-treated cells; loss of homeostasis did not necessarily produce simultaneous loss of viability, as TMS-treated cells remained viable for 30 min while $CH_3HgCl$-treated cells became apoptotic within 1 min. Nonetheless, the YAC-1 cells proceeded to cell death more slowly, remaining early apoptotic after 4 hr, when almost all $HgCl_2$- and *p*-CMB-treated cells were necrotic.

These findings indicate the two groups of mercury compounds may alter responses to polarized stimuli and induce cell death by distinct pathways, one involving an apparently abortive signal and the other mediated by much more profound disruption of cellular homeostasis. Within the larger patterns there are further differences between the effects produced by each Hg compound, likely reflecting the combined influence of pharmaco–kinetic and –dynamic factors governing access to and interactions with

different cellular targets leading to cell death. These distinct targets may in turn be reflected in the different immune effects produced by these compounds *in vivo*.

## ACKNOWLEDGEMENTS

I wish to thank Drs. Barry Blakley and Mark Wickstrom , my supervisors, for contributing advice and support in completion of this thesis. I thank the members of my graduate student committee, Drs. Don Hamilton, Gillian Muir, George Forsyth, Alan Rosenberg and Baljit Singh. I must also offer my most heartfelt thanks to Alan Buckpitt for his patience, wisdom and humour, for trusting me with a project that had no guarantee of success and which was more often than not a failure. I wish to thank all the instructors and veterinary students I met teaching pharmacology and toxicology pursuing during my PhD. Without teaching as an outlet to compensate for the "challenge" of research I doubt I ever would have finished. Finally, I wish to say thank you to my parents, once again, for having taught me that learning was its own reward.

I have been supported throughout this project by the WCVM Interprovincial graduate scholarship funds.

> *"The glory of science is not in a truth more absolute than the truth of Bach or Tolstoy, but in the act of creation itself. The scientist's discoveries impose his own order on chaos, as the composer or painter imposes his; an order that always refers to limited aspects of reality, and is based on the observer's frame of reference, which differs from period to period as a Rembrandt nude differs from a nude by Manet."*
>
> - Arthur Koestler

*"Sometimes a scream is better than a thesis."*

- Ralph Waldo Emerson

## TABLE OF CONTENTS

## LIST OF TABLES

## LIST OF FIGURES

## LIST OF ABBREVIATIONS

| | |
|---|---|
| **Anti-PTyr** | Mouse-anti-phosphotyrosine antibody |
| **Anti-Tub** | Mouse-anti-tubulin antibody |
| **APC** | Antigen presenting cell |
| **B lymphocyte** | Bursa cell equivalent (antibody producing) |
| **BSA** | Bovine serum albumin |
| **CD--** | Cluster of differentiation designation for cell surface markers, e.g. CD3 |
| **$CD4^+$** | CD 4 positive cell (helper T lymphocyte) |
| **$CD8^+$** | CD 8 positive cell (cytotoxic T lymphocyte) |
| **$CH_3HgCl$** | Methylmercuric chloride |
| **CTL** | Cytotoxic T lymphocyte |
| **CTLA-4** | Cytotoxic T lymphocyte antigen 4 |
| **$\Delta\Psi_m$** | Mitochondrial transmembrane potential |
| **DAG** | Diacylglycerol |
| **DMSO** | Dimethylsulfoxide |
| **ERM** | Ezrin, radixin and moesin cytoskeleletal linker proteins |
| **FBS** | Fetal bovine serum |
| **GAM** | Goat anti-mouse IgG antibody |
| **GSH** | Glutathione |
| **HAM** | Hamster anti-mouse IgG antibody |
| **Hg** | Mercury |
| **$HgCl_2$** | Mercuric chloride |
| **IC** | Immune complex |
| **ICAM** | Intercellular adhesion molecule (integrin) |
| **IFNγ** | Interferon-γ |
| **IFNGR** | Interferon-γ receptor |
| **IgG** | Immunoglobulin subtype G |
| **$IP_3$** | Inositol 1,4,5-trisphosphate |
| **IL-...** | Interleukin designation, e.g., 1, 2, 10 |
| **JNK** | c-Jun N-terminal kinase |
| **LFA** | Lymphocyte function-associated antigen (intergrin) |
| **MAH** | Mouse-anti-hamster IgG antibody |
| **MAP kinase** | Mitogen activated protein kinase |
| **mIg** | Membrane-bound immunoglobulin |
| **MMP** | Mitochondrial membrane permeabilization |
| **MT** | Microtubule |
| **MTOC** | Microtubule organizing centre (pericentriolar material) |
| **MTT** | Methylthiazolyldiphenyl-tetrazolium bromide |
| **PBL** | Peripheral blood lymphocyte |
| **PBS** | Phosphate buffered saline |
| **PBS/BSA** | PBS/1% bovine serum albumin/0.1% $NaN_3$ |
| ***p*-CMB** | *Para*-chloromercuribenzoate |
| **PFA** | Paraformaldehyde |
| **PI** | Propidium iodide |

| | |
|---|---|
| **PKC** | Protein kinase C |
| **PLC-γ1** | Phospholipase C-γ1 |
| **PLL** | Poly-L-lysine |
| **PT** | Mitochondrial permeability transition |
| **PTK** | Protein tyrosine kinase |
| **PTPase** | Protein tyrosine phosphatase |
| **PTPC** | Permeability transition pore complex |
| **PTyr** | Phosphotyrosine |
| **PTyr-P** | Phosphotyrosine phosphorylation |
| **TNP** | Trinitrophenol |
| **TR-WGA** | Texas Red-conjugated wheat germ agglutinin |
| **RPM** | Revolutions per minute |
| **RT** | Room temperature |
| **-SH** | Sulfhydryl group |
| **sIg** | Soluble/circulating immunoglubulin |
| **SMAC** | Supramolecular activation complex (immunological synapse) |
| **TCR** | T-cell receptor |
| **$T_H$** | Helper T lymphocyte |
| **T lymphocyte** | Thymic lymphocyte |
| **TMS** | Thimerosal |
| **TNF** | Tumour necrosis factor |
| **WGA** | Wheat germ agglutinin |
| **YP** | YOPRO-1 dye |

# 1.0 INTRODUCTION

Mercury continues to be a serious environmental and occupational contaminant (Aronson, 1998; Barregard et al., 1999b; Counter and Buchanan, 2004; Eto, 2000; Hansen and Danscher, 1997; Hultman and Enestrom, 1992; Kaiser, 1998; Kanluen and Gottlieb, 1991; Nierenberg et al., 1998; Risher et al., 2002). Mercury is highly toxic to the nervous (Clarkson, 1987; Eto, 1997, 2000) and renal systems (Girardi et al., 1996; Graeme and Pollack, 1998), and can be lethal in some cases (Kulig, 1998; Siegler et al., 1999). However, alterations in immune function may be seen at levels well below those producing overt nervous or renal effects (Dieter et al., 1983; Moszczyanski et al., 1998; Park et al., 2000; Queiroz and Dantas, 1997a, b; Queiroz et al., 1994a; Queiroz et al., 1994b).

The immune effects produced by mercury (Hg) are diverse and difficult to explain within the framework of any current model of mercury toxicity. On one hand, mercury can induce thymic atrophy (Kosuda et al., 1996), inhibit lymphocyte proliferation, suppress both humoral and cellular immune function (Jiang and Moller, 1995, 1996; Kosuda et al., 1996; Loftenius et al., 1997; Pelletier et al., 1987a; Sapin et al., 1977), and increase the risk and severity of human malaria infection (Silbergeld et al., 2000). On the other hand, mercury may stimulate lymphocyte proliferation (Jiang and Moller, 1996), and can even induce a transient, genetically determined Type-2 (or T-helper-2-like or

antibody-mediated) autoimmune disease in susceptible rats and mice (Druet et al., 1979b; Sapin et al., 1982). These results may indicate that a percentage of the human population, as yet undetected in general surveys, may be genetically predisposed to the immunotoxic effects of mercury.

Mercury-induced autoimmune disease in laboratory animals has therefore become an established model of human autoimmune disease. However, despite intensive study, the nature of genetic susceptibility to mercury-induced autoimmune disease and the underlying biochemical mechanisms responsible for the toxicity of mercury and other heavy metals are largely unknown. Many mechanisms for the toxic effects of mercury have been proposed, yet none of these models on its own provides an adequate explanation of all the immune alterations produced by mercury.

Most immunotoxicologic research has involved examination of the cellular effects of immunotoxicants. Few studies have examined toxic effects at the level of signal transduction and none have examined toxicant effects on the 'immunologic synapse', the specialised form of receptor-mediated cell-to-cell communication that is at the heart of immune system activation and regulation. The immunologic synapse presents a unique opportunity to study immunotoxicant effects on signal transduction in both time and space.

The cells of the immune system exist largely as independent units, until called upon to coordinate their activities in response to an antigenic threat. In the presence of the appropriate antigenic stimulus, antigen-derived peptide fragments are presented to helper or cytotoxic T lymphocytes by the major histocompatibility complex (MHC: class I or II) on the surface of B lymphocytes, antigen presenting cells (APCs), virally infected

or neoplastic cells. Only T lymphocytes bearing the clonotypic T cell receptor (TCR) specific for that peptide/MHC combination recognise and bind the peptide/MHC receptor in the area of contact between the cells. Antigen-specific activation of the surface receptors creates a 'synapse', with a localised area of signalling created in the area of contact between the cells. The localisation of signalling triggers the responding cells to polarize cytoskeletal and secretory machinery (microtubule organizing centre [MTOC] and Golgi apparatus) toward the area of contact, allowing specific release of soluble mediators like cytokines or perforins directly in the synaptic junction.

Given that mercury and other immunotoxicants may interfere with many of the signalling pathways that are involved in the formation of a stable immunologic synapse, and that these toxicants generally do not act in a localised fashion, there is potential for immunotoxicants to produce an aberrant, non-polarized intracellular signal. Such aberrant signalling may alter normal cell-to-cell communications, and possibly induce cell death and/or abortive activation of lymphocytes.

Many of the effects of mercury have been attributed to high-affinity sulfhydryl (-SH) group binding (Rothstein, 1972). Among several theories for the biochemical target or mechanism of mercury toxicity in various tissue types are: (1) cross-linking of membrane phospholipid head groups to reduce membrane fluidity (Delnomdedieu and Allis, 1993; Girault et al., 1996); (2) aggregation of membrane receptors or other thiol group interactions to induce aberrant signaling (Nakashima et al., 1994; Pu et al., 1996; Rahman et al., 1993; Rosenspire et al., 1998); (3) alteration or blockade of membrane $Ca^{++}$ channels (Sirois and Atchison, 1996, 2000); (4) inhibition of $Na^{+}/K^{+}$-ATPase activity and subsequent loss of osmotic control of cell volume (Ballatori and Boyer,

1996; Ballatori et al., 1988; Chanez et al., 1989); (5) direct intracellular activation or inhibition of signal transduction components, such as protein kinase C (Badou et al., 1997), *ras*.GTP (Mattingly et al., 2001), caspase-3 (Whitekus et al., 1999) or tyrosine phosphatases (Lander et al., 1992); (6) inhibition of myosin ATPase activity (Vassallo et al., 1999); (7) inhibition of microtubule assembly or deaggregation of microtubules (Brown et al., 1988; Imura et al., 1980; Keates and Yott, 1984; Miura et al., 1984; Sager et al., 1983; Vogel et al., 1985); (8) activation of redox-sensitive signalling cascades, either directly or indirectly, as a result of generalised oxidative stress (generation of reactive oxygen species and lipid peroxidation), consumption of glutathione and induction of the mitochondrial permeability transition (Brawer et al., 1998; InSug et al., 1997; Naganuma et al., 1990; Nath et al., 1996; Pintado et al., 1995; Shenker et al., 1999; Shenker et al., 1998, 2000; Shenker et al., 1993b) and (9) some effects may also be mediated by modulation of gene transcription, including those coding for metallothionein (Koropatnick and Zalups, 1997), glutathione, γ-glutamyl cysteine synthetase, glutathione disulfide (GSSG) reductase, GSH peroxidase, and several enzymes involved in cellular energetics (Lash and Zalups, 1996).

As mercury must first pass the cell membrane in order to interact with intracellular targets, it is possible that toxicity is produced by multiple mechanisms, involving both membrane and intracellular components. Regardless of the proximal target, it appears that a common target or indicator of mercury toxicity in most organs, including the immune system, is (10) disruption of intracellular calcium homeostasis (Badou et al., 1997; MacDougal et al., 1996; Pintado et al., 1995; Sirois and Atchison, 2000; Smith et al., 1987; Tan et al., 1993).

Comparative concentration-response studies of the effects of both organic and inorganic mercury on lymphocyte cell surface receptor expression, and their relationship to lymphocyte intracellular signalling, proliferation and cell death are needed. We propose that immunotoxicant binding of critical lymphocyte surface receptors or intracellular targets produces an aberrant non-polarized intracellular signal. We believe this global (i.e., non-localised) signal prevents normal polarization of signalling machinery, cytoskeleton and secretory apparatus towards the area of contact formed between antigen-specific lymphocytes and complementary antigen presenting cells (APCs; B-cells, macrophages or dendritic cells). We expect that, under most circumstances, in the absence of appropriate spatio-temporal stimuli by which to orient the cytoskeleton and secretory machinery, the lymphocyte response to a toxicant-mediated stimulus will therefore be abortive. However, at certain optimal toxicant concentrations, the toxicant signal may mimic a polarized signal sufficiently to activate lymphocytes in non-antigen-specific fashion. We anticipate that non-localized signalling may therefore provide a basis for both the immunosuppressive, stimulatory and autoimmune effects of mercury.

Selected aspects of polarised signalling in T lymphocytes were studied in a model of the immunologic synapse using anti-CD3-coated latex microbeads as surrogate antigen-presenting cell to induce polarisation responses from YAC-1 lymphoma cells.

Mercury compounds having differing chemical properties (organic vs inorganic mercury, pKa, presumed or known ability to penetrate cell membranes and suspected or known effects on immune function) were selected for the study. The four compounds selected were mercuric chloride ($HgCl_2$), methyl mercuric chloride ($CH_3HgCl$), *p*-

chloromercuribenzoate (*p*-CMB), and ethylmercurithiosalicyclate, also known as thimerosal (TMS).

The goal of this project was to study concentration-response effects of mercury on lymphocyte signalling events triggered by polarised ligation of cell surface receptors. In doing so, we hoped to elucidate the role of aberrant lymphocyte activation and induction of anergy or apoptosis in the immunosuppressive and autoimmune effects of mercury. The results of the research herein may provide a link to the molecular mechanisms and genetic basis of immune dysfunction induced by mercury and other metals *in vivo*.

We anticipate that aberrant, non-localized signalling may similarly disrupt polarized responses to receptor-mediated signals in other organ systems, and, in particular, may underlie the toxic effects of metals like mercury in the nervous system. In addition, this research may provide a common etiology for toxin-induced $Th_2$-like autoimmune syndromes produced by drugs such as captopril, penicillamine and gold sodium thiomalate (Delfraissy et al., 1984; Hill, 1986; Hoorntje et al., 1980; Robinson et al., 1986; Wooley et al., 1980). Convergence of antigen-mediated signalling through cell surface antigens and toxicant-mediated cell signalling may have significant implications for other areas of immunology, including modulation of immune responses, therapy of $Th_1$-like autoimmune disease and the pathogenesis of multiple chemical sensitivity.

# 2.0 LITERATURE REVIEW

## 2.1 The Immune System as a sensory organ

The immune system evaluates and responds to the antigenic environment of the body, detecting tissue damage, foreign microbes and certain chemical signals. The immune system is therefore sometimes considered a sensory organ, somewhat analogous to the nervous system. Like the nervous system, the immune system consists of primary or central tissue components and a vast network of peripheral or secondary components that penetrate almost all other organs of the body. The cells of the nervous system are connected in neural networks, but lymphocytes and corresponding antigen-presenting cells (APCs) or target cells do not form gap junctions or couple their respective cytoplasmic compartments (Singer, 1992). Instead, the cells of the immune system exist largely as independent units, creating response networks as needed in response to antigenic threats.

## 2.2 The Mobile Synapse

### 2.2.1 Specific antigen recognition and presentation

Lymphoid cells are quite mobile within tissues and also traffic in the vascular or lymphoid circulation, thus maximizing the likelihood of encountering antigen in both the fluid (extracellular, lymph and blood) and intracellular environments and providing the

appropriate response. Although distinct subsets of lymphoid cells provide immune surveillance for either environment, they share many common features.

Foreign (non-self) epitopes on antigens present in the fluid compartments may be recognized in their native conformation by circulating soluble immunoglobulin (sIg). Foreign antigen trapped by circulating sIg is phagocytosed by antigen presenting cells (APCs). Alternately, foreign antigen may be internalized after binding to membrane-bound immunoglobulin (mIg) on B lymphocytes. The internalized foreign antigen is processed through the endosomal/lysosomal compartments to generate short peptide fragments. These peptides are returned to the cell surface, held in the groove of a special receptor found on antigen presenting cells, termed Class II major histocompatibility complexes (Class II MHC) on APCs. The class II MHC/peptide complexes form a specific ligand recognized by the complementary T-cell receptor/CD3 receptor complex (TCR/CD3) on T lymphocytes, generally of the CD4+ helper subset (Chien and Davis, 1993). Through this antigen-specific interaction a localised area of signalling, or "synapse", is created in the area of contact between the cells (Qi et al., 2001).

Similarly, foreign proteins of intracellular origin (produced by neoplastic cells, viruses or intracellular parasites) are processed into short peptide fragments in the cytoplasm of the affected cell and returned to the surface on class I MHC via the endoplasmic reticulum. Class I MHC is present on all nucleated cells of the body. In a healthy cell, class I MHC presents an array of proteins derived from the interior of the cell. These "normal" peptides do not elicit T lymphocyte responses as, during T lymphocyte maturation within the thymus, lymphocytes with TCRs that avidly bind self peptide/MHC class I on thymic epithelial cells are deleted via apoptosis. However,

cytotoxic T lymphocytes (CTLs) will recognise foreign peptide/Class I MHC complexes, to form an antigen-specific signalling complex similar to that for B/helper T lymphocyte conjugates (Montoya et al., 2002; Qi et al., 2001).

### 2.2.2 Binary interactions: Cell-to-cell adhesion and intercellular communication

Local signalling complexes or synapses arise only between cells bearing a particular clonotypic T-cell receptor and APCs bearing the corresponding peptide/MHC recognised by that TCR (Berridge, 1997b). The key features of these processes have been extensively studied in helper T and B lymphocyte (acting as APC) couples (Hodes and Singer, 1984; Kupfer et al., 1991; Kupfer and Singer, 1989b; Kupfer et al., 1986b; Kupfer et al., 1987b; Kupfer et al., 1994; Sanders et al., 1988), but many are shared by activated CTL/target cell (Kupfer and Dennert, 1984; Kupfer et al., 1985; Kupfer and Singer, 1989a; Kupfer et al., 1986a; Podack and Kupfer, 1991) and natural killer (NK)/target cell (Johansson and Nannmark, 1996; Kupfer et al., 1985) couples.

As reviewed by Singer (1992), when sufficient concentrations of receptor and corresponding ligand are present on the membrane, the formation of a few transcellular receptor-ligand pairings creates an area of localised cell-to-cell contact. This initial adhesion may allow sufficient time for other receptors to diffuse through the membrane toward the area of contact (McCloskey and Poo, 1986) and facilitate the formation of additional receptor-ligand pairs (Singer, 1992). As a consequence, the responding cells may become flattened together (Kupfer et al., 1994; Montoya et al., 2002), or form interdigitating villous processes (in the case of CTLs (Foa et al., 1988; Zagury et al., 1979)), to maximise both the area of close cell-to-cell contact and number of receptor-

ligand pairs. The adhesion is further stabilised by ligation and aggregation of non-specific intercellular adhesion molecules (ICAMs), which may also provide accessory signals (Podack and Kupfer, 1991; Singer, 1992).

The intial interaction of a small number of peptide-bearing Class II MHC's on B lymphocyte APCs with clonotypic TCR/CD3 complexes delivers a first signal to the $T_H$ lymphocyte (Kupfer and Singer, 1989b). This signal stimulates a chemical or conformational change in the helper T lymphocyte function-associated antigen (LFA-1 integral membrane protein or integrin) receptors, likely mediated by protein kinase C (PKC) phosphorylation, to greatly increase their affinity for the monotypic ICAMs-1 and 2 on APCs (Kupfer and Singer, 1989b). In another PKC-dependent process (Burn et al., 1988; Kupfer et al., 1990), the actin-binding cytoskeletal linker molecule talin becomes associated with ligand-bound LFA (Kupfer et al., 1986a; Sedwick et al., 1999). Talin stabilises the LFA-mediated adhesion, forming a transmembrane linkage between the extracellular matrix and the cytoskeleton (Kupfer et al., 1990), and may also mediate fusion of Golgi-derived vesicles with the cell membrane (Podack and Kupfer, 1991).

An additional signal, requiring a larger concentration of antigen and more extensive syn-capping of CD4 and T-cell receptors, is needed to trigger cytoskeletal reorientation (Monks et al., 1997) and subsequent $T_H$ lymphocyte proliferation (Kupfer and Singer, 1989b). Further mutual co-capping of TCR/peptide-MHC pairs generally does not occur in the absence of high concentrations of processed antigen on the B lymphocyte APC and a significant LFA/ICAM-mediated intercellular adhesion (Kupfer and Singer, 1989b). The TCR may also undergo a conformational change with increased affinity for the CD4 receptor (normally independent of TCR/CD3), which then interacts

with non-peptide-bearing portions of the B lymphocyte MHC (Kupfer et al., 1987a; Sakihama et al., 1995).

### 2.2.3 Reorientation of the cytoskeleton and Golgi apparatus for specific activation

Reorientation of the $T_H$ lymphocyte microtubule organizing centre (MTOC; the nucleation centre for microtubule polymerization) and the associated Golgi apparatus occurs within minutes of cell contact and precedes cytokine synthesis by several hours (Kupfer et al., 1991). The cytoskeletal reorientation process is not completely understood, but it is thought that microtubules (MTs) in the area of cell contact become attached to the cell membrane and exert torque to pull it (Singer, 1992) and the Golgi apparatus (Rios and Bornens, 2003) toward the contact zone. In antigen-specific $T_H$/B-APC or CTL/target cell conjugates, only the $T_H$ lymphocyte (Kupfer et al., 1986b) or CTL (Kupfer and Dennert, 1984) undergoes cytoskeletal reorientation. While multiple B lymphocytes may bind a given $T_H$ cell, those facing the $T_H$ MTOC and its secretory machinery preferentially proliferate. Other B lymphocytes bound to the same $T_H$ lymphocyte but not adjacent to the $T_H$-MTOC remain in interphase (Kupfer et al., 1994).

Cytoskeletal involvement is thought to maintain the adhesion and signalling for extended periods (Valitutti et al., 1995). Prolonged cell-to-cell contact (several minutes to a couple of hours for CTLs (Vyas et al., 2002); up to 20-30 hr for naive B or T lymphocytes (Iezzi et al., 1998; Kupfer et al., 1991; Kupfer et al., 1994; Van Seventer et al., 1992) may be necessary to create a sustained calcium signal, assemble a stable signalling scaffold from the membrane to the interior of the cell and induce gene transcription and protein translation (Podack and Kupfer, 1991; Valitutti and

Lanzavecchia, 1997). Golgi-derived vesicles containing newly-synthesised proteins may then track along MTs to fuse with the cell membrane in the contact zone (Mizuno and Singer, 1993; Singer, 1992).

The secretory products contained in the Golgi vesicles have no antigenic specificity in their action *in vitro* (Kupfer et al., 1991). Functional specificity may nonetheless be imposed through polarized delivery of cytokines and local insertion of newly expressed receptors only into the restricted intercellular space created by the three-dimensional structure of the adhesion (Kupfer et al., 1986a; Poo et al., 1988). In B-APC/$T_H$ lymphocyte pairs, the $T_H$ lymphocyte releases cytokines into the 'synapse': where a corresponding receptor is present on the attached B lymphocyte, a signal may then be specifically delivered to the B lymphocyte without activation of bystander cells (Kupfer et al., 1991). The polarization response may also direct delivery of endosomes to the area of contact, providing additional TCRs and signalling components to augment or prolong signal transduction (Das et al., 2004; Ehrlich et al., 2002).

The cytotoxic T lymphocyte accomplishes unidirectional cell killing of target cells in a similar fashion (Kupfer et al., 1986a). Membrane-bound lytic granules (containing membrane pore-forming cytolysin or perforin, and granzyme serine esterases) are reoriented toward the contact zone and fuse with the inner surface of the CTL membrane. The contents are released into the intercellular cleft, delivering the lethal hit only to the attached cell, while sparing other cells in the vicinity (Kupfer et al., 1985; Kupfer et al., 1986a; Poenie et al., 1987; Stinchcombe et al., 2001; Zagury et al., 1979). Both membrane and secreted proteins originating from the Golgi may activate apoptosis pathways in the target cell, including that mediated by tumour necrosis factor (TNF)

(Podack and Kupfer, 1991) and the membrane-associated cytokine Fas ligand (Suda et al., 1995).

### 2.2.4 The supramolecular activation complex (SMAC)

The specialised three-dimensional contact formed between cells following antigen recognition has been termed the supramolecular activation complex (SMAC) or immunological synapse (Monks et al., 1998). The arrangement and components of the SMAC in various cell types can vary (Montoya et al., 2002; O'Keefe et al., 2004; Potter et al., 2001; Roda Navarro et al., 2004; Standeven et al., 2004; Vyas et al., 2002). The following general description refers to naive $T_H$/B-APC interactions.

Grakoui *et al* (1999) have described SMAC formation as a 3-stage process: initial junction formation, followed by MHC-peptide transport and later stabilization of the SMAC. The SMAC initially contains a zone of large integrin family adhesion molecules (LFA-1/ICAM pairs) several microns wide and spanning 30-40 nm between the two cells (Dustin, 2002). The integrin junction creates a fulcrum for propulsion of an outer ring of T lymphocyte membrane into close apposition with the APC hrough cytoskeletal rearrangement (Grakoui et al., 1999a). The smaller TCR molecules in the zone of apposition may then interact with peptide-MHC on the APC, with TCR/peptide-MHC pairs spanning a 15 nm distance in a ring surrounding the integrin junction (Dustin, 2002). Over the following minutes, the engaged TCRs are transported toward the centre of the contact zone in an actin-dependent process: it is thought that multiple TCRs are consumed in serial fashion during this period, each only binding the MHC for seconds (Grakoui et al., 1999a). As a result, the mature SMAC contains a central zone of TCR/MHC-peptide pairs surrounded by a ring of integrins (Grakoui et al., 1999a; Monks

et al., 1998). In a CD3-dependent process, the large mucin CD43 (the most abundant molecule on the surface of T lymphocytes) is actively excluded from the T lymphocyte/APC contact site (Sperling et al., 1998), co-localising with ERM (ezrin-radixin-moesin) family cytoskeletal adaptor proteins in a membrane domain distal to the site of TCR engagement (Allenspach et al., 2001; Cullinan et al., 2002; Delon et al., 2001). CD43 may function as a barrier to nonspecific T lympocyte/APC interactions that is removed as a result of T lymphocyte activation (Allenspach et al., 2001; Sperling et al., 1998).

There is some controversy as to whether subsequent receptor clustering into the SMAC is mediated by active cytoskeletal rearrangements (Al-Alwan et al., 2001; Blanchard and Hivroz, 2002) or as a result of spontaneous self-assembly (Qi et al., 2001). It has been suggested that passive diffusion of TCRs is sufficient to supply the SMAC (Favier et al., 2001), although others have shown movement of TCRs into the SMAC at speeds significantly greater than unrestricted diffusion (Moss et al., 2002). Nonetheless, engagement of LFA/ICAM and CD28/B7 co-stimulatory pathways may enhance the myosin motor protein-driven movement of actin-linked membrane receptors on the T lymphocyte into the area of contact through cytoskeletal reorientation, thus amplifying the localised TCR-mediated signal (Wulfing and Davis, 1998; Wulfing et al., 2002).

While a minimal signal does not create productive T lymphocyte responses, the early integrin-mediated adhesion may commit the cell to the formation of a mature SMAC, capable of orchestrating responses which are not dependent on TCR signalling alone (Freiberg et al., 2002; Wulfing et al., 1998). The interaction of individual signalling components within the SMAC may also serve to generate signal patterns that

would not otherwise be created in response to random receptor aggregation (Bromley et al., 2001; Monks et al., 1998) and enable amplification of signals even as the TCR becomes partially desensitised by serial engagement (Dustin, 2003).

### 2.2.5 Intracellular signalling cascades in the T lymphocyte

The lymphocyte response to T-cell receptor-mediated activation signals may be to proliferate, become anergic (transiently unresponsive to otherwise appropriate stimuli (Sloan Lancaster et al., 1994a) ) or to die. The nature of the response is determined by the developmental stage of the lymphocyte, the type and activation state of the APC (Rothoeft et al., 2003), and by the number, kinetics and quality of the receptor/ligand interactions (Irvine et al., 2002; Valitutti and Lanzavecchia, 1997; Viola et al., 1997b). In immature thymocytes, TCR/CD3 activation by self-peptides stimulates apoptosis (thus establishing self-tolerance), while non-reactive cells are permitted to mature. Naive lymphocytes encountering antigen in the absence of appropriate co-stimulation tend to become anergic. When stimulated by sub-optimal signals, mature lymphocytes may become anergic or apoptotic; more optimal signalling may induce proliferation and development into effector lymphocytes. Mature activated/memory T lymphocytes do not generally require co-stimulation (Farber et al., 1997) and form mature immunological synapses more quickly than naive lymphocytes (Watson and Lee, 2004). The following discussion will briefly describe signalling events in mature lymphocytes after primary antigen exposure.

It should be noted that T lymphocyte signalling is very complex and may involve several different signalling cascades. Nonetheless, tyrosine phosphorylation of intracellular proteins appears to be the initial event following interaction of the clonotypic

TCR with antigen/MHC complexes. The TCR itself does not have tyrosine kinase activity: TCR kinase activity is restricted to intracellular portions of the ζ-subunit of the invariant CD3 receptor associated with the TCR. The TCR-mediated signalling involves formation of stable complexes of the TCR with co-receptors (CD4/8) and intracellular kinases, including ZA*P*-70, $p56^{lck}$ and $p59^{fyn}$ (Berridge, 1997b). The activity of these kinases is regulated by both kinases and phosphatases. A critical regulatory element appears to be the tyrosine phosphatase associated with the CD45 membrane receptor, which helps to maintain the *src*-family protein tyrosine kinase (PTK) $p56^{lck}$ in the active dephosphorylated state (D'Oro et al., 1997; Ucker et al., 1994; Volareviac et al., 1990; Volareviac et al., 1993; Volareviac et al., 1992). The $p56^{lck}$ kinase is associated with cytoplasmic tails of CD4 or CD8 co-receptors. The CD4 receptor recruits $p56^{lck}$ to translocate to the cytoskeleton at the T lymphocyte/APC interface (Caplan and Baniyash, 1996), while co-operation between CD4 and the co-stimulatory receptor CD28 leads to autophosphorylation of $p56^{lck}$ (Holdorf et al., 2002). Activated $p56^{lck}$ kinase in turn phosphorylates immunoreceptor tyrosine-based activation motifs (ITAMs) on the cytoplasmic tails of CD3 subunits (Farber et al., 1997). The ZA*P*-70 PTK binds the ITAMs and is itself phosphorylated and activated for downstream signalling (Berridge, 1997b; Farber et al., 1997; Ucker et al., 1994). The signalling activity of the *src*- and related *syk*-family kinases returns to basal levels within 30 min, after which additional signalling pathways may serve to prolong the signalling process (Dustin, 2003).

This initial TCR triggering creates a wave of phosphorylation events in the cell, inducing the formation of multi-protein signalling complexes, and ultimately influencing gene transcription (Schmitz et al., 2003). Activated ZA*P*-70 phosphorylates tyrosine

residues on the adapter molecule linker for activation of T cells (LAT) and other proteins, which then recruit other proteins involved in activation of the *Ras* and calcium signalling pathways. These include phospholipase-Cγ1 (PLC-γ1), which translocates to the cell membrane upon phosphorylation. Increased catalytic activity of PLC-γ1 leads to production of diacylglycerol (DAG) and inositol 1,4,5-trisphosphate ($IP_3$) from hydrolysis of membrane-derived phosphatidylinositol. DAG production, in conjunction with *src*-family tyrosine kinase TCR signalling (Thebault and Ochoa-Garay, 2004), phosphatidylinositol 3-kinase (PI3-K) co-stimulation and actin cytoskeleton reorganization (Altman and Villalba, 2002; Sanchez-Lockhart et al., 2004), stimulates membrane translocation and activation of protein kinase C-θ (PKC-θ) (Altman et al., 2000; Diaz-Flores et al., 2003). Activation of PKC-θ is an important step in TCR-mediated proliferation (Monks et al., 1997), inducing interleukin-2 (IL-2) synthesis through the activator protein-1 (A*P*-1) and nuclear factor-kappaB (NF-κB) transcription factors (Altman et al., 2000; Isakov and Altman, 2002); PKC-θ provides an important survival signal to T lymphocytes (Altman and Villalba, 2002), promoting T lymphocyte cell cycle progression and regulating programmed cell death (Isakov and Altman, 2002). Stimuli that fail to result in PKC-θ translocation and activation also fail to induce proliferation (Monks et al., 1997).

Activation of $IP_3$ receptors on the endoplasmic reticulum results in a transient release of calcium ($Ca^{2+}$) stores (Berridge, 1997a; Gardner, 1989). This brief $IP_3$ and $Ca^{2+}$ signal is insufficient to induce full lymphocyte activation (Gardner, 1989; Van Seventer et al., 1992). However, depletion of intracellular $Ca^{2+}$ stores induced by inositol 1,4,5-trisphosphate ($IP_3$) activates stores-operated $Ca^{2+}$ channels in the plasma

membrane, creating both sustained $Ca^{2+}$ signalling (Lewis and Cahalan, 1995) and oscillations in intracellular $Ca^{2+}$ ($[Ca^{2+}]_i$) levels (Donnadieu et al., 1992; Gray et al., 1988) through feedback control of the stores-operated channels (Berridge, 1997a; Tsien and Tsien, 1990). At the bulk population level, the pulses create cytoplasmic $Ca^{2+}$ levels approximately 1.5 to 3 times the resting level (~ 100 nM) (Berridge, 1997a; Gardner, 1989). Near-membrane $Ca^{2+}$ concentrations at sites of intense signal activity may reach even higher levels (Etter et al., 1996). The localised and/or pulsatile increases in $[Ca^{2+}]_i$ may allow for targeting of $Ca^{2+}$-mediated effects and prolonged signalling without activation cytotoxicity (Donnadieu et al., 1992). The sustained entry of $Ca^{2+}$ through the cell membrane regulates the turnover of active PKC to support the signalling response (Gardner, 1989); PKC-θ co-operates with the calmodulin/ $Ca^{2+}$-activated serine/threonine phosphatase calcineurin to activate gene transcription for IL-2 synthesis (Altman et al., 2000; Berridge, 1997a; Isakov and Altman, 2002).

### 2.2.6 Potentially antigenic peptides and the immunological synapse

It has been proposed that the immunological synapse serves as a checkpoint for lymphocyte activation, by providing a framework within which the T lymphocyte may discriminate qualitative, quantitative and temporo-spatial differences in $T_H$/APC cell surface receptor interactions (Anton van der Merwe et al., 2000; Blanchard and Hivroz, 2002; Grakoui et al., 1999a; Lanzavecchia and Sallusto, 2001): such differences may be translated as distinct $Ca^{2+}$ signals, cytoskeletal rearrangements and lymphocyte responses.

The range of biologic effects produced by various MHC-peptide combinations appears to be a function of the half-life of the TCR/MHC-peptide interaction (Grakoui et

al., 1999a). Optimal stimulation of the TCR is achieved with peptide/MHC ligands having off-rates for binding corresponding to the minimum receptor engagement period required to trigger signalling. High affinity binding does not activate T lymphocytes efficiently, as low rates of dissociation limit the number of TCRs bound. Low affinity binding may lead to dissociation before any signal is transduced (Valitutti and Lanzavecchia, 1997).

The helper T lymphocyte is thought to sample its environment through receptor interactions. The T lymphocyte is remarkably sensitive to TCR ligation, responding with transient $Ca^{2+}$ signals to as few as 30 peptide-MHC ligands. Co-expression of the CD4 receptor allows transient $Ca^{2+}$ signalling in response to even a single agonist peptide-MHC ligand (Irvine et al., 2002). Re-organization of molecules in the contact zone begins in the presence of about ten agonists (Irvine et al., 2002; Purbhoo et al., 2004). Provided the binding kinetics are optimal, even a small number of peptides (100-200 per APC) presented by an APC may engage large numbers of TCRs through serial recruitment and triggering of TCRs (Valitutti and Lanzavecchia, 1997). Given the TCR has been engaged for a requisite period of time, the complex may then dissociate without loss of signal transduction and the MHC-peptide ligand may bind another TCR. A single MHC-peptide ligand may thus bind several hundred TCRs in an hour (Valitutti and Lanzavecchia, 1997).

Proliferation and production of cytokines are stimulated following triggering of 8,000 or more TCRs. Signal amplification by LFA-1/ICAM, CD28/B7or other co-stimulatory interactions appears to reduce the number of TCR ligation events required to activate naive lymphocytes (Viola and Lanzavecchia, 1996). This signalling process is

self-limiting, as a result of gradual down-regulation of TCR expression (Valitutti and Lanzavecchia, 1997) due to PTK- or PKC-dependent endocytic recycling of the TCR (Geisler, 2004). While TCR down-regulation may attenuate signalling, it may also ensure an internal store of TCR that can be rerouted to the immunological synapse (Geisler, 2004).

The density of TCR/peptide-MHC complexes clustered within the SMAC and the proportion of cells forming mature SMACs are correlated with subsequent lymphocyte proliferation. A threshold concentration of at least 60 agonist MHC-peptide complexes per $um^2$ in the central SMAC is thought to "lock in" a proliferative response (Grakoui et al., 1999a). The T lymphocytes form fewer conjugates and fail to form SMACs with APCs presenting peptides at lower concentrations (Sperling et al., 1998) or presenting antagonist peptides (regardless of peptide density) (Monks et al., 1998).

The antigenic peptides presented by APCs may also have agonist, weak agonist, antagonist, and null properties, producing different types of adhesions and $Ca^{2+}$ signals (Chen et al., 1998; Grakoui et al., 1999a; Grakoui et al., 1999b; Wulfing et al., 1997): even a single amino acid substitution may alter the outcome of TCR/MHC-peptide interactions (Chien and Davis, 1993; Grakoui et al., 1999a; Robey and Allison, 1995; Sloan Lancaster et al., 1994a; Sloan Lancaster et al., 1994b; Viola et al., 1997a). Agonist, weak agonist and antagonist MHC-peptide combinations each accumulate in the area of contact, although null and antagonist MHC-peptides do not form full SMACs or stop lymphocyte migration (Grakoui et al., 1999a; Grakoui et al., 1998). Both full agonist and weak agonist peptides stop migration, and induce central accumulation of TCRs, but the density of central cluster of TCRs is lower for the weak agonist. In

addition, synapses formed with APCs presenting both antagonist and agonist peptides display reduced MHC density within the central SMAC. The responding T lymphocytes fail to arrest migration, and show reduced $Ca^{2+}$ flux, IL-2 secretion and proliferation (Sumen et al., 2004).

Only the most robust $Ca^{2+}$ signals stimultate T lymphocyte proliferation. The duration of the delay between the first $T_H$/APC contact and the onset of the $Ca^{2+}$ signal correlates with the strength of the stimulus, with stronger agonist stimuli giving a more rapid $Ca^{2+}$ response (Wulfing et al., 1997). However, in an apparent feedback control mechanism, ligation of the CD-28-related cell-surface receptor cytotoxic T lymphocyte-associated antigen 4 (CTLA-4) following T lymphocyte activation downregulates cytokine production and cell cycle progression (Ostrov et al., 2000). Both CD28 and CTLA-4 bind the B7 counter-receptor on APCs; however, CTLA-4 normally localizes to an intracellular compartment, while co-stimulatory CD28 is expressed on the T lymphocyte surface. CTLA-4 accumulates at the immunological synapse proportionate to the strength of the TCR signal (Egen and Allison, 2002). The immunological synapse may therefore boost weak antigenic signals and attenuate overly strong signalling (Lee et al., 2003).

### 2.2.7 Selective engagement of signalling components and the cytoskeleton in response to T-cell receptor (TCR) ligation and supramolecular activation complex (SMAC) formation

The assembly of a signalling scaffold beneath the SMAC and the distribution of calcium signals within the lymphocyte are dependent on the nature of the TCR/MHC-peptide interaction and the architecture of the SMAC (Grakoui et al., 1999a; Monks et al.,

1998; Pizzo et al., 2004; Pizzo and Viola, 2004). Many components of intracellular signalling cascades and the cytoskeleton may assemble beneath the mature SMAC: these include: PKC θ; $p56^{lck}$ (associated with CD4); talin, ezrin and other submembranous cytoskeletal linker proteins; actin fibres; and the MTOC (Kwan Lim et al., 1998; Monks et al., 1998; Monks et al., 1997; Schaefer et al., 2004; Tomas et al., 2002).

Different patterns of TCR stimulation may produce distinct $Ca^{2+}$ signals. *In vitro* treatment of human leukemia cells with soluble anti-CD3 antibody (anti-CD3) alone produces a transient $Ca^{2+}$ signal, beginning 2-3 min after addition of the antibody and returning to baseline within 15 min. $Ca^{2+}$ signals in response to polarised signals from microsphere-fixed anti-CD3 are of similar amplitude but persist for 1 hr. In the presence of competitive soluble anti-CD3, $Ca^{2+}$ responses to polarised stimuli from fixed anti-CD3 are reduced in duration and the TCRs rapidly desensitized (Hashemi et al., 1996).

After polarised stimulation of naive $T_H$ lymphocytes with antigen presented by APCs, there is a delay of several minutes before $[Ca^{2+}]_i$ levels begin to rise, after which oscillations occur at approximately 2 min intervals (Donnadieu et al., 1992). The $[Ca^{2+}]_i$ levels remain elevated for at least 1–4 hrs (Donnadieu et al., 1992; Van Seventer et al., 1992). In an actin- and extracellular $Ca^{2+}$-dependent process, normally spherical $T_H$ lymphocytes may adopt flattened and elongated morphologies, a response not seen after stimulation with soluble anti-CD3 antibody (Donnadieu et al., 1992).

In CTLs, synapse formation and $Ca^{2+}$ mobilisation patterns may reflect different activation thresholds for the dual functions of cytotoxicity and cytokine production (Faroudi et al., 2003). The formation of the CTL synapse can be initiated by binding of high levels of LFA-1 (Marwali et al., 2004; Somersalo et al., 2004). Immature CTLs

selectively activated to cytotoxicity lack a mature immunological synapse while exhibiting a low threshold polarised secretion of lytic granules and spike-like patterns of $Ca^{2+}$ mobilisation (Faroudi et al., 2003). The interaction of mature CTLs with target cells results in a mature immunological synapse (Faroudi et al., 2003) accompanied by an almost immediate smooth and sustained 4–6 fold increase in $[Ca^{2+}]_i$ (Poenie et al., 1987) and subsequent cytokine production (Faroudi et al., 2003). The $Ca^{2+}$ signal is maximal within 30 to 60 s and returns to baseline over 15 to 20 min. The $Ca^{2+}$ signal has two spatially and temporally distinct components. Transient $Ca^{2+}$ mobilization from intracellular stores occurs distal to target cell contact zone (Gray et al., 1988; Poenie et al., 1987). A more prolonged signal proximal to the target cell is created by extracellular $Ca^{2+}$ influx (Gray et al., 1988). Inappropriate targets cells evoke no changes in $[Ca^{2+}]_i$ (Poenie et al., 1987). In contrast, $[Ca^{2+}]_i$ is distributed almost homogeneously throughout the cell volume after stimulation of the Jurkat T cell line with the mitogenic lectin phytohemagglutinin (Maltsev et al., 1994).

The T lymphocyte MTOC becomes reoriented toward the site of TCR signalling in response to optimal concentrations of antigen (Monks et al., 1997), regardless of whether integrins or co-stimulatory molecules are engaged (Lowin Kropf et al., 1998; Sedwick et al., 1999). Reorientation is dependent on TCR-activated phosphorylation of TCR ITAMs by $p56^{lck}$ (Lowin Kropf et al., 1998) and extracellular $Ca^{2+}$ (Kupfer et al., 1985) but not on LFA-1 engagement or talin rearrangement (Sedwick et al., 1999). Where the APC presents sub-optimal concentrations of agonist or antagonist peptide, talin is clustered in the contact zone, but not PKC, and the MTOC remains randomly oriented (Grakoui et al., 1999a; Monks et al., 1998).

## 2.4 Mercury

Although the chemical form may be altered by enzymatic activity and interaction with other chemicals, all forms of mercury are toxic (Fernando, 1995). Because of its toxicity and persistence, mercury continues to be a serious environmental and occupational contaminant (Aronson, 1998; Barregard et al., 1999a; Counter and Buchanan, 2004; Eto, 2000; Hansen and Danscher, 1997; Hultman and Enestrom, 1992; Kaiser, 1998; Kanluen and Gottlieb, 1991; Nierenberg et al., 1998; Risher et al., 2002). For this reason, mercury ranks #3 on the US ATSDR (Agency for Toxic Substances and Disease Registry) priority list of hazardous substances.

### 2.4.1 Mercury in the environment

While natural mercury accounts for a significant proportion of the global mercury cycle, anthropogenic inputs are currently thought to exceed natural sources. Global atmospheric deposition of mercury from anthropogenic sources, including coal burning, waste incineration and ore refining, is estimated to be 4,000 t per year and rising at a rate of 1 – 2 % per year (Fitzgerald, 1995; Slemr and Langer, 1992). Current environmental mercury loads in North America are 3–4 times greater than prior to the industrial revolution (Evers et al., 1998).

Mercury is found in the Earth's crust in an elemental form or combined with sulfur, most commonly as cinnabar (mercury (II) sulfide, HgS) (vanLoon and Duffy, 2000). In water and sediments, mercury is found as Hg(0), Hg(+1 or I) and Hg(+2 or II) species depending on redox and other environmental factors; in aerobic conditions, Hg(+2 or II) predominates. In the absence of other complexing agents, mercury forms mono and dihydroxy complexes in water. However, Hg(II) readily forms complexes with

chloride ions in water, such that $HgCl_2$ becomes the dominant species, even at very low chloride concentrations (vanLoon and Duffy, 2000). Mercury binds organic matter strongly through interactions with sulfur-, oxygen- and nitrogen-containing functional groups (Rothstein, 1972). The Hg(II) form can also form a stable bond with carbon, to create methylmercury. The monomethylmercury ion ($CH_3Hg^+$) complexes readily with chloride or sulfur ions, as $CH_3HgCl$ or $(CH_3Hg)_2S$. Further methylation results in the formation of volatile and lipid-soluble (and therefore extremely toxic) dimethylmercury $(CH_3)_2Hg$ (vanLoon and Duffy, 2000).

Unlike other heavy metals, mercury can biomagnify and bioaccumulate as methylmercury (Mason et al., 2001). Mercury in aquatic environments is largely bound to surface sediments, but may be released under oxidizing conditions as soluble mercury (II) chloro species. Plants growing in the water can accumulate chloromercurials, or methylation within the organic sediments can create lipid soluble species that are taken up into aquatic organisms and passed up the food chain to fish (vanLoon and Duffy, 2000).

### 2.4.2 Mercury toxicity

Humans are usually exposed to organic mercury, most commonly through consumption of methylmercury-contaminated fish and shellfish. Less commonly, humans have been exposed to other organomercurials used as topical disinfectants (thimerosal [TMS] and merbromin) or preservatives in medical preparations (TMS) and grain products (both methyl and ethyl mercurials), in the manufacture of paints (phenylmercury), in industrial processes and in the calibration of certain analytical laboratory equipment (dialkyl mercurials) (Risher et al., 2002). Occupational exposure

can become significant in the manufacture of chlor-alkali batteries (Barregeard et al., 1997), fluorescent bulbs (Soleo et al., 1997) and other products containing mercury (Moszczyanski et al., 1998). In recent years, there has been growing concern regarding mercury exposure in dental care workers and individuals with a heavy burden of dental amalgam in teeth (Bates et al., 2004; Corbin and Kohn, 1994; Dodes, 2001; Ekstrand et al., 1998; Fan et al., 1997; Lindow et al., 2003; Ritchie et al., 2004; Ritchie et al., 2002). A controversial theory linking thimerosal exposure from childhood vaccines and autism has been proposed (Ball et al., 2001; Clements, 2004; Verstraeten et al., 2003; Vojdani et al., 2003; Westphal and Hallier, 2003). More recently, an association between autism and increased atmospheric deposition of mercury was demonstrated (Palmer et al., in press); further, autistic children have been shown to have reduced mercury elimination (Holmes et al., 2003).

Organic and elemental mercury are highly toxic to the central nervous system (CNS) (Clarkson, 1987; Eto, 1997, 2000; Eto et al., 1999), although toxicity may also involve the renal, respiratory, hepatic, immune, dermal, and gastrointestinal systems (Risher et al., 2002). Symptoms of neurologic toxicity include visual abnormalities, sensory impairment of the extremities, cerebellar ataxia, hearing loss, muscle weakness, tremor and mental deterioration (Kazantzis, 2002; Vettori et al., 2003). Renal effects, first evident as proteinuria, may accompany CNS signs, or may be evident without significant neurotoxicity (Kazantzis, 2002).

Inorganic mercury salts primarily affect the renal system, leading to acute tubular necrosis (Eto et al., 1999; Girardi et al., 1996; Graeme and Pollack, 1998). Proteinuria is often immediate following direct, dose-related toxic injury. However, in secondary, and

largely dose-independent, immune-mediated injury, proteinuria may be delayed several weeks to months. Mercury-related glomerulopathy occurs as part of a lupus-like syndrome, involving a variety of autoantibodies, most prominently antinuclear antibodies (Barregeard et al., 1997; Hill, 1986; Kazantzis et al., 1962; Tubbs et al., 1982).

### 2.4.3 Immunotoxicologic effects of mercury

While nervous or renal system impairments are characteristic of acute mercury toxicity in humans, alterations in immune function may be seen in the absence of overt nervous or renal effects (Dieter et al., 1983; Kazantzis, 2002; Moszczyanski et al., 1998; Park et al., 2000; Queiroz and Dantas, 1997a, b; Queiroz et al., 1994a; Queiroz et al., 1994b; Silbergeld et al., 2000; Silva et al., 2004).

The immune effects mercury are diverse and difficult to explain within the framework of current models of mercury toxicity. Mercury can induce thymic atrophy (Kosuda et al., 1996); suppress humoral (Blakley et al., 1980; Shenker et al., 1993a) and cellular immunity (Nakatsuru et al., 1985), and natural killer activity (Cai et al., 1988); increase tumour frequency (Blakley, 1984); and increase susceptibility to malaria infection in mice (Silbergeld et al., 2000). Mercury is also a known contact-sensitizing agent (Kazantzis, 2002; Pirker et al., 1993; Rowat, 1998; Santucci et al., 1998; Stejskal et al., 1996). Mercury may also stimulate lymphocyte proliferation (Jiang and Moller, 1995, 1996; Loftenius et al., 1997; Pelletier et al., 1988), and can induce transient Type-2 (T-helper-2-like) autoimmune disease in genetically susceptible rats (Druet et al., 1978; Sapin et al., 1977) and mice (Hultman and Enestrom, 1992; Warfvinge et al., 1995), and similar autoimmune dysfunction in mercury-exposed humans (Silva et al., 2004). Mercuric chloride ($HgCl_2$)-treated animals develop glomerulonephritis and proteinuria,

increased serum IgE, T lymphocyte-dependent polyclonal B lymphocyte activation and increased auto-antibody to glomerular basement membrane, immunoglobulins, DNA and nucleolar components (Bernaudin et al., 1979; Druet et al., 1979a; Druet et al., 1979b; Druet et al., 1978; Hultman and Enestrom, 1992; Pelletier et al., 1987b; Sapin et al., 1977). Immune system activation and immune complex (IC) deposition are also seen in genetically susceptible rats given dental amalgam restorations (Hultman et al., 1998), and in mice (Warfvinge et al., 1995) and rats (Hua et al., 1993) exposed to mercury vapour or thimerosal (TMS) (Havarinasab et al., 2004). Methyl mercuric chloride ($CH_3HgCl$) can induce antinucleolar antibody in susceptible mice, but the B lymphocyte response is less than for $HgCl_2$, with minimal increases in serum IgE and no systemic IC deposits (Hultman and Hansson-Georgiadis, 1999).

Evidence of human systemic autoimmune activation by mercury similar to that seen in laboratory animals is sparse (Barregeard et al., 1997; Dantas and Queiroz, 1997; Kazantzis et al., 1962; Tubbs et al., 1982). Recently, a more convincing association was demonstrated among Brazilians living and working gold mining sites, among which 40% of had antinuclear (ANA) and antinucleolar autoantibodies (AnoA). In upstream populations exposed to methylmercury primarily through consumption of fish contaminated by gold mining activities, both the prevalence and levels of autoantibodies were approximately half those seen in the gold mining community, but still several fold greater than those in a reference site with lower mercury exposures (Silva et al., 2004).

#### 2.4.3.1 Mercury and autoimmune disease in laboratory animals

Chronic administration of $HgCl_2$ can induce dysregulation of the immune system in susceptible strains of rats (Druet et al., 1978; Sapin et al., 1977) and mice (Hultman

and Enestrom, 1992; Warfvinge et al., 1995). After several weeks of oral or subcutaneous $HgCl_2$ administration, treated animals develop glomerulonephritis and proteinuria, coincident with the appearance of both granular and linear anti-glomerular basement membrane IgG deposits. Increased serum IgE and proteinuria are characteristic of the autoimmune syndrome, in conjunction with T -dependent polyclonal B lymphocyte activation and dose-dependent production of various autoantibodies (glomerular basement membrane, immunoglobulins, DNA and nucleolar components, myeloperoxydase) (Bernaudin et al., 1979; Druet et al., 1979a; Druet et al., 1979b; Druet et al., 1978; Hultman and Enestrom, 1992; Pelletier et al., 1987b; Sapin et al., 1977; Warfvinge et al., 1995). Over the course of several weeks, autoantibody levels gradually return to normal even in the face of continued mercury exposure (Castedo et al., 1994). Thereafter, susceptible rats are resistant to subsequent mercury challenges, likely due to activation of suppressor cells (Bowman et al., 1984; Mathieson et al., 1991) and/or $T_H$-1-like effector functions (Castedo et al., 1994; Dubey et al., 1993). In addition to renal damage and peripheral immune activation, splenic and lymph nodes hyperplasia and severe thymic atrophy, with loss of double-positive $CD^{4+}CD^{8+}$ thymocytes and extensive disorganization of the cortical and medullary architecture, are seen within 15 days following mercury treatment. Lewis (LEW) strain rats are resistant to these immunotoxic effects, suggesting a role for a genetic control of this immune response, linked, in part, to MHC phenotype (RT-1 locus) (Kosuda et al., 1996; Sapin et al., 1982). In certain models, there is evidence of tissue injury in many organs, including gastrointestinal vasculitis, similar to that seen in graft-versus-host disease (Mathieson et al., 1992) and polyarthritis (Kiely et al., 1995).

A similar autoimmune syndrome is seen in genetically susceptible strains of mice exposed to $HgCl_2$ (Hultman et al., 1992). After 5-6 weeks of $HgCl_2$ administration, mice from strains carrying the H-$2^s$ (A.SW and SJL) or H-$2^q$ haplotype develop antibodies to the nucleolar protein fibrillarin and systemic immune complex (IC) deposits. Intermediate responder strains, like BALB/C (H-$2^d$), develop only IC deposits, and most strains like the A.TL (H-$2^{tl}$) and DBA/2 (H-$2^d$) strains are resistant to systemic autoimmunity, indicating non-H-2 genes also regulate the response to mercury (Abedi Valugerdi and Moller, 2000; Johansson et al., 1998). Susceptible mice show a mild mesangial glomerulopathy, accompanied by mesangial $IgG_1$ antibody (and to a lesser extent $IgG_{2a}$ and C3 complement) immune complex deposition (Hultman et al., 1989).

Resistance or susceptibility to mercury-induced autoimmunity may be partly a function of antibody-dominant or T helper-2 ($T_H$-2) lymphocyte activation, although some involvement of $T_H$-1-type and other cytokines is also postulated (Bagenstose et al., 1998b; Hu et al., 1999; Kono et al., 1998). Generalised T lymphocyte proliferation and activation occurs in response to mercury administration, as indicated by an increase of IL-2-producing cells, and increased expression of the IL-2-receptor proteins CD25 and CD122 and of the proliferation marker CD71 on days 2-4 in susceptible strains. This is followed by a long-lasting increase in the number of cytokine-producing T lymphocytes, dominated by $CD4^+$ lymphocytes, with a late predominance of the $T_H$-2-associated IL-4 producing lymphocytes (Johansson et al., 1997). While a $T_H$-2-dominated response leads to a faster and stronger B cell activation, IL-4 production is not necessary for induction of autoimmunity by mercury (Bagenstose et al., 1998b; Johansson et al., 1997). And although cytokines that support $T_H$-1 functions, e.g. IL-12, can down-regulate the AnoA

and serum IgG1 levels, they do not significantly affect IgE induction, indicating the various manifestations of mercury-induced autoimmunity are independently regulated (Bagenstose et al., 1998a).

Genetically determined differences in mercury toxicokinetics may also affect the onset and strength of the autoimmune response. Mercury deposition in the kidneys and spleen of $HgCl_2$-exposed mice is correlated with the dose (Hultman and Enestrom, 1992). Whole-body mercury retention in various inbred strains of mice exposed to $^{203}HgCl_2$ in drinking water reaches steady state after 4-5 weeks (Griem et al., 1997; Hultman and Nielsen, 2001). In susceptible mice, thymic mercury concentrations increase with continued exposure, though steady state levels in blood and liver are reached after four weeks, and in spleen and kidney after eight weeks. In strains with low susceptibility, steady-state mercury concentrations in spleen, blood and liver are lower (Griem et al., 1997). The ANoA titre in susceptible congenic H-$2^{as}$ mice is correlated with whole-body retention and organ accumulation of mercury; but like susceptibility in general, the H-2 locus does not account for all the genetic difference in toxicokinetics (Hultman and Nielsen, 1998). The anti-fibrillarin response may be driven, in part, by the kinetics of mercury accumulation in susceptible strains, leading to rapid initial modification of fibrillarin by mercury followed by a dose-dependent T lymphocyte-dependent immune response driven by the modified fibrillarin (Hultman and Nielsen, 2001; Nielsen and Hultman, 2002), with AFA appearing in serum after two weeks (Hultman and Nielsen, 2001).

Altered ratios of $T_H$-1 and $T_H$-2 lymphocytes are often observed along with oligoclonal utilization of certain TCR-beta chains in dysregulated immune states. In

$HgCl_2$-stimulated T lymphocytes from the responder BALB/c or SJL mice and the non-responder DBA/2 mice, T lymphocytes bearing a certain set of TCR-beta chains are activated only in mercury autoimmune-susceptible mice, which is inhibited by depletion of V beta $CD^{8+}$ T lymphocytes (Jiang and Moller, 1996). Exposure of BALB/c mice to $HgCl_2$ induces an oligoclonal response with increases of $Vbeta^{5+}$, $Vbeta^{7+}$, and $Vbeta^{13+}$ $CD4^{+}$ splenic T lymphocytes (Heo et al., 1997). As such, $HgCl_2$ may activate murine T lymphocytes *in vitro* in a fashion similar to a superantigen, bypassing the usual constraints on antigen presentation.

Other forms of mercury may also trigger autoimmunity. Mercury vapour produces autoimmune manifestations similar to $HgCl_2$ in mice (Warfvinge et al., 1995) and rats (Hua et al., 1993), as can TMS (although a higher absorbed dose of mercury is needed) (Havarinasab et al., 2004). Susceptible ($H\text{-}2^{s}$) mice treated with subcutaneous injections of $CH_3HgCl$ develop ANoA targeting fibrillarin, although the general (polyclonal) and specific (ANoA) B lymphocyte response is less than that seen with $HgCl_2$, with minimal increases in serum IgE and no systemic immune complex (IC) deposits (Hultman and Hansson-Georgiadis, 1999). Dental amalgam restorations also give rise to immune system activation and systemic IC deposits in genetically susceptible rats (Hultman et al., 1998).

The mercury body burden in occupationally exposed humans is comparable to the lowest observable effect level (LOEL) for autoantibodies in mice (Warfvinge et al., 1995). The effects of mercury in laboratory animals may indicate that a percentage of the population, may be at a greater risk of mercury immune toxicity (Barregeard et al., 1997). The mercury-induced autoimmune syndrome shares many features of diseases like

systemic lupus erythematosus, making it popular model for autoimmunity. This research has uncovered many of the cellular effects of mercury and led to the development of a plethora of biochemical mechanisms thought to be responsible for them.

### 2.4.4 Proposed mechanisms for mercury toxicity

Some, if not all, mercury effects on immune function likely involve interaction with thiol (-SH) groups. As such, thiol-containing compounds inhibit mercury-induced immune effects *in vitro* and *in* vivo (Hu et al., 1997). However, physico-chemical differences between organic and inorganic mercury may make it difficult to identify specific mechanisms for mercury toxicity. Some proposed mechanisms may represent targets of all forms of mercury; however, certain mechanisms involve only membrane-based target sites, while others are intracellular, to which ionised $Hg^{2+}$ may have limited access. The effects of $Hg^{2+}$ may therefore be quite different in cell free systems than in whole cell models.

Cellular binding and uptake studies with mercury have shown that approximately 66% of $Hg^{2+}$ accumulated by renal cortical epithelial cells exposed to 1 uM $HgCl_2$ for 30 min was membrane bound (Endo et al., 1995a, b). Accumulation of $Hg^{2+}$ is thought to be bi-phasic: initial non-specific electrostatic binding to membranes is followed by internalization (Foulkes, 1988; Gutknecht, 1981). Internalisation of a proportion of $Hg^{2+}$ is dependent on energy and temperature, suggesting involvement of active transport mechanisms (Endo et al., 1995a). Candidate transporters influencing $Hg^{2+}$ uptake include the $HCO_3^-/Cl^-$ transporter (Endo et al., 1997) and those used by essential metals (Ballatori, 2002). The transporter binding sites for essential divalent metals appear to be somewhat non-specific, allowing transport of toxic metals such as $Cd^{2+}$ and $Pb^{2+}$ into and

around the cell (Ballatori, 2002). In the only study of $Hg^{2+}$ uptake by lymphocytes, during the initial 15-30 min period after exposure to radioactive $^{203}HgCl_2$, $^{203}Hg$ was found only in membranes, but was later found bound to non-histone proteins in the nucleus (Nordlind, 1985). However, using the fluorescent dye BTC-5N to measure $Hg^{2+}$ in the cytosol, nanomolar $Hg^{2+}$ levels are seen within minutes of $Hg^{2+}$ application in association with a rise in $[Ca^{2+}]_i$, indicating $Hg^{2+}$ must enter the hepatocytes for this $Ca^{2+}$ increase to occur (Nathanson et al., 1995). Although significant accumulation of $Hg^{2+}$ does not appear to occur until after mercury-induced disruption the membrane barrier, organic $CH_3HgCl$ can penetrate the cells without any noticeable damage to the membrane (Nakada and Imura, 1982). Transmembrane transfer of $CH_3HgCl$ has been suggested to involve several systems: 1) organic anion transport; 2) facilitated diffusion of D-glucose; 3) cysteine-facilitated transport; and 4) $Cl^-$ ion transport (Wu, 1995). Cysteinal sulfhydryl (–SH) group binding creates $CH_3Hg$-L-cysteine, which may be transported into the cell (and across the blood-brain barrier) by the same mechanisms used for methionine (Kerper et al., 1992). Inside the cell, some $CH_3HgCl$ is released and binds GSH. The resulting $CH_3HgCl$-glutathione complex may be a substrate for proteins that transport glutathione S-conjugates out of the brain capillary endothelial cells into the brain interstitial space (Ballatori, 2002; Kerper et al., 1996).

#### 2.4.4.1 Mercury interactions with membranes

Cell membranes are the first potential target for mercury toxicity. Cross-linking of primary amines on polar heads of phosphatidylserine and phosphatidylethanolamine lipids by $Hg^{2+}$ may increase lipid-lipid affinity, which alone or in combination with increased protein-protein and reduced protein-lipid affinities, may reduce membrane

fluidity and alter the spatial arrangement of membrane receptors by "squeezing" membrane proteins out of the lipid medium (Delnomdedieu and Allis, 1993; Girault et al., 1997). Such receptor rearrangements may mimic those occurring in response to physiologic ligands. Similarly, membrane divalent $Hg^{2+}$ may non-specifically cross-link thiol (–SH) groups on lymphocyte cell surface receptors, to alter receptor conformation and/or produce receptor aggregation and induce aberrent signal transduction (Nakashima et al., 1994; Pu et al., 1995). Aggregation (i.e. patching and capping) of CD3, CD4, Thy-1 and CD45 receptors has been observed in $HgCl_2$-treated murine splenic cultures. Receptor aggregation was associated with activation of the *src* family protein tyrosine kinase $p56^{lck}$ and heavy tyrosine phosphorylation of intracellular proteins (Nakashima et al., 1994; Rahman et al., 1993). Although the mechanism of triggering these events is redox-linked, phosphotyrosine-containing proteins and $p56^{lck}$ do not form aggregates directly through thiol-mediated bonds (Katano et al., 1995) and phosphorylation required an intact membrane. However, heavy phosphorylation was observed only at relatively high concentrations (> 0.2 mM $HgCl_2$) and cell death ensued rapidly (Nakashima et al., 1994). In contrast, 48 hr exposure to $HgCl_2$ was mitogenic at concentrations below those producing observable tyrosine phosphorylation with transient exposure (Nakashima et al., 1994). Other studies have shown moderate increases in phosphorylation at 0.1 to 1.0 uM $HgCl_2$ (Rosenspire et al., 1998), or phosphorylation of specific proteins without increasing overall phosphorylation (McCabe et al., 1999). Electrophoretic analysis shows numerous proteins are specifically phosphorylated in response to high concentrations of $Hg^{2+}$, including a 52-kDa Shc protein, extracellular signal-regulated kinase 1 (ERK1), and p44, ERK2 p42 and the c-Jun amino terminal kinase p54 of the

mitogen-activated protein kinase MAPK family (Akhand et al., 1998). However, mercury-induced aggregation of cell membrane receptors may induce distinct downstream intracellular phosphorylation patterns (Pu et al., 1996).

Membrane $Ca^{2+}$ channels may also be targets of $Hg^{2+}$ and methylmercury (Busselberg, 1995; Girardi and Elaias, 1998; Sirois and Atchison, 1996, 2000). Heavy metal ions may directly block voltage activated L/N and T type calcium channels in excitable cells *in vitro* (Busselberg, 1995). Both $Hg^{2+}$ and *p*-chloromercuribenzoate reduce passive, non-AT*P*-dependent $Ca^{2+}$ influx into hepatic plasma membrane vesicles *in vitro* (Bygrave et al., 1989). In contrast, other studies report elevation of $[Ca^{2+}]_i$ in response to metal exposure (Badou et al., 1997; McNulty and Taylor, 1999; Tan et al., 1993), alone or in conjunction with uptake of the metal (McNulty and Taylor, 1999); metal uptake through $Ca^{2+}$ channels in the absence of significant $Ca^{2+}$ signalling may also be seen (Hinkle et al., 1987; Tomsig and Suszkiw, 1991); uptake of metals into the cell may be triggered in part by depletion of $[Ca^{2+}]_i$ stores (Kerper and Hinkle, 1997). Increased $[Ca^{2+}]_i$ in neuronal preparations treated with methyHg *in vitro* has been attributed to non-specific increases in membrane permeability secondary to mercury-related loss of energy production (Kauppinen et al., 1989). Similar non-specific changes in membrane cation permeability have been seen with TMS (Gukovskaya et al., 1992).

In addition, mercury may inhibit $Na^+/K^+$-ATPase activity (Anner, 1997; Ballatori and Boyer, 1996; Ballatori et al., 1998; Chanez et al., 1989; Kaplan and Mone, 1985; Lewis and Bowler, 1983). Hepatocyte $Na^+/K^+$-ATPase activity is more sensitive to the effects of $Hg^{2+}$ than $CH_3HgCl$. Over 60 min, cells treated with 50 uM $HgCl_2$ swelled to double the volume of controls and failed to return to normal volume after placement in

hypotonic media (Ballatori et al., 1988). $Na^+/K^+$-ATPase activity in isolated canine renal (Kaplan and Mone, 1985) and rat brain synaptic membrane (Lewis and Bowler, 1983) preparations have been shown to be very sensitive to TMS, although inhibition was greater for $HgCl_2$ than for TMS in rat fetal brain homogenate (Chanez et al., 1989).

#### 2.4.4.2 Intracellular targets for mercury

Mercury may target intracellular components, though it is often uncertain whether the effects are direct or indirect. Direct activation of the $Ca^{2+}$/calcineurin-dependent pathway and protein kinase C (PKC) have both been implicated in $HgCl_2$-induced IL-4 gene expression by murine T lymphocyte hybridomas. In this model, $HgCl_2$ also induced a PKC-dependent $Ca^{2+}$ influx through L-type $Ca^{2+}$ channels (Badou et al., 1997). In the WEHI-231 B lymphocyte cell line, activation of PKC through B-cell receptor (BCR) ligation leads to induction of apoptosis. Non-toxic $HgCl_2$ concentrations, producing no change in overall tyrosine phosphorylation attenuate the growth inhibitory effects of BCR cross-linking but have no effect on the negative growth signal generated by direct activation of PKC with phorbol 12-myristate 13-acetate (McCabe et al., 1999). In contrast, $Hg^{2+}$ inhibits the activity of, and the binding of regulatory ligands to soluble PKC (Speizer et al., 1989). Organomercurials, including methyl mercury, phenyl mercury and *p*-chloromercuribenzoic acid (*p*-CMB), inhibit soluble PKC through thiol binding in a similar fashion, though greater concentrations are required (Inoue et al., 1988).

Mercury may interact with the *Ras*/MAP kinase (mitogen activated protein kinase) signal transduction pathway. Subtoxic concentrations of $HgCl_2$ stimulate *Ras*.GTP in the Jurkat human T lymphocytic cell line, but fail to increase MAP kinase

activation. Selective inhibition of T cell receptor-mediated Ras and MAP kinase activation is also seen with $HgCl_2$ exposure, though activation of MAP kinase by phorbol diesters remains intact (Mattingly et al., 2001). The $Hg^{2+}$ ion has also been shown to activate protein tyrosine phosphatases (PTPase's) and $p56^{lck}$ without increasing tyrosine phosphorylation. Phosphorylation was only seen at concentrations producing PTPase inhibition (Lander et al., 1992).

The cytoskeleton presents several potential targets for mercury. Organic $CH_3HgCl$ selectively targets microtubules (MTs) (Brown et al., 1988; Imura et al., 1980; Miura et al., 1984; Sager et al., 1983; Vogel et al., 1985), in a time- and concentration-dependent fashion (Castoldi et al., 2000), while actin microfilaments remain intact, even in cells showing complete MT deaggregation (Wasteneys et al., 1988). Vimentin intermediate filaments are also spared except at concentrations causing extensive MT disassembly (Sager, 1988; Wasteneys et al., 1988). The inorganic $Hg^{2+}$ ion is a more potent inhibitor of *in vitro* tubulin polymerisation than $CH_3HgCl$, producing complete inhibition at 25 uM $Hg^{2+}$ (Miura et al., 1984) as compared to 30-50 uM $CH_3HgCl$ (Miura et al., 1984; Vogel et al., 1985). However, immunofluorescence studies in intact mouse glioma cells indicate $CH_3HgCl$ disrupts the MT network at an early stage of growth inhibition, while $Hg^{2+}$ has no effect on MTs for at least 1 hr (Miura et al., 1984). This $CH_3HgCl$-related MT disruption is known to interfere with cell cycle progression. G2/M-phase (prometaphase/metaphase) arrest is an important event in the development of apoptosis after $CH_3HgCl$ exposure, similar to that seen with colchicine (Miura et al., 1999). Neuronal MT de-polymerisation in response to 1 uM $CH_3HgCl$ precedes the onset of cell death by several hours (Castoldi et al., 2000). Thimerosal is also a potent MT

disruptor ($IC_{30}$= 0.03 mM) (Brunner et al., 1991), producing cell-cycle arrest (Alexandre et al., 2003) and loss of spindle chromosome-sorting fidelity (Voutsinas et al., 1997).

Activation of redox-sensitive signalling cascades has been demonstrated for all forms of mercury. Redox signalling may be activated directly or indirectly, as a result of generalised oxidative stress (generation of reactive oxygen species and lipid peroxidation), consumption of glutathione (GSH) and induction of the mitochondrial permeability transition (Brawer et al., 1998; InSug et al., 1997; Naganuma et al., 1990; Nath et al., 1996; Pintado et al., 1995; Shenker et al., 1999Shenker, 2000 #1964; Shenker et al., 1998; Shenker et al., 1993b). Cells with high levels of GSH are resistant to $HgCl_2$ toxicity while cells with low levels of GSH are extremely sensitive. Both T and B lymphocytes and monocytes exposed to $HgCl_2$ exhibit a dose-dependent decrease in GSH content with a concomitant reduction in glutathione disulfide (GSSG) levels. Lymphocyte and monocyte GSH generation is inhibited by $HgCl_2$, although GSH reductase and GSH peroxidase are unaffected (Shenker et al., 1993b). Strain-dependent differences in thiol levels in particular subsets of CD4+ lymphocytes and subset-specific modification of thiol levels may contribute to differential effects of $HgCl_2$ lymphocytes from autoimmune-susceptible and -resistant strains (Roos et al., 1997).

Hydrogen peroxide production and expression of redox-sensitive genes (heme oxygenase and members of the *bcl* family) are stimulated by $HgCl_2$ in renal cells *in vitro* and *in vivo* (Nath et al., 1996). In T lymphocytes exposed to $CH_3HgCl$, a profound reduction in mitochondrial redox potential ($\Delta\rho_m$) occurs early, in conjunction with a decline in GSH levels within 1 h. Subsequently, the generation of reactive oxygen species (ROS) creates a further decrease in thiol reserves. The induction of oxidative

stress and the mitochondrial permeability state may then lead to activation of death-signalling pathways (Shenker et al., 1999). Similar changes are seen in monocytes treated with $CH_3HgCl$ (InSug et al., 1997). Mitochondrial dysfunction and the development of the mitochondrial permeability transition may result in the release of cytochrome c, a factor that promotes apoptosis. While $CH_3HgCl$ causes a significant increase in cytosolic cytochrome c from human T lymphocytes, $HgCl_2$ does not affect cytosolic cytochrome c (Shenker et al., 2000).

Modulation of gene transcription may be responsible for some of the effects of mercury. Renal GSH levels increase after exposure to a subtoxic dose of $HgCl_2$ (0.5 uM/kg), in conjunction with increases in gamma-glutamylcysteine synthetase, glutathione disulfide (GSSG) reductase and GSH peroxidase activities (Lash and Zalups, 1996). The levels of c-jun mRNA and c-Jun protein are elevated in LLC-PK1 cells exposed to 10 – 20 uM $HgCl_2$ (Matsuoka et al., 2000). Pretreatment of human monocytic leukemia cells with sub-toxic concentrations of $HgCl_2$ (2 uM) for 20 hrs has no effect on proliferation potential or metabolic activity, but induces metallothionein mRNA and metallothionien protein accumulation (Koropatnick and Zalups, 1997). Both activation of the cell-death mediators caspase-8, -9, and -3 and increased expression of caspase-8 and -9 are seen in human T lymphocytes following $CH_3HgCl$ exposure (Shenker et al., 2002).

#### 2.4.4.3 Mercury and intracellular calcium

Although mercury toxicity may involve both membrane and intracellular components, a final common pathway for mercury toxicity is likely disruption of intracellular calcium ($[Ca^{2+}]_i$) homeostasis (Badou et al., 1997; Komulainen and Bondy, 1987; MacDougal et al., 1996; Pintado et al., 1995; Sirois and Atchison, 2000; Smith et

al., 1987; Tan et al., 1993). While both $CH_3HgCl$ (0.02-2 uM) and $HgCl_2$ (0.01-1 uM) increase $[Ca^{2+}]_i$ in rat splenic lymphocytes in a concentration-dependent manner, the mechanisms may differ. The increase produced by $CH_3HgCl$ is both rapid and sustained, while $HgCl_2$ causes a slow rise in $[Ca^{2+}]_i$. The effects of the mercury compounds are not initially associated with reduced membrane integrity, however, membrane damage is seen after 15 min (Tan et al., 1993).

The increased $[Ca^{2+}]_i$ seen after $HgCl_2$ exposure may be a function of aberrant activation of signalling mechanisms. The $HgCl_2$ induces a protein kinase C-dependent $Ca^{2+}$ influx through L-type $Ca^{2+}$ channels in murine T lymphocyte hybridomas. The $Hg^{2+}$-induced signal is transient, being approximately 15 min in duration (Badou et al., 1997). Similar results are seen in leukocytes from a marine teleost fish, *Sciaenops ocellatus*. At 10 uM or greater, $HgCl_2$ induces rapid influx of extracellular $Ca^{2+}$, along with growth inhibition and tyrosine phosphorylation. Lower concentrations that activate fish lymphocyte growth (0.1-1 uM) induce a slower sustained rise in intracellular calcium but do not produce detectable protein tyrosine phosphorylation (MacDougal et al., 1996).

Both $CH_3HgCl$ and TMS appear to influence $[Ca^{2+}]_i$ primarily through inhibition of ATP production and/or increased non-specific membrane permeability. In a guinea pig synaptosomal model, $CH_3HgCl$ increases synaptosomal $Ca^{2+}$ levels by two distinctive mechanisms. At 30 uM $CH_3HgCl$, $Ca^{2+}$ increases moderately secondary to loss of ATP production. At 100 uM $CH_3HgCl$, synaptosomal $Ca^{2+}$ is dramatically increased as both mitochondrial and anaerobic energy production cease and plasma membrane ionic permeability increases (Kauppinen et al., 1989). The effects of $CH_3HgCl$ cannot be inhibited with either $Ca^{2+}$ or $Na^+$ channel blockers (Komulainen and Bondy, 1987). A bi-

phasic 10-fold increase in $[Ca^{2+}]_i$ is seen in in thymic lymphocytes exposed to TMS (5-100 uM), with the second phase producing the most dramatic increase. Mobilization of $Ca^{2+}$ from intracellular stores does not contribute significantly, as TMS, like $CH_3HgCl$, non-specifically increases membrane ion permeability (Gukovskaya et al., 1992). However, in lymphocytes the TMS-induced rise in $[Ca^{2+}]_i$ seems to be due to both a release of intracellular stores and influx of extracellular $Ca^{2+}$ (Pelassy et al., 1994).

#### 2.4.4.4 Mercury-induced apoptosis and necrosis

Both $HgCl_2$ and $CH_3HgCl$ reduce human peripheral lymphocyte viability, but the chemical form of mercury and the cell model used may influence the expression of particular components of the cell death pathways.

Human peripheral T lymphocytes exposed to $HgCl_2$ or $CH_3HgCl$ show morphological (nuclear hyperchromaticity, fragmentation and condensation of nucleoplasm, destruction of cytoplasmic organelles and loss of membrane integrity) and biochemical (reduced phospholipid synthesis) changes consistent with apoptotic cell death (Shenker et al., 1992a; Shenker et al., 1993a). In contrast, concentration- and time-dependent changes characteristic of both apoptosis and necrosis are seen in murine hybridomas and T lymphocytes exposed to $HgCl_2$ (Akhand et al., 1998; Aten et al., 1995; Prigent et al., 1995). In mouse T lymphocytes, DNA fragmentation is seen at 1 uM $Hg^{2+}$ but not at 10 uM or more. However, cell death in both concentration ranges is partly inhibited by protein kinase inhibitors such as staurosporine and herbimycin A, indicating a protein phosphorylation-linked signal is involved in $Hg^{2+}$-mediated cell death regardless of whether DNA fragmentation is seen (Akhand et al., 1998).

Methyl mercuric chloride is approximately 5-10 times more potent an inducer of cell death than $HgCl_2$ (Shenker et al., 1992a; Shenker et al., 1993a). At low concentrations (0-5 uM) of $CH_3HgCl$, human T lymphocytes and monocytes exhibit changes in light scatter and vital dye exclusion patterns, and plasma membrane lipid organization consistent with apoptosis. Treated cells show thiol depletion and a decrease in mitochondrial transmembrane potential (psi $\triangle$m), and may be predisposed to damage from mercury-potentiated reactive oxygen species (ROS) formation (InSug et al., 1997; Shenker et al., 1998). As many as 1/3 of lymphocytes become apoptotic within 1 hr of exposure to $CH_3HgCl$, yet only 2/3 are apoptotic after 24 hrs of continued exposure, with 1/3 remaining viable. When activated by mitogens, T lymphocytes are protected from apoptogenic effects of the organomercurials (Shenker et al., 1997).

Within 1 hr of exposure, both $CH_3HgCl$ and $HgCl_2$ induce a mitochondrial membrane permeability transition, reducing both the transmembrane potential and the intracellular pH, and increasing reactive oxygen species (ROS) (Shenker et al., 2000), in association with reduced glutathione (GSH) content and activation of the caspase cascade (Shenker et al., 2002). The two forms of mercury differ with respect to release of cytochrome C, an event often accompanying the permeability transition. The $CH_3HgCl$ causes a significant increase in cytosolic cytochrome c from human T lymphocytes, with no accompanying changes in levels of the anti-apoptotic protein Bcl-2, while $HgCl_2$ does not affect cytosolic cytochrome c but does increase Bcl-2 (Shenker et al., 2000). Transfected cell lines displaying increased levels of anti-apoptotic protein human Bcl-2 are resistant to $HgCl_2$-induced cell death but susceptibility to apoptosis induced by an

anti-CD3 antibody is unaffected, suggesting receptor-mediated stimuli trigger different pathways leading to cell death than those activated by $Hg^{2+}$ (Aten et al., 1995).

Mercury may produce dysregulation of physiological cell death pathways. In the Jurkat human leukemic cell line, low levels ($\leq$ 10 uM) of $HgCl_2$ abrogate anti-CD95 (Fas)-mediated apoptosis and enhance cell survival, possibly through blockade of an unknown plasma membrane proximal signaling event upstream of CD95 (Fas)-induced caspase-3 activation (McCabe et al., 2005; Whitekus et al., 1999). TNF-alpha-induced caspase-3 activation is not affected by $Hg^{2+}$ (McCabe et al., 2005). However, treatment with $CH_3HgCl$ induces activation of caspase-8, -9, and -3 along with increased expression of caspase-8 and -9 (Shenker et al., 2002).

## 2.5 Proposed mechanism for effects of mercury in lymphocytes

We proposed that the immunotoxic effects of inorganic mercury ($Hg^{2+}$) and perhaps other compounds, like *p*-chloromercuribenzoate [*p*-CMB], that are charged at physiologic pH and penetrate membranes poorly) are produced, at least initially, through global triggering of normal membrane-dependent signalling mechanism. In contrast, those of organic mercury compounds ($CH_3HgCl$ and perhaps also thimerosal [TMS]), which penetrate membranes more easily, are mediated primarily by increased non-specific membrane permeability and intracellular effects, including inhibition of ATP production and dissolution of microtubules. In either case, we expected that non-localized signalling would be incompatible with normal lymphocyte activation in most circumstances.

Specifically, we hypothesized that, initially, divalent $Hg^{2+}$ acts to simultaneously trigger various T lymphocyte receptors all over the surface of the cell, either through

high-affinity protein sulfhydryl interactions or by altering membrane lipid ordering. These membrane-dependent perturbations produced by $Hg^{2+}$ may differ, spatially and temporally, from those normally occurring in the localized area of contact between an APC and an antigen-specific lymphocyte. Simultaneous globalised triggering of TCRs and associated signalling cascades may inhibit polarization of the cytoskeleton and secretory machinery and directed shape changes or motility. Further, it was anticipated these effects would be accompanied by down-regulation of the TCR in response to receptor triggering, as occurs with physiologic ligation (Valitutti et al., 1997), but would occur before effects at other intracellular targets for mercury (particularly microtubule integrity) are seen – and before the activation of cell death pathways.

In contrast, organomercurial compounds with greater lipid solubility and thus more rapid penetration into the cell, were expected to damage membranes non-specifically and to increase membrane permeability, without triggering down-regulation of surface receptors to an appreciable extent. Some of the subsequent intracellular targets of $CH_3HgCl$ or TMS could be the same or similar to those activated down-stream by $Hg^{2+}$-receptor activation, but the time course of effects was expected to be different. Organomercurial compounds were therefore expected to produce significant effects on polarised signalling events only in conjunction with – and not prior to – loss of microtubule integrity and the onset of cell death.

The pattern of cell death was expected to differ for both forms of mercury, with inorganic $Hg^{2+}$ producing predominantly apoptosis over all but the highest concentrations studied and at all time periods, and organomercurial compounds possibly producing apoptosis at low concentrations, with necrosis dominating at higher concentrations and

with continued exposure, secondary to the loss of membrane integrity and loss of calcium homeostasis.

To test our hypothesis, a simple model of the immunological synapse, amenable for use with multiple samples and experiments, was required. One possibility was to maintain an antigen-specific T lymphocyte culture along with an appropriate APC line and a source of antigen or antigen-derived peptides. An alternative strategy used in this study was to create a surrogate antigen-presenting cell to induce polarisation responses from an immortalised cell line (Hashemi et al., 1996; Lowin Kropf et al., 1998) thus avoiding the need to maintain two cell lines and a specific antigen to activate the cells.

The YAC-1 Moloney virus transformed T lymphocytic line was chosen because of the ease of maintaining continuous cultures without specialised media and known surface expression of complete CD3 receptors and associated co-receptors (Lindvall et al., 1997). A surrogate antigen-presenting cell (APC) was created by coating 6.0 um latex microspheres with anti-CD3 antibody. By mixing and centrifuging the cells and beads together, the YAC-1 cells became bound to the beads, often moving over the surface to completely engulf the bead (and in some cases more than one bead). Although no anti-co-stimulatory receptor antibody was used, and the rigid antibody-coated bead did not allow receptors from both cells to migrate or diffuse through the membrane or formation of the ‘bull’s eye’ 3-dimensional supramolecular activation complex (SMAC), this did not seem to affect the reorientation response, as the MTOC came to lie adjacent to the bead, similar to events occurring in antigen-specific lymphocyte-APC conjugates.

Mercury compounds having differing chemical properties (organic vs inorganic mercury, pKa, presumed or known ability to penetrate cell membranes and suspected or

known effects on immune function) were selected for study (see Table 2.1). The four compounds were mercuric chloride ($HgCl_2$), methyl mercuric chloride ($CH_3HgCl$), *p*-chloromercuribenzoate (*p*-CMB), and thimerosal (TMS; ethylmercurithiosalicyclate).

Mercuric chloride was selected for the study as a known immunotoxicant capable of inducing autoimmune disease. Inorganic mercury is also thought to penetrate membranes less quickly than methyl mercury in physiologic solutions, where it is likely present as polychloride anions (Foulkes, 2000) with poor lipid solubility. Methyl mercuric chloride was selected as an organic mercurial compound which primarily produces immunosuppressant effects but can, with appropriate exposures, also induce a form of autoimmune dysfunction that differs from that produced by $HgCl_2$ (Hultman and Hansson-Georgiadis, 1999). Monomethyl mercury is thought to pass through cell membranes more rapidly than inorganic mercury, owing to the increase in lipid solubility provided by the methyl group and the likelihood that in physiologic solutions the compound remains uncharged, i.e. methylmercuric choride (Foulkes, 2000). *Para*-chloromercuribenzoate (*p*-CMB) was selected as an organic mercury compound thought to penetrate membranes somewhat less rapidly than $CH_3HgCl$ (possibly as a result of ionization at physiologic pH) and because *p*-CMB effects on lymphocytes were unknown. Thimerosal, a drug, vaccine, and medical fluid preservative, was also included in the assays, owing to recent controversy regarding possible links between childhood vaccination and autism (Ball et al., 2001; Clements, 2004; Verstraeten et al., 2003; Vojdani et al., 2003; Westphal and Hallier, 2003). Thimerosal (TMS) can also induce a systemic autoimmune syndrome very similar to that seen after treatment with inorganic mercury in genetically susceptible mice, although a higher absorbed dose is required.

However, the immune changes produced by TMS, like $HgCl_2$, differ from the weaker and more restricted autoimmune reaction observed after treatment with an equipotent dose of methylmercury (Havarinasab et al., 2004). As an organomercurial compound with significant carbon character, it was expected that the unionised parent compound TMS could penetrate membranes quickly, but it has also been shown that the thiosalicylate group may dissociate following protein binding to leave an ethyl mercury group attached to proteins (Pintado et al., 1995).

In order to assess the effects of 5 and 30 min exposures to each of the four mercury compounds on immunological synapse formation, the percentage of YAC-1 cells forming conjugates, and the percentage of conjugated cells showing morphological and cytoskeletal reorganization in response to anti-CD3 binding were obtained. Concentration-response profiles for selected signalling events, including TCR/CDE receptor expression, protein tyrosine phosphorylation, microtubule integrity, and intracellular calcium levels were determined after 1, 5, 30 min and 4 hrs after initiation of mercury exposure. The pattern of cell death, whether apoptotic or necrotic, was also studied for the same four time points, and overall cell viability assessed 24 hrs after the initiation of either 5, 30 min or 4 hr mercury exposures. These experimental objectives are outlined in Chapter 3 and the specific procedures described in Chapter 4.

**Table 2.1** Summary of mercury compounds used in the study

| Chemical Name | Molecular Formula | Structure | F.W. | Toxicity data |
|---|---|---|---|---|
| Mercuric Chloride | $HgCl_2$ | 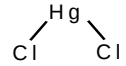 | 271.5 | $LD_{50}$ oral:<br>Rat = 1 mg/kg<br>Mouse = 5 mg/kg |
| *para*-Chloro-Mercuriben-zoate | $C_7H_4ClHgO_2.H$ | 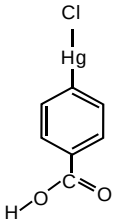 | 357.16 | $LD_{50}$ intraperitoneal:<br>Mouse = 25 mg/kg |
| Methyl Mercuric Chloride | $CH_3HgCl$ | 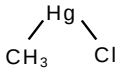 | 251.08 | $LD_{50}$ oral:<br>Rat = 29 mg/kg<br>Mouse = 57 mg/kg |
| Thimerosal | $C_9H_9HgNaO_2S$ | 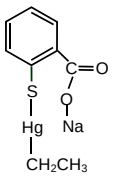 | 404.84 | $LD_{50}$ oral:<br>Rat = 75 mg/kg<br>Mouse = 91 mg/kg |

# 3.0 OBJECTIVES OF THESIS

## 3.1 Central Hypothesis

The central hypothesis of this study was that the interaction of some forms of mercury with cell membrane or intracellular targets may mimic receptor-mediated binding of antigen and produce aberrent cellular activation.

It was proposed that the toxic effects of inorganic mercury ($Hg^{2+}$) and other forms of mercury that penetrate membranes poorly (*p*-CMB) initially occur at the level of the cell membrane, while more lipid-soluble organomercurial compounds that rapidly penetrate to the cell interior have more pronounced intracellular effects. It was expected that $Hg^{2+}$ membrane interactions could produce concentration-dependent stimulation or inhibition of lymphocyte activation by altering membrane-dependent intracellular signalling events and assembly of cytoskeletal components. This aberrant, global antigen-independent signal may then alter lymphocyte responses to normal polarised stimuli, produce transient activation of some lymphocytes and/or lead to cell death.

## 3.2 Overall Project Objective

The main objective of this research was to undertake a preliminary study of the effects of various forms of mercury on selected components of receptor-mediated signalling pathways in T lymphocytes, including responses to polarised stimuli.

## 3.3 Specific Aims

The specific aims of the study were to examine the concentration-response effects of several forms of mercury on YAC-1 lymphoma cell on

I Viability and manner of cell death,

II Cytoskeletal integrity,

III TCR/CD3 expression, protein tyrosine phosphorylation and intracellular calcium levels, and

IV Morphology and polarization responses.

## 3.4 Specific Aim I: Viability and Cell Death

### 3.4.1 Broad Objective

The broad objective of Specific Aim I was to compare the effects of brief *in vitro* exposures to various forms of mercury (Hg) on YAC-1 lymphoma cell viability and to assess the manner of cell death (apoptosis or necrosis) at those concentrations producing loss of T lymphocyte viability.

### 3.4.2 Null Hypotheses

All forms of mercury – organic vs inorganic, simple salt vs aromatic compound – will have equivalent toxicity, as measured by the [$IC_{50}$], the concentration required to kill 50% of the YAC-1 cells following *in vitro* exposure. The toxicity of each of the mercury compounds will increase with increasing exposure. All forms of mercury will induce cell death in similar fashion – either apoptotic or necrotic – with similar kinetics. The addition of anti-CD3 antibody coated 6.0 um latex microspheres, to provide an activation stimulus through localised activation of CD3 receptors on the YAC-1 cells, will not affect the viability of mercury-treated YAC-1 cell cultures.

### 3.4.3 Specific Objectives

a) To assess the effect of brief *in vitro* exposures to mercury compounds on YAC-1 cell 24-hr viability. The MTT assay was selected for initial range-finding studies, where lymphocyte viability was assessed at 24 hr following 5 min, 30 min or 4 hr exposures to mercury and the results expressed as an [$IC_{50}$] for each mercury compound. On the basis of the results of this assay, the range of mercury concentrations selected for the remainder of the study was 0.01 to 100 uM.

b) To assess the effect of addition of anti-CD3-coated beads on the 24-hr viability of mercury-treated YAC-1 cells, where beads were added either before or after the mercury (not all assays required the beads, their effects needed to be assessed).

c) To develop an inexpensive high-throughput *in vitro* assay for detection of toxicant-induced apoptosis and/or necrosis, using flow cytometric techniques.

d) Having established the range of concentrations producing toxicity, to assess the manner and kinetics of cell death in mercury-treated YAC-1 cells, following 1 min, 5 min, 30 min or 4 hr exposures. A YOPRO-1 (YP)/propidium iodide (PI) dye exclusion assay was used to assess whether mercury-treated cells were viable (Y*P*-/$PI^-$), early apoptotic ($YP^+/PI^-$) or late apoptotic/necrotic ($YP^+/PI^+$).

## 3.5 Specific Aim II: Cytoskeletal integrity

### 3.5.1 Broad Objective

The broad objective of Specific Aim III was to quantitatively assess the effects of brief *in vitro* exposures to mercury on selected components of the cytoskeleton of YAC-1 lymphoma cells and to compare these results to those of Specific Aims I and II above.

### .5.2 Null Hypothesis

Mercury treatment will have no effect on the quantity of microtubules, actin microfilaments, vimentin filaments or talin in YAC-1 lymphoma cells.

### 3.5.3 Specific Objectives

a) To develop flow cytometric methods for the quantititive assessment of cytoskeletal components in YAC-1 lymphoma cells.

b) To assess the effects of brief *in vitro* mercury exposure on YAC-1 lymphoma cell microtubules, following flow cytometric assessment of mean fluorescence following indirect immunofluorescent staining of beta-tubulin sub-units.

c) To assess the effects of brief *in vitro* mercury exposure on YAC-1 lymphoma cell actin microfilaments, following flow cytometric assessment of mean fluorescence following staining of actin with fluorochrome-conjugated phalloidin. Exposure periods selected for objectives (b) and (c) were 1, 5 and 30 min and 4 hrs.

## 3.6 Specific Aim III: TCR/CD3 expression, protein tyrosine phosphorylation and intracellular calcium levels

### 3.6.1 Broad objective

The broad objective of Specific Aim III was to assess the effects of *in vitro* mercury exposures on selected components of receptor-mediated cell signalling cascades in YAC-1 lymphoma cells, for comparison with the results of Specific Aims I and II.

### 3.6.2 Null Hypothesis

Mercury treatment will have no effect on cell-surface CD3 receptor expression, protein tyrosine phosphorylation levels or intracellular calcium levels in YAC-1 cells.

### 3.6.3 Specific Objectives

a) To develop flow cytometric methods for quantitative assessment of the effects of brief *in vitro* mercury exposures on cell surface CD3 receptor expression and intracellular protein tyrosine phosphorylation.

b) To assess the effects of brief *in vitro* mercury exposure on YAC-lymphoma cell surface CD3 receptor expression, by flow cytometric assessment of mean CD3 fluorescence following indirect immunofluorescent staining of CD3 receptors.

c) To assess the effects of brief *in vitro* mercury exposure on YAC-1 lymphoma cell protein tyrosine phosphorylation, following flow cytometric assessment of mean intracellular phosphotyrosine fluorescence following indirect immunofluorescent staining of phosphotyrosine residues. Exposure periods selected for objectives (b) and (c) were 1 min, 5 min, 30 min and 4 hrs.

d) To develop high throughput assays to assess the effects of brief *in vitro* mercury exposures on intracellular $Ca^{2+}$ $[Ca^{2+}]_i$ levels.

e) To assess the effects of brief *in vitro* mercury exposure on $[Ca^{2+}]_i$ in YAC-1 lymphoma cells. Exposure periods selected for this assay were 1 min, 5 min, 15 min, 30 min and 4 hr.

## 3.7 Specific Aim IV: Morphology and polarization responses

### 3.7.1 Broad Objective

The broad objective of Specific Aim IV was to assess the effects of mercury on the model of the immunologic synapse and to compare the effects with those seen in the viability assays in Specific Aims I - III.

### 3.7.2 Null Hypotheses

Mercury treatment will not affect the percentage of YAC-1 cells forming conjugates with anti-CD3 antibody-coated beads, morphologic responses or cytoskeletal re-orientation of the following YAC-1 cell binding to the beads. Mercury treatment will not alter the appearance of the microtubules, microtubule organizing centre or Golgi apparatus.

### 3.7.3 Specific Objectives

a) To establish a method for visualising the effects of mercury on polarised signalling events using fluorescent microscopic techniques.

b) To evaluate the effects of brief (5 and 30 min) *in vitro* exposures to mercury on the percentage of YAC-1 cells forming conjugates with anti-CD3 antibody-coated 6.0 latex microspheres.

c) To assess the effects of 5 and 30 min *in vitro* exposures to mercury on the percentage of YAC-1 cells altering their morphology to wrap around at least 50% of the circumference of the anti-CD3 bead following bead binding.

d) To assess the effects of 5 and 30 min *in vitro* exposures to mercury on the percentage of YAC-1 cells reorienting the MTOC and Golgi complex to a position directly adjacent to the area of bead contact bead following anti-CD3 bead binding.

e) To evaluate the effects of brief *in vitro* exposure to mercury on the appearance of YAC-1 cell microtubules and MTOC

# 4.0

# CELL DEATH AND CYTOTOXIC EFFECTS IN YAC-1 LYMPHOMA CELLS FOLLOWING EXPOSURE TO VARIOUS FORMS OF MERCURY.

## 4.1 Relationship to overall project

The results and discussion included in Chapter 4 encompass Specific Aim I Objectives c and d, and Specific Aims II and III.

It was originally planned that real-time measurement of changes in $[Ca^{2+}]_i$ levels over 60 minutes post-mercury exposure would be performed using fluorometric assessment of Fluo-3 calcium indicator dye-loaded cells; however, like other cells of the lymphocytic lineage (Sommer et al., 1994), the YAC-1 cells actively extrude the dye into the medium, producing spurious fluorescence signals when bound to free $Ca^{2+}$ in the medium. Instead, an alternate methodology was developed, using flow cytometric evaluation of $[Ca^{2+}]_i$ in mercury-exposed dye-loaded cells chilled and washed free of the mercury at specific time-points (see Materials and Methods, below).

In addition, mercury effects on intermediate filament vimentin and the cytoskeletal linker protein talin were to be assessed; both proved to be nearly undetectable with available antibodies, and assessment of mercury effects on these cytoskeletal components were subsequently deleted from the study objectives.

## 4.2 ABSTRACT

The effects of 1 min – 4 hr exposures to four mercury compounds (mercuric chloride [$HgCl_2$], methyl mercuric chloride [$CH_3HgCl$], *p*-chloromercuribenzoate [*p*-CMB] and thimerosal [TMS; ethylmercurithiosalicylate) on cell death, microtubules, actin, CD3 receptor expression, protein tyrosine phosphorylation (PTyr-P), and intracellular calcium ($[Ca^{2+}]_i$) levels were investigated in YAC-1 lympoma cells using flow cytometry. After 4 hr, YOPRO-1 (YP) and propidium iodide (PI) dye uptake indicated all forms of mercury tested were toxic at concentrations ranging from 25.8 – 48.4 uM, with two distinct patterns of effects. Early apoptosis was prolonged for $CH_3HgCl$- and TMS-treated cells, with more than 50% remaining $YP^+/PI^-$ after 4 hr. Both $CH_3HgCl$ and TMS induced complete loss of β-tubulin fluorescence, indicative of microtubule depolymerization and inhibition of tubulin synthesis and/or β-tubulin degradation, while F-actin fluorescence diminished to a lesser degree and only after loss β-tubulin. In addition, $CH_3HgCl$ and TMS induced an almost immediate two-fold increase in CD3 fluorescence, with levels returning to baseline within minutes. With continued exposure, CD3 fluorescence was reduced to approximately 50% of baseline values. Both compounds also increased PTyr-P two- to three-fold immediately, with levels returning to baseline at 4 hr. Similarly, two- to three-fold increases in $[Ca^{2+}]_i$ were noted after 1 min exposure; $[Ca^{2+}]_i$ increased progressively, reaching levels five- to eight-fold greater than control values. In contrast, dye uptake was delayed with $HgCl_2$ and *p*-CMB, although cell death proceeded rapidly, with almost all non-viable cells being late apoptotic ($YP^+/PI^+$) by 4 hr. Exposure to *p*-CMB produced early reductions in F-actin, and after 4 hr, complete loss of F-actin with only partial reduction of total β-tubulin was

seen with both *p*-CMB and $HgCl_2$. CD3 expression and PTyr-P were reduced slightly within minutes after exposure to $HgCl_2$, while *p*-CMB produced similar effects on CD3 only at 4 hr, at which time PTyr-P was increased two- to three-fold. Both compounds increased $[Ca^{2+}]_i$ within minutes, though levels remained under twice the baseline concentration after 15 min exposure. With continued exposure, $[Ca^{2+}]_i$ increased to levels two- to five-fold greater than corresponding control values. These findings indicate the two groups of mercury compounds may induce cell death by distinct pathways, reflecting interactions with different cellular targets leading to cell death.

## 4.3 INTRODUCTION

Many of the proposed targets for mercury (Hg) toxicity are also components of the localized supramolecular activation complex (SMAC) or 'immunological synapse' formed between antigen-presenting cells (APCs) and responding lymphocytes (Monks et al., 1998). While antigenic stimuli are restricted to the localized SMAC, mercury may interact non-specifically with thiol (-SH) groups throughout the cell. Non-localized mercury impacts may mimic antigen-mediated signalling at certain concentrations, but the effects are likely not optimal under most circumstances. In the absence of appropriate spatio-temporal signal organization normally provided by APCs, the lymphocyte response may be to activate cell death pathways. Alternately, mercury may transiently activate a small percentage of cells in a non-antigen-specific fashion. Aberrant global signalling, and variations thereof produced by different forms of mercury, may provide a basis for both the immunosuppressive and stimulatory effects of mercury.

Mercury can induce thymic atrophy (Kosuda et al., 1996); suppress humoral (Blakley et al., 1980; Shenker et al., 1993a) and cellular immunity (Nakatsuru et al.,

1985), and natural killer activity (Cai et al., 1988); increase tumour frequency (Blakley, 1984); and reduce host immunity to and severity of malaria infection in mice (Silbergeld et al., 2000). Mercury may also stimulate lymphocyte proliferation (Jiang and Moller, 1995), and can induce transient Type-2 (T-helper-2-like) autoimmune disease in genetically susceptible rats (Druet et al., 1978; Sapin et al., 1977) and mice (Hultman and Enestrom, 1992; Warfvinge et al., 1995).

As a result, multiple targets for mercury toxicity have been proposed including: membrane receptors (Nakashima et al., 1994); protein kinase C (Badou et al., 1997), tyrosine phosphorylation (Rosenspire et al., 1998); microtubules (Brown et al., 1988); and intracellular calcium (Badou et al., 1997; Tan et al., 1993)). Some of the difficulty in identifying specific mechanisms for mercury toxicity may be a function of physico-chemical differences between organic and inorganic mercury. Some targets (e.g. membrane receptors) are considered specific for divalent $Hg^{2+}$; others may be targets of all forms of mercury, although the chemical form may determine whether primary or secondary.

Patching and capping of CD3, CD4, Thy-1 and CD45 receptors have been observed in lymphocytes exposed to $HgCl_2$, with cell death ensuing rapidly thereafter. Receptor aggregation was associated with activation of $p56^{lck}$ and co-localisation of phosphotyrosine (PTyr)-containing proteins (Nakashima et al., 1994), both of which require an intact cell membrane (Nakashima et al., 1994; Rahman et al., 1993). Increased PTyr-P also occurs in cells exposed to $CH_3HgCl$ (Colombo et al., 2004) or TMS (Kim et al., 2002).

Microtubule integrity is also altered following exposure to $HgCl_2$, $CH_3HgCl$ or TMS. Depolymerization of microtubules by $CH_3HgCl$ specifically inhibits tubulin synthesis (Miura et al., 1998), and both $CH_3HgCl$ and TMS inhibit cell cycle progression (Alexandre et al., 2003; Wasteneys et al., 1988) with subsequent apoptosis (Castoldi et al., 2000; Miura et al., 1999). However, $Hg^{2+}$ is a more potent inhibitor of *in vitro* tubulin polymerization than $CH_3HgCl$ (Miura et al., 1984), although growth inhibition is generally seen without significant loss of microtubules (Imura et al., 1980).

In rat splenic lymphocytes, $CH_3HgCl$ produces a rapid and sustained concentration-dependent increase in intracellular calcium ($[Ca^{2+}]_i$), while $HgCl_2$ causes a slow rise (Tan et al., 1993). Increased $[Ca^{2+}]_i$ in $CH_3HgCl$-treated neuronal synaptosomal membrane preparations has been attributed to increased membrane permeability secondary to loss of ATP production (Kauppinen et al., 1989). Similarly increased cation permeability occurs in thymic lymphocytes exposed to TMS (Gukovskaya et al., 1992) in conjunction with release of intracellular stores (Pelassy et al., 1994). In contrast, $HgCl_2$ induces protein kinase C (PKC)-dependent $Ca^{2+}$ influx through membrane $Ca^{2+}$ channels in murine T lymphocyte hybridomas (Badou et al., 1997).

We studied the effects of short-term (1 min– 4 hr) exposures to $HgCl_2$, $CH_3HgCl$, *p*-chloromercuribenzoate (*p*-CMB), and TMS (ethylmercurithiosalicylate; see Table 2.1) on lymphocyte cell death, microtubules, actin, CD3 receptor expression, PTyr-P, and $[Ca^{2+}]_i$ levels. In physiologic solutions, inorganic $Hg^{2+}$ is present as a polychloride anion with poor lipid solubility (Foulkes, 2000). Inorganic $Hg^{2+}$ may therefore produce effects at the membrane before significant intracellular accumulation occurs. Likewise, *p*-CMB was selected as an organomercurial compound thought to penetrate membranes more

slowly than $CH_3HgCl$ (as a result of ionization), and whose immune effects are also unknown. The medical preservative TMS was included because of controversy regarding possible links between childhood vaccination and autism (Verstraeten et al., 2003; Vojdani et al., 2003; Westphal and Hallier, 2003). Unionised TMS penetrates membranes quickly, but the thiosalicylate group may dissociate following protein binding to leave the toxic ethyl mercury moiety attached to proteins (Pintado et al., 1995).

We hypothesized that the immunotoxic effects of inorganic mercury ($Hg^{2+}$ and perhaps other compounds, like *p*-chloromercuribenzoate (*p*-CMB), that are charged at physiologic pH and are presumed to penetrate membranes poorly) are produced, at least initially, through global triggering of various membrane receptors with increased protein tyrosine phosphorylation PTyr-P) and down-regulation of the T-cell receptor (TCR), as occurs with physiologic ligation (Valitutti et al., 1997). Receptor–based effects were anticipated to occur before effects on microtubule integrity and before the activation of cell death pathways. In contrast, the organomercurial compounds $CH_3HgCl$ and TMS, with greater lipid solubility and more rapid entry into the cell, were not expected to interact with receptors or produce down-regulation. Some of the subsequent intracellular targets of $CH_3HgCl$ or TMS could be the same or similar to those activated down-stream by $Hg^{2+}$-receptor activation, but the time course of effects was expected to be different. Both $CH_3HgCl$ and TMS were therefore expected to produce significant effects only in conjunction with – and not prior to – loss of microtubule integrity and the onset of cell death.

## 4.4 MATERIALS AND METHODS

Unless otherwise noted, all laboratory disposables and chemicals/reagents were obtained from VWR (Mississauga, ON) and Sigma-Aldrich (Oakville, ON), respectively.

### 4.4.1 Preparation of mercury solutions

Stock solutions (10 mM) of each mercury compound were prepared in deionized distilled $H_2O$. The TMS was completely soluble in water. The $HgCl_2$ (ICN Pharmaceuticals, Costa Mesa, CA) was dissolved in 500 uL 1 N HCl (al-Sabti, 1994); $CH_3HgCl$ (Alfa Inorganics, Ventron, Beverly, MA, USA) in 1 mL of acetone (al-Sabti, 1994); and *p*-CMB (ICN) in 2.0 mL of 1N NaOH. Working dilutions of mercury solutions were prepared in complete RPMI at two times (0.02 – 200 uM) the final concentration (0.01 – 100 uM).

### 4.4.2 Cultured cell line

The YAC-1 murine Moloney virus-transformed lymphoma cell line (American Type Culture Collection, Rockville, MD) was grown in continuous culture in complete medium [RPMI with L-glutamine supplemented with 10% fetal bovine serum (FBS; Canadian Life Technologies, Burlington, ON) and 10 mM HEPES buffer]. For all experiments, a suspension of $4 \times 10^6$ live cells/mL was prepared and held in a humidified incubator at 37 C with 5% $CO_2$ for 60-90 min before use.

### 4.4.3 Preparation of 96-well plates and addition of cells

Ten uL of mercury solutions or media were added to the appropriate well of a 96-well U-bottom tissue culture plate. The plate was placed in a humidified incubator at 37 C with 5% $CO_2$ for a minimum of 30 minutes. After pre-incubation, 10 uL of the $4 \times 10^6$

cells/mL cell suspension were added to the mercury-loaded plates. The plates were returned to the incubator for 1 min, 5 min, (15 min for calcium assay), 30 min or 4 hr.

### 4.4.4 Dye exclusion assay for apoptosis or necrosis

The manner of cell death was assessed using a YOPRO-1 (YP; Molecular Probes) and propidium iodide (PI) dye exclusion assay (Idziorek et al., 1995), with modifications as noted below. The day prior to the assay, 100 uL of the working YAC-1 cell suspension was set aside and held overnight in an incubator in a sealed tube. These predominantly non-viable cells were used as positive control cells for the staining procedure and to set flow cytometer signal compensations (unstained and YOPRO-, PI-, and dual-stained wells), while unstained viable cells provided negative control cells.

After incubation, the plates were immediately placed on finely crushed ice and 180 uL of ice-cold RPMI/0.5% FBS were added to each well. The plates were centrifuged for two min at 1200 RPM to recover the cell pellets. The cells were washed three more times with ice cold medium to remove the mercury before flow cytometric acquisition. The plates were returned to the ice for all pipetting procedures. Five uL of non-viable cells were added to each of four wells set aside for stain control wells. Seventy uL of a 0.2 uM YOPRO in ice-cold plain RPMI or media were added as appropriate, followed by 10 uL of 10 ug/mL PI. The plates were held on ice for 30 min before flow cytometric acquisition, which was completed within two hrs thereafter.

### 4.4.5 Fixation of cells for immunofluorescent and phalloidin staining

At the end of the desired incubation period, the cells were immediately fixed by adding 80 uL of 4% paraformaldehyde in phosphate buffered saline (PBS) for 30 min. After fixation, the plates were centrifuged at 1200 RPM for 2 min to recover the cell

pellets and the plates washed three times with 180 uL PBS. After staining, the plates were centrifuged at 1200 RPM for 5 min to recover the cell pellets and the wells washed once with PBS before flow cytometric data acquisition.

### 4.4.6 Indirect immunofluorescent staining of tubulin fluorescence

One hundred uL of a 1:250 dilution of mouse anti-β-tubulin antibody (anti-Tub) in PBS/1% bovine serum albumin (PBS/BSA) with 0.1% saponin (SAP) were added to each well for 30 min at room temperature (RT). Stain control wells included unstained wells and wells stained with of mouse-anti-hamster IgG antibody (MAH; Cedarlane, Hornby, ON). The plates were centrifuged at 1200 RPM for 5 min to recover the cell pellets and the wells washed once with 180 uL PBS. The anti-Tub antibody was detected by adding 100 uL of a 1:250 dilution of Alexa®-488 goat-anti-mouse IgG antibody (GAM-488; Molecular Probes/Invitrogen, Burlington, ON) in PBS/BSA/SAP for 30 min at RT.

### 4.4.7 Actin staining with phalloidin

One hundred uL of a 1:800 dilution of Oregon-Green®-phalloidin (OG-phall; Molecular Probes) in PBS/BSA/SAP were added to each well for 30 min at RT.

### 4.4.8 Indirect immunofluorescent staining of cell surface CD3 receptors

CD3 receptors were detected using a three-layer indirect immunofluorescence technique. One hundred uL of a 1:250 dilution of hamster-anti-mouse anti-CD3 (anti-CD3; Cedarlane) in PBS/BSA were added to each well for 30 min. Stain control groups included wells stained with anti-trinitrophenol (anti-TNP; Cedarlane) isotype control antibody or media alone, followed by secondary and tertiary antibodies. The plates were centrifuged at 1200 RPM for 5 min to recover the cell pellets and the wells were washed

once more with plain PBS. The anti-CD3 antibody was detected by adding 100 uL of a 1:300 dilution of MAH in PBS/BSA for 30 min, washing the plate twice before adding 100 uL of a 1:250 dilution of GAM-488 in PBS/BSA for 30 min.

### 4.4.9 Indirect immunufluorescent staining of intracellular phosphotyrosine residues

Intracellular phosphotyrosine (PTyr) residues were detected using an indirect immunofluorescence technique (Far et al., 1994). One hundred uL of a 1:250 dilution of mouse anti-phosphotyrosine (anti-PTyr) in PBS/BSA with 0.1% saponin (PBS/BSA/SAP) were added to each well for 30 min. Stain control groups included wells stained with MAH. The plates were centrifuged at 1200 RPM for 5 min to recover the cell pellets and the wells washed once more with PBS. The anti-PTyr antibody was detected by adding 100 uL of a 1:250 dilution GAM-488 in PBS/BSA/SAP for 30 min.

### 4.4.10 Detection of intracellular calcium with Fluo-3

Intracellular calcium $[Ca^{2+}]_i$ levels in the mercury-treated YAC-1 cells were evaluated using the cell-permeant $Ca^{2+}$ indicator dye Fluo-3-AM (Molecular Probes) in a flow cytometric assay (Maltsev et al., 1994; Verburg-Van Kemenade et al., 1998) modifiied for use with multiple samples as indicated below. While divalent cations may interact with calcium indicator dyes and interfere with $Ca^{2+}$-related fluorescence signals, this effect is minimal for Fluo-3 at free $Hg^{2+}$ concentrations up to 5 uM (Marchi et al., 2000). Intracellular free $Hg^{2+}$ concentrations are likely very low, as the high affinity of metal ions for proteins and other biological molecules prevents charged metal ions from diffusing across membranes or through ion channels passively without reacting with their components or with proteins in the extracellular fluid (Foulkes, 2000). The Fluo-3 was

prepared as 2 uL aliquots of a 1 mM fluo solution in DMSO and frozen for future use in individual experiments. At the time of the assay, 18 uL of complete RPMI were added to a 2 uL aliquot of Fluo-3 and mixed well to make a working Fluo-3 solution. For a vehicle control treatment, 2 uL of DMSO were added to 18 uL of complete RPMI.

For Fluo-3 dye loading, the 4 x $10^6$ cells/mL suspension was removed from the incubator after 55 min and 1.0 mL aliquots of the cells were dispensed into Eppendorf tubes. Three uL of the working solution of the Fluo-3 dye, DMSO vehicle or complete RPMI were added to the cells. Each tube was vortexed briefly and the cells returned to the incubator for 30 min. After incubation, the cells were centrifuged at 6000 RPM for 45 sec to recover the cell pellets. The cells were washed twice more and then resuspended in 1.0 mL of pre-warmed ($37^oC$) complete RPMI. Ten uL of dye-loaded or DMSO-treated cells were immediately added to the prepared mercury-loaded plates. The plates were returned to a humidified incubator at $37^0C$ with 5% $CO_2$ for 1 min, 5 min, 15 min, 30 min. An additional stain control included an aliquot of Fluo-3-loaded cells placed on ice immediately after the dye loading procedure. Like other lymphocytic cells (Sommer et al., 1994), the YAC-1 lymphoma cell line appeared to transport organic acids like the Fluo-3 dye out of the cells. Fluo-3-MFI in dye-loaded cells held on ice was not significantly different from untreated cells at 1, 5 and 15 min. After 30 -90 min, Fluo-3-MFI was greater in the cells held on ice than in untreated cells, but was still less than that obtained in any of the mercury treatment groups (data not shown). By 4 hr, dye loading in cold cells was greater than in control or treated cells and this time point was dropped.

After incubation, the plates were immediately placed on finely crushed ice, 180 uL of ice-cold RPMI/0.5% FBS added to each well and the plates centrifuged for 2 min at

1200 RPM to recover the cell pellets. The cells were washed three times with ice cold media and the cell pellets were re-suspended by vortexing for 1-2 sec. The plates were returned to the ice, seating the plate firmly to contact the ice and 80uL of ice cold plain RPMI were added to each well. Data was acquired by flow cytometry within 90 min.

### 4.4.11 Flow cytometric acquisition

The Epics ELITE® flow cytometer (Beckman Coulter, Mississauga, ON) was configured with forward and side scatter parameters in linear and PMT2 and PMT3 fluorescence channels in logarithmic modes. Each acquisition contained 1000 events. The PMT2 (YP/green channel) and PMT3 (PI/red channel) sensitivities were adjusted using single-stained dead cells to obtain peak fluorescence at the second decade ($10^2$). Compensation was set with dual-stained dead cells to obtain a uniform population in the upper right ($YP^+/PI^+$; see Fig. 4.1-B), untreated dual-stained live cells in the lower left ($YP^-/PI^-$; see Fig 4.1-A), and early apoptotic cells in the lower part of the upper left quadrant ($YP^+/PI^-$; see Fig. 4.1-B) of the PMT2/PMT3 dot plot. The dot plots were analyzed with Expo32® software (Beckman Coulter) and the results expressed as the percentage of cells in each quadrant. For tubulin, actin, CD3, PTyr, and calcium assays, mean fluorescence in the PMT2 channel was expressed as the percent control response.

### 4.4.12 Statistical Analysis

All statistical analyses were performed using Prism® software (GraphPad Software Incorporated, San Diego, CA). The significance of mercury and control treatment effects were analysed using the Kruskal-Wallis one-way ANOVA. No post tests were performed if the overall p value for the ANOVA was > 0.05. For all analyses,

treatment values differing from control values with $p < 0.05$ were considered significantly different.

## 4.5 RESULTS

### 4.5.1 YP/PI Dye Exclusion

***Mercuric Chloride ($HgCl_2$):*** After 1 or 5 min exposure to $HgCl_2$, there were no effects on YAC-1 cell viability (see A, Figs. 4.2, 4.3-I and 4.3-II). Effects on viability were clearly evident after 30 min at 70 – 100 uM ($p < 0.001$, see Fig 4.2-A). At 100 uM, approximately 70% of YAC-1 cells were non-viable, among which approximately 2/3 were early apoptotic ($YP^+/PI^-$) and 1/3 were late apoptotic/necrotic ($YP^+/PI^+$; see figure 4.3-III-A). At 4 hr, $HgCl_2$ continued to reduce viability at 50 – 100 uM ($p < 0.001$, see Fig. 4.2-A). At 60 – 100 uM $HgCl_2$, approximately 95% of cells were non-viable (see Fig 4.2-A), of which approximately 85% were late apoptotic/necrotic, and 15% early apoptotic (see Fig. 4.3-IV-A).

***Para-Chloromercuribenzoate (p-CMB):*** *P*-CMB treatment did not affect viability after 1 or 5 min exposures (see B, Figs. 4.2, 4.3-I and 4.3-II). After 30 min, while overall YAC-1 cell viability for the *p*-CMB treatment group remained greater than 85% even at 100 uM (see Fig. 4.2-B), loss of viability was significant at 90 – 100 uM ($p < 0.001$). The percentages of apoptotic and necrotic cells were generally equal among non-viable *p*-CMB-treated cells at this time (see Fig. 4.3-III-B). After 4 hr, loss of viability for *p*-CMB-treated cells was significant at 30 – 100 uM (see Fig 4.2-B, $p < 0.001$). Despite the lack of effect in the first 30 min, by 4 hr approximately 95% of the YAC-1 cells were non-viable at *p*-CMB concentrations of 60 – 100 uM, of which

approximately 85% were late apoptotic/necrotic and 15% early apoptotic (see Fig. 4.3-IV-B), similar to effects seen with $HgCl_2$.

***Methyl Mercuric Chloride ($CH_3HgCl$):*** Reductions in viability were already evident at 1 min for $CH_3HgCl$ at 60 – 100 uM ($p < 0.05$, see Fig. 4.2-C). The loss of viability was consistent with early apoptosis with no necrosis, even where over 80 % of the YAC-1 cells were $YP^+$ (see Figure 4.3-I-C). After 5 min, $CH_3HgCl$ toxicity had increased, with reductions in viability at 40–100 uM ($p < 0.05$, see Fig. 4.2-C), and 70 – 80% of cells were early apoptotic at 60–100 uM $CH_3HgCl$, while only 5 – 10 % were late apoptotic/necrotic (see Figure 4.3-II-C). As at 1 and 5 min, after 30 min 70 – 80% of cells remained $YP^+/PI^-$ at 60 – 100 uM $CH_3HgCl$, and 10% were late apoptotic/necrotic (Fig. 4.3-III-C). After 30 min or 4 hr, YAC-1 viability was reduced at 30 – 100 uM ($p < 0.001$ for each, see Fig. 4.2-C). At 4 hr, approximately 40% of the almost 90% non-viable cells were late apoptotic/necrotic (see Fig. 4.3-IV-C), and 60% remained early apoptotic at ≤ 80 uM. At higher concentrations, the percentages of early apoptotic and late apoptotic/necrotic cells were approximately equal.

***Thimerosal (TMS):*** There was no effect of TMS treatment on viability after 1 or 5 min (see Fig. 4.2-D). TMS cytotoxicity increased at 30 min, with effects seen at 40 – 100 uM ($p < 0.001$, see Fig. 4.2-D) and viability reduced approximately 70% at 100 uM. Approximately 2/3 of non-viable TMS-treated cells were early apoptotic and 1/3 late apoptotic/necrotic, similar to the $CH_3HgCl$ treatment group (see Fig. 4.3-III-D). By 4 hrs, YAC-1 cell viability was reduced at 20 – 100 uM ($p < 0.001$), with 90% loss of viability at concentrations 50 – 100 uM (see Fig. 2-D). As seen with $CH_3HgCl$, despite early loss of viability, a slightly greater percentage of non-viable cells remained early

apoptotic at ≤ 60 uM TMS, while at higher concentrations more were late apoptotic/necrotic (see Fig. 4.3-IV-D).

### 4.5.2 β-Tubulin

Indirect immunofluorescence detection of β-tubulin did not distinguish between monomeric subunits, dimers or polymerised protein. The mean fluorescence intensity (β-Tub-MFI) was therefore a measure of total β-tubulin levels in each cell.

***Mercuric Chloride ($HgCl_2$)*:** After 1 or 5 min exposure to all concentrations of $HgCl_2$, β-Tub-MFI in the YAC-1 cells was not significantly different from untreated control cells. After 30 min, reductions in β-tubulin staining were noted at 70 – 100 uM ($p < 0.05$), with β-Tub-MFI reduced to 81 – 49% of control values. After 4 hrs, β-Tub-MFI was further reduced to 47 – 22% of control values at 60 – 100 uM (see Fig. 4.4-A).

***Para-Chloromercuribenzoate (p-CMB)*:** After 1 min exposure to all tested concentrations of *p*-CMB, β-Tub-MFI in the YAC-1 cells was not significantly different from untreated control cells. After 5 min, β-tubulin staining was reduced to 67 – 64% of control values at 70 – 100 uM ($p < 0.001$). Although the concentration/response curves for $HgCl_2$ and *p*-CMB were very similar at 30 min, the overall *p*-value for the *p*-CMB regression was only 0.07. But as with $HgCl_2$, β-Tub-MFI in *p*-CMB-treated cells did not drop below 50% of control values at this time. After 4 hr, β-Tub-MFI was reduced to 47 – 23% of control fluorescence at 50 – 100 uM ($p < 0.001$; see Fig. 4.4-B).

***Methyl Mercuric Chloride ($CH_3HgCl$)*:** Progressive effects on β-Tub-MFI were evident after $CH_3HgCl$ exposure at 20 – 100 uM for each of the 1 min, 5 min, 30 min or 4 hr time periods ($p < 0.001$, 0.01, 0.001 and 0.05 respectively). Reductions in β-tubulin staining to between 80 – 46% of control values were seen after just one min, with similar

reductions to 80 – 40% noted at 5 min. After 30 min exposure, β-tubulin fluorescence was reduced to 25 – 10% of control levels at the highest concentrations tested and was virtually undetectable after 4 hrs (see Fig. 4.4-C).

***Thimerosal (TMS)*:** Effects on β-Tub-MFI were evident at 10 – 100 uM TMS at all time periods ($p < 0.001$ for each). After just one min, β-tubulin fluorescence was reduced to 71 – 47% of control values, and to 71 – 43% at 5 min. After 30 min exposure, β-tubulin staining was reduced to 29 - 9% of control levels at the highest concentrations tested, and was virtually undetectable after 4 hr (see Fig. 4.4-D), similar to effects seen with $CH_3HgCl$.

### 4.5.3 F-Actin

Phalloidin binds primarily to polymerised filamentous actin (F-actin), but does not distinguish between large and small filaments (Cooper, 1987; Howard and Meyer, 1984). The MFI (Phall-MFI) was therefore as measure of F-actin levels in the cell.

***Mercuric Chloride ($HgCl_2$)*:** There was a trend toward reduced Phall-MFI in the YAC-1 cells after 1 min exposure to all tested concentrations of $HgCl_2$ ($p = 0.09$), but no such trend was evident after 5 min. After 30 min or 4 hr, reductions were noted at 60 – 100 uM ($p < 0.001$ and 0.05, respectively). After 30 min, phalloidin fluorescence was reduced to between 76 – 41% of control values at these concentrations. By 4 hr Phall-MFI was almost undetectable, being reduced to 7% of control values at the highest concentrations tested (see Fig. 4.5-A).

***Para-Chloromercuribenzoate (p-CMB)*:** After a 1 min *p*-CMB exposure, Phall-MFI was reduced to between 65 – 41% of control values at 50 – 100 uM ($p < 0.05$). Similar effects were seen after 5 min, with fluorescence reduced to 81 – 32% at 40 uM

and 60–100 uM ($p < 0.01$). After 30 min, Phall-MFI was further reduced to 60 – 26% of control values at 30 – 100 uM ($p < 0.05$). However, by 4 hr, effects were significant only at 50–100 uM ($p < 0.001$), with Phall-MFI reduced to 5% of control values, similar to effects seen with $HgCl_2$ (see Fig. 4.5-B).

***Methyl Mercuric Chloride ($CH_3HgCl$)*:** There were no effects on Phall-MFI after 1 min exposure to $CH_3HgCl$. Phall-MFI was reduced to 74 – 68% of control values at 80–100 uM after 5 min ($p < 0.05$), with similar levels (73 – 61% of control values) seen at 30–100 uM after 30 min ($p < 0.001$). After 4 hr, Phall-MFI was 58 – 41% at 30 – 100 uM ($p < 0.001$; see Fig. 4.5-C).

***Thimerosal (TMS)*:** Phall-MFI was unchanged after 1 min exposure to TMS. After 5 min, phalloidin fluorescence was reduced to 81 – 60% of control values at 60 – 100 uM ($p < 0.01$). After 30 min, Phall-MFI was further reduced to 57 –3 5% at 30 – 100 uM ($p < 0.001$). By 4 hr, reductions to 49 – 23% of control levels were seen at 20 – 100 uM ($p < 0.05$; see Fig. 4.5-D).

### 4.5.4 Cell surface CD3 receptor expression

***Mercuric Chloride ($HgCl_2$)*:** There was a trend toward reduced MFI in CD3-stained YAC-1 cells (CD3-MFI) after 1 min exposure to $HgCl_2$ ($p = 0.11$). After 5 min, CD3 fluorescence in YAC-1 cells was reduced to 83 – 69% of control values at 40 – 100 uM ($p < 0.001$). However, after 30 min, there were again no significant effects. At 4 hr, reductions similar to those seen at 5 min were noted at 50 – 100 uM, (79 – 65%; $p < 0.01$; see Fig 4.6-A).

***Para-Chloromercuribenzoate (p-CMB)*:** After 1, 5 or 30 min exposure to *p*-CMB, CD3-MFI was not significantly different from untreated control cells. After 4 hr,

CD3-MFI was reduced to 80 – 65% of control values at 30 –1 00 uM ($p < 0.01$), over which range of concentrations CD3-MFI appeared to plateau (see Fig. 4.6-B).

***Methyl Mercuric Chloride ($CH_3HgCl$)*:** After 1 min, CD3 fluorescence in $CH_3HgCl$-treated cells was increased to approximately 132 – 191% of control values at 30 ($p < 0.05$) and 50–100 uM ($p < 0.001$). However there were no effects on CD3-MFI after 5 or 30 min exposure to $CH_3HgCl$. After 4 hr exposure, CD3 staining was reduced to 75 – 48% of control values at 30–100 uM ($p < 0.01$; see Fig. 4.6-C).

***Thimerosal (TMS)*:** Cell surface CD3 fluorescence was increased to approximately 127 – 214% of control values after 1 min exposure to TMS at 50 – 100 uM ($p < 0.05$ and 0.001, respectively). After 5 min, CD3-MFI remained elevated at 40 ($p < 0.001$) and 60 – 100 uM ($p < 0.001$), though to a lesser extent than seen at 1 min (128 – 164%). However, after 30 min, no effects were apparent. After 4 hrs, CD3 fluorescence was reduced to 53 – 38% at 20 – 100 uM ($p < 0.001$), and as for *p*-CMB, appeared to have reached a plateau (see Fig. 4.6-D).

### 4.5.5 Intracellular Phosphotyrosine (PTyr) Residues

***Mercuric Chloride ($HgCl_2$)*:** The MFI in PTyr-stained YAC-1 cells (PTyr-MFI) was reduced to approximately 77 – 66% of control values at 70 – 100 uM after 1 min exposure to $HgCl_2$ ($p < 0.05$) and to a slightly lesser extent (to 89 – 83%) after 5 min ($p < 0.001$). However, no effects were evident after 30 min or 4 hr exposures (see Fig. 4.7-A).

***Para-Chloromercuribenzoate (p-CMB)*:** After 1, 5 or 30 min exposure to *p*-CMB, there were no effects on PTyr-MFI. After 4 hr, PTyr fluorescence increased to approximately 149 – 279% of control values at 50 – 100 uM ($p < 0.05$; see Fig. 4.7-B).

***Methyl Mercuric Chloride ($CH_3HgCl$)*:** Intracellular PTyr fluorescence was increased to approximately 127–227% of control values after 1 min exposure to 50 – 100 uM $CH_3HgCl$ ($p < 0.05$). After 5 min, PTyr-MFI was increased to 118 – 318% at 40 – 100 uM ($p < 0.05$). Increasing the exposure period to 30 min produced marked effects, increasing PTyr-MFI to 117 – 460% at 50 – 100 uM $CH_3HgCl$ ($p < 0.05$). However, by 4 hr, although there was a trend toward elevated PTyr MFI ($p = 0.09$), PTyr fluorescence had fallen (see Fig. 4.7-C).

***Thimerosal (TMS)*:** After 1 min exposure to TMS, PTyr-MFI was increased to 152 – 264% of control values at 50–100 uM ($p < 0.001$). Similar increases (to 136 – 314%) were seen at ≥ 20 uM after 5 min ($p < 0.001$). PTyr-MFI had fallen after 30 min, but was still increased approximately to 123 – 165% as compared to untreated cells at 10 uM ($p < 0.05$) and 30 – 100 uM ($p < 0.05$). After 4 hr, there were no effects of TMS on PTyr- MFI (see Fig. 4.7-D).

### 4.5.6 Intracellular Calcium ($[Ca^{2+}]_i$)

***Mercuric Chloride ($HgCl_2$)*:** Mean $[Ca^{2+}]_i$ as assessed by Fluo-3-MFI, was increased approximately to approximately 114 – 175% of control values in YAC-1 cells exposed to 40 – 100 uM $HgCl_2$ for 1 min ($p < 0.05$). After 5 min exposure, Fluo-3-MFI increased to 142–221%, and after 15 min to 119 – 173%, over the same range of concentrations ($p < 0.001$ and 0.01 respectively). After 30 min, more marked effects were evident at 50 – 100 uM, with Fluo-3-MFI increased to 176 – 463% as compared to untreated cells ($p < 0.05$; see Fig. 4.8-A).

***Para-Chloromercuribenzoate (p-CMB)*:** Fluo-3-MFI was slightly elevated, reaching approximately 110 – 136% of control treatment values after 1 min exposure to

60 – 80 and 100 uM *p*-CMB ($p < 0.05$). Similar small increases were seen after 5 min at 40–100 uM (107 – 126%; $p < 0.05$) and 15 min at 60 – 100 uM (116 – 123%; $p < 0.01$). After 30 min, Fluo-3-MFI had increased more dramatically to 140 – 304% at 30 – 100 uM *p*-CMB ($p < 0.05$; see Fig. 4.8-B).

***Methyl Mercuric Chloride ($CH_3HgCl$)*:** After 1 min exposure to $CH_3HgCl$, Fluo-3-MFI increased to 208 – 288% of control values at 40 – 100 uM uM ($p < 0.01$), and still further to 160 – 426% at 20 – 100 uM after 5 min exposure ($p < 0.05$). Similar increases (to 158 – 365%) in Fluo-3-MFI were seen after 15 min exposures to 40 – 100 uM $CH_3HgCl$ ($p < 0.05$). Fluo-3 fluorescence increased dramatically after 30 min exposure, with levels approximately 313 – 826% of values seen in untreated cells at 30 – 100 uM $CH_3HgCl$ ($p < 0.01$; see Fig. 4.8-C).

***Thimerosal (TMS)*:** Fluo-3-MFI increased 183 – 316% as compared to control values after 1 min at 20 – 100 uM TMS ($p < 0.001$). After 5 min, slightly greater elevations in Fluo-3 fluorescence were noted at 10 – 100 uM TMS (to 242–356%; $p < 0.001$). After 5 min, increased Fluo-3-MFI (250 – 290%; $p < 0.001$) similar that seen at 1 min was evident at 40 – 100 uM TMS. After 30 min, Fluo-3 fluorescence increased markedly at 20 – 100 uM ($p < 0.001$), with levels increasing 272 – 505% as compared to untreated control cells (see Fig. 4.8-D).

## 4.6 DISCUSSION

After 4 hr incubation, the relative cytotoxicities of the mercury compounds were TMS > $CH_3HgCl$ > *p*-CMB > $HgCl_2$, consistent with other *in vitro* models (Shenker et al., 1992a; Shenker et al., 1992b; Van Horn et al., 1977). The chemical structures of the mercury compounds likely account for the differences in toxicity, as chemically similar

forms of mercury (e.g. methyl-, ethyl- and phenylmercury) produce toxicity at equimolar mercury concentrations (InSug et al., 1997). The relative toxicities of these compounds *in vivo* are $HgCl_2$ > $CH_3HgCl$ > *p*-CMB > TMS (see Table 2.1), reflecting the influence of toxicokinetic parameters not present *in vitro*. In human T lymphocytes, $CH_3HgCl$ is approximately 5-10 times more cytotoxic than $HgCl_2$ (Shenker et al., 1992a; Shenker et al., 1993a), although less than a two-fold difference was observed in the dye exclusion assay reported here.

Two general patterns of effects were observed, one for $HgCl_2$ and *p*-CMB, the other for $CH_3HgCl$ and TMS, indicating the two groups of mercury compounds may induce cell death by distinct pathways, although individual differences are also evident in this and other assays. Cell death proceeds rapidly to late apoptosis/necrosis for $HgCl_2$ and *p*-CMB. Both $HgCl_2$ and *p*-CMB induced moderate reductions in CD3 expression. For $HgCl_2$, these reductions first occurred within minutes, while for *p*-CMB they were not evident until the 4 hr time point. The $HgCl_2$ also induced a small, but almost immediate drop in PTyr-P, with levels returning to normal thereafter, while *p*-CMB had no effects until the 4 hr time point, at which time PTyr-P was increased two- to three-fold. Neither $HgCl_2$ nor *p*-CMB affected β-tubulin levels at early time points, and significant β-tubulin staining remained after 4 hr treatment. The $HgCl_2$ effects on β-tubulin and F-actin were quite similar in magnitude and time-course, while reductions in phalloidin staining were evident almost immediately with *p*-CMB treatment, coincident with a modest increase in $[Ca^{2+}]_i$ and prior to effects in other assays. After 4 hr, F-actin levels were almost undetectable in both $HgCl_2$- and *p*-CMB-treated YAC-1 cells. Both compounds increased $[Ca^{2+}]_i$ within minutes, though levels remained less than twice

baseline levels after 15 min exposure. With continued exposure, $[Ca^{2+}]_i$ increased two- to five-fold over baseline levels.

Different patterns were seen with $CH_3HgCl$ and TMS, both of which induced an almost immediate two-fold increase in CD3 fluorescence, with levels returning to baseline within minutes. With continued exposure, CD3 fluorescence was reduced to approximately 50% of baseline values. Both compounds also induced immediate two- to three-fold increases in PTyr-P, which returned toward baseline levels at 4 hr. Both $CH_3HgCl$ and TMS induced rapid and complete loss of β-tubulin staining, while actin filaments dissociated only after reductions in β-tubulin staining, and to a lesser degree, with approximately 25% and 50% remaining in $CH_3HgCl$- and TMS-treated cells, respectively. Similarly, two- to three-fold increases in $[Ca^{2+}]_i$ were noted after just 1 min exposure to either $CH_3HgCl$ and TMS. The $[Ca^{2+}]_i$ increased progressively with continued exposure, reaching levels five- to eight-fold greater than control values.

The delay in onset of YP/PI dye uptake following $HgCl_2$ or *p*-CMB exposure as compared to $CH_3HgCl$ may be a function of relatively slower passage of these mercurial compounds into the cell interior to produce effects. Alternately, the onset of apoptosis/necrosis may be delayed following interactions at the cell surface/interior. Changes in CD3 expression, PTyr-P and $[Ca^{2+}]_i$ preceded loss of microtubule or F-actin integrity and dye-uptake in $HgCl_2$-treated cells, while F-actin appeared to be an early and specific target of *p*-CMB, with effects preceding dye uptake and all other changes. In contrast, the effects produced by $CH_3HgCl$ are suggestive of rapid penetration of $CH_3HgCl$ to the cell interior, resulting in almost immediate induction of an early apoptotic ($YP^+/PI^-$) state, coincident with effects on all other assays except F-actin levels.

It is also possible rapid apoptosis was triggered by non-specific changes in membrane permeability, though such changes might be expected to be accompanied by influx of PI. The slightly slower onset of dye uptake in TMS-treated cells may reflect the degree of ionization of this compound, its larger size or protein binding of the ethylmercury moiety following dissociation from the parent TMS. Nonetheless, TMS almost immediately increased CD3 expression, PTyr-P and $[Ca^{2+}]_i$, and reduced tubulin while sparing actin, similar to effects seen with $CH_3HgCl$. A slow progression from apoptosis through late necrosis was not unexpected, at least for $CH_3HgCl$. In previous studies, as many as 1/3 of lymphocytes became apoptotic within 1 hr of exposure to $CH_3HgCl$, yet only 2/3 were apoptotic after 24 hr of continued exposure (Shenker et al., 1997). However, in all mercury treatments, a percentage of cells passed through the $YP^+/PI^-$ stage before becoming $YP^+/PI^+$, perhaps indicating activation of both necrotic and apoptotic cell death pathways, with the dominant death phenotype at 4 hr determined by the relative speed of each process (Unal-Cevik et al., 2004).

The different patterns of cytotoxicity may reflect differences in mercury -induced apoptotic cascades seen in other cell types. Both $CH_3HgCl$ and $HgCl_2$ induce the development of a mitochondrial membrane permeability transition. Cytochrome-c is released in to the cytosol in $CH_3HgCl$-treated human T lymphocytes, with no accompanying changes in levels of the anti-apoptotic protein Bcl-2. In contrast, $HgCl_2$ has no affect on cytochrome-c, but increases Bcl-2 (Shenker et al., 2000). Activation of the caspase cascade and phosphatidylserine exposure on the plasma membrane during apoptosis requires ATP, while necrosis involves passive degradation (Buttgereit et al., 2000); ATP depletion after initiation of apoptosis can lead to suspension of the apoptotic

process, with subsequent death by cell lysis (Volbracht et al., 1999). The $Hg^{2+}$ ion increases cellular ATP levels early and at low concentrations, although ATP levels later drop with more prolonged exposures, particularly at higher concentrations of $Hg^{2+}$ (Carranza-Rosales et al., 2005; Silles et al., 2005). Both $CH_3HgCl$ and TMS reduce ATP production and increase non-specific membrane permeability, which may lead to increased intracellular calcium levels, and ultimately, cell death (Gukovskaya et al., 1992; Kauppinen et al., 1989; Pelassy et al., 1994).

Microtubules serve as scaffolds for apoptosis signaling pathways and modulate the activity of apoptosis-regulating molecules (Mollinedo and Gajate, 2003). Suppression of microtubule dynamics by either microtubule-disrupting or -stabilizing agents blocks the cell cycle at the metaphase/anaphase [G2/M] transition, leading to cell death by apoptosis (Abal et al., 2003; Jordan, 2002; Mollinedo and Gajate, 2003). Microtubules appeared to be primary, or at least early, targets of $CH_3HgCl$ and TMS in this study, with marked loss of β-tubulin fluorescence preceding the onset of late apoptosis/necrosis. The similarity between patterns of β-tubulin staining in $CH_3HgCl$- and TMS-treated cells indicates that, like $CH_3HgCl$, TMS may inhibit tubulin synthesis. Both agents also appear to enhance tubulin degradation, producing a complete loss of β-tubulin staining within a matter of hours. In contrast, in $HgCl_2$- and *p*-CMB-treated cells, loss of microtubule integrity was coincident with dye uptake. The moderate reduction in β-tubulin levels produced by $HgCl_2$ and *p*-CMB may be the result of partial inhibition of tubulin synthesis following microtubule disassembly and/or incomplete tubulin degradation. Although actin filaments are relatively insensitive to the effects of some forms of mercury, actin appeared to a specific target of *p*-CMB. However, the distinction

between primary or secondary effects must also take into account the influence of confounding factors affecting both microtubule and F-actin integrity, including intracellular calcium levels (Gremm and Wegner, 2000; Karr et al., 1980; O'Brien et al., 1997). Cytoskeletal dynamics are also coupled to lymphocyte signal transduction pathways (Sechi and Wehland, 2004) that may be targeted by mercury.

It is postulated that $HgCl_2$ produces aberrant aggregation and activation of cell surface receptors (Nakashima et al., 1994; Pu et al., 1995) and/or PKC activation (Badou et al., 1997), but TCR/CD3 receptor down-regulation has not been reported. Down-regulation of TCR/CD3 receptors is an early event following TCR triggering (Dietrich et al., 2002; Salio et al., 1997) or protein kinase C (PKC) activation (Cantrell et al., 1985), and is associated with increased PTyr-P (Kastrup et al., 2000; Lauritsen et al., 1998). Down-regulation of TCR/CD3 receptors may be achieved by increasing endocytic internalization, decreasing exocytosis (with or without increasing degradation of internalized receptors) or by a combination of both mechanisms (Liu et al., 2000). When triggered by large amounts of antibody or agonist peptides, TCR/CD3 receptor expression is reduced 80% or more (Dietrich et al., 2002; Salio et al., 1997) as a result of increased intracellular retention and degradation of the TCR/CD3 complexes (Liu et al., 2000). In contrast, activation of intracellular PKC by phorbol esters increases TCR/CD3 receptor internalization 10-fold (Menne et al., 2002) without affecting exocytosis or receptor degradation (Salio et al., 1997). As a result, TCR/CD3 expression falls to approximately 50% of normal levels (Dietrich et al., 2002; Menne et al., 2002). Specific inhibition of constitutive TCR/CD3 exocytosis by brefeldin A (Dietrich et al., 2002) or primiquine (Das et al., 2004) reduces surface TCR/CD3 expression only 20 or 30%,

respectively, similar to reductions produced by $HgCl_2$ or *p*-CMB. The $Hg^{2+}$ ion may have nonetheless produced partial receptor down-regulation through agonist-like membrane interactions or PKC activation. Indiscriminate cross-linking of multiple surface receptor types by $Hg^{2+}$ or mercury-induced phosphorylation may not mimic the high receptor occupancy (Bachmann et al., 1997) or receptor clustering and assembly into lipid rafts (Miceli et al., 2001) needed for complete down-regulation.

The early increase in CD3 and PTyr-P fluorescence seen with $CH_3HgCl$ and TMS was unexpected, as increased PTyr-P might otherwise be associated with TCR/CD3 down-regulation. In previous studies of TCR/CD3 expression, no increase was noted 2–5 min following agonist triggering or PKC activation (Dietrich et al., 2002; Liu et al., 2000). However, in $CH_3HgCl$ or TMS-treated cells, CD3 fluorescence had returned to baseline within 5 min, and the initial increase could easily have been missed without an earlier time point. T lymphocytes can u*p*-regulate TCR/CD3 expression (D'Oro et al., 1997) by decreasing receptor endocytosis (Lauritsen et al., 2001). In resting lymphocytes, 70–85% of the cycling TCR/CD3 pool is found at the cell surface (Liu et al., 2000). Decreased endocytosis would not therefore be expected to increase CD3 expression two-fold unless the intracellular pool is larger in YAC-1 cells than in normal lymphocytes (Matsuda et al., 1994). It is tempting to suggest the early increase in PTyr staining was responsible for later down-regulation of CD3 receptor expression. However, the reduction in CD3 expression was less than with receptor-triggered PTyr-P, although it was similar to that seen with PKC activation.

Sustained PTK activation is also required to maintain increased $[Ca^{2+}]_i$ in T lymphocytes following stimulation by APCs (Muller et al., 1999), but the converse does

not appear to be true, at least in TMS-exposed cells, where increased PTyr-P is not thought to be a consequence of increased $[Ca^{2+}]_i$ (Kim et al., 2002). As such, while observed simultaneously, the early increase in PTyr-P in $CH_3HgCl$- and TMS-treated YAC-1 cells may have been responsible for the dramatic concomitant increase in Fluo-3 fluorescence. Alternately, non-specific increases in permeability (Gukovskaya et al., 1992; Kauppinen et al., 1989) or activation of intracellular or membrane $Ca^{2+}$ channels (Pelassy et al., 1994) could account for the observed effects. The more modest increase in $[Ca^{2+}]_i$ over the initial 15 min of $HgCl_2$ exposure was consistent with previous studies in which $HgCl_2$-exposed rat T lymphocytes showed a transient (15 min) rise in $[Ca^{2+}]_i$, thought to have resulted from PKC-dependent $Ca^{2+}$ influx through L-type membrane channels (Badou et al., 1997). However, TCR/CD3 down-regulation consistent with PKC activation was not seen in this study. Further disruption of $[Ca^{2+}]_i$ homeostasis, with levels up to 5-fold greater than baseline, was evident by 30 min, coincident with the onset of YP/PI dye uptake but prior to effects on actin or tubulin.

The findings presented here indicate the two groups of mercury compounds induce cell death at different rates, possibly reflecting the more rapid penetration of $CH_3HgCl$ and TMS to the cell interior as compared to $HgCl_2$ and *p*-CMB. However, they also suggest the mercury compounds may have different specificities and produce toxic effects by different mechanisms. These patterns extend to effects on microtubules, actin and selected intracellular signalling components involved in the formation of the immunological synapse and lymphocyte activation/cell death. Although a receptor-mediated mechanism has been proposed for $Hg^{2+}$, and microtubules are thought to be a primary target of $CH_3HgCl$ and TMS, mercury in all its forms is considered non-specific

and can interact directly with sulfhydryl (-SH) groups on targets other than membrane receptors, PKC, microtubules or other cellular components postulated to be specific targets of mercury. Even if initially acting through these pathways, mercury may therefore produce more complex effects than agonist ligands or target-specific chemicals. Nonetheless, in this study, a relatively specific effect on F-actin was evident for *p*-CMB. However, at concentrations altering $[Ca^{2+}]_i$, $HgCl_2$-treated YAC-1 cells show responses distinct from those produced by physiologic stimuli, including slightly reduced PTyr-P, and partial CD3 down-regulation. The organomercurial compounds $CH_3HgCl$ and TMS produced high levels of PTyr-P and moderate down-regulation of CD3 expression, though neither produced CD3 down-regulation equivalent to that seen with agonist ligation. It is therefore uncertain whether a receptor-based mechanism for $Hg^{2+}$-related effects remains plausible, or whether such a stimulus can produce only an abortive signal. In addition, while microtubule deaggregation precedes cell death in $CH_3HgCl$- and TMS-treated cells, and appears to be accompanied by inhibition of tubulin synthesis, the distinction between primary and secondary effects of these mercury compounds is made more difficult by the concomitant appearance of markedly increased PTyr-P and $[Ca^{2+}]_i$. Additional investigations aimed at identifying the sequence of these events is warranted in order to define the initial targets of mercury toxicity and their impact upon lymphocyte signaling and immune regulation.

**Figure 4.1:** (A) Representative dot-plot of untreated YAC-1 lymphoma cells stained on ice with YOPRO-1 (YP) and propidium iodide (PI) dyes, showing greater than 90% viable cells ($YP^-/PI^-$) as highlighted within the oval; (B) Representative dot-plot of YAC-1 cells after 4 hr exposure to methyl mercuric chloride ($CH_3HgCl$) and subsequent staining with YP and PI dyes, indicating viable cells ($YP^-/PI^-$), early apoptotic ($YP^+/PI^-$) cells within the small oval, and late apoptotic/necrotic ($YP^+/PI^+$) cells highlighted within the larger oval.

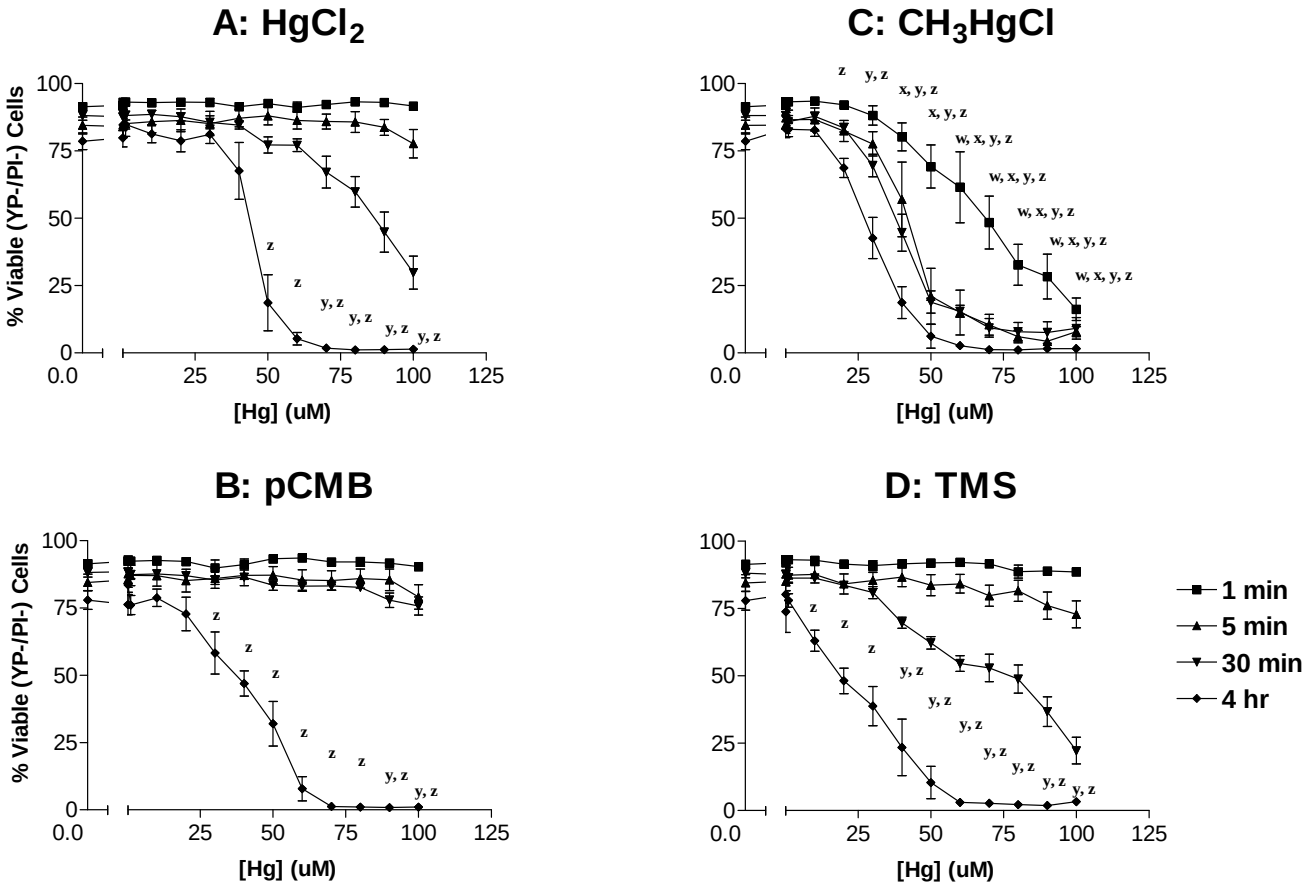


**Figure 4.2:** Effects of mercuric chloride ($HgCl_2$; A), *p*-chloromercuribenzoate (*p*-CMB; B), methylmercuric chloride ($CH_3HgCl$; C) and thimerosal (TMS; D) on YAC-1 lymphoma cell viability following *in vitro* exposures of 1 min, 5 min, 30 min or 4 hr duration, expressed as the percentage of the control treatment (RPMI) viable ($YP^-/PI^-$) cells, as measured by flow cytometry following incubation of mercury -treated cells with cell viability indicator dyes YOPRO-1 and propidium iodide on ice (n ± SEM; n = minimum of 5 replicates for each data point; w, x, y and z indicate values differing significantly from control values for the 1 min, 5 min, 30 min and 4 hr exposure periods, respectively, $p < 0.05$).

Fig. 4.3 I

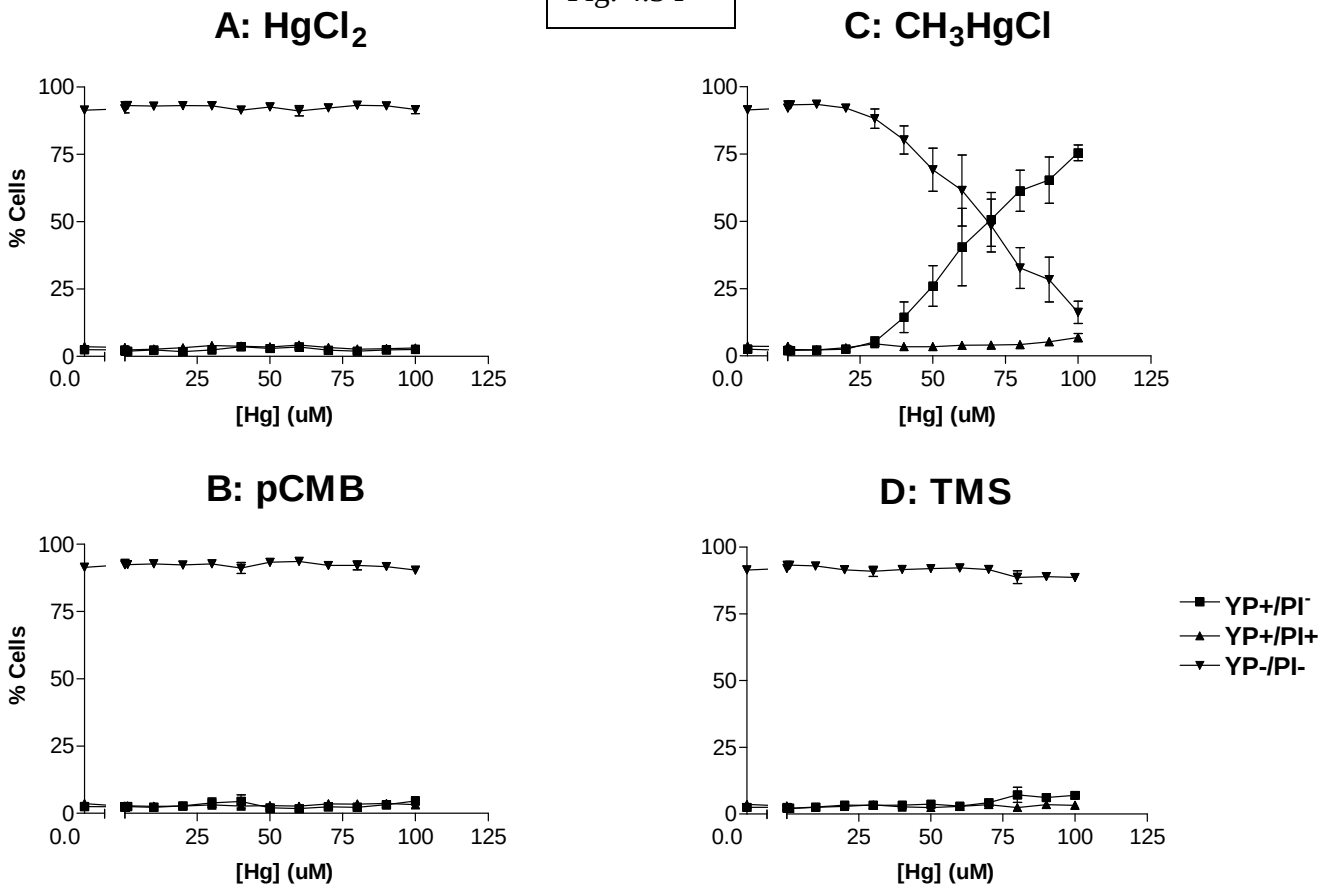


**Figure 4.3-I to IV**: Effects of mercuric chloride ($HgCl_2$, A), *p*-chloromercuribenzoate (*p*-CMB; B), methylmercuric chloride ($CH_3HgCl$; C) and thimerosal (TMS; D) on YAC-1 lymphoma cell death following *in vitro* exposures of 1 min (I), 5 min (II), 30 min (III) or 4 hr (IV) duration, expressed as the percentage of cells in each of three categories: (i) YOPRO-1 negative/propidium iodide negative ($YP^-/PI^-$; live), (ii) $YP^+/PI^-$ (early apoptotic), and (iii) $YP^+/PI^+$ (late apoptotic/necrotic), as measured by flow cytometry following incubation of mercury -treated cells with the dyes on ice (n ± SEM; n = minimum of 5 replicates for each data point).

Fig. 4.3 II

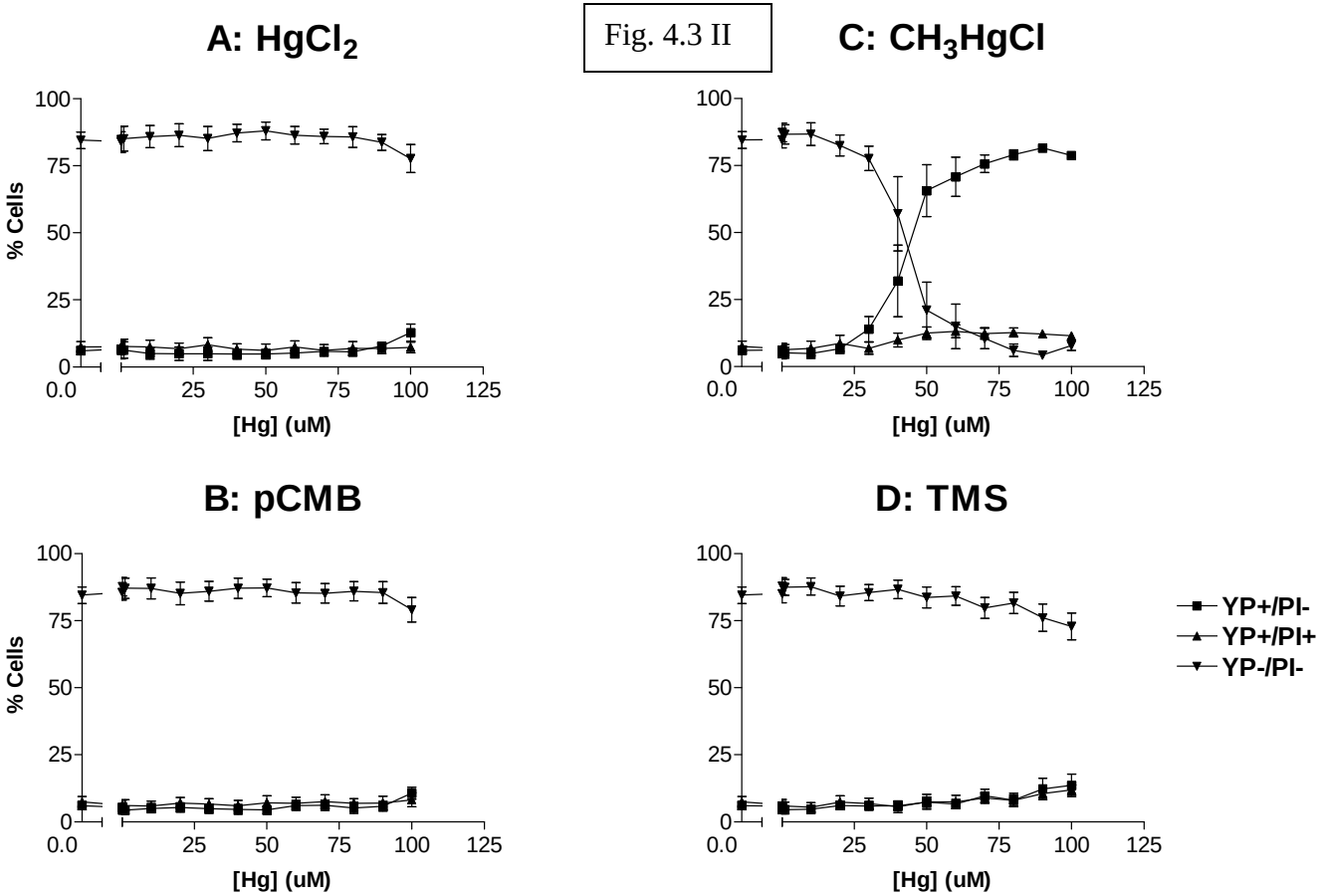

Fig. 4.3 III

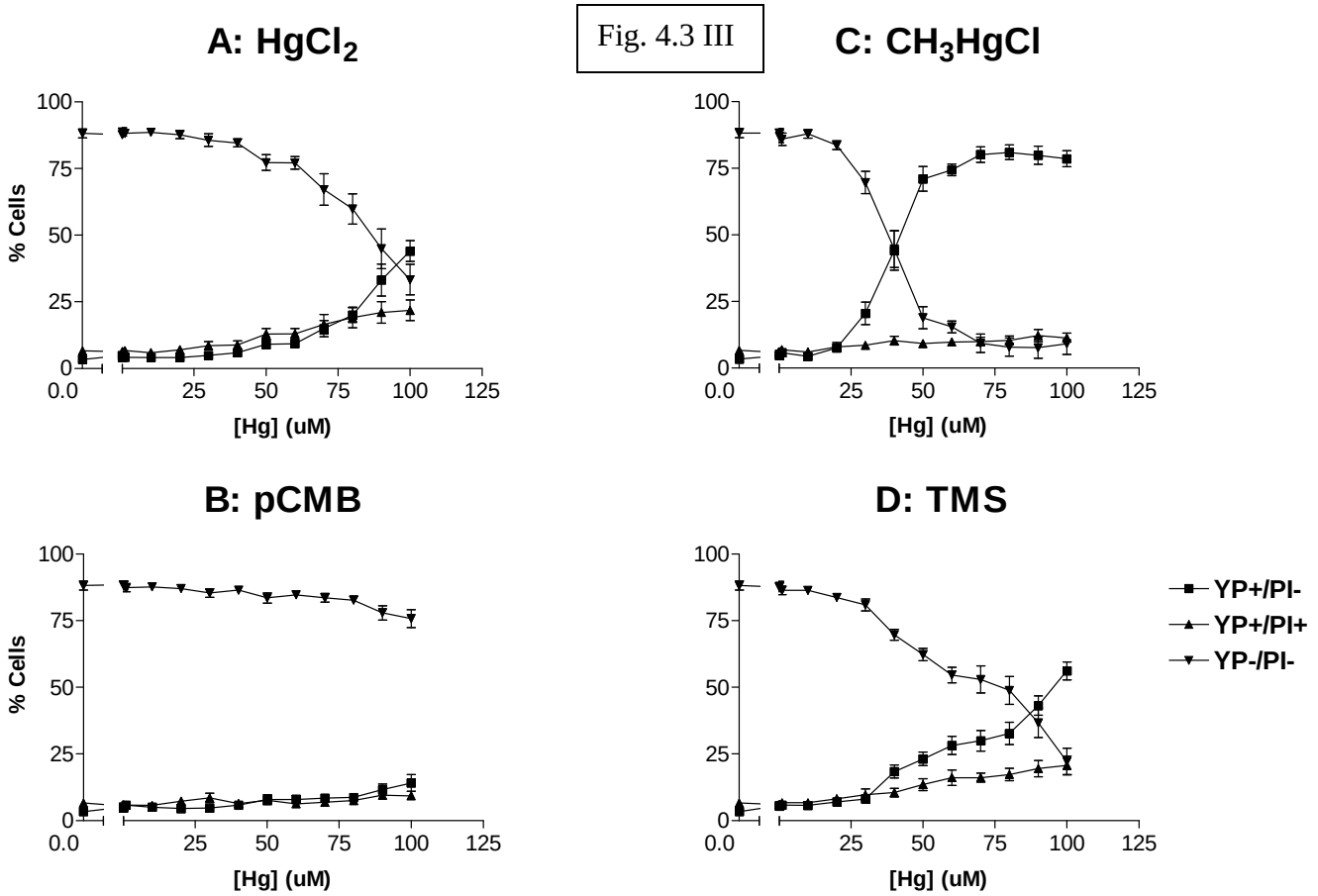
A: HgCl2
C: CH3HgCl
B: pCMB
D: TMS
% Cells
[Hg] (uM)
0.0
25
50
75
100
125
0
25
50
75
100
YP+/PI-
YP+/PI+
YP-/PI-

Fig. 4.3 IV

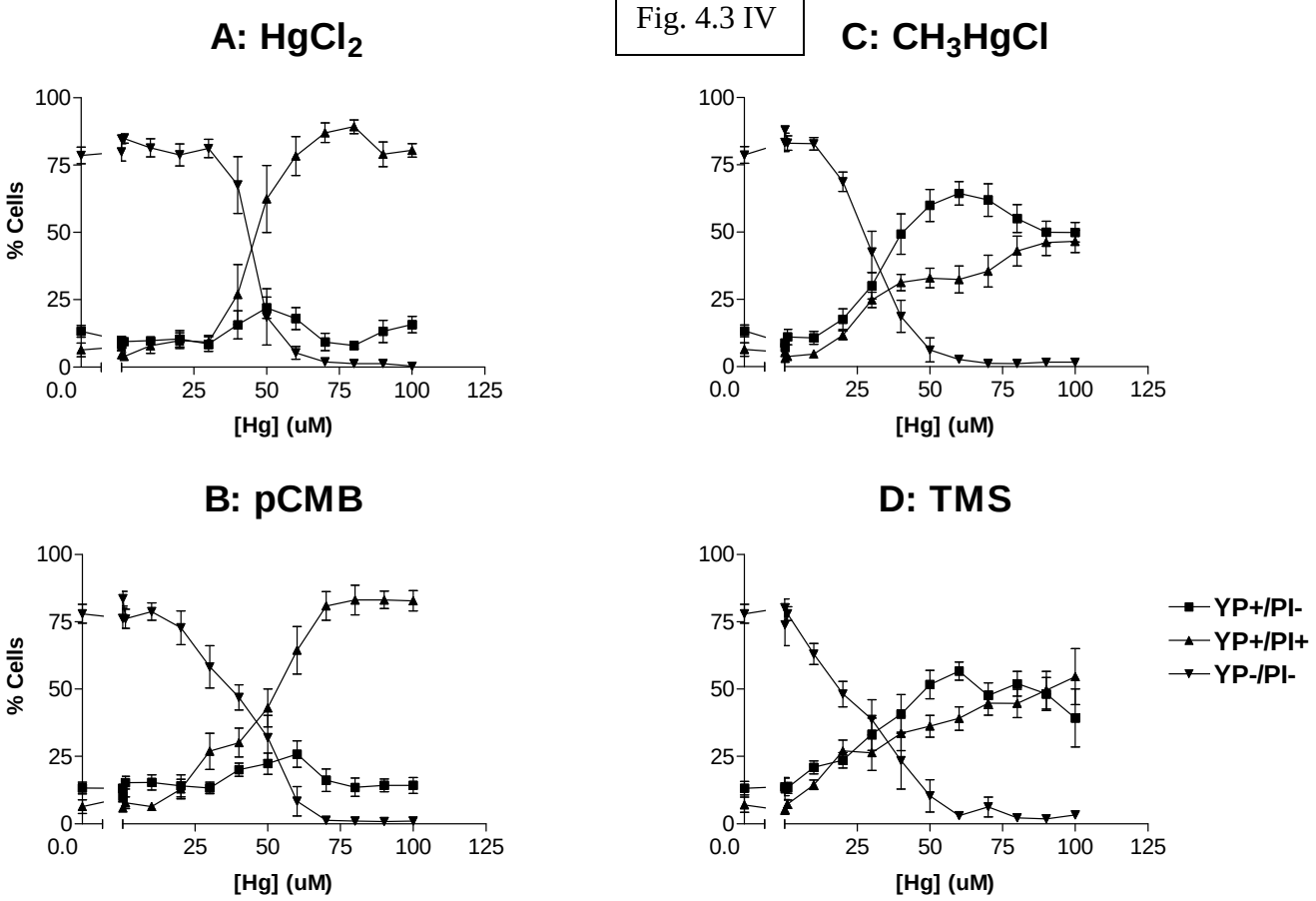
A: HgCl2
C: CH3HgCl
B: pCMB
D: TMS
% Cells
[Hg] (uM)
0.0
25
50
75
100
125
0
25
50
75
100
YP+/PI-
YP+/PI+
YP-/PI-

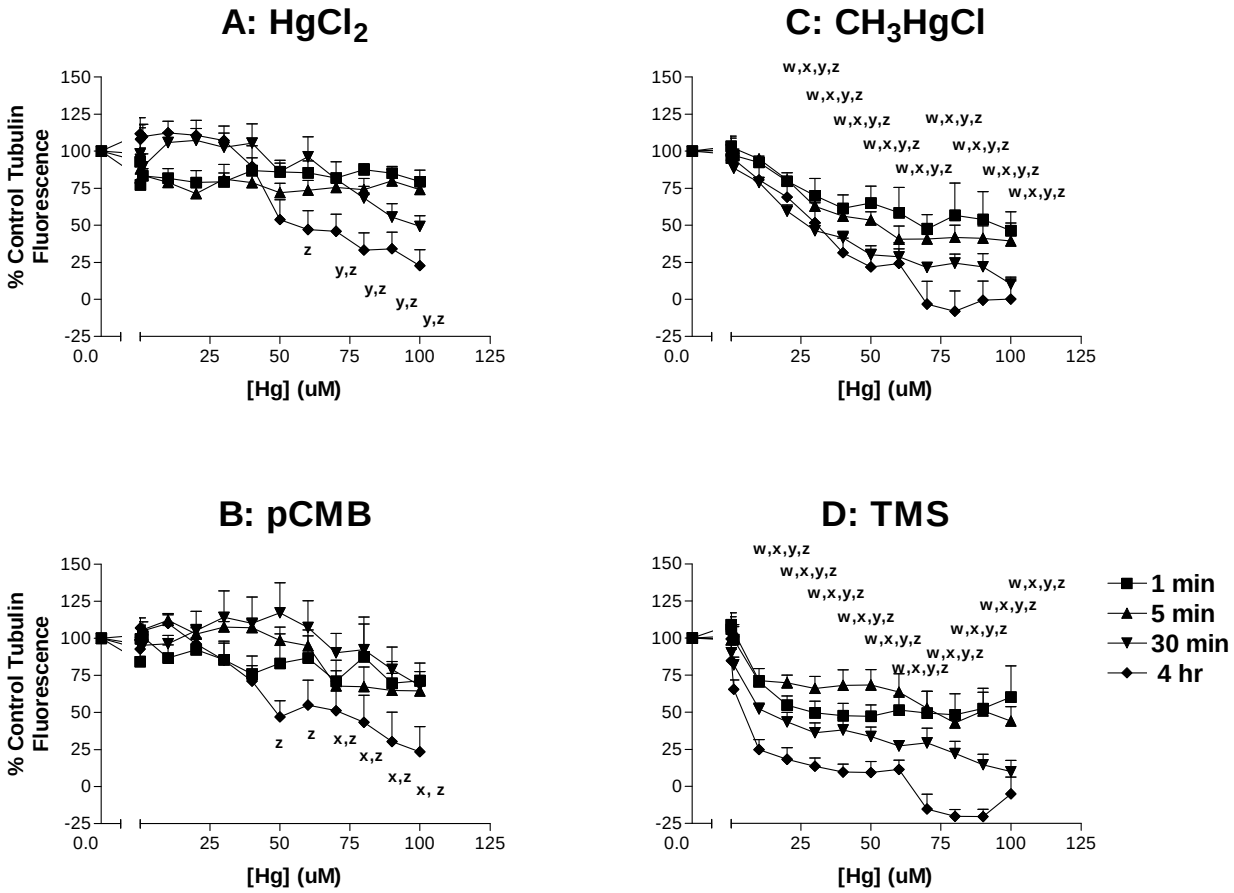


**Figure 4.4:** Effects of mercuric chloride ($HgCl_2$; A), *p*-chloromercuribenzoate (*p*-CMB; B), methylmercuric chloride ($CH_3HgCl$; C), and thimerosal (TMS; D) on YAC-1 lymphoma cell β-tubulin levels following 1 min, 5 min, 30 min or 4 hr *in vitro* exposures, expressed as a percentage of the control treatment (RPMI) fluorescence, as measured by flow cytometry following indirect immunofluorescent staining of intracellular β-tubulin (mean ± SEM; n = minimum of 5 replicates for each data point; w, x, y and z indicate values differing significantly from control values at 1 min, 5 min, 30 min or 4 hr, respectively, $p < 0.05$].

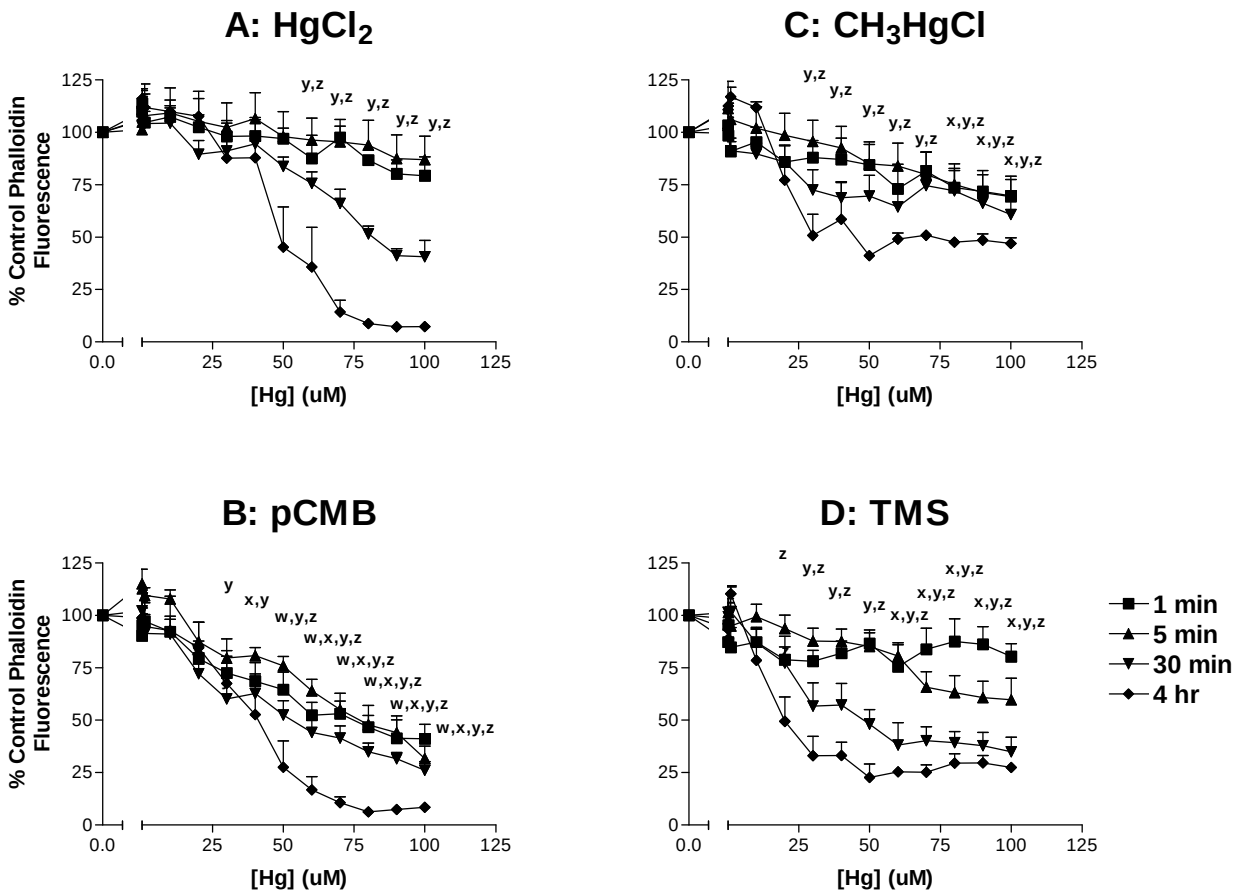


**Figure 4.5:** Effects of mercuric chloride ($HgCl_2$; A), *p*-chloromercuribenzoate (*p*-CMB; B), methylmercuric chloride ($CH_3HgCl$; C), and thimerosal (TMS; D) on YAC-1 lymphoma cells F-actin levels following 1 min, 5 min, 30 min or 4 hr *in vitro* exposures, expressed as a percentage of the control treatment (RPMI) fluorescence, as measured by flow cytometry following staining of intracellular F-actin with fluorochrome-conjugated phalloidin (mean $\pm$ SEM; n = minimum of 5 replicates for each data point, except 1 min, where n = 3; w, x, y and z indicate values differing significantly from control values at 1 min, 5 min, 30 min or 4 hr, respectively, $p < 0.05$].

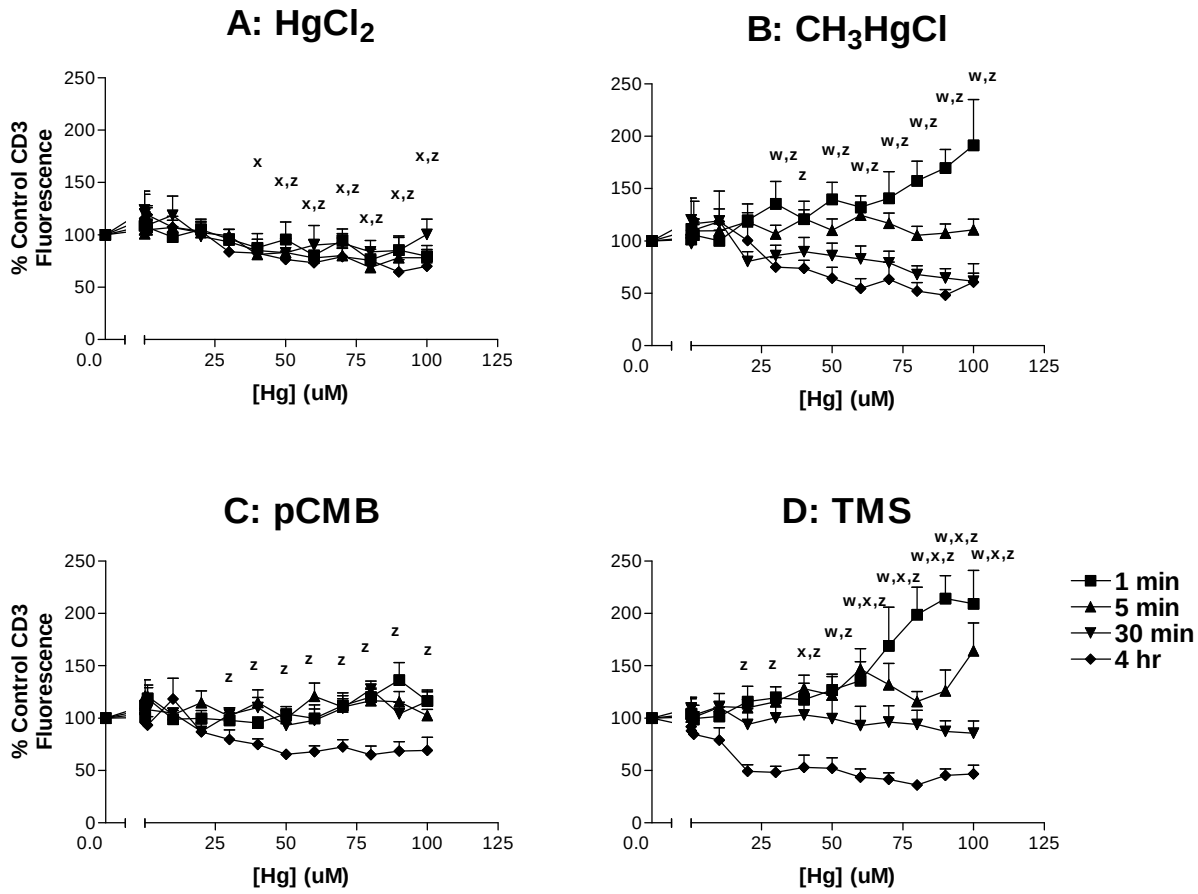


**Figure 4.6:** Effects of mercuric chloride ($HgCl_2$; A), *p*-chloromercuribenzoate (*p*-CMB; B), methylmercuric chloride ($CH_3HgCl$; C), and thimerosal (TMS; D) on YAC-1 lymphoma cell surface CD3 receptor expression following 1 min, 5 min, 30 min or 4 hr *in vitro* exposures, expressed as a percentage of the control treatment (RPMI) fluorescence, as measured by flow cytometry following indirect immunofluorescent staining of CD3 receptors (mean + SEM; n = minimum of 5 replicates for each data point; w, x, y and z indicate values differing significantly from control values at 1 min, 5 min, 30 min or 4 hr, respectively, $p < 0.05$].

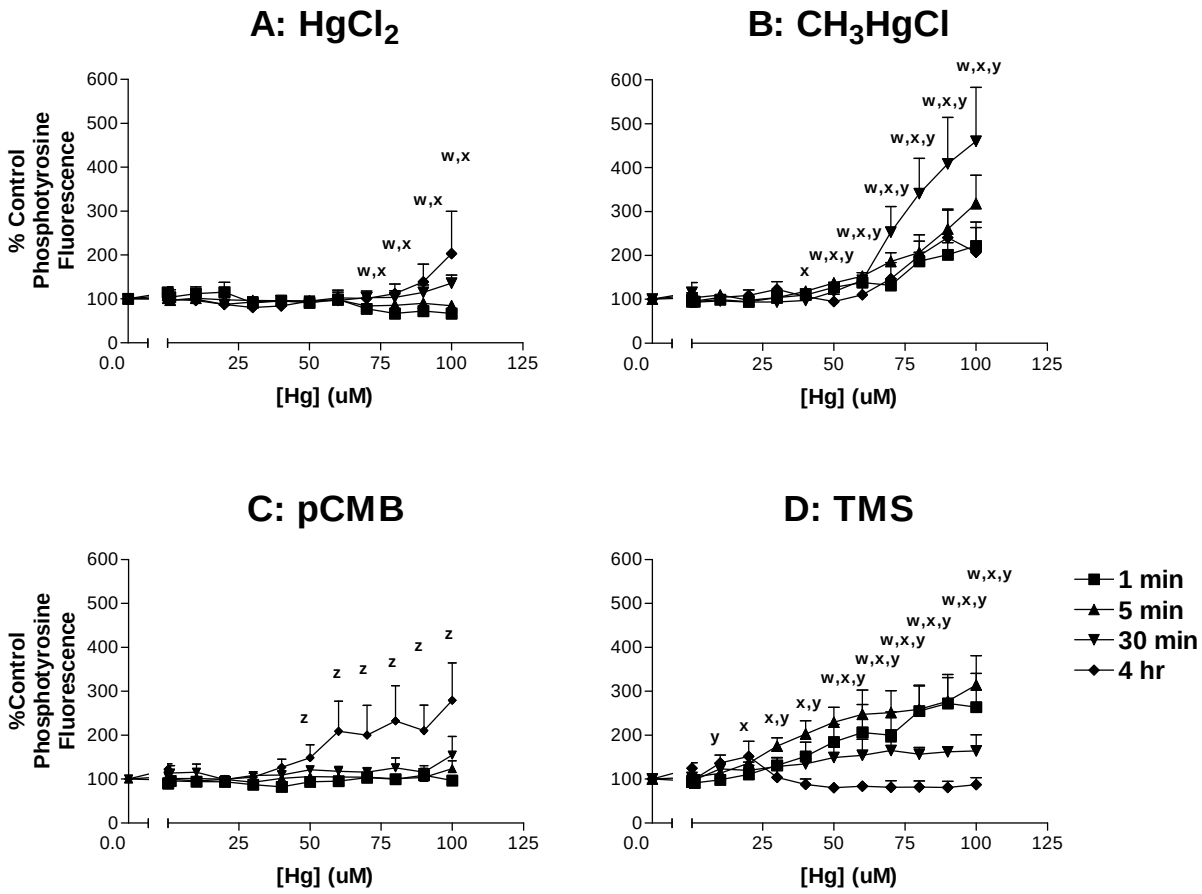


**Figure 4.7**: Effects of mercuric chloride ($HgCl_2$; A), *p*-chloromercuribenzoate (*p*-CMB; B), methylmercuric chloride ($CH_3HgCl$; C), and thimerosal (TMS; D) on YAC-1 lymphoma cells intracellular phosphotyrosine levels following 1 min, 5 min, 30 min or 4 hr *in vitro* exposures, expressed as a percentage of the control treatment (RPMI) fluorescence, as measured by flow cytometry following indirect immunofluorescent staining of intracellular phosphotyrosine residues (mean + SEM; n = minimum of 5 replicates for each data point; w, x, y and z indicate values differing significantly from control values at 1 min, 5 min, 30 min or 4 hr, respectively, $p < 0.05$].

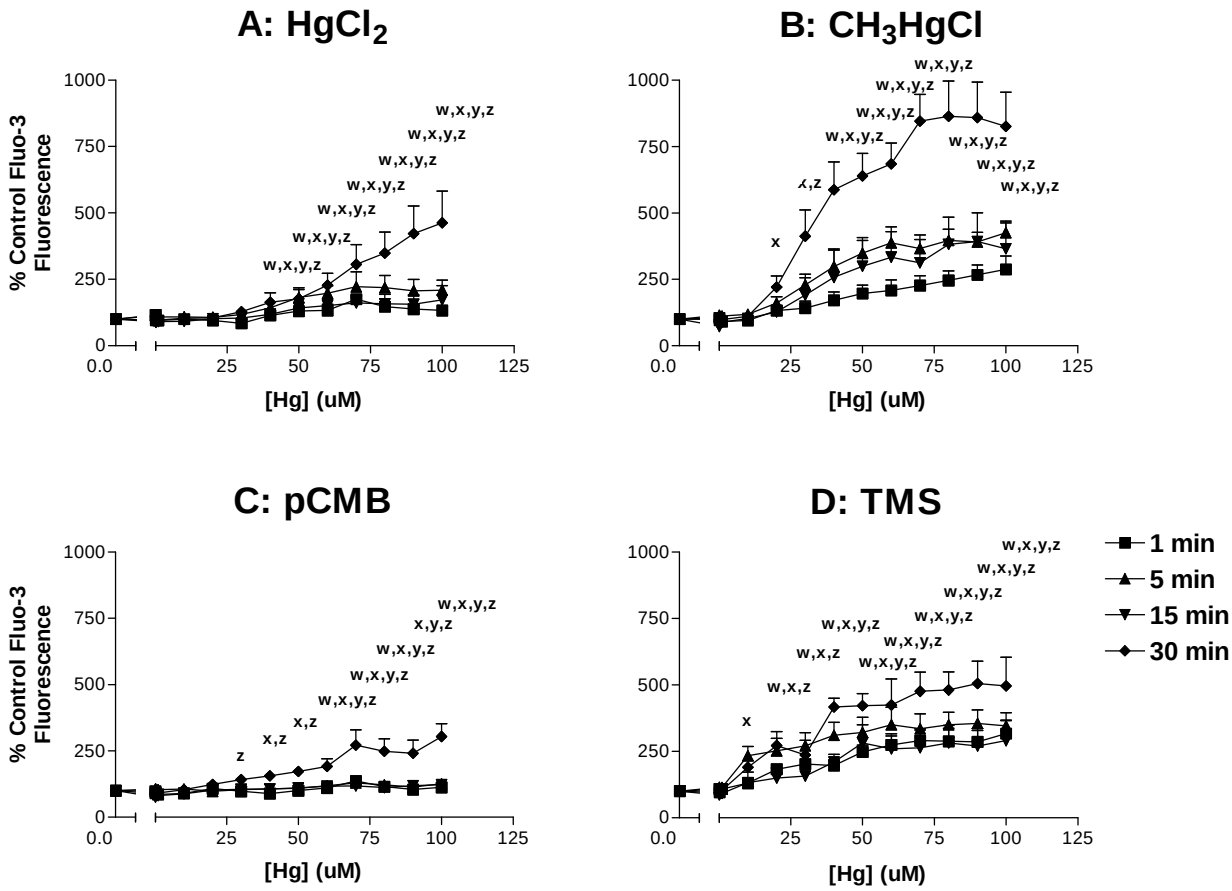


**Figure 4.8:** Effects of mercuric chloride ($HgCl_2$; A), *p*-chloromercuribenzoate (*p*-CMB; B), methylmercuric chloride ($CH_3HgCl$; C), and thimerosal (TMS; D) on YAC-1 lymphoma cells intracellular calcium levels following 1, 5, 15 or 30 min *in vitro* exposures, expressed as a percentage of the control treatment (RPMI) fluorescence, as measured by flow cytometry following Fluo-3 calcium indicator dye loading (mean + SEM; n = minimum of 5 replicates for each data point, except 15 min, where n = 2; w, x, y and z indicate values differing significantly from control values at 1, 5, 15 or 30 min, respectively, $p < 0.05$].

# 5.0

# CYTOSKELETAL POLARIZATION RESPONSES IN THE YAC-1 LYMPHOMA CELL LINE FOLLOWING EXPOSURE TO VARIOUS MERCURY COMPOUNDS.

## 5.1 Relationship to overall project

The results and discussion included in Chapter 5 encompass Specific Aim IV. The results of this study were compared with those in Chapter 4, to assess whether effects on cytoskeletal components and viability preceded altered responses to polarised stimuli, as was anticipated for $HgCl_2$, or were coincident with reduced polarization responses, as was expected for $CH_3HgCl$ or TMS.

## 5.2 ABSTRACT

This study investigated the effects of exposures to 0.01 – 100 uM concentrations of various mercury compounds (mercuric chloride [$HgCl_2$], methyl mercuric chloride [$CH_3HgCl$], *p*-chloromercuribenzoate [*p*-CMB] and thimerosal [TMS; ethylmercurithiosalicylate]) on selected aspects of polarised signalling in T lymphocytes using an *in vitro* model of the immunological synapse. YAC-1 lymphoma cells were conjugated to anti-CD3 antibody-coated 6.0 uM latex beads after 5 or 30 min mercury pre-treatment, fixed and the microtubules, microtubule organizing centre (MTOC) and Golgi apparatus identified by indirect immunofluorescent staining of beta tubulin and

fluorochrome-conjugated wheat germ agglutinin, respectively. The percentage of cells forming conjugates with anti-CD3 or control beads, altering their morphology to wrap around or reorienting to lie adjacent to the attached bead were determined by light and fluorescent microscopy. Two general patterns of responses were observed. After 5 min pre-incubation, both $CH_3HgCl$ and TMS produced moderate reductions in MTOC reorientation, with pronounced effects on morphologic responses. These effects were accompanied by a decrease in microtubule and MTOC staining. After 30 min, all bead-binding variables were markedly inhibited by $CH_3HgCl$ or TMS, accompanied by a concentration-dependent loss of microtubules, MTOC and Golgi staining. In contrast, neither $HgCl_2$ nor *p*-CMB inhibited conjugate formation, morphologic responses, MTOC reorientation or the appearance of microtubules/MTOC in YAC-1 cells after 5 min pre-treatment. After a 30 min pre-incubation, all bead binding variables were reduced by $HgCl_2$ and *p*-CMB, in the absence of the marked loss of microtubule, MTOC and Golgi staining seen with concentrations of $CH_3HgCl$ or TMS producing similar effects on bead binding.

## 5.3 INTRODUCTION

Cell-to-cell adhesion and intercellular communication are critical to the development, activation and maturation of the immune system. However, unlike solid organs, the cells of the immune system exist largely as independent units until called upon to coordinate their activities in response to an antigenic threat. Interactions between cells of the immune system do not involve gap junctions or other means of coupling the respective cytoplasmic compartments (Singer, 1992). Lymphocytes and corresponding antigen presenting cells (APCs; B lymphocytes, macrophages or dendritic cells) or target

(neoplastic or virus-infected) cells instead form a specialised three-dimensional adhesion and signalling complex termed the supramolecular activation complex (SMAC) or 'immunological synapse' (Monks et al., 1998). The immunological synapse presents a unique opportunity to study the effects of immunotoxicants such as mercury (Hg) in both time and space.

The key features of SMAC formation have been extensively studied in helper T ($T_H$) and B lymphocyte (acting as APC) couples (Kupfer and Singer, 1989b; Kupfer et al., 1986b; Kupfer et al., 1987b). Many of these are shared by activated cytotoxic T lymphocyte (CTL)/target (Kupfer and Dennert, 1984; Kupfer et al., 1985; Kupfer and Singer, 1989a) and natural killer (NK)/target (Kupfer et al., 1983) cell couples. In the presence of an appropriate antigenic stimulus, antigen-derived peptide fragments are presented to $T_H$ lymphocytes by the major histocompatibility complex (MHC) on the surface of APCs. $T_H$ lymphocytes bearing the corresponding clonotypic T-cell receptor (TCR) recognise and bind the peptide/MHC. Antigen-specific activation of surface receptors creates a localised signalling complex, and triggers reorientation of the T lymphocyte cytoskeletal and secretory machinery (microtubule organizing centre or MTOC and the Golgi apparatus) toward the area of contact. Soluble mediators may then be specifically released from the T lymphocyte directly in the synaptic junction (Kupfer et al., 1991), without unnecessary activation (Kupfer et al., 1994) or killing (Kupfer et al., 1986a) of bystander cells. The immunological synapse thus serves as a checkpoint for lymphocyte activation, providing a framework within which T lymphocytes may discriminate qualitative, quantitative and spatio-temporal differences in $T_H$/APC cell surface receptor interactions: such differences may be translated as distinct calcium

signals, cytoskeletal rearrangements and lymphocyte responses (Anton van der Merwe et al., 2000; Grakoui et al., 1999a; Lanzavecchia and Sallusto, 2001).

The immunological synapse prevents lymphocyte activation by inappropriate antigens, but it is vulnerable to chemical agents that do not act in a localised fashion. Modulation of protein kinase C (PKC) activity by bryostatin or bisindolylmaleimide can inhibit reorientation of the MTOC in CTL/target cell couples (Nesic et al., 1998). Similarly, mercury may interact with many of the components of the SMAC and downstream signalling cascades, including: membrane receptors (Nakashima et al., 1994; Pu et al., 1996; Rahman et al., 1993); protein kinase C (Badou et al., 1997), tyrosine phosphorylation (Rosenspire et al., 1998) or tyrosine phosphatases (Lander et al., 1992); microtubules (Brown et al., 1988; Miura et al., 1984; Sager et al., 1983); redox-sensitive signalling cascades (InSug et al., 1997; Shenker et al., 1993a; Shenker et al., 2002); and intracellular calcium (Badou et al., 1997; Smith et al., 1987; Tan et al., 1993).

Various forms of mercury, both organic and inorganic, are known to be cytotoxic to lymphocytes and to produce immune dysregulation. Mercuric chloride ($HgCl_2$) and methyl mercuric chloride ($CH_3HgCl$) reduce human peripheral lymphocyte viability *in vitro* (Shenker et al., 1992a; Shenker et al., 1993a), while the mercurial medical preservative thimerosal induces apoptosis in the Jurkat human T lymphocytic leukemia cell line (Makani et al., 2002). Mercury can induce thymic atrophy (Kosuda et al., 1996); inhibit lymphocyte proliferation (Shenker et al., 1992b); suppress humoral (Blakley et al., 1980; Shenker et al., 1993a) and cellular immunity (Nakatsuru et al., 1985), and natural killer activity (Cai et al., 1988); increase tumour frequency in mice exposed to carcinogens (Blakley, 1984); and increase the risk and severity of human malaria

infection (Silbergeld et al., 2000). Mercury may also stimulate lymphocyte proliferation (Jiang and Moller, 1995, 1996; Loftenius et al., 1997; Pelletier et al., 1988), act as a hapten to stimulate mercury -specific lymphocytes (Stejskal et al., 1999), and can induce a transient, genetically determined Type-2 (T-helper-2-like or antibody-mediated) autoimmune disease in susceptible rats and mice (Druet et al., 1979b; Hultman and Hansson-Georgiadis, 1999; Pelletier et al., 1987a; Sapin et al., 1982). Similar autoimmune dysfunction in humans is seen in mercury-exposed humans (Silva et al., 2004).

To date there have been no investigation of mercury effects on the immunological synapse. However, $HgCl_2$ has been shown to alter intracellular signalling and inhibit polarization in response to chemotactic gradients in neutrophils (Contrino et al., 1988; Worth et al., 2001). Binding of critical lymphocyte surface receptors or intracellular targets by mercury may produce an aberrant non-polarised intracellular signal. The mercury-induced signal may mimic antigen-mediated signalling at certain mercury concentrations, but is likely not optimal under most circumstances. This global signal may prevent normal reorientation of the lymphocyte signalling scaffold, cytoskeleton and secretory apparatus in response to physiologic stimuli. In the absence of appropriate spatio-temporal stimuli by which to initiate reorientation, the lymphocyte response to mercury-mediated stimuli may simply be to activate cell death pathways. Alternately, mercury may transiently activate a small percentage of cells in a non-antigen-specific fashion. The global stimulus may also trigger non-specific release of soluble mediators and inappropriate activation of bystander cells. Aberrant global signalling may thus provide a basis for both the immunosuppressive and -stimulatory effects of mercury. In

this study, the effects of four mercury compounds on selected aspects of polarised signalling were investigated using an *in vitro* model of the immunological synapse.

## 5.4 MATERIALS AND METHODS

Unless otherwise noted, all laboratory disposables were obtained from VWR International (Mississauga, ON) and all chemicals and reagents were purchased from Sigma-Aldrich (Oakville, ON).

### 5.4.1 Preparation of mercury solutions

Mercury compounds having differing chemical properties (organic vs inorganic mercury, presumed or known ability to penetrate cell membranes and suspected or known effects on immune function) were selected for the study. The four compounds selected were mercuric chloride ($HgCl_2$), *p*-chloromercuribenzoate (*p*-CMB), methyl mercuric chloride ($CH_3HgCl$), and ethylmercurithiosalicyclate, also known as thimerosal (TMS). Stock solutions (10 mM) of each mercury compound were prepared in dd$H_2O$. The TMS was completely soluble in water, but $HgCl_2$ (ICN Pharmaceuticals, Costa Mesa, CA) was dissolved in 500 uL 1 N HCl (al-Sabti, 1994); $CH_3HgCl$ (Alfa Inorganics, Ventron, Beverly, MA, USA) in 1 mL of acetone (al-Sabti, 1994); and *p*-CMB (ICN) in 2.0 mL of 1N NaOH. The solutions were filter-sterilized, aliquotted and frozen at -20$^{o}$C until required. Working dilutions of mercury treatments were prepared in complete RPMI medium (RPMI with L-glutamine supplemented with 10% fetal bovine serum [FBS; all Canadian Life Technologies, Burlington, ON] and 10 mM HEPES buffer) at two times (0.02 – 200 uM) the final concentration (0.01 – 100 uM).

### 5.4.2 Cultured cell line

The YAC-1 murine Moloney virus-transformed lymphoma cell line (H-$2^a$, $CD3^+$, $TCR_{..}$, $CD45^+$, $CD4^-/8^-$; (Lindvall et al., 1997)) was obtained from the American Type Culture Collection (TIB-160; ATCC, Rockville, MD). The cells were grown in continuous culture in complete medium. After washing, counting and determination of viability using trypan blue exclusion, the cell concentration was adjusted to 4 x $10^6$ live cells/mL and the suspension incubated in a humidified incubator at $37^0$C with 5% $CO_2$ for 60-90 minutes before use.

### 5.4.3 Preparation of multi-well slides

Glass slides (2" x 3"; Corning) were coated with 15 uL of a 1 mg/mL solution of poly-L-lysine (PLL, >300 000 MW) in water and allowed to air dry. Multi-well slide membranes were prepared from a commercial window coating film (Concord Window Film, Danbury, CT) by first cutting the film slightly smaller than the slide, and then using a plain paper hole punch to create the wells (8/slide). The upper surface of the membrane was washed thoroughly with cotton swab soaked in 70% ethanol. The lower surface was lightly coated with a thin film of warmed glycerol jelly (50 mL water, 5 g gelatin, 50 mL glycerol) applied with a cotton swab. The membrane was firmly applied to a PLL-coated slide and left for at least one hour.

### 5.4.4 Preparation of anti-CD3 antibody-, poly-L-lysine (PLL)- and mercury-treated anti-CD3-coated microbeads

Anti-CD3-coated latex microbeads were used as surrogate antigen-presenting cells to induce polarisation responses from YAC-1 lymphoma cells. Antibody-coated and control beads were prepared with a passive adsorption technique under sterile

conditions, after the method of Lowin-Kropf *et al* (1998). Fifty uL of 6.0 um red-dyed carboxylate-modified latex beads (~2 x $10^8$ beads/ml; Polysciences, Warrington, PA) were placed in an micro-centrifuge tube (Eppendorf) with 950 uL plain phosphate buffered saline (PBS; Sigma-Aldrich) and centrifuged for 2 min at 6000 RPM. The bead pellet was recovered and the beads were washed twice more and then resuspended in 1.0 mL of PBS. Ten µg (20 µL) of anti-CD3 antibody (0.5 mg/mL; Cedarlane, Hornby, ON) or 10 µL of a 1 mg/mL filter-sterilized solution of PLL were added. The beads were placed on a rotary shaker at room temperature (RT) for 90 min. The beads were washed two more times and resuspended in PBS with 1% BSA to block any unbound sites and then placed on a rotary shaker for 30 min. The stained and blocked beads were washed three times in plain PBS, resuspended and stored for a maximum of four weeks in 1.0 mL plain PBS (to give a final bead concentration of $10^7$ beads/mL).

For each experiment, an appropriate volume of the stock suspensions of anti-CD3- or PLL-coated beads were diluted 1:4 in complete RMPI, to give a working dilution of 2 x $10^6$ beads/mL. The working dilution of the anti-CD3-coated beads was used to prepare mercury -treated control beads. Aliquots of anti-CD3-coated beads were transferred to each of four micro-centrifuge tubes. An appropriate volume of the 1 mM working dilutions of $HgCl_2$, $CH_3HgCl$, *p*-CMB or TMS was added to the bead suspension to give a final concentration of 100 uM Hg. The beads were incubated with the mercury for 30 min, washed three times in plain RPMI for one min at 6000 RPM, and resuspended in complete media. The prepared beads were placed in a humidified incubator at 37 C with 5% $CO_2$ until required.

### 5.4.5 Preparation of 96-well plates and addition of cells

Ten uL of the four mercury solutions, control treatments or media were added to the appropriate well of a 96-well U-bottom tissue culture plate (Nunc). The plate was placed in a humidified incubator at 37 C with 5% $CO_2$ for a minimum of 30 min. After pre-incubation, 10 uL of the prepared cell suspension were added to the mercury -loaded plates. The plates were then returned to the incubator for 5 or 30 min for the anti-CD3 bead conjugation assay.

### 5.4.6 Cell-bead conjugation

At the end of the 5 or 30 min mercury incubation, 10 uL of prepared anti-CD3-, mercury-treated anti-CD3- or PLL-coated beads or media were added to the appropriate wells. The plates were then vortexed gently for one min and centrifuged for ten min at 1200 RPM to bring the cells and beads into contact. After centrifugation, 180 uL of RPMI/0.5% FBS are added to each well and the plates centrifuged at 1200 RPM for two min to recover the cell pellets. After removing 180 uL of supernatant, the plates were vortexed vigourously for 10 s. The remaining cell-bead suspensions were quickly transferred to the appropriate well of the prepared multi-chambered slides and allowed to settle for 5 min. The cells were fixed by adding 50 uL of 4% paraformaldehdye in PBS to each well for 30 min. The paraformaldehyde was removed and the wells washed three times with 100 uL PBS.

### 5.4.7 Fluorescence staining of microtubules and Golgi apparatus

The location of the Golgi apparatus was identified using fluorochrome-congugated wheat germ agglutinin (WGA) after the method of Kupfer *et al* (1983) (Kupfer et al., 1983; see Fig 5.1-B). The WGA binds to N-acetylglucosaminyl (NAG)

residues in the cell, primarily in the trans-Golgi compartment. The cells were permeabilised by adding 20 uL of PBS containing 1% bovine serum albumin (BSA), 0.1 % saponin and 0.1% $NaN_3$ (PBS/BSA/Sap) to each well for 20 min. The permeabilisation solution was removed, and non-specific WGA binding sites on the endoplasmic reticulum were blocked by adding 20 uL of a 100 ug/mL Concanavalin-A (ConA) solution in PBS/BSA to each slide well for 20 min. The ConA was removed and the wells washed once with plain PBS. A 100 ug/mL solution of Texas-Red WGA (TR-WGA; Molecular Probes, Eugene, OR) was prepared in 0.15% Triton X-100 (J.T. Baker Chemical Co., Phillipsburg, NJ) in PBS containing 1% BSA (PBS/BSA) and centrifuged at 6000 RPM for 2 min to remove any protein aggregates. Twenty uL of the TR-WGA solution were added to each well for 30 min. Stain control wells included unstained wells, wells stained only with TR-WGA (and no anti-tubulin antibody) and wells blocked with 10 mM N-acetylglucosamine (NAG; Sigma-Aldrich) in PBS/BSA. The TR-WGA was removed and the wells washed once with plain PBS.

The location of the microtubules (MT) and microtubule-organising centre (MTOC) were identified with an indirect immunofluorescence technique, after the method of Kupfer *et al* (1982 and 1983; see Fig. 5.1-A). Twenty uL of a 1:250 dilution of mouse anti-β-tubulin (anti-Tub) in PBS/BSA/Sap were added to each well for 30 mins. The anti-Tub was removed and the wells washed once with PBS. The anti-Tub antibody was detected by adding 20 uL of a 1:250 dilution of Alexa®-488 goat-anti-mouse IgG antibody (GAM-488; Molecular Probes) in PBS/BSA/SAP for 30 min. The GAM-488 was removed and the wells washed once with plain PBS. Stain control wells included unstained wells and wells stained with anti-Tub/GAM only (and no TR-WGA), or with

mouse-anti-hamster IgG isotype control antibody (MAH; Cedarlane, Hornby, ON) followed by secondary antibody staining.

The location of the well was marked on the underside of the slides before removing the membrane. A drop of ProLong AntiFade® mounting medium (Molecular Probes) was added to each well and cover slips applied.

### 5.4.8 Scoring of conjugate formation, morphologic responses and microtubule organizing centre (MTOC)/Golgi reorientation

The response of the YAC-1 cells to anti-CD3 or control bead binding was assessed by light and fluorescent microscopy. The percentage of cells forming conjugates with anti-CD3 or control beads, the morphology of YAC-1 cells bound to beads, and the orientation of the MTOC/Golgi with respect to the bound bead were evaluated microscopically for each well using a 40X phase-contrast or 60X dry objective. To determine the percentage of cells forming conjugates, two hundred cells/well were counted and the number of cells binding beads (including cells with multiple beads attached or multiple cells contacting a single bead) were recorded. Incidental contact was distinguished from stable conjugate formation first on the basis of continued contact through vortexing, staining and wash steps and also by observations of a slight deformation of the YAC-1 cell in the area of contact (as assessed by phase or differential interference contrast microscopy).

To assess the morphologic and MTOC/Golgi polarization responses to bead binding, one hundred single-cell/single-bead conjugates were scored for each well. Morphologic responses (see Fig. 5.2) were scored as: (1) wrapped (where the cell contact area extended at least halfway around the circumference of the bead, as assessed by

placing the cross-hairs of the microscope photo mask over the bead); (2) touching (where area of contact was minimal and the YAC-1 cell retained a roughly spherical shape); or (3) elongated (where the area of contact was minimal or wrapped around the bead while the cell adopted an elongated morphology, such that the length of the cell exceeded two times its width). The orientation of the MTOC/Golgi (see Fig. 5.3) was assessed relative to the position of the bead. The MTOC/Golgi orientation was scored as: (1) adjacent (directly adjacent to or flattened onto the bead); (2) neutral (in the middle of the cell or on the side opposite the area of bead contact); or (3) elongated (stretched the length of cell with an elongated morphology). Where the MTOC was not visualised, the location of the Golgi was scored, if present. In cells where neither the MTOC or Golgi were seen, a 'not identified' score was assigned. The results were expressed as the percentage of cells in each category. The general appearance of the microtubules, MTOC and Golgi were also noted. Because scoring of slides for these assays is extremely time-consuming, 60 uM was the maximum concentration of $CH_3HgCl$, *p*-CMB and TMS tested at 30 min.

### 5.4.9 Statistical Analysis

All statistical analyses were performed using Prism® statistical software (GraphPad Software Incorporated, San Diego, CA). The [$IC_{50}$] values for mercury effects ([Hg] producing 50% reduction as compared to control treatments) were obtained from non-linear regression of data after log transformation of x values ([Hg]), with T-tests for comparison of [$IC_{50}$] values. The significance of mercury and control treatment effects were analysed using the Dunnett's one-way analysis of variance (ANOVA). No post tests were performed if the overall p value for the ANOVA was > 0.05. For all

analyses, treatment values differing from control values at the level of $p < 0.05$ were considered significantly different.

## 5.5. RESULTS

### 5.5.1 Formation of conjugates with anti-CD3 antibody-coated beads

At a cell:bead ratio of 2:1, approximately 40 and 33% of untreated YAC-1 cells formed stable conjugates with the anti-CD3-coated beads at the 5 and 30 min time points respectively (see Fig. 5.4-A and D, control values).

***Mercuric Chloride ($HgCl_2$)*:** After 5 min pre-treatment with $HgCl_2$, the percentage of YAC-1 cell-bead conjugates was not significantly different from untreated control cells. After 30 min, effects were noted at 60 – 100 uM $HgCl_2$ ($p < 0.001$), with an [$IC_{50}$] of 47.1 uM (see Table 5.1 and Fig 5.5-A).

***Para-Chloromercuribenzoate (p-CMB)*:** After 5 min pre-treatment, *p*-CMB had no effect on YAC-1 conjugate formation. After 30 min, conjugate formation was reduced at 30 – 100 uM *p*-CMB ($p < 0.001$), with an [$IC_{50}$] of 22.3 uM (see Table 5.1 and Fig. 5.5-B).

***Methyl Mercuric Chloride ($CH_3HgCl$)*:** After 5 min pre-treatment, $CH_3HgCl$ produced no effects on conjugate formation. However, $CH_3HgCl$-treated cells acquired a rounded morphology and tended to form larger aggregates than untreated, $HgCl_2$- or *p*-CMB-treated cells. Anti-CD3 beads located within the aggregates contacted many cells, increasing the percentage of conjugates scored. After 30 min exposure, conjugate formation was reduced at 10 – 100 uM $CH_3HgCl$ ($p < 0.05$; [$IC_{50}$] = 7.2 uM; see Table 5.1 and Fig. 5.5-C).

***Thimerosal (TMS)*:** Like $CH_3HgCl$-treated cells, TMS-treated cells acquired rounded morphology and formed large aggregates, within which many cells contacted any entrapped beads. There was a trend toward reduced conjugate formation after 5 min pre-treatment with TMS (overall $p = 0.09$). The effects became more pronounced after 30 min, with conjugate formation reduced at 10 – 100 uM TMS ($p < 0.001$; $[IC_{50}] = 3.8$ uM; see Table 5.1 and see Fig. 5.5-D).

***Bead treatment control groups*:** Pre-treatment of anti-CD3 beads with 100 uM of each of the mercury compounds had no effect on conjugate formation. The percentage of PLL-coated bead conjugates was also not significantly different from anti-CD3 bead conjugates. However, only approximately 6 and 7% of untreated YAC-1 cells formed conjugates with isotype control anti-TNP antibody-coated beads at the 5 or 30 min time points, respectively ($p < 0.001$ for both 5 and 30 min; see Fig. 5.8-A and D).

### 5.5.2 Morphology of cells conjugated to anti-CD3 antibody-coated beads

At either the 5 or 30 min time points, approximately 53% of untreated YAC-1 cells forming stable conjugates with the anti-CD3-coated beads also engulfed the bead (see Fig. 5.4 B and E, control values), either partially (at least 50% of the circumference of the bead) or completely (occasionally engulfing more than one bead, data not shown).

***Mercuric Chloride ($HgCl_2$)*:** There was a trend toward a reduction in conjugated YAC-1 cells wrapping around the attached bead after 5 min pre-treatment with $HgCl_2$ (overall $p = 0.14$). After 30 min, effects were noted at 40 – 100 uM $HgCl_2$ ($p < 0.05$), with an $[IC_{50}]$ of 50.0 uM (see Table 5.2 and Fig 5.6-A).

***Para-Chloromercuribenzoate (p-CMB)*:** After 5 min exposure, *p*-CMB had no effect on YAC-1 morphologic responses. The *p*-CMB inhibited bead-wrapping after 30

min, with significant reductions noted at 20 – 100 uM ($p < 0.001$; [$IC_{50}$] = 23.5 uM; see Table 5.2 and Fig. 5.6-B).

***Methyl Mercuric Chloride ($CH_3HgCl$):*** After 5 min pre-treatment with $CH_3HgCl$, the percentage of YAC-1 cells wrapping around the attached bead was reduced at 20 – 100 uM ($p < 0.05$; [$IC_{50}$] = 21.8 uM, see Table 5.2). After 30 min exposure, morphologic responses were further reduced, with effects noted at concentrations of 10 – 100 uM $CH_3HgCl$ ($p < 0.001$; [$IC_{50}$] = 5.7 uM; see Table 5.2 and Fig. 5.6-C).

***Thimerosal (TMS)*:** A 5 min exposure to TMS reduced YAC-1 morphologic responses at 10 – 100 uM ($p < 0.05$; [$IC_{50}$] = 5.4 uM, see Table 5.2). After 30 min the concentration response curve was somewhat different, although statistically, TMS effects on morphology were relatively unchanged, with an [$IC_{50}$] value of 5.4 uM and effects again seen at 10 – 100 uM ($p < 0.001$; see Table 5.2 and Fig 5.6-D).

***Bead treatment controls*:** Pre-treatment of anti-CD3 beads with the mercury compounds had no effect on morphologic responses. Morphologic changes in response to PLL or isotype control anti-TNP antibody-coated beads were reduced as compared to the anti-CD3 bead response, with between 3 and 7% of untreated wrapping around the bead at the 5 or 30 min time points ($p < 0.001$ for both PLL and TNP beads at 5 or 30 min; see Fig. 5.8-B and E).

### 5.5.3 Reorientation of the microtubule organizing centre (MTOC) and Golgi apparatus in response to anti-CD3 bead binding

Approximately 55 and 53% of untreated YAC-1 cells forming stable conjugates with the anti-CD3-coated beads also had the microtubule organizing centre (MTOC)

lying adjacent to the bead at the 5 and 30 min time points, respectively (see Fig. 5.8-C to F, control values).

***Mercuric Chloride ($HgCl_2$)*:** The percentage of conjugated YAC-1 cells reorienting the MTOC towards the attached bead was not significantly different from untreated control cells after 5 min pre-treatment with $HgCl_2$. No changes in the appearance of the microtubules, MTOC and Golgi were detectable microscopically at this time. After 30 min, effects were noted at 60 - 100 uM ($p < 0.001$; [$IC_{50}$] = 60.1 uM; see Table 5.3 and Fig 5.7-A). These reductions in polarization responses were not accompanied by a loss of microtubule/MTOC staining, except at 80-100 uM $HgCl_2$ (see Fig. 5.10-A), where the MTOC was not visualized in some cells though MTOC staining generally appeared normal (see Figs. 5.4-A to C). Occasionally, failure to identify the MTOC was associated with increased peripheral tubulin staining (see 5.4-B) or the appearance of randomly oriented microtubules throughout the cell (see 5.4-C).

***Para-Chloromercuribenzoate (p-CMB)*:** After 5 min exposure, *p*-CMB had no effect on YAC-1 cytoskeletal reorientation responses (see Fig. 5.7-B). As for $HgCl_2$, no changes in the appearance of the microtubules, MTOC and Golgi were detectable microscopically at this time. The MTOC reorientation response was inhibited after 30 min at 40 – 100 uM ($p < 0.001$; [$IC_{50}$] = 41.2 uM; see Table 5.3 and Fig. 5.10-B). These reductions in polarization responses were not accompanied by a loss of microtubule/MTOC staining. Where it was not possible to identify the MTOC (see Fig. 5.10-B), the loss of the MTOC was associated with increased peripheral tubulin staining or the appearance of randomly oriented microtubules throughout the cell (see Fig. 5.4-D).

***Methyl Mercuric Chloride ($CH_3HgCl$)***: There was a trend toward reduced reorientation responses after 5 min pre-treatment with $CH_3HgCl$ ($p = 0.0585$), but it was not possible to calculate an [$IC_{50}$] value (see Table 5.3). The effects were partly a function of a loss in microtubule staining, which was first evident at concentrations just above those reducing the percentages of YAC-1 cells exhibiting polarized reorientation responses. The loss of microtubule staining progressed to complete loss of an identifiable MTOC or Golgi at higher concentrations of $CH_3HgCl$ (see Fig. 5.10-C). After 30 min exposure, reorientation responses were significantly reduced, with effects noted at 20 – 100 uM ($p < 0.001$; [$IC_{50}$] = 18.2 uM; see Table 5.3 and Fig. 5.7-C). The loss of polarization responses was associated with marked loss of microtubule and MTOC staining (see Fig. 5.4-E), and concomitant loss of Golgi staining (see Fig. 5.9 and 10-C).

***Thimerosal (TMS)*:** A 5 min exposure to TMS reduced YAC-1 reorientation responses at 20 – 100 uM ($p < 0.05$; [$IC_{50}$] = 20.5 uM, see Table 5.3). As for $CH_3HgCl$, the effects reflected reduced microtubule staining (see Fig. 5.9 and 10-D). After 30 min TMS effects noted at 10 – 100 uM ($p < 0.001$; [$IC_{50}$] = 9.3 uM, see Table 5.3 and Fig 5.7-D). Similar to $CH_3HgCl$ and the effects seen at 5 min, the loss of polarization responses at 30 min was associated with marked loss of microtubule and MTOC staining (see Fig. 5.4-F), and concomitant loss of Golgi staining (see Fig. 5.10-D).

***Bead treatment controls*:** Pre-treatment of anti-CD3 beads with the mercury compounds had no effect on MTOC reorientation. Reorientation of the MTOC toward PLL-coated beads occurred in approximately 22 and 18% of conjugated YAC-1 cells at the 5 or 30 min time points, respectively ($p < 0.001$ for both 5 and 30 min; see Fig. 5.8-C and F). Among the untreated YAC-1 cells bound to isotype control anti-TNP antibody-

coated beads, approximately 16 and 21% of had the MTOC adjacent to the bead at the 5 or 30 min time points, respectively ($p < 0.001$ for both 5 and 30 min; see Fig. 5.8-C and F).

## 5.6 DISCUSSION

The anti-CD3 coated latex microbeads provided a simple model to study the effects of mercury on the immunological synapse. However, as the anti-CD3 antibody is held rigid on the bead surface, the model does not allow for co-aggregation and migration of cell surface receptors as typically occurs during formation of cell-to-cell conjugates (Anton van der Merwe et al., 2000). The YAC-1 cells nonetheless formed stable conjugates with the anti-CD3-coated beads and specifically induced both morphologic changes and reorientation of intracellular structures in response to bead binding. While the YAC-1 cells formed conjugates with PLL-coated beads at levels similar to anti-CD3 beads, wrapping of the beads did not occur. In addition, reorientation of the MTOC was seen in less than 25% of cells bound to the PLL beads, a figure considered consistent with random MTOC orientation (Lowin Kropf et al., 1998). Isotype control anti-TNP antibody-coated beads failed to induce conjugate formation, morphologic responses or MTOC reorientation.

All forms of mercury tested reduced formation of cell-bead conjugates and morphologic and polarization responses to bead binding. The $CH_3HgCl$ and TMS were the most potent inhibitors of bead-related variables, while the curves for the *p*-CMB data tended to fall intermediate to those produced by $CH_3HgCl$ and TMS and that of $HgCl_2$. In addition, there were two general patterns of responses produced by the mercury compounds. The data plots, [$IC_{50}$] values and effects on microtubules produced by

$CH_3HgCl$ and TMS were quite similar. After 5 min pre-incubation, both $CH_3HgCl$ and TMS produced moderate reductions in MTOC reorientation, with pronounced effects on morphologic responses. These effects were accompanied by a decrease in microtubule and MTOC staining. After 30 min, all the bead-binding parameters were markedly inhibited at low concentrations of $CH_3HgCl$ or TMS, accompanied by a concentration-dependent loss of microtubules and identifiable MTOC or Golgi complex. The loss of discernable Golgi structures stained with WGA is likely due to coincident loss of the associated microtubule array. The Golgi apparatus is actively maintained in a perinuclear position through the action of microtubules, molecular motor activity and other factors (Rios and Bornens, 2003). The fate of the microtubules and Golgi complex are interlinked during normal mitotic cycling (Moskalewski and Thyberg, 1990) and also following treatment with microtubule-disrupting drugs (Robbins and Gonatas, 1964; Rogalski and Singer, 1984). While the toxicity of $CH_3HgCl$ is thought to involve multiple mechanisms (Ponce et al., 1994), methylmercury has been shown to specifically attack microtubules in cultured cells at concentrations that inhibit cell growth (Brown et al., 1988; Cadrin et al., 1988; Imura et al., 1980; Sager, 1988; Wasteneys et al., 1988). TMS is also a known spindle poison capable of disrupting cellular microtubules (Voutsinas et al., 1997) and inhibiting *in vitro* tubulin polymerization (Brunner et al., 1991; Wallin and Hartley-Asp, 1993). Similarly, in this study, the loss of microtubule integrity in $CH_3HgCl$- and TMS-treated YAC-1 cells appears to underlie the reductions in conjugate formation, and morphologic and cytoskeletal reorientation responses in the anti-CD3-coated bead binding assay.

In contrast, alterations in bead-binding parameters occurred without discernable loss of microtubules in $HgCl_2$- and *p*-CMB-treated YAC-1 cells. Neither $HgCl_2$ nor *p*-CMB inhibited conjugate formation, morphologic responses, MTOC reorientation or the appearance of microtubules/MTOC in YAC-1 cells after 5 min pre-treatment. After 30 min pre-incubation, all bead binding variables were reduced by $HgCl_2$ and *p*-CMB, in the absence of the marked loss of microtubule, MTOC and Golgi staining seen with concentrations of $CH_3HgCl$ or TMS producing similar effects on bead binding. This result is consistent with other studies, where mercuric ion ($Hg^{2+}$) has been shown to disrupt microtubule networks only to the same extent as other cellular organelles (Imura et al., 1980). As $Hg^{2+}$ is a more potent inhibitor of *in vitro* tubulin polymerization than $CH_3HgCl$ (Imura et al., 1980; Miura et al., 1984), it would appear unlikely that free $Hg^{2+}$ was present in the cytosol at the time when the loss of bead-binding responses was observed.

However, inhibition of cytoskeletal polarization in $HgCl_2$- and *p*-CMB-treated YAC-1 cells may nonetheless have been due to minor losses in assembled microtubules (particularly in the cortical regions most intimately involved in morphologic responses to cell-bead binding) not evident to the naked eye by fluorescence microscopy, similar to reductions in endocytosis and subsequent processing following low-dose colcemid exposure producing only minimal microtubule disruption (Caron et al., 1985). Where the MTOC or Golgi were not clearly identifiable in $HgCl_2$ and, in particular, *p*-CMB-treated cells, it was not due to loss of overall tubulin staining, but rather to loss of an identifiable MTOC within cells with otherwise normal microtubule architecture. Less commonly, failure of polarization was seen in cells with an apparently normal amount of

microtubules scattered haphazardly throughout the cell or concentrated at the periphery. The significance of this finding is unknown. It is possible that these effects were artefacts of the fixation procedure, as cells with similar microtubule arrangements were occasionally seen in other treatment groups, or the effect may perhaps be secondary to disengagement of microtubules from the MTOC or cell membrane attachments, disruption of actin or other cytoskeletal components. Alternately, stabilization of microtubules similar to that produced by chemotherapeutic agents like taxol (Abal et al., 2003) could theoretically prevent the cytoskeletal remodelling necessary for polarization response. However, in cytotoxic T lymphocytes (CTL), microtubule stabilization by taxol has no effect on CTL polarization or release or cytotoxic granules toward target cells (Knox et al., 1993).

Morphologic and polarization results obtained after 30 min pre-incubation with higher concentrations of the mercury compounds must nonetheless be interpreted with caution as conjugate formation was almost completely inhibited: the results, particularly for higher mercury concentrations, often reflect scoring of less than 100 cell-bead conjugates. As such, the results may be appear skewed, as seen, for example, by the trend to more normal MTOC polarization responses at 30 min for 50 and 60 uM TMS, following almost complete inhibition of the response at lower concentrations (see Fig. 5 D).

The reductions in bead binding responses were not a function of mercury blockade of variable (binding) regions on the anti-CD3 antibody, as pre-treatment of the anti-CD3 beads with 100 uM concentrations of each of the mercury compounds did not affect conjugate formation, morphology or polarization responses in the YAC-1 cells. It

is therefore considered unlikely that mercury effects in the bead conjugation assays occurred secondary to blockade of CD3 epitopes.

Given the complexity of the formation of the immunological synapse, multiple mechanisms may underlie the inhibition of lymphocyte polarization by mercury compounds. The cytoskeletal polarization response may involve multiple signalling components, from ligation and activation of cell surface receptors, to the formation of stable signalling scaffolds within the cell and creation of gradients of intracellular calcium across the cytosol – all of which may be influenced by mercury treatment. The bead-binding assays may therefore produce results that may not correlate well with those seen in assays where the beads were not used. However, the appearance of microtubules, the MTOC and Golgi in both conjugated and unconjugated cells were similar, suggesting mercury treatment did not have different effects as a result of bead binding.

While a microtubule-centred mechanism for the effects of $CH_3HgCl$ or TMS on lymphocyte polarization responses is attractive, actin microfilament and microtubule networks are interconnected, and are also linked to the cell membrane through integrins and cytoskeletal linker proteins which participate in the formation of the immunological synapse and associated signalling complexes (Burn et al., 1988; Das et al., 2002; Faure et al., 2004; Kupfer et al., 1990). However, reduced polarization responses in $HgCl_2$- and *p*-CMB-treated YAC-1 cells may involve additional mechanisms, including subtle cytoskeletal alterations not apparent on a visual examination of cell-bead conjugates. We are therefore quantifying tubulin and actin levels in YAC-1 cells exposed to the four mercury compounds, and assessing TCR/CD3 receptor expression, and intracellular

phosphotyrosine and calcium levels to further elucidate the mechanisms of the altered bead binding responses.

**Table 5.1:** Effects of mercuric chloride ($HgCl_2$,), methylmercuric chloride ($CH_3HgCl$), *p*-chloromercuribenzoate (*p*-CMB) and thimerosal (TMS) on the percentage of YAC-1 lymphoma cells forming conjugates with anti-CD3 antibody-coated 6.0 um latex beads following 5 or 30 min exposure *in vitro* with subsequent addition of the beads. The concentration producing 50% reduction in conjugate formation ([$IC_{50}$]) was calculated by non-linear regression of concentration-response data normalized to % control response [% control response = (% Hg-treated cells conjugated with anti-CD3-coated beads - % cells binding isotype control antibody-coated beads)/(% treatment control conjugated cells - % cells binding control beads); n = minimum of five replicates for each data point].

| Time (min) | **[$IC_{50}$] (uM)** | | | |
|---|---|---|---|---|
| | **$HgCl_2$** | ***p*-CMB** | **$CH_3HgCl$** | **TMS** |
| **5** | --- | --- | --- | --- |
| **30** | 47.1 | 22.3 | 7.2 | 3.8 |

**Table 5.2:** Effects of mercuric chloride ($HgCl_2$,), methylmercuric chloride ($CH_3HgCl$), *p*-chloromercuribenzoate (*p*-CMB) and thimerosal (TMS) on the percentage of YAC-1 lymphoma cells (conjugated to anti-CD3 antibody-coated 6.0 um latex beads) wrapping around at least 50% of the circumference of the bead following 5 or 30 min exposure *in vitro* with subsequent addition of the beads. The concentration producing 50% reduction in cells wrapping the beads ($[IC_{50}]$) was calculated by non-linear regression of concentration-response data normalized to % control response [% control response = (% Hg-treated cells wrapping around anti-CD3-coated beads - % cells wrapping isotype control antibody-coated beads)/(% treatment control wrapped cells - % cells wrapping control beads); n = minimum of five replicates for each data point].

| Time (min) | $[IC_{50}]$ (uM) | | | |
|---|---|---|---|---|
| | **$HgCl_2$** | ***p*-CMB** | **$CH_3HgCl$** | **TMS** |
| **5** | --- | --- | 21.8 | 5.4 |
| **30** | 50.0 | 23.5 | 5.7 | 5.3 |

**Table 5.3:** Effects of mercuric chloride ($HgCl_2$,), methylmercuric chloride ($CH_3HgCl$), *p*-chloromercuribenzoate (*p*-CMB) and thimerosal (TMS) on the percentage of YAC-1 lymphoma cells (conjugated to anti-CD3 antibody-coated 6.0 um latex beads) having the microtubule organizing centre (MTOC) and/or Golgi apparatus oriented directly adjacent the bead following 5 or 30 min exposure *in vitro* with subsequent addition of the beads. The concentration producing 50% reduction in cells reorienting the MTOC next to the beads ($[IC_{50}]$) was calculated by non-linear regression of concentration-response data normalized to % control response [% control response = (% Hg-treated cells reoriented toward anti-CD3-antibody-coated beads - % cells reoriented toward isotype control antibody-coated beads)/(% treatment control reoriented cells - % cells reoriented toward control beads); n = minimum of four replicates for each data point].

| Time (min) | $[IC_{50}]$ (uM) | | | |
|---|---|---|---|---|
| | **$HgCl_2$** | ***p*-CMB** | **$CH_3HgCl$** | **TMS** |
| **5** | --- | --- | 60.1 | 20.5 |
| **30** | 60.1 | 41.2 | 18.2 | 9.3 |

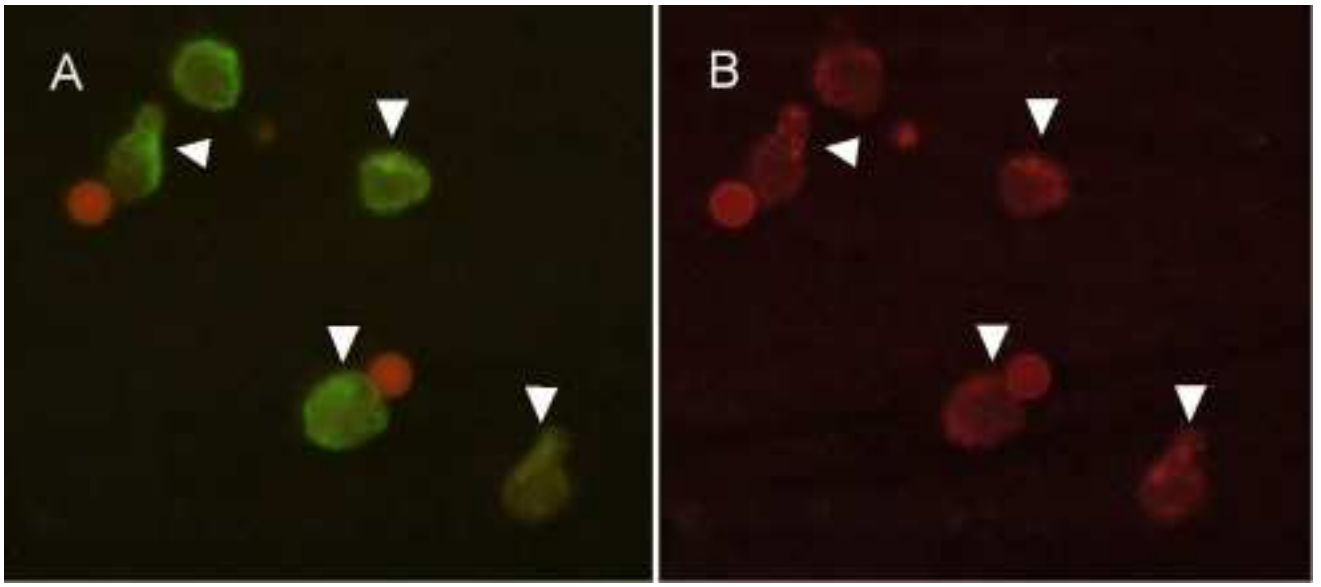


**Figure 5.1:** Identification of (**A**) the microtubule organizing centre (MTOC; arrowheads) in YAC-1 lymphoma cells bound to anti-CD3 antibody-coated 6 uM latex microspheres by indirect immunofluorescence staining of β-tubulin with mouse anti-β-tubulin antibody and Alexa-488®-conjugated goat-anti-mouse IgG (GAM) antibody and (**B**) counterstaining with Texas-Red®-conjugated wheat germ agglutinin (WGA) to identify the trans-Golgi (arrowheads).

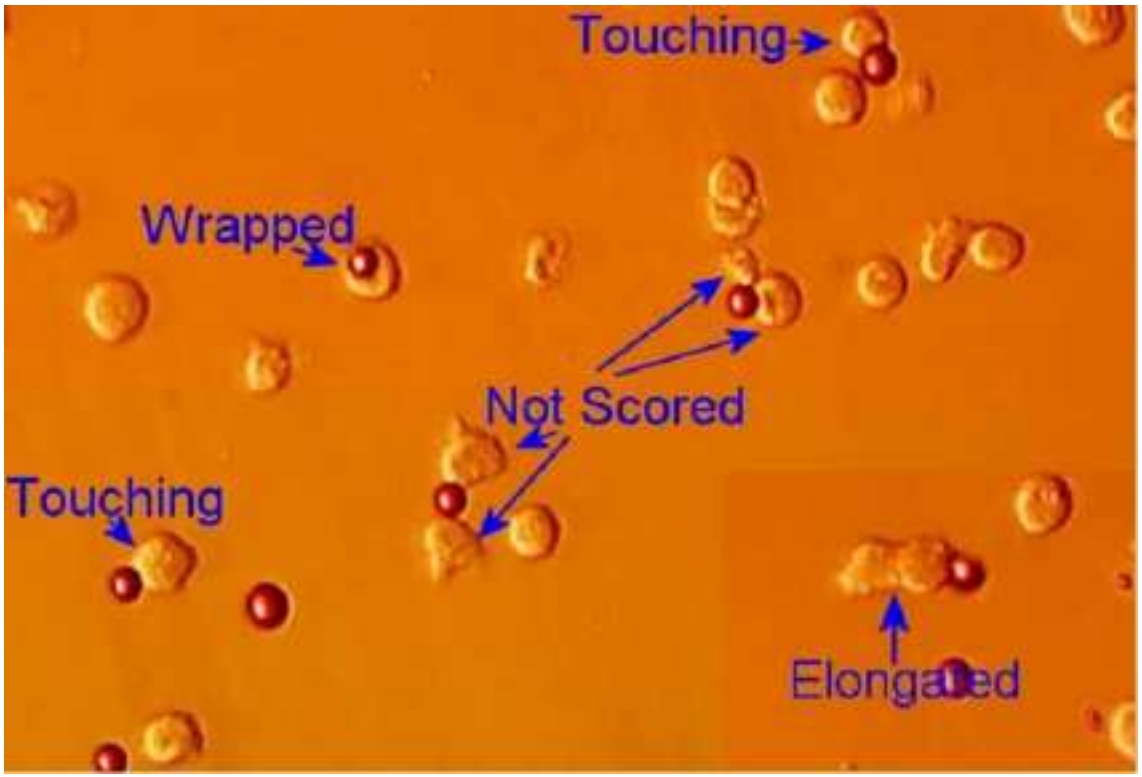


**Figure 5.2:** Illustration of scoring of morphologic responses of YAC-1 cells to anti-CD3 bead binding. Single cell/bead conjugates were scored as: (1) wrapped (where the cell contact area extended at least halfway around the circumference of the bead, as assessed by placing the cross-hairs of the microscope photo mask over the bead); (2) touching (where area of contact was minimal and the YAC-1 cell retained a roughly spherical shape); or (3) elongated (where the area of contact was minimal or wrapped around the bead while the cell adopted an elongated morphology, such that the length of the cell exceeded two times its width). Conjugates of more than one cell or bead were not scored.

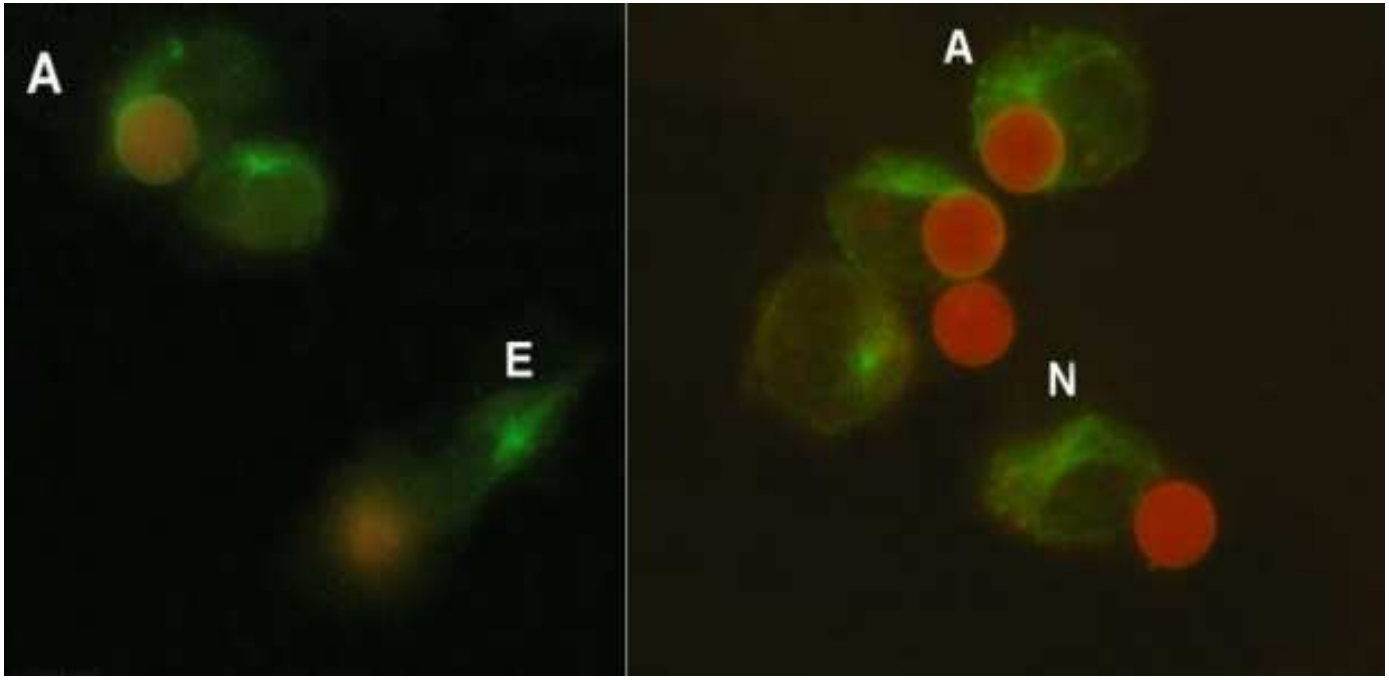


**Figure 5.3:** Illustration of scoring of microtubule organizing center (MTOC) orientation of YAC-1 cells to anti-CD3 bead binding. Single cell/bead conjugates were scored as: (1) adjacent (directly adjacent to or flattened onto the bead; A); (2) neutral (in the middle of the cell or on the side opposite the area of bead contact; N); or (3) elongated (stretched the length of cell with an elongated morphology; E). Where the MTOC was not visualised, the location of the Golgi was scored, if present. In cells where neither the MTOC or Golgi were seen, a 'not identified' score was assigned. Conjugates of more than one cell or bead were not scored.

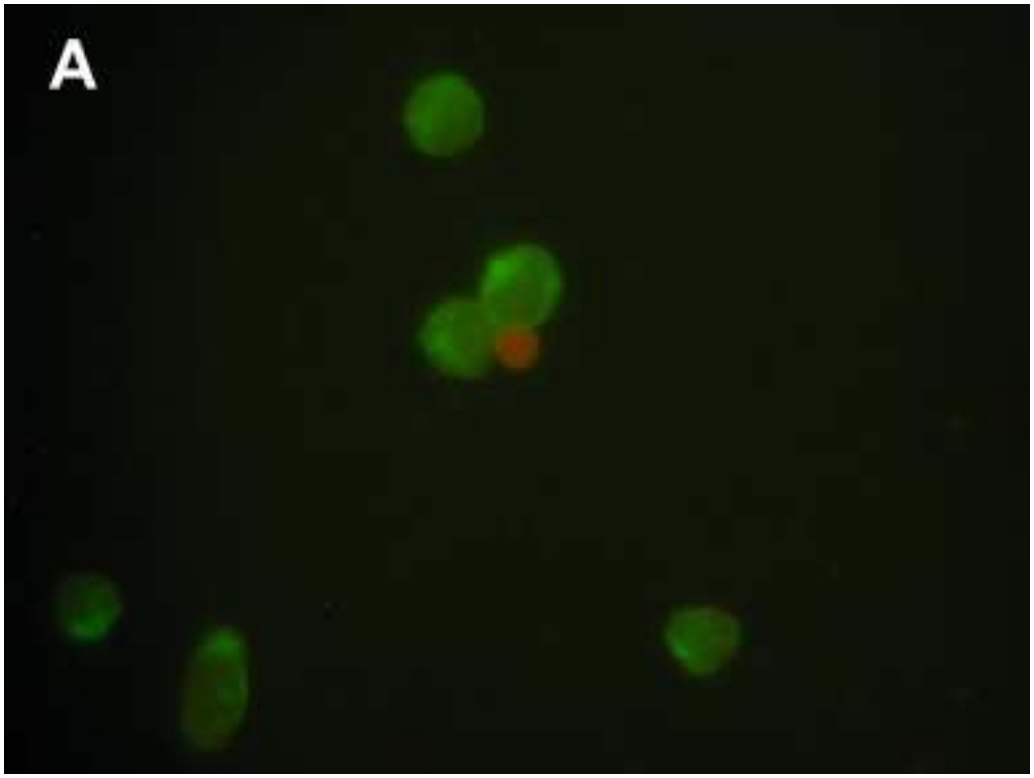


**Figure 5.4:** Representative images of -β-tubulin fluorescence YAC-1 cells conjugated to anti-CD3 beads and treated for 30 min with (**A**) 90 uM mercuric chloride ($HgCl_2$); (**B**) 100 uM $HgCl_2$ (arrowhead indicates YAC-1 cell with increased peripheral staining and loss of identifiable microtubule organizing center [MTOC]); (**C**) 80 uM $HgCl_2$ (arrowhead indicates YAC-1 cell with randomly oriented microtubules); (**D**) 60 uM *p*-chloromercuribenzoate (*p*-CMB; arrowhead indicates YAC-1 cell with randomly oriented microtubules); (**E**) 30 uM methylmercuric chloride ($CH_3HgCl$); (**F**) 20 uM thimerosal (TMS).

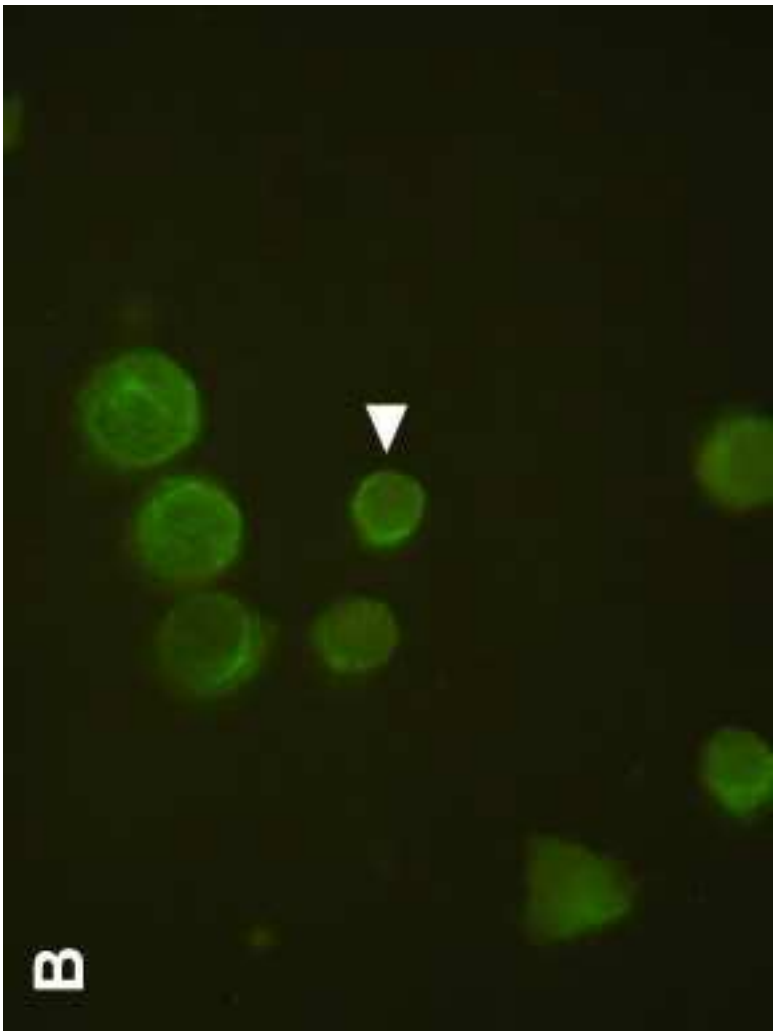
B

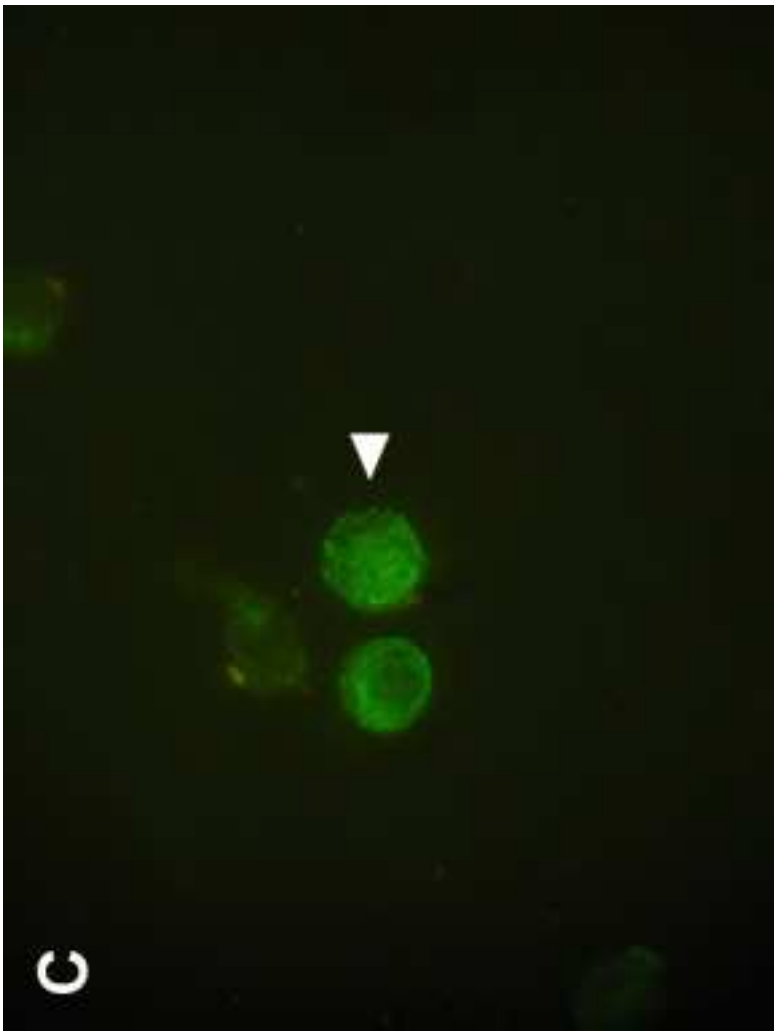
C

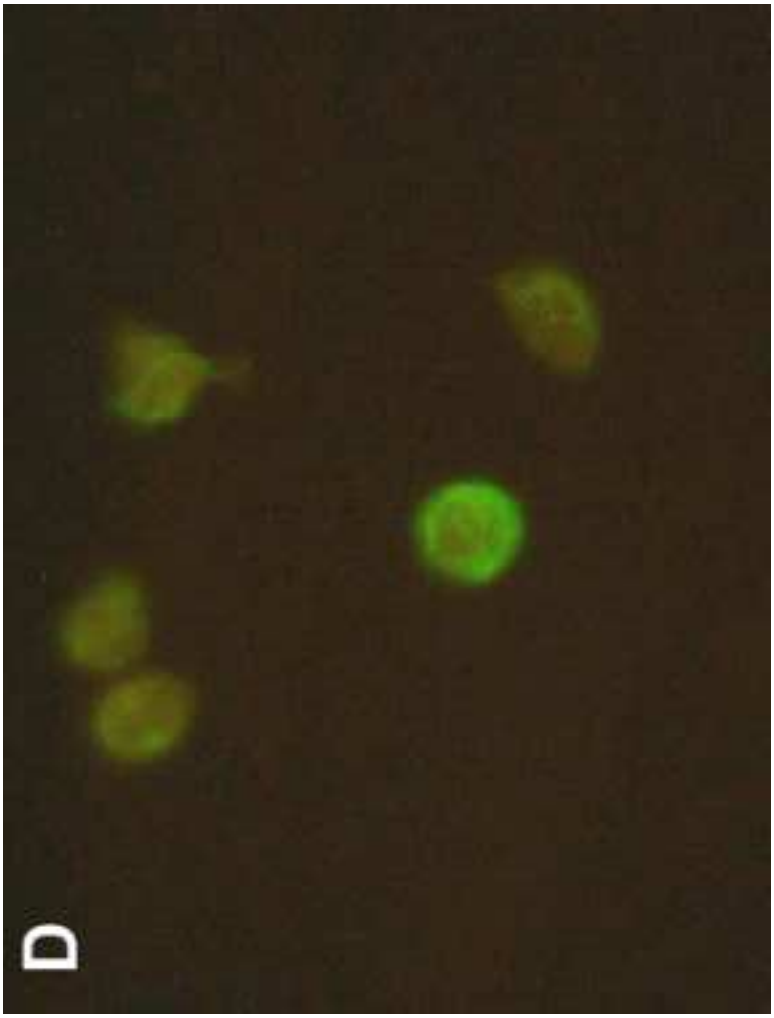
D

E

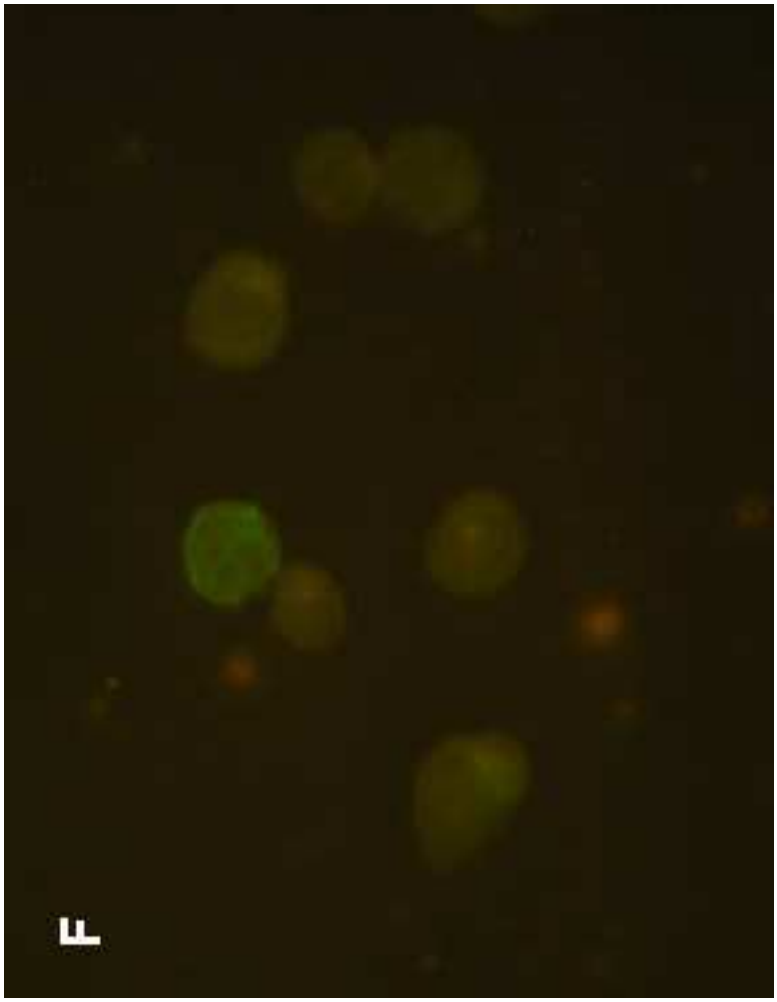
E

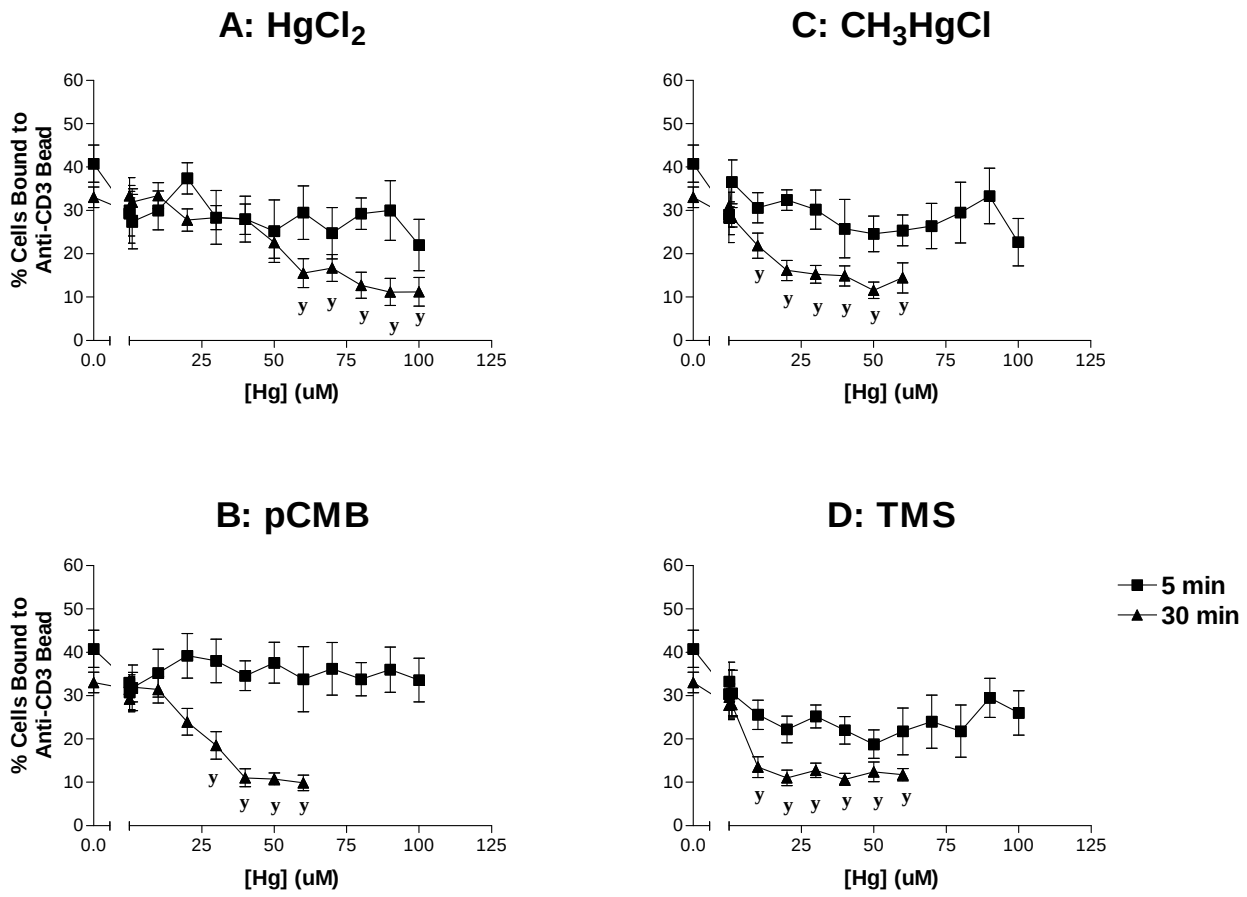


**Figure 5.5:** Effects of mercuric chloride ($HgCl_2$; A), *p*-chloromercuribenzoate (*p*-CMB; B), methylmercuric chloride ($CH_3HgCl$; C), and thimerosal (TMS; D) on the percentage of YAC-1 lymphoma cells forming conjugates with anti-CD3 antibody-coated 6.0 um latex beads following 5 min or 30 min exposure *in vitro* with subsequent addition of the beads (mean ± SEM; n = minimum of 5 replicates for each data point; y indicates values differ significantly from control treatment values at 30 min, $p < 0.05$).

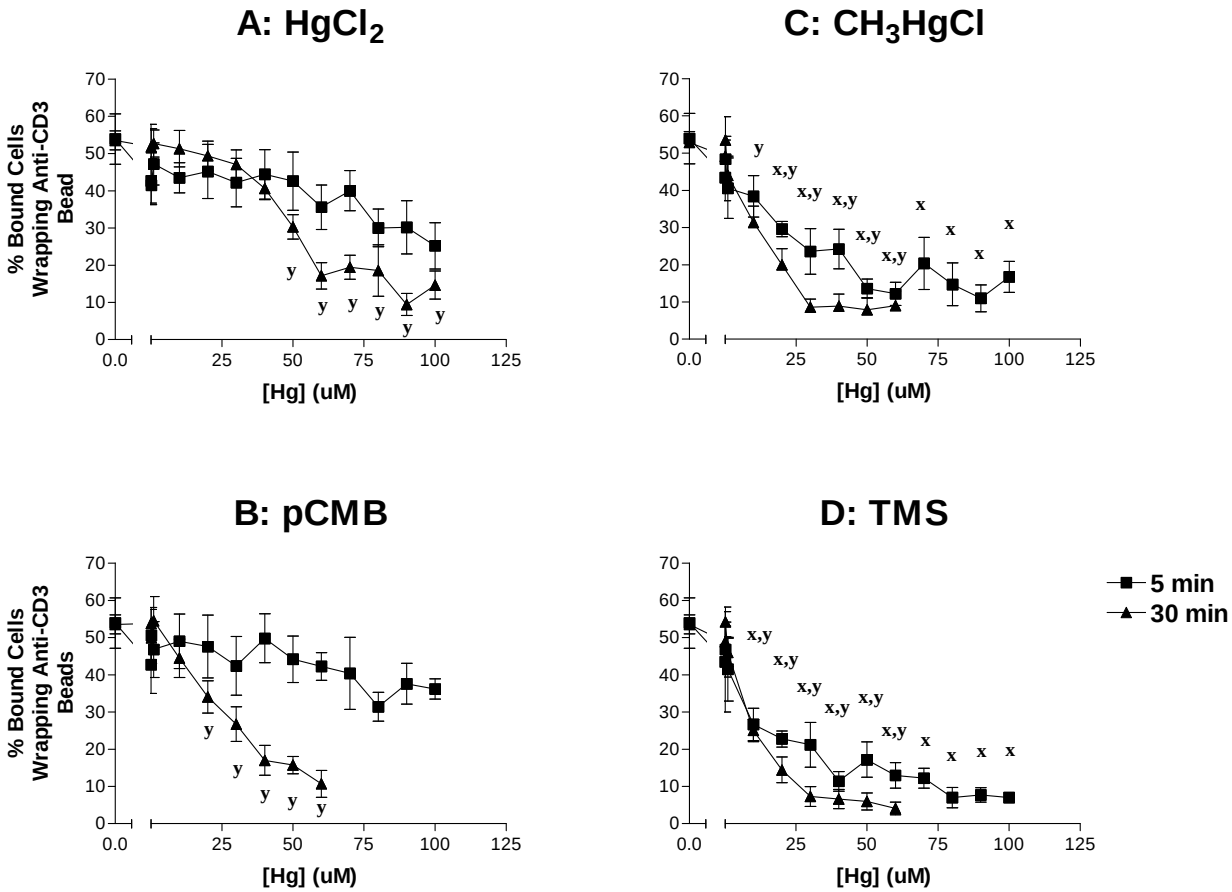


**Figure 5.6:** Effects of mercuric chloride ($HgCl_2$; A), *p*-chloromercuribenzoate (*p*-CMB; B), methylmercuric chloride ($CH_3HgCl$; C), and thimerosal (TMS; D) on the percentage of YAC-1 lymphoma cells conjugated to anti-CD3 antibody-coated 6.0 um latex beads wrapping around at least 50% of the circumference of the bead following 5 min or 30 min exposure *in vitro* with subsequent addition of the beads (mean ± SEM; n = minimum of 5 replicates for each data point; x and y indicate values differ significantly from control treatment values at 5 and 30 min respectively, $p < 0.05$).

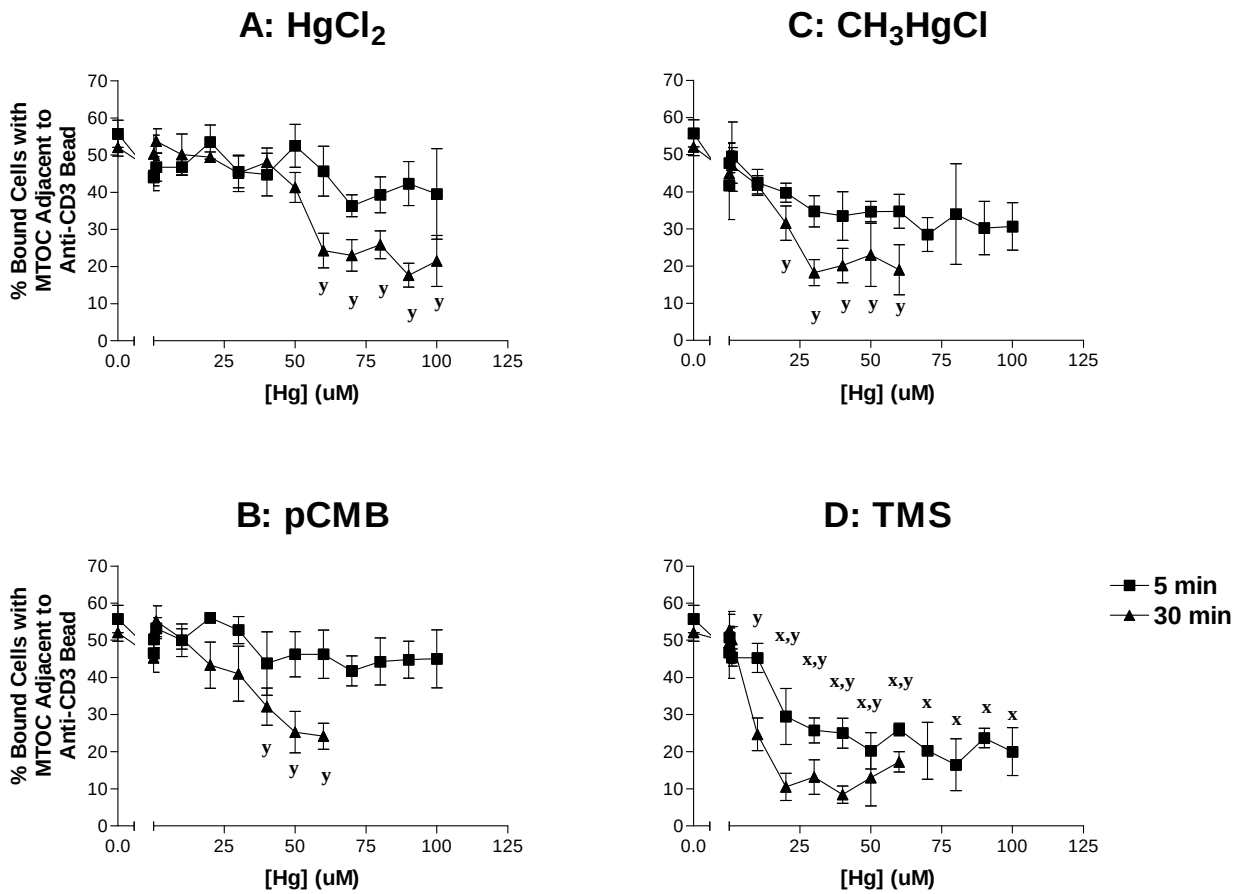


**Figure 5.7:** Effects of mercuric chloride ($HgCl_2$; A), *p*-chloromercuribenzoate (*p*-CMB; B), methylmercuric chloride ($CH_3HgCl$; C), and thimerosal (TMS; D) on the percentage of YAC-1 lymphoma cells conjugated to anti-CD3 antibody-coated 6.0 um latex beads with the microtubule organizing centre (MTOC) oriented directly adjacent the bead following 5 min or 30 min exposure *in vitro* with subsequent addition of the beads (mean ± SEM; n = minimum of 4 replicates for each data point; x and y indicate values differ significantly from control treatment values at 30 min, $p < 0.05$).

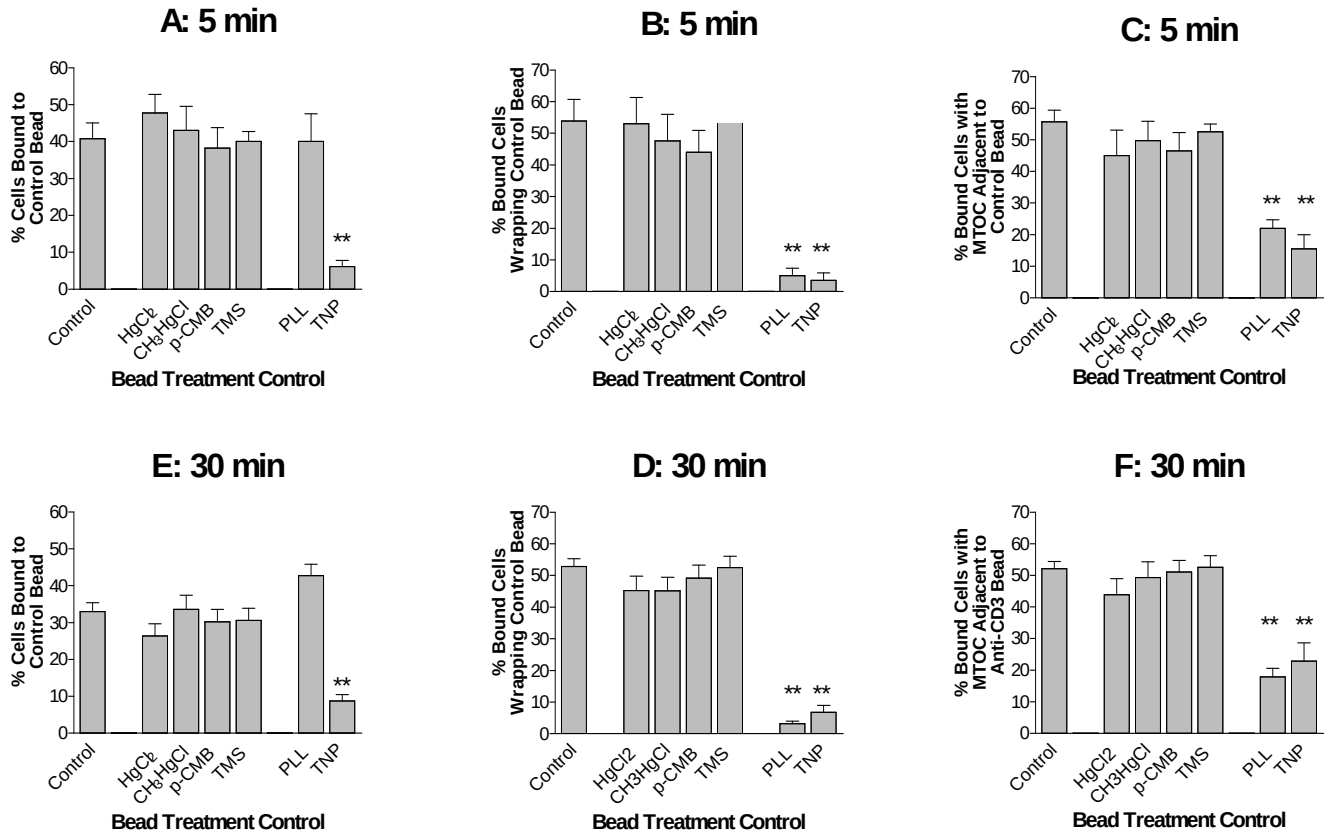


**Figure 5.8:** Effects of mercuric chloride ($HgCl_2$)-, methylmercuric chloride ($CH_3HgCl$)-, *p*-chloromercuribenzoate (*p*-CMB)- or thimerosal (TMS)-treated anti-CD3 beads, or poly-L-lysine (PLL)- and anti-trinitrophenol antibody (TNP)-coated 6.0 um latex beads on the percentage of YAC-1 lymphoma cells forming cell-bead conjugates (A, D), wrapping around at least 50% of the bead circumference (B, E) or having with the microtubule organizing centre (MTOC) oriented directly adjacent to the bead (C, F) following 5 (A, B, C) and 30 min (D, E,F) incubation with untreated media *in vitro* with subsequent addition of the beads; (mean + SEM; n = minimum of 4 replicates for each data point; * and ** indicate values differ significantly from anti-CD3 bead control values, $p < 0.05$ and $p < 0.001$, respectively).

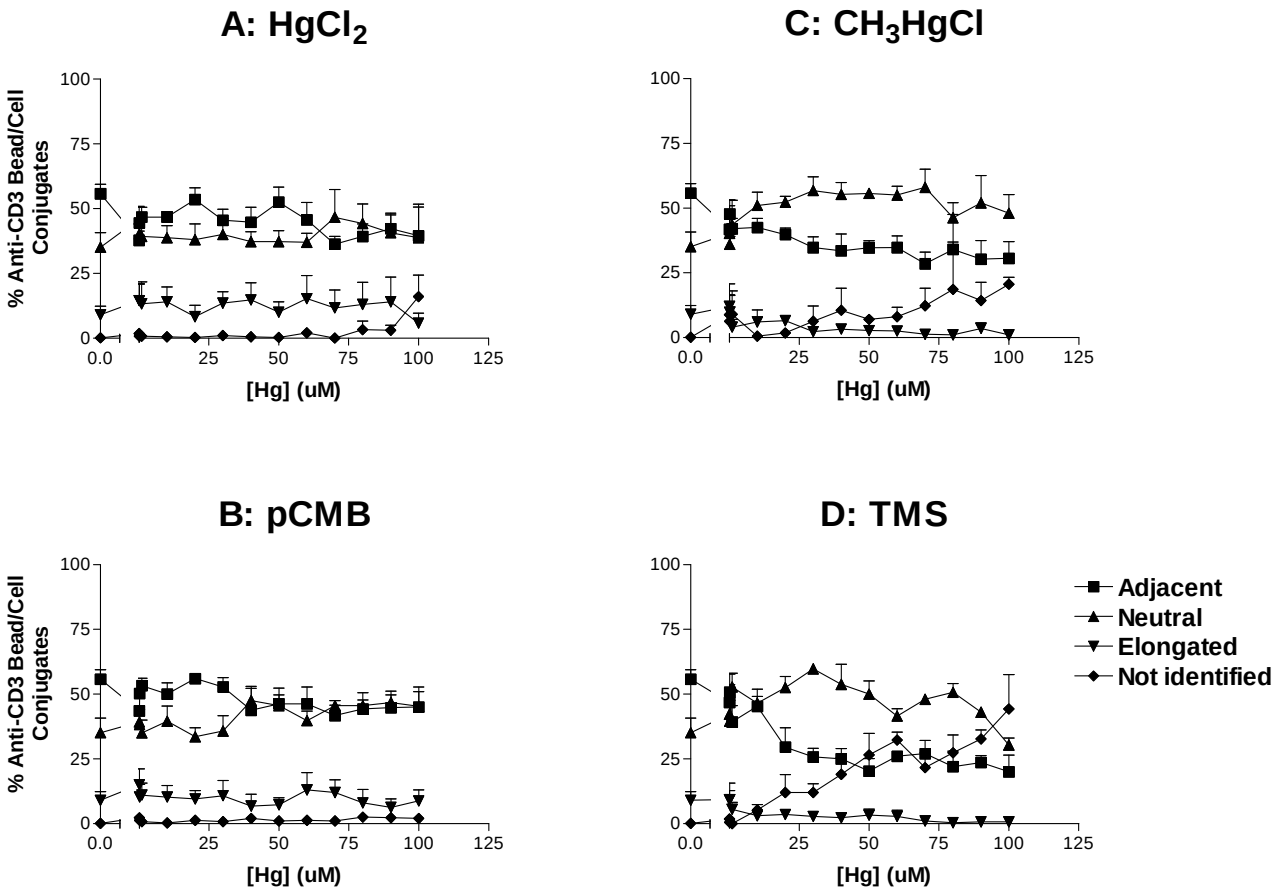


**Figure 5.9:** Effects of mercuric chloride ($HgCl_2$; A), *p*-chloromercuribenzoate (*p*-CMB; B) methylmercuric chloride ($CH_3HgCl$; C), and thimerosal (TMS; D) on the percentage of YAC-1 lymphoma cells conjugated to anti-CD3 antibody-coated 6.0 um latex beads having the microtubule organizing centre (MTOC) oriented in each of four positions [(i) directly adjacent to the bead, (ii) neutral (centrally located or on the opposite side of the cell from the bead), (iii) elongated (MTOC extends the length of the cell, which is itself elongated) and (iv) not identified] following 5 min exposure *in vitro* with subsequent addition of the beads (mean + SEM; n = min of 4 replicates for each data point).

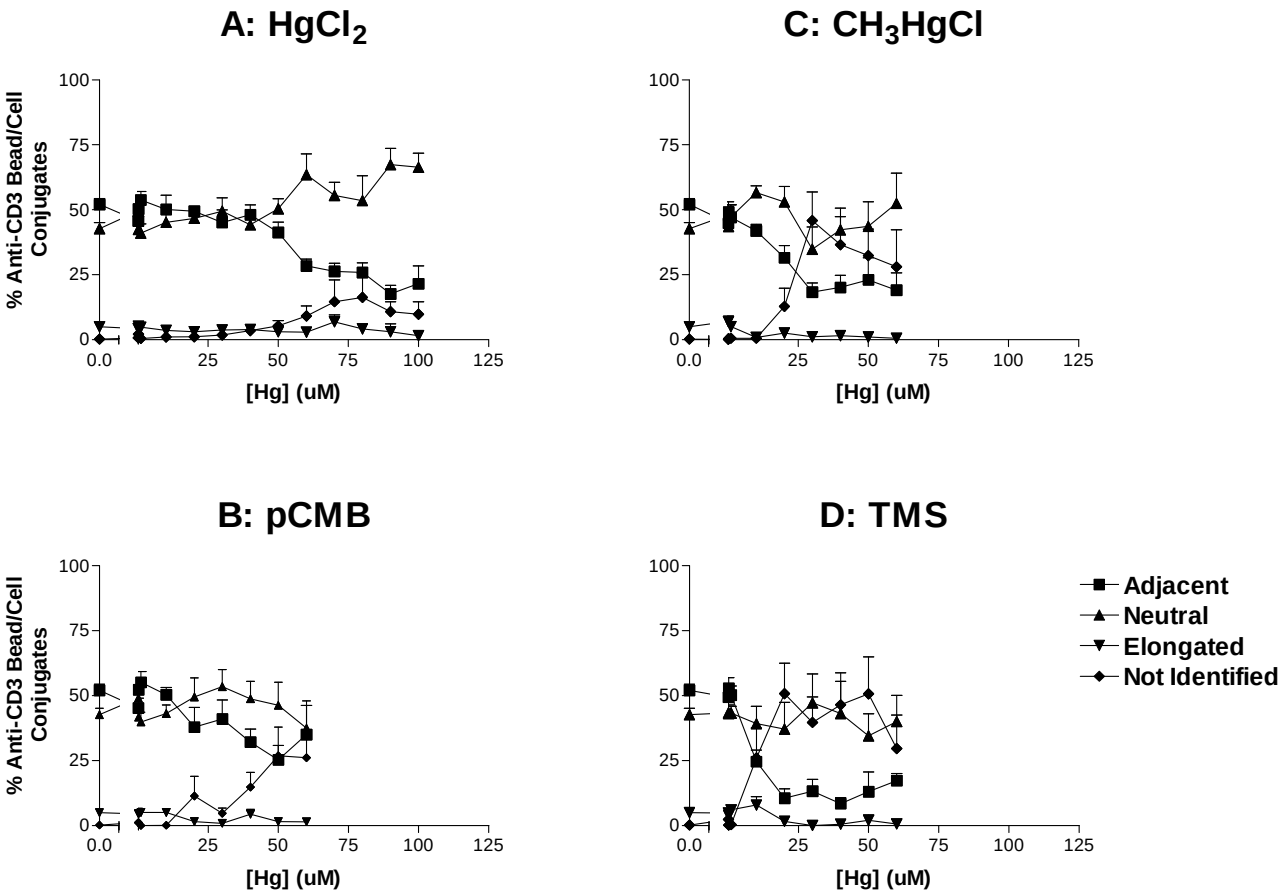


**Figure 5.10:** Effects of mercuric chloride ($HgCl_2$; A), *p*-chloromercuribenzoate (*p*-CMB; B) methylmercuric chloride ($CH_3HgCl$; C), and thimerosal (TMS; D) on the percentage of YAC-1 lymphoma cells conjugated to anti-CD3 antibody-coated 6.0 um latex beads having the microtubule organizing centre (MTOC) oriented in each of four positions [(i) directly adjacent to the bead, (ii) neutral (centrally located or on the opposite side of the cell from the bead), (iii) elongated (MTOC extends the length of the cell, which is itself elongated) and (iv) not identified] following 30 min exposure *in vitro* with subsequent addition of the beads (mean + SEM; n = min of 4 replicates for each data point).

# 6.0

# EFFECTS OF BRIEF EXPOSURES TO VARIOUS FORMS OF HG ON YAC-1 LYMPHOMA CELL VIABILITY

## 6.1 Relationship to overall project

This material comprises the results of Specific Aim I, objectives (a) and (b, referring to the methylthiazolyldiphenyl-tetrazolium bromide (MTT) assay of cell viability. As this data was primarily used to establish appropriate ranges of mercury concentrations to be used for the assays to follow, or in the case of specific objective (b), did not produce any particularly interesting effects, it was not included in the first manuscript (Chapter 4). However, there were some unexpected findings that did prove interesting.

## 6.2 ABSTRACT

Cell viability, as assessed by the methylthiazolyldiphenyl-tetrazolium bromide (MTT) assay, was examined in YAC-1 lymphoma cells 24 hr after 1 min – 4 hr exposures to 0.01 – 100 uM concentrations of various mercury compounds (mercuric chloride [$HgCl_2$] methyl mercuric chloride [$CH_3HgCl$], *p*-chloromercuribenzoate [*p*-CMB] and thimerosal [TMS; ethylmercurithiosalicylate]). All forms of mercury tested were toxic to the YAC-1 cell line at micromolar concentrations, ranging from 3.3 – 43.6 uM, with distinct patterns of effects evident in each assay. The concentration-response

curves in the MTT assay were similar 24 hr after 5 min, 30 min or 4 hr exposures for $HgCl_2$ and $CH_3HgCl$. In contrast, both *p*-CMB and TMS exhibited enhanced 24-hr cytotoxicity with increasing exposure time. These findings indicate the two groups of mercury compounds may induce cell death by distinct pathways.

## 6.3 INTRODUCTION

Refer to section 4.3, for relevant background information and rationale.

## 6.4 MATERIALS AND METHODS

### 6.4.1 Preparation of mercury solutions

The preparation of the mercury solutions is described in section 4.4.1

### 6.4.2 Cultured cell line

The preparation of the YAC-1 lymphoma cell line is described in section 4.4.2.

### 6.4.3 Preparation of 96-well plates and addition of cells

Ten uL of the four mercury solutions or media were added to the appropriate well of a 96-well U-bottom tissue culture plate (Nunc, VWR). The plate was placed in a humidified incubator at 37 C with 5% $CO_2$ for a minimum of 30 minutes. After pre-incubation, 10 uL of the prepared cell suspension were added to the mercury-loaded plates. The plates were then returned to the incubator for 5 min, 30 min or 4 hr for the MTT assay.

### 6.4.4 Methylthiazolyldiphenyl-tetrazolium Bromide (MTT) Assay

The MTT (3-[4,5-dimethylthiazol-2-yl]2,5-diphenyl tetrazolium bromide) assay (Mosmann, 1983) was used to assess cell viability 24 hr after brief mercury exposures, with modifications as noted below. The MTT assay is a colorimetric assay system which measures the reduction of a tetrazolium component (MTT) into an insoluble formazan

product by the mitochondria of viable cells. At the end of the mercury exposure, 180 uL of RPMI containing 0.5% fetal bovine serum (RPMI/0.5%FBS) were added to each well and the plates centrifuged at 1200 RPM for two min to recover the cell pellets. The plates were washed three more times and the pellets resuspended in 100 uL complete RPMI. The plates were returned to the incubator for a total of 24 hrs after the addition of cells to the mercury. After 24 hrs, 50 uL of media were removed from each well. Ten uL of 1% saponin (Sigma-Aldrich) in PBS were added to one well of untreated cells (lysis control) and the cell pellet resuspended by gentle trituration. Five uL of MTT reagent (5 mg/mL in phosphate buffered saline [PBS]; Sigma-Aldrich) were added to all wells and the plate returned to the incubator for four hr. After four hr of incubation, 45 uL of media were withdrawn from the wells. One hundred uL of acid alcohol (isopropanol with 0.4 % 1 N HCl) were added to each well to develop the blue colour of the MTT reagent. The intensity of the colour reaction was recorded in a microplate reader (Molecular Devices, Sunnyvale, CA) in dual-filter mode, with the read filter set at 565 uM and the reference filter set at 630 uM. The YAC-1 cell viability was expressed as an adjusted value with reference to the background value (lysis control) as follows:

$$\text{Adjusted \% Control Response} = \frac{(\text{Reading} - \text{Background})}{(\text{No Treatment} - \text{Background})}$$

### 6.4.5 Modifications to MTT (methylthiazolyldiphenyl-tetrazolium bromide (MTT) assay methodology for addition of anti-CD3 beads

The MTT assay was modified to maintain the relationship of cell numbers and mercury concentration with the addition of anti-CD-coated beads. The mercury was

added to the plates as in basic MTT assay method (see Chapter 4 for basic method). Anti-CD3 coated beads were prepared as in Chapter 5.

#### 6.4.5.1 Viability of YAC-1 cells, with addition of anti-CD3 beads before exposure to mercury

The cells were prepared at a concentration of 8 x $10^6$ cells/mL and the anti-CD3-, Hg-treated anti-CD3-, anti-TN*P*- or PLL–coated beads were prepared at 4 x $10^6$ beads/mL. After the pre-incubation of the prepared cell suspension, equal volumes of cells and beads were mixed in 12 x 75 mm polystyrene tubes (Falcon, VWR), vortexed for 1 min and then centrifuged at 1200 RPM for 10 mins to bring the cells and beads into contact. After centrifugation, the plates were vortexed vigourously for 10 secs to break up large cell-bead clumps and to resuspend the cell-bead pellets. Ten uL of cell-bead mixture or complete RPMI were added to the appropriate wells, including all assay controls indicated in section 4.6.1.2 above. The plates were gently vortexed for 10 secs and then returned to a humidified incubator at 37 C with 5% $CO_2$ for 5 min, 30 min or 4 hours. At the end of the incubation period, the cell-bead pellets were gently re-suspended and then 180 uL of RPMI/0.5% FBS was added to each well and the plates centrifuged for 2 min at 1200 RPM to recover the cell pellets. The cells were washed three more times and the cell pellets resuspended in 100 uL complete RPMI. The plates were then returned to the incubator for a total of 24 hrs from the time of the addition of cells to the mercury.

After 24 hr, the plates were removed from the incubator and the remainder of the MTT assay was completed as described in section 4.6.1.2.

#### 6.4.5.2 Viability of YAC-1 cells, with addition of anti-CD3 beads after exposure to mercury

Anti-CD3-, Hg-treated anti-CD3-, anti-TN*P*- or PLL–coated beads were prepared as in section 4.5. The preparation of the cells and plates was as indicated in section 4.6.1.1. At the end of the pre-incubation periods for the cells and plates, 10 uL of YAC-1 cells or complete RPMI (to create assay control wells similar to those in 4.6.1.1. and additional control wells for use of the anti-CD3 beads: beads in media without cells, untreated cells without beads, untreated cells with beads, untreated cells with Hg-treated beads, untreated cells with beads lysed before addition of the MTT reagent, and media only) were added to each well and the plates gently vortexed. The plates were returned to a humidified incubator at 37 C with 5% $CO_2$ for 5 min, 30 min or 4 hours.

### 6.4.6 Statistical Analysis

All statistical analyses were performed using Prism® statistical software (GraphPad Software Incorporated, San Diego, CA). The [$IC_{50}$] values for mercury effects were obtained from non-linear regression of data after log transformation of x values ([Hg]), with T-tests for comparison of [$IC_{50}$] values. The significance of mercury and control treatment effects in the MTT assay were analysed using the Kruskal-Wallis non-parametric one-way analysis of variance and Dunn's multiple comparison tests. For all analyses, treatment values differing from control values at the level of $p < 0.05$ were considered significantly different.

## 6.5 RESULTS

### 6.5.1 Viability of YAC-1 cells, without addition of anti-CD3 beads

All of the mercury compounds tested were toxic to the YAC-1 lymphoma line (see Figs 6.1 and 6.2), but the kinetics of cell death and the $IC_{50}$ values (see Table 6.1), as measured by the MTT assay, differed significantly between the mercury treatments.

***$HgCl_2$ without anti-CD3 beads:*** After 5 min exposure to $HgCl_2$, followed by washing and incubation for 24 hrs, YAC-1 cell viability was significantly reduced at concentrations $\geq$ 50 uM ($p < 0.01$, see Fig. 6.1-A; [$IC_{50}$] = 46.0 uM, see Table 6.1). After 30 min or 4 hr, the cytotoxicity of $HgCl_2$ ([$IC_{50}$] = 41.6 uM and 43.6 uM, respectively; see Table 6.1) and concentration-response curves were similar to the effects produced following a five min exposure (see Fig 6.1-A and Table 6.1), although at 4 hr, YAC-1 viability was reduced at $\geq$ 40 uM ($p < 0.01$, see Fig. 6.1-A).

***Para-Chloromercuribenzoate (p-CMB) without anti-CD3 beads:*** After 5 min exposure, *p*-CMB had no effect on YAC-1 viability (see Fig. 6.1-B). The *p*-CMB began to alter viability after 30 min, with significant reductions in viability at $\geq$ 40 uM ($p < 0.01$, see Fig. 6.1-B), but the effects were not sufficient to calculate an [$IC_{50}$]. The *p*-CMB cytotoxicity continued to increase with exposure time. The viability was reduced at $\geq$ 30 uM after 4 hr ($p < 0.01$, see Fig 6.1-B; [$IC_{50}$] = 33.0 uM, see Table 6.1).

***Methyl Mercuric Chloride ($CH_3HgCl$) without anti-CD3 beads:*** After a 5 min exposure, $CH_3HgCl$ reduced the 24-hr viability at $\geq$ 30 uM ($p < 0.01$, see Fig. 6.1-C; [$IC_{50}$] = 28.5 uM, see Table 6.1). After 30 min, the cytotoxicity ([$IC_{50}$] = 25.1 uM, see Table 6.1) was similar to the effects produced following a 5 min exposure. By 4 hr, the cytotoxicity of $CH_3HgCl$ had increased slightly ([$IC_{50}$] = 20.7 uM), with effects seen at $\geq$ 20 uM ($p < 0.01$), although the concentration-response curve was remarkably similar to that produced following a 5 or 30 min exposure (see Fig 6.1-C and Table 6.1).

***Thimerosal (TMS) without anti-CD3 beads:*** A 5 min exposure to TMS reduced YAC-1 cell viability at ≥ 30 uM ($p < 0.05$, see Fig. 6.1-D; [$IC_{50}$] = 46.0 uM, see Table 6.1). Cytotoxicity associated with TMS increased with exposure time, with [$IC_{50}$] values of 12.6 uM and 3.3 uM and effects seen at ≥ 20 and 10 uM after 30 min and 4 hr exposures, respectively ($p < 0.001$ for each; see Fig 6.1-D and Table 6.1).

***Control Treatments without anti-CD3 beads:*** There were no significant effects produced by the control treatments after either 5 min, 30 min or 4 hr exposure (see Fig. 6.2).

### 6.5.2 Viability of YAC-1 cells, with addition of anti-CD3 beads before mercury exposure

***$HgCl_2$ with anti-CD3 beads added before mercury exposure:*** After 5 min exposure, the 24 hr [$IC_{50}$] of $HgCl_2$ was 59.3 uM (see Fig 6.2-A and Table 6.2), a value significantly higher than when the beads were not added (see Table 6.4), and significant reduction in viability was seen only at ≥ 70 uM. Prior addition of anti-CD3 beads increased 30 min $HgCl_2$ toxicity ([$IC_{50}$] = 35.0 uM; see Tables 6.2. and 6.4) as compared to addition of the beads after mercury. After 4 hr, the toxicity of $HgCl_2$ ([$IC_{50}$] = 44.5 uM; see Table 6.2), was significantly different from that produced by 30 min exposure, but similar to that produced in the absence of anti-CD3 beads (see Table 6.4).

***p-CMB with anti-CD3 beads added before mercury exposure:*** The *p*-CMB had no effect on overall YAC-1 viability after a 5 min exposure (see Fig. 6.2-B), and it was not possible to calculate an [$IC_{50}$]. The toxicity of *p*-CMB increased after 30 min exposure, sufficient to calculate an [$IC_{50}$] of 44.2 uM, similar to that obtained in the absence of the beads (see Tables 6.2 and 6.4). After 4 hr of mercury exposure, *p*-CMB

was the only treatment for which addition of anti-CD3 beads significantly affected toxicity, which was reduced relative to the value obtained without beads ([$IC_{50}$] = 41.1 uM; see Tables 6.2 and 6.4).

***$CH_3HgCl$ with anti-CD3 beads added before mercury exposure:*** The addition of beads before a 5 min exposure to $CH_3HgCl$ produced effects on viability ([$IC_{50}$] = 29.4 uM]) similar to results seen without addition of anti-CD3 beads (see Fig. 6.2-C and Tables 6.2 and 6.4). After 30 min exposure, the toxicity of $CH_3HgCl$ ([$IC_{50}$] = 17.7 uM) was significantly greater than that obtained at 5 min and after 30 min exposure without the addition of beads (see Tables 6.2 and 6.4).

***TMS with anti-CD3 beads added before mercury exposure:*** Prior addition of anti-CD3 beads increased the toxicity of a 5 min TMS exposure ([$IC_{50}$] = 17.7 uM; see Fig. 6.2-D and Table 6.2), producing significant reductions in viability at $\geq$ 20 uM. After 30 min, the toxicity of TMS ([$IC_{50}$] = 8.4 uM) was significantly greater than that produced by 5 or 30 min exposures without beads, although the 4 hr [$IC_{50}$] of 1.9 uM was similar to that obtained in the absence of the beads (see Table 6.4).

***Cell and bead treatment control groups with beads added before mercury exposure*:** Neither control treatments (concanavalin A and anti-CD3), or prior addition of Hg-treated bead controls or anti-CD3 beads or bead treatment control PLL- or anti-TNP isotype-control antibody-coated beads any effect on YAC-1 viability (see Fig 6.4).

### 6.5.3 Viability of YAC-1 cells, with addition of anti-CD3 beads after mercury exposure

***$HgCl_2$ with anti-CD3 beads added after mercury exposure:*** After 5 min exposure to $HgCl_2$, the 24 hr [$IC_{50}$] was 60.8 uM (see Fig. 6.5-A and Table 6.3), a value

significantly higher than when the beads were not added (see Table 6.4), and significant reduction in viability was seen only at ≥ 70 uM. After 30 min, the toxicity of $HgCl_2$ ($[IC_{50}]$ = 42.6 uM) was significantly different from that seen at 5 min, but not from that produced by an equivalent exposure without the addition of anti-CD3 beads (see Table 6.4). After 4 hrs, the toxicity of $HgCl_2$ ($[IC_{50}]$ = 40.8 uM) was not significantly different from that produced by 30 min exposure (see Table 6.4).

***p-CMB with anti-CD3 beads added after mercury exposure:*** As seen in the absence of anti-CD3 beads, *p*-CMB had no effect on YAC-1 viability after a 5 min exposure, except for reductions seen at 70 and 100 uM (see Fig. 6.5-B). After 30 min, the $[IC_{50}]$ was 47.0 uM, and not significantly different from values obtained without the beads at 30 min (see Tables 6.3 and 6.4). After 4 hr exposure, *p*-CMB toxicity was increased ($[IC_{50}]$ = 23.5 uM), and was the only treatment for which the $[IC_{50}]$ was reduced relative to the value obtained without beads at this time (see Table 6.4).

***$CH_3HgCl_2$ with anti-CD3 beads added after mercury exposure:*** The addition of the beads did not alter $CH_3HgCl$ toxicity after 5 min exposure, with YAC-1 viability reduced at ≥ 40 uM ($[IC_{50}]$ = 29.2 uM), similar to that seen without beads (see Fig. 6.5-C and Tables 6.3 and 6.4). After 30 min, the toxicity of $CH_3HgCl$ ($[IC_{50}]$ = 26.4 uM) was not significantly different from values obtained at 5 min or from those obtained without the beads at 30 min. The toxicity of $CH_3HgCl$ was increased after 4 hr, to give an $IC_{50}$ value of 17.1 uM, a value similar to that obtained in the absence of the beads (see Tables 6.3 and 6.4).

***TMS with anti-CD3 beads added after mercury exposure:*** The addition of the beads increased 5 min TMS toxicity ($[IC_{50}]$ = 15.2 uM) and significant reduced viability

at ≥ 20 uM (see Fig. 6.5-D and Tables 6.3 and 6.4). The toxicity of TMS after a 30 min exposure was not significantly different from that obtained at 5 min or without the beads ([$IC_{50}$] = 11.8 uM). After 4 hr, the toxicity of TMS was increased, to give an [$IC_{50}$] of 1.9 uM, similar to that obtained in the absence of the beads (see Table 6.4).

***Cell and bead treatment control groups with anti-CD3 beads added after mercury exposure***: Neither control treatments (concanavalin A and anti-CD3), Hg-treated bead controls (anti-CD3 beads pre-treated with 100 uM solution of each of the mercury compounds tested) or anti-CD3 beads or bead treatment control poly-L-lysine (PLL)- or anti-TNP isotype-control antibody-coated beads any effect on YAC-1 viability (see Fig. 6.6).

## 6.6 DISCUSSION

The MTT assay was used to establish appropriate mercury concentrations for use in other assays. Initially, concentrations from 0.01 to 50 uM, with exposure periods of 30 mins and 4 hrs were selected. However, in subsequent assays some mercury effects appeared very rapidly, and additional 1, 5 and 15 min exposures were added for some assays, and the maximal concentration extended to 100 uM for all treatment groups.

After an initial 4 hr incubation with the mercury compounds, with or without the addition of anti-CD3 beads, the relative toxicities at 24 hrs post-treatment, as expressed by the [$IC_{50}$] values (see Chapter 4) were TMS > $CH_3HgCl$ > *p*-CMB > $HgCl_2$. The very high toxicity of TMS (6-fold greater than $CH_3HgCl$) is consistent with other models. As little as 0.02 – 0.1 uM TMS has been shown to be toxic corneal endothelial cultures (Takahashi, 1982; Van Horn et al., 1977). These findings may be of concern given than TMS has been included in vaccines as a preservative – intramuscular injection of TMS

bypasses GI absorption and hepatic metabolism, distributing the compound directly to the injection site and any associated inflammatory response.

In addition, each of the mercury compounds produced complete loss of YAC-1 cell viability within a very narrow range of concentrations (10 – 30 uM). This result may reflect the homogeneity of the cell line with respect to redox status, pro- vs. anti-apoptotic signalling components, and protective reserves (anti-oxidants, glutathione, etc.) or other factors that influence mercury toxicity. Alternatively, mercury may be sequestered by binding to thiol (-SH; sulfhydryl) and other binding sites on albumen or other non-diffusible proteins in the medium (Foulkes, 1974), with free mercury present in the media only after saturation of albumen and other proteins. Mercury toxicity may also be a threshold phenomenon, requiring a certain proportion of membrane or intracellular targets to be bound by mercury before effects are seen. Regardless of the actual mechanism responsible for the steep concentration-response curves, it was evident that all subsequent assays needed to be carefully optimised to provide meaningful comparisons of the results.

Perhaps most unexpected was the lack of effect of increasing exposure time on the toxicity of $HgCl_2$ or $CH_3HgCl$. The concentration response curves for the 5 min, 30 min and 4 hr treatments were virtually identical (see Figure 6.1-A and -C) and the [$IC_{50}$] values were not significantly different (except at 4 hrs for $CH_3HgCl$; see Table 6.1). In contrast, TMS, and *p*-CMB in particular, showed significant effects of increasing exposure times. The ethylmercury moiety has been shown to be the toxic principle of TMS. The toxicity of ethyl- and methylmercury are thought to be quite similar (Magos, 2001; Shenker et al., 1997). The clear difference in the kinetics of toxicity of TMS and

$CH_3HgCl$ in the MTT assay would suggest that ethylmercury does not rapidly dissociate from TMS in the YAC-1 cell model. As both *p*-CMB and TMS contain carboxyl groups, the effects may nonetheless reflect the degree of ionisation of these compounds at pH = 7.4 or their larger size, slowing their diffusion and entry into the cell, and thus the speed at which these compounds diffuse across the lipid cell membrane to produce intracellular effects. The effects of *p*-CMB were delayed to a greater extent than for TMS, possibly as a function of lower overall toxicity and/or greater ionisation. During optimisation of the assay protocols, *p*-CMB toxicity was observed to be markedly influenced by the pH of the media (as was $HgCl_2$), however TMS toxicity appeared to be much less sensitive to pH. The assay protocol was modified to include a 30 min incubation of the mercury - loaded 96-well plates in a $CO_2$ incubator to equilibrate the pH of all wells prior to addition of the cells. The results may also represent a certain degree of reversibility of *p*-CMB and TMS effects, such that with continued exposure, the cells become irreversibly committed to die.

The very rapid effects of $HgCl_2$ are more difficult to explain, given that $HgCl_2$ was also the least toxic of the mercury compounds studied. This result may to some extent reflect the mechanics of the assay: the wash steps to remove the mercury after the initial exposure 'pulse' require a significant amount of time (around 15 min). During the initial wash steps some residual mercury may still be present in the media and thus the '5 min' exposure may therefore more accurately reflect an 8 to 10 min exposure – thereafter, further exposure to $HgCl_2$ does not appear to increase toxicity – though what may be occurring in that 8 - 10 minute period remains to be explained.

Theoretically, both $HgCl_2$ and $CH_3HgCl$ could enter cells equally rapidly – with the lower toxicity of $HgCl_2$ being a function of different potential target sites. Diffusion of uncharged $HgCl_2$ from protein-free media through lipid bilayers has been demonstrated (Gutknecht, 1981). However, $HgCl_2$ is thought be present mainly as an anionic polychloride in physiologic solutions (Foulkes, 1991). Given the very high affinity of metal ions for proteins and other biological molecules, it is unlikely that $Hg^{2+}$ diffuses through membranes or ion channels passively without reacting with their components, or with proteins in extracellular fluid. Membrane transfer of metals may instead be mediated by diffusible metal complexes (Foulkes, 2000). In other *in vitro* models of $HgCl_2$ toxicity, mercury was found only in membranes for 15-30 minutes post-exposure (Nordlind, 1985). After longer exposures, most mercury was still bound to membranes (Endo et al., 1995a). Maximal uptake of mercury by human peripheral T lymphocytes occurred within 1 to 3 hr following $CH_3HgCl$ treatment; in contrast, mercury uptake was not maximal until 3-6 hr after $HgCl_2$ exposure (Shenker et al., 1992b). These findings would suggest $Hg^{2+}$ does not easily pass through membranes to the cytosol.

The lack of effect of increasing duration of $HgCl_2$ or $CH_3HgCl$ exposure may have nonetheless been a function of membrane binding and subsequent internalisation of mercury through normal membrane trafficking. Upon exposure to $HgCl_2$, external membrane binding sites (–SH, –OH, etc.) may have been saturated (or binding reached some threshold level) at $HgCl_2$ concentrations greater than 40 uM. Upon subsequent internalization of membranes, a lethal ‘hit’ (immediate or delayed) may have been delivered to the interior of the cell, and further accumulation of mercury was not required

for cell death. The mechanism of such a 'hit', whether somehow related to membrane-bound mercury or to mercury that is subsequently released from internalised membranes, is not known.

The anti-CD3 beads were to be added to the YAC-1 cell cultures as surrogate antigen presenting cells in subsequent assays (see Chapter 5). As such, it was important to assess their effects on viability in the MTT assay. A cell:bead ratio of 2:1 was found to be optimal, generally resulting in a maximum of 30 % of cells binding beads under most circumstances. If the proportion of beads was increased, the cells and beads tended to form large aggregates, making assessment of the YAC-1 cell orientation virtually impossible (see Chapter 5) and potentially shielding cells at the the centre from mercury exposure. At the 2:1 cell:bead ratio, the addition of anti-CD3 beads had no effect on viability of untreated YAC-1 cells. This was not entirely unexpected, as unlike some cell lines, the virus-transformed YAC-1 cell line proliferates (possibly maximally) without cytokine or antigenic stimulation and with only 30% cell-bead conjugates, any effect related to the anti-CD3-coated beads was not expected to be dramatic.

It was also of interest to determine whether a polarized stimulus could 'rescue' cells from mercury toxicity. All of the mercury compounds tested continued to be toxic to the YAC-1 lymphoma line when anti-CD3 beads were added immediately before or after the mercury exposure, similar to effects seen where the anti-CD3 beads were not added. However, some effects of bead addition were noted at 5 min, where the toxicity of $HgCl_2$ was slightly reduced and TMS toxicity was slightly increased. Some additional effects of addition of beads were also noted with 30 min exposures to $HgCl_2$, $CH_3HgCl$ and TMS and following 4 hr exposure to $CH_3HgCl$ and *p*-CMB. These effects may have

been a function of the variability of the MTT assay and the small number of replicates; if genuine, the effects of anti-CD3 binding appeared most likely to affect the outcome of mercury treatment if occurring within minutes of, or possibly before, the initiation of mercury treatment. For subsequent bead-binding assays, the beads were nonethless added immediately before mercury treatment, as the effects of mercury on early signalling events were of primary interest for this study. Regardless, some caution in interpreting the effects of $HgCl_2$ and TMS in bead-binding assays was warranted (although cytoskeletal effects, at least, appeared similar in both bound and unbound cells; see Chapter 5).

The findings presented here may indicate the two groups of mercury compounds induce cell death by distinct pathways, but despite overall similarities in patterns of cytotoxicity produced by $HgCl_2$ and $CH_3HgCl$, and by *p*-CMB and TMS, the individual differences in the pattern of effects produced by each these compounds may reflect interactions with different cellular targets leading to cell death. Those different targets may, in turn, reflect the physicochemical properties of each of the compounds, and the ease with which they pass from the membrane to the cell interior

**Table 6.1:** Effects of mercuric chloride ($HgCl_2$), *p*-chloromercuribenzoate (*p*-CMB), methylmercuric chloride ($CH_3HgCl$) and thimerosal (TMS) on YAC-1 lymphoma cell 24-hr viability, as measured by the colorimetric MTT (methylthiazolyldiphenyl-tetrazolium bromide) assay of mitochondrial activity, following *in vitro* exposures of 5 min, 30 min or 4 hr duration, expressed as the concentration producing 50% reduction in viability (24-hr [$IC_{50}$]; calculated by non-linear regression of concentration-response data; n = minimum of 5 replicates for each data point).

| | **[$IC_{50}$] (uM)** | | | |
|---|---|---|---|---|
| **Time** | **$HgCl_2$** | ***p*-CMB** | **$CH_3HgCl$** | **TMS** |
| **5 min** | 46.0 [a, x] | -- | 28.5 [b, x] | 36.1 [c, x] |
| **30 min** | 41.6 [a, x] | -- | 25.1 [b, x] | 12.6 [c, y] |
| **4 hr** | 43.6 [a, x] | 33 [b] | 20.7 [c, y] | 3.3 [d, z] |

[a, b, c, d] Indicate significant differences due to treatment effects: where letters for the different mercury treatments of a specific time period are the same, the [$IC_{50}$] values between treatments do not differ; different letters indicate the values are significantly different from each other, $p < 0.05$.

[x, y, z] Indicate significant differences due to exposure time: where letters for different time periods for a mercury treatment are the same, the [$IC_{50}$] values between time periods do not differ; different letters indicate the values are significantly different from each other, $p < 0.05$.

**Table 6.2:** Effects of mercuric chloride ($HgCl_2$), methylmercuric chloride ($CH_3HgCl$), *p*-chloromercuribenzoate (*p*-CMB) and thimerosal (TMS) on the 24 hr-viability of YAC-1 lymphoma cells previously conjugated to anti-CD3 antibody-coated 6.0 um latex beads, following *in vitro* exposures of 5 min, 30 min or 4 hr duration, expressed as the concentration producing 50% loss of viability (24-hr [$IC_{50}$]; calculated by non-linear regression of concentration-response data; n = minimum of 5 replicates for each data point), as measured by the colorimetric MTT (methylthiazolyldiphenyl-tetrazolium bromide) assay of mitochondrial activity.

| | **[$IC_{50}$] (uM)** | | | |
|---|---|---|---|---|
| **Time** | **$HgCl_2$** | ***p*-CMB** | **$CH_3HgCl$** | **TMS** |
| **5 min** | 59.3 [a, x] | -- | 29.4 [b, x] | 17.7 [c, x] |
| **30 min** | 35 [a, y] | 44.2 [b, y] | 17.9 [c, y] | 8.4 [d, y] |
| **4 hr** | 44.5 [a, z] | 41.2 [a, y] | 25.9 [b, x] | 5.5 [c, y] |

[a, b, c, d] Indicate significant differences due to treatment effects: where letters for the different mercury treatments of a specific time period are the same, the [$IC_{50}$] values between treatments do not differ; different letters indicate the values are significantly different from each other, $p < 0.05$.

[x, y, z] Indicate significant differences due to exposure time: where letters for different time periods for a mercury treatment are the same, the [$IC_{50}$] values between time periods do not differ; different letters indicate the values are significantly different from each other, $p < 0.05$.

**Table 6.3:** Effects of mercuric chloride ($HgCl_2$,), methylmercuric chloride ($CH_3HgCl$), *p*-chloromercuribenzoate (*p*-CMB) and thimerosal (TMS) on YAC-1 lymphoma cell 24-hr viability following *in vitro* exposures of 5 min, 30 min or 4 hr duration with subsequent addition of anti-CD3 antibody-coated 6.0 um latex beads, expressed as the concentration producing 50% loss of viability (24-hr [$IC_{50}$]; calculated by non-linear regression of concentration-response data; n = minimum of 5 replicates for each data point) as measured by the colorimetric MTT (methylthiazolyldiphenyl-tetrazolium bromide) assay of mitochondrial activity.

| | **[$IC_{50}$] (uM)** | | | |
|---|---|---|---|---|
| **Time** | **$HgCl_2$** | ***p*-CMB** | **$CH_3HgCl$** | **TMS** |
| **5 min** | 60.8 [a, x] | -- | 29.2 [b, x] | 15.2 [c, x] |
| **30 min** | 42.6 [a, y] | 47.0 [a, x] | 26.4 [b, x] | 11.8 [c, x] |
| **4 hr** | 40.8 [a, y] | 23.5 [b, y] | 17.1 [c, y] | 1.9 [d, y] |

[a, b, c, d] Indicate significant differences due to treatment effects: where letters for the different mercury treatments of a specific time period are the same, the [$IC_{50}$] values between treatments do not differ; different letters indicate the values are significantly different from each other, $p < 0.05$.

[x, y, z] Indicate significant differences due to exposure time: where letters for different time periods for a mercury treatment are the same, the [$IC_{50}$] values between time periods do not differ; different letters indicate the values are significantly different from each other, $p < 0.05$.

**Table 6.4:** Comparison of the effects of mercuric chloride ($HgCl_2$; A), methylmercuric chloride ($CH_3HgCl$; B), *p*-chloromercuribenzoate (*p*-CMB; C) and thimerosal (TMS; D) on the 24-hr viability of YAC-1 lymphoma cells with either no anti-CD3 antibody coated 6.0 latex beads added, with anti-CD3 beads added after mercury (Hg) exposure or where the YAC-1 cells have previously been conjugated to anti-CD3 beads, following *in vitro* mercury exposures of 5 min, 30 min or 4 hr duration, expressed as the concentration producing 50% loss of viability (24-hr [$IC_{50}$]; calculated by non-linear regression of concentration-response data), as measured by the colorimetric MTT (methylthiazolyldiphenyl-tetrazolium bromide) assay of mitochondrial activity.

| | **A: $HgCl_2$** | | |
|---|---|---|---|
| | **No Beads** | **Beads After Hg** | **Beads Before Hg** |
| **5 min** | 46.0 | 60.8 | 59.3 |
| **Sig Diff** [a] | x | y | y |
| **30 min** | 41.6 | 42.6 | 35 |
| **Sig Diff** | x | x | y |
| **4 hr** | 43.6 | 40.8 | 44.5 |
| **Sig Diff** | x | x | x |

| | **B: $CH_3HgCl$** | | |
|---|---|---|---|
| | **No Beads** | **Beads After Hg** | **Beads Before Hg** |
| **5 min** | 28.5 | 29.2 | 29.4 |
| **Sig Diff** | x | x | x |
| **30 min** | 25.1 | 26.4 | 17.9 |
| **Sig Diff** | x | x | y |
| **4 hr** | 20.7 | 17.1 | 25.9 |
| **Sig Diff** | x | x | y |

| | **C: *p*-CMB** | | |
|---|---|---|---|
| | **No Beads** | **Beads After Hg** | **Beads Before Hg** |
| **5 min** | n/a | n/a | n/a |
| **Sig Diff** | x | x | x |
| **30 min** | n/a | 47 | 44.2 |
| **Sig Diff** | x | x | x |
| **4 hr** | 33 | 23.5 | 41.2 |
| **Sig Diff** | x | y | z |

| | **D: TMS** | | |
|---|---|---|---|
| | **No Beads** | **Beads After Hg** | **Beads Before Hg** |
| **5 min** | 36.1 | 15.2 | 17.7 |
| **Sig Diff** | x | y | y |
| **30 min** | 12.6 | 11.8 | 8.4 |
| **Sig Diff** | x | x | y |
| **4 hr** | 3.3 | 1.9 | 5.5 |
| **Sig Diff** | x | x | x |

[a] Sig Diff (significant differences): Where letters in no bead, beads after mercury and beads before mercury treatment columns of a time period are the same the [$IC_{50}$] values between treatments do not differ; different letters indicate the values are significantly different from each other, $p < 0.05$.

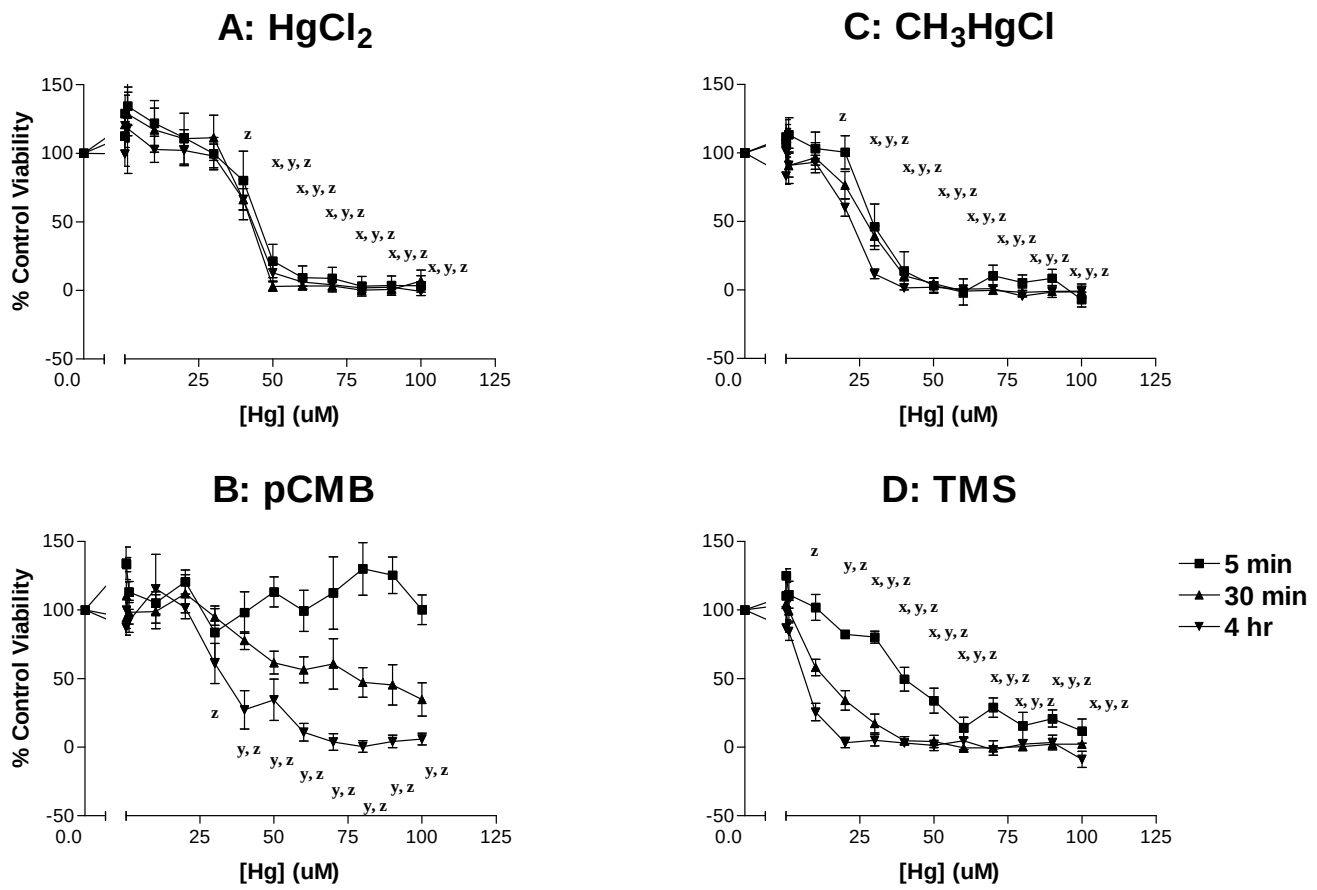


**Figure 6.1:** Effects of mercuric chloride ($HgCl_2$, A), *p*-chloromercuribenzoate (*p*-CMB; B), methylmercuric chloride ($CH_3HgCl$; C) and thimerosal (TMS; D) on YAC-1 lymphoma cell 24-hr viability following *in vitro* exposures of 5 min, 30 min or 4 hr duration, as measured by the colorimetric MTT (methylthiazolyldiphenyl-tetrazolium bromide) assay of mitochondrial activity [adjusted % control response = (reading - background)/(RPMI control treatment - background); mean ± SEM; n = minimum of replicates for each data point; x, y and z indicate values differing significantly from control values for the 5 min, 30 min and 4 hr exposure periods, respectively, $p < 0.05$].

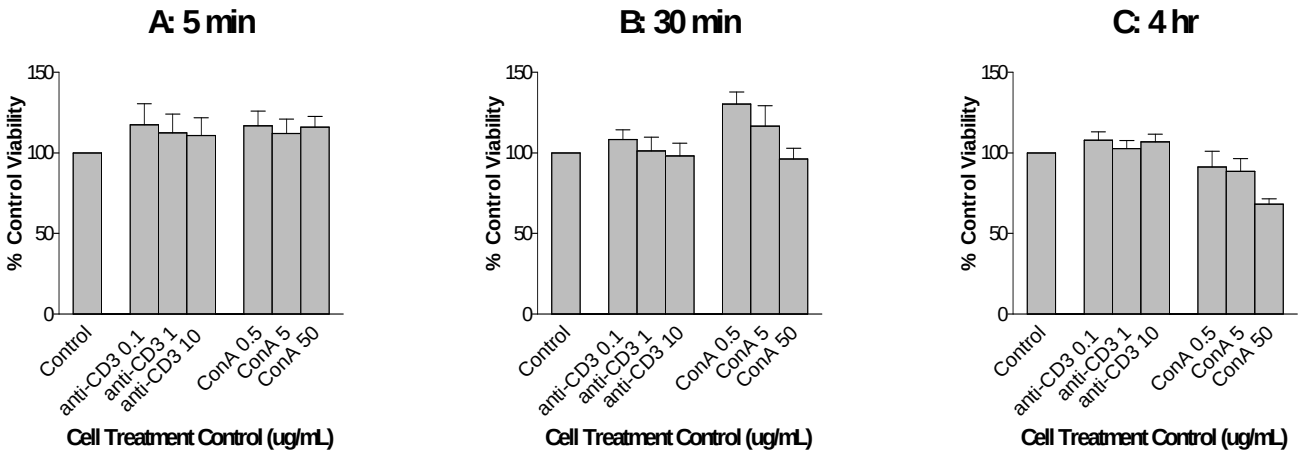


**Figure 6.2:** Effects of concanavalin-A (ConA) and anti-CD3 antibody control treatments on YAC-1 lymphoma cell 24-hr viability after *in vitro* exposures of 5 min (A), 30 min (B) or 4 hr (C) duration, as measured by the colorimetric MTT (methylthiazolyldiphenyl-tetrazolium bromide) assay of mitochondrial activity [% control response = (reading - background)/(RPMI control treatment - background); mean ± SEM; n = minimum of 5 replicates for each data point].

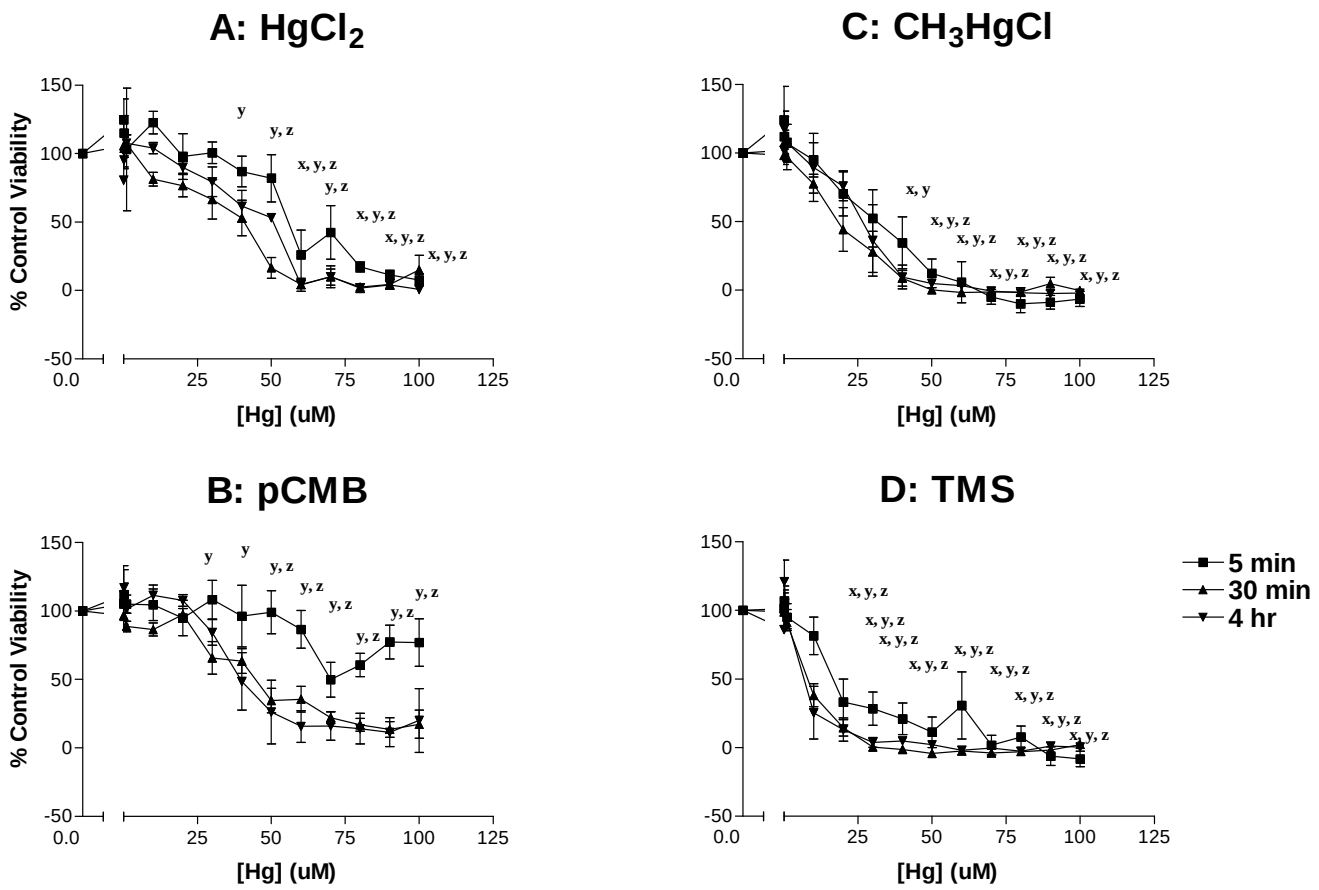


**Figure 6.3:** Effects of mercuric chloride ($HgCl_2$, A), *p*-chloromercuribenzoate (*p*-CMB; B), methylmercuric chloride ($CH_3HgCl$; C) and thimerosal (TMS; D) on the 24-hr viability of YAC-1 lymphoma cells previously conjugated to anti-CD3 antibody-coated 6 uM latex beads, following *in vitro* exposures of 5 min, 30 min or 4 hr duration, as measured by the colorimetric MTT (methylthiazolyldiphenyl-tetrazolium bromide) assay of mitochondrial activity [adjusted % control response = (reading - background)/(RPMI control treatment - background); mean ± SEM; n = minimum of 5 replicates for each data point, except at 4 hr, where n = 3; x, y and z indicate values differing significantly from control values for the 5 min, 30 min and 4 hr exposure periods, respectively, $p < 0.05$].

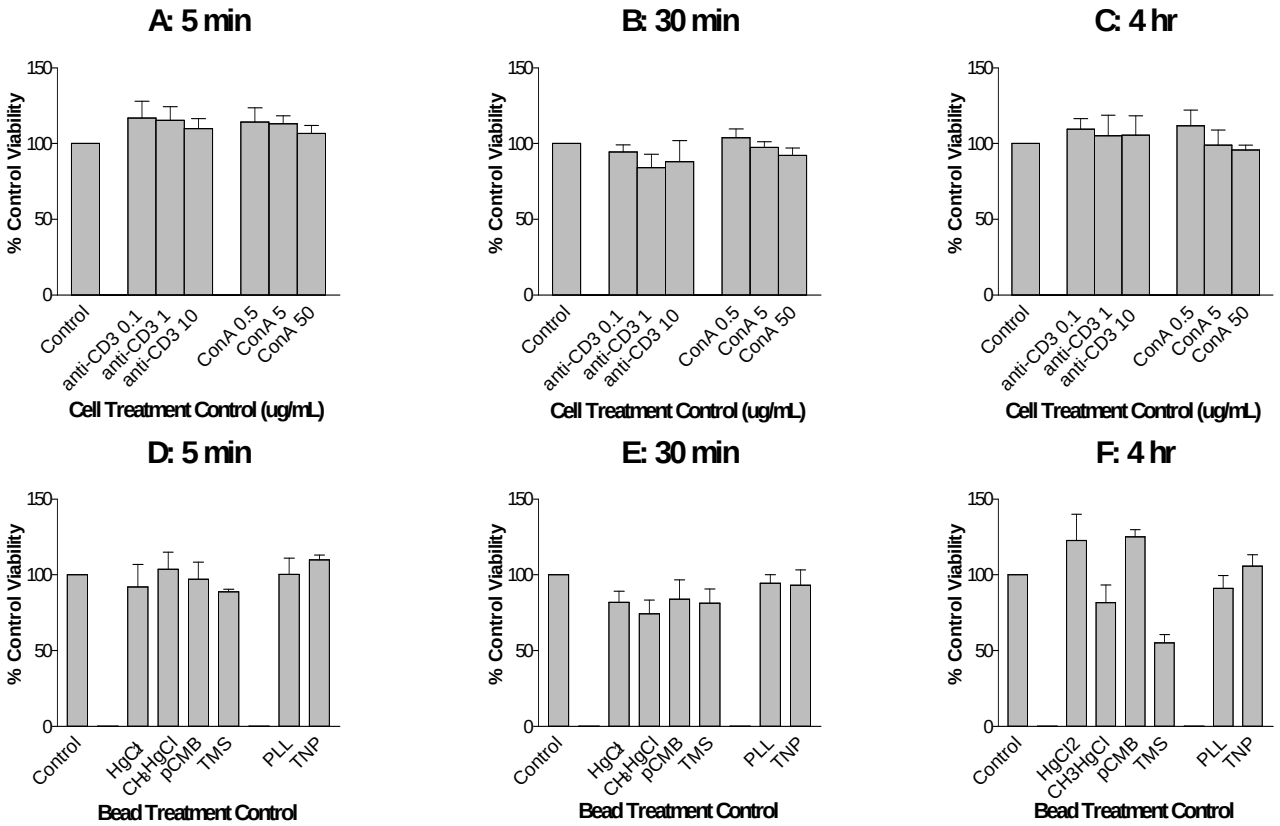


**F**

**Figure 6.4:** Effects of 5 min, 30 min or 4 hr *in vitro* exposures to concanavalin-A (ConA) and anti-CD3 antibody control treatments and addition of anti-CD3 beads (A-C) or addition of mercuric chloride- ($HgCl_2$), methylmercuric chloride- ($CH_3HgCl$), *p*-chloromercuribenzoate-(*p*-CMB) or thimerosal- (TMS) treated anti-CD3-coated, poly-L-lysine- (PLL) or anti-trinitrophenol- (TNP) coated 6.0 um latex beads to untreated cells after 5 min, 30 min or 4 hrs (D-F) on YAC-1 lymphoma cell 24-hr viability, as measured by the colorimetric MTT (methylthiazolyldiphenyl-tetrazolium bromide) assay of mitochondrial activity [adjusted % control response = (reading–background)/(no treatment–background); mean + SEM; n = minimum of 5 replicates for each data point, except at 4 hr, where n = 3].

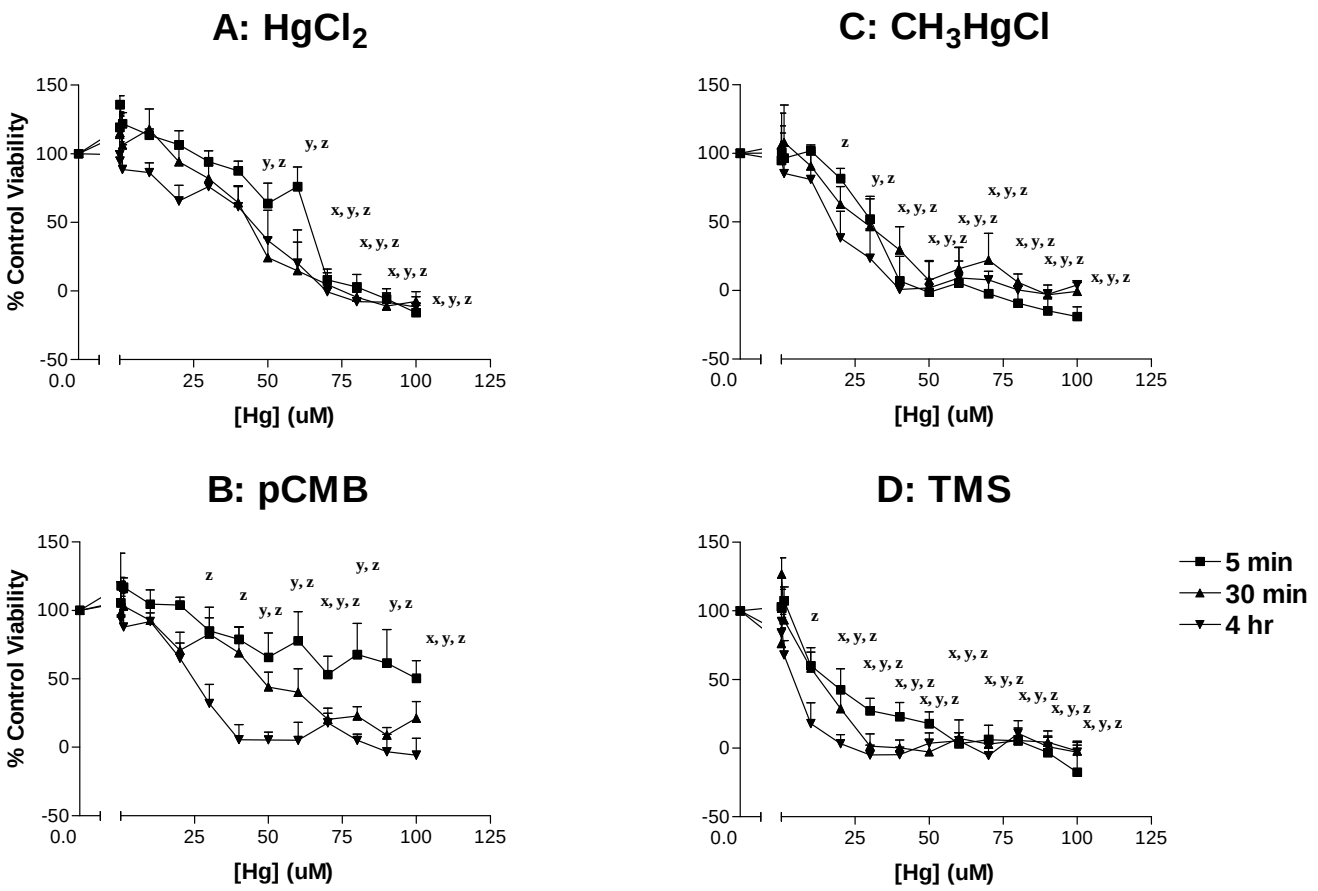


**Figure 6.5:** Effects of mercuric chloride ($HgCl_2$, A), *p*-chloromercuribenzoate (*p*-CMB; B), methylmercuric chloride ($CH_3HgCl$; C) and thimerosal (TMS; D) on the 24-hr viability of YAC-1 lymphoma cells conjugated to anti-CD3 antibody-coated 6 uM latex beads following *in vitro* exposures of 5 min, 30 min or 4 hr duration, as measured by the colorimetric MTT (methylthiazolyldiphenyl-tetrazolium bromide) assay of mitochondrial activity [adjusted % control response = (reading - background)/(RPMI control treatment - background); mean ± SEM; n = minimum of 5 replicates for each data point; x, y and z indicate values differing significantly from control values for the 5 min, 30 min and 4 hr exposure periods, respectively, $p < 0.05$].

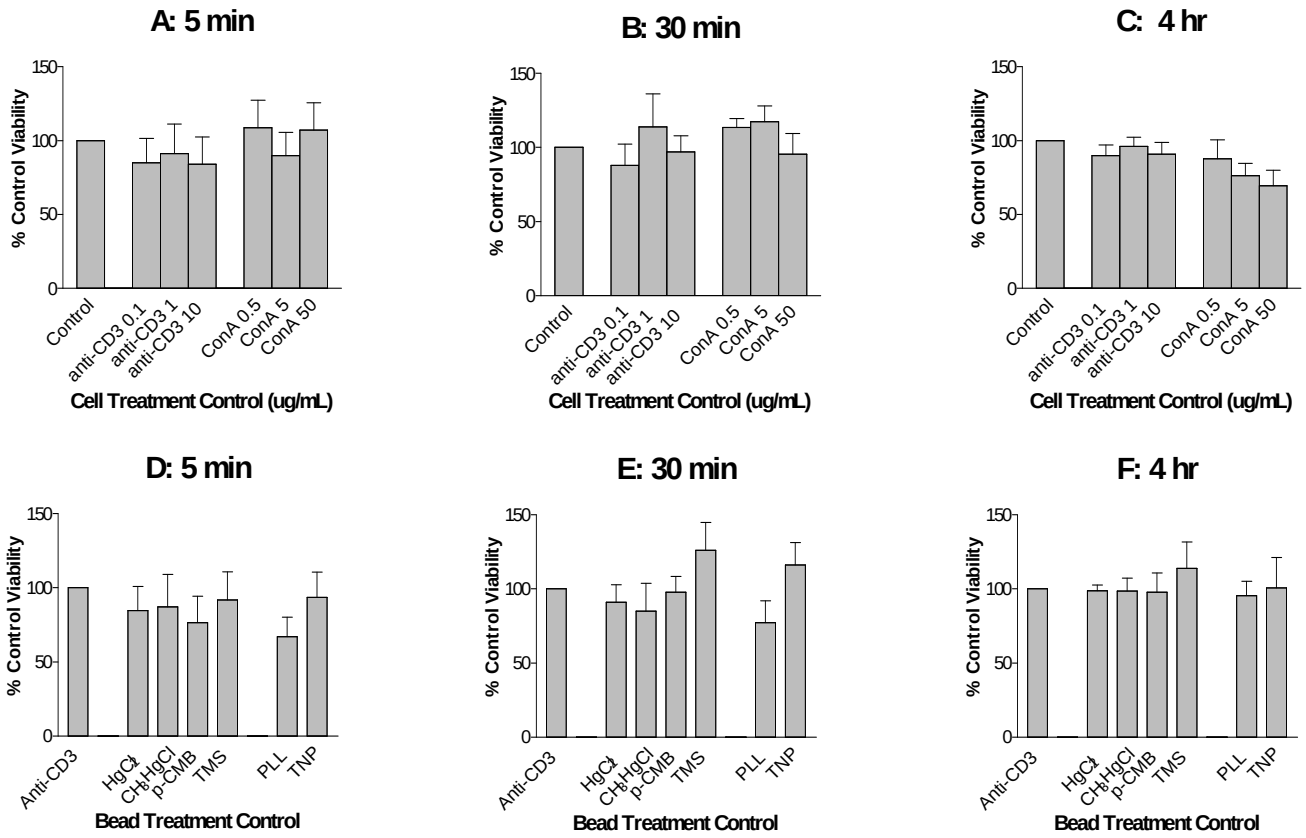


**Figure 6.6:** Effects of 5 min, 30 min or 4 hr *in vitro* exposures to concanavalin-A (ConA) and anti-CD3 antibody control treatments (A-C) or addition of mercuric chloride- ($HgCl_2$), methylmercuric chloride- ($CH_3HgCl$), *p*-chloromercuribenzoate- (*p*-CMB) and thimerosal- (TMS) treated anti-CD3-coated, poly-L-lysine- (PLL) and anti-trinitrophenol-(TNP)-coated 6.0 uM control beads to untreated cells after 5 min, 30 min or 4 hrs (D-F) on 24 -hr viability of YAC-1 lymphoma cell previously conjugated to anti-CD3-coated beads (A-C) or bead treatment controls (D-F), as measured by the colorimetric MTT (methylthiazolyldiphenyl-tetrazolium bromide) assay of mitochondrial activity [adjusted % control response = (reading - background)/(no treatment - background); mean + SEM; n = minimum of 5 replicates for each data point, except F, n = 2].

# 7.0 GENERAL DISCUSSION

## 7.1 Premise

The potential for immunotoxicants, and in particular mercury, to produce failure of pattern recognition within the localized supramolecular activation complex (SMAC) or 'immunological synapse' formed between antigen-presenting cells (APCs) and responding lymphocytes was the focus of this project.

While antigenic stimuli are restricted to the localized SMAC, mercury may interact non-specifically with thiol (-SH) groups throughout the cell. Non-localized mercury impacts may perhaps mimic antigen-mediated signaling at certain concentrations and for short periods; however, the effects are likely not optimal under most circumstances, creating interference with normal signaling pathways and activating cell death pathways to protect the body against inappropriate immune activation.

Further, the physico-chemical properties of various forms of mercury may influence the events leading to loss of viability and the manner of cell death, which may in turn underlie the different effects of various forms of mercury on immune function.

## 7.2 The Trouble with Targeting Mercury Effects

Mercury is a non-specific toxicant, binding to sulfhydryl (-SH; and to a lesser extent other) functional groups on virtually any protein on or in the cell. Unfortunately, even in experiments designed to identify particular targets of mercury, it is often difficult to discern whether such effects are direct or indirect, as multiple extra- and intracellular

targets may be triggered more-or-less simultaneously. Some of the difficulty in identifying specific targets for mercury toxicity is also likely a function of physico-chemical differences between organic and inorganic mercury. Some targets (e.g. membrane receptors) are considered specific for divalent $Hg^{2+}$, while other downstream signaling components may be targets of all forms of mercury, though the kinetics of such effects may differ. In some cases, cell free models have been used to try to isolate mercury effects at the molecular levels; however, the effects may differ from those seen whole cell models, as seen with the inhibition of microtubule assembly by $Hg^{2+}$ and $CH_3HgCl$.

Despite these difficulties, the functional consequences of non-specific mercury effects on the immunological synapse may nonetheless give some insight as to how mercury toxicity is manifested. The immunological synapse (or supramolecular activation complex; SMAC) is a four-dimensional pattern-recognition framework within which the lymphocyte can distinguish dangerous from harmless antigenic stimuli and target the effector response accordingly. But while antigenic stimuli are restricted to the localized area of contact created by the immunological synapse, many cellular components involved in spatio-temporal patterning of the immunological synapse are susceptible to aberrant activation or inhibition by chemical agents such as mercury. Such global signals may not be optimal for T lymphocyte activation, especially for naive T lymphocytes. Without an appropriate directional stimulus with which to orient reorganization of signalling scaffolds, the cytoskeleton and secretory functions, the lymphocyte may essentially become ‘confused’. ‘Confused’ lymphocytes may be unable to respond to normal polarized stimuli, and also need to be eliminated in order to prevent

the possibility of inappropriate activation and non-targeted release of cytokines or cytolytic factors. The immunological synapse is but one of many mechanisms preventing inappropriate immune activation and autoimmunity, but it has two potential weaknesses: first, if large numbers of lymphocytes become 'confused' simultaneously, their subsequent pre-emptive elimination may leave the host with reduced defences; second, if somehow breached, the loss of this one defence may circumvent many of the other protective measures. In both cases, the disruption may be transient, but if order is not restored promptly, the host may become immuno-compromised or fall victim to its own rampaging immune system, both of which may be seen with various forms of mercury.

### 7.3 Using the Immunological Synapse to Study Mercury

Specifically, we proposed that the immunotoxic effects of inorganic $Hg^{2+}$ (and perhaps other compounds, like *p*-chloromercuribenzoate, that are likely charged at physiologic pH and penetrate membranes poorly) are produced, at least initially, through global triggering of normal membrane-dependent signaling mechanisms at the cell surface. We expected this non-antigen specific receptor activation could inhibit polarization of cytoskeleton and secretory machinery in lymphocytes responding to localized stimuli, in conjunction with down-regulation of the TCR in response to receptor triggering, but before any significant effects at other intracellular targets for mercury (particularly microtubule integrity) are seen – and before the activation of cell death pathways. In most naive lymphocytes, the abortive non-localized stimulus created by $Hg^{2+}$ may activate receptor-mediated apoptotic cell death pathways as part of the immune system's 'failsafe' mechanisms to avoid inappropriate immune activation, while possibly transiently activating a small percentage of cells in a non-antigen-specific fashion.

In contrast, organomercurial compounds, such as methyl mercuric chloride ($CH_3HgCl$) and thimerosal (TMS), with greater lipid solubility and thus more rapid penetration into the cell, were expected disrupt microtubules and increase membrane permeability non-specifically without activating or down-regulating cell surface receptors to an appreciable extent. Some of the subsequent intracellular targets of $CH_3HgCl$ or TMS could be the same or similar to those activated down-stream by $Hg^{2+}$-receptor activation, but effects on polarized signaling events would be seen in conjunction with – and not prior to – loss of microtubule and organelle integrity and other intracellular effects associated with the onset of cell death.

The patterns of cell death, while likely showing components of both apoptosis and necrosis depending on concentration, were expected to differ in time course for both groups of mercury compounds – with inorganic $Hg^{2+}$ producing predominantly apoptosis at all time points and over all but the highest concentrations studied, and $CH_3HgCl$ and TMS possibly producing apoptosis at low concentrations, but with necrosis becoming dominant at higher concentrations and with continued exposure, secondary to the loss of membrane integrity and increasing intracellular calcium.

### 7.4 Methylthiazolyldiphenyl-tetrazolium Bromide (MTT) Assay

After 4 hr incubation, the relative cytotoxicities of the mercury compounds in the MTT assay were TMS > $CH_3HgCl$ > *p*-CMB > $HgCl_2$. While it may be argued that the concentrations at which viability was affected are too high to be environmentally or clinically relevant, the YAC-1 cells were exposed to a large range of concentrations (0.01 to 100 uM). Transformed cell lines do not respond to normal growth-inhibitory stimuli and may also prove more resistant to toxicity. As such, mercury concentrations

producing effects in the YAC-1 cells may be relatively, but not directly, comparable to cells *in vivo* or in freshly isolated lymphocytes. Each mercury compound tested nonetheless produced effects in each of the additional assays at similar concentrations to those producing loss of viability, allowing direct inter-assay comparisons – and a glimpse into the differences between mercury compounds that share the same toxic principle.

*In vitro* cytotoxicity often increases with increasing exposure, as was seen with *p*-CMB and TMS, although at some point no further toxic effects are expected. However, the lack of effect of increasing exposures to $HgCl_2$ and $CH_3HgCl$ beyond a 5 min exposure in the MTT assay was unexpected, especially for $HgCl_2$. The data are consistent with three possible scenarios: 1) both compounds penetrate cells extremely rapidly, to produce cytotoxicity within minutes thereafter, although previous studies indicate this is unlikely for charged and highly reactive $Hg^{2+}$ (Foulkes, 1991, 2000; Nordlind, 1985; Shenker et al., 1992b); 2) either form of mercury produces almost immediate effects, regardless of whether that mercury has penetrated to the cell interior – with $HgCl_2$ likely producing those effects before significant intracellular accumulation; 3) toxicity is a function of early saturation of a critical target by $HgCl_2$ or $CH_3HgCl$, whether in the cell interior or at the membrane (with toxicity in the latter case related to effects at the membrane, and/or upon membrane internalization). The first possibility became less likely upon consideration of the results of the YP/PI dye exclusion and other assays.

### 7.5 Dye Exclusion Assay

The delay in onset of YP/PI dye uptake following $HgCl_2$ or *p*-CMB exposure as compared to $CH_3HgCl$ may be a function of relatively slower passage of $HgCl_2$ or *p*-CMB into the cell interior to produce effects. Alternately, the onset of apoptosis/necrosis

may be delayed following interactions at the cell surface or interior. In contrast, the effects produced by $CH_3HgCl$ are suggestive of rapid penetration of $CH_3HgCl$ to the cell interior, resulting in almost immediate induction of an early apoptotic ($YP^{low}/PI^{neg}$) state, coincident with effects on all other assays except F-actin levels. It is also possible rapid apoptosis was triggered by non-specific changes in membrane permeability, though such changes might be expected to be accompanied by influx of PI. The slightly slower onset for TMS effects may reflect the degree of ionization of this compound, its larger size or protein binding of the ethylmercury moiety following dissociation from the parent TMS. While it was expected that $CH_3HgCl$ and TMS would both produce greater disruption of cellular homeostasis than $HgCl_2$ and *p*-CMB, is was also anticipated that such changes would be incompatible with cell survival and would hasten cell death by necrosis. Despite these early and profound changes in the intracellular environment, for both $CH_3HgCl$ and TMS, progression through apoptosis through late necrosis was slower than for $HgCl_2$ or *p*-CMB.

### 7.6 Flow Cytometric Assessment of CD3 Expression, Phosphotyrosination, B-Tubulin, F-Actin and Intracellular Calcium Levels

Although a receptor-mediated mechanism has been proposed for $Hg^{2+}$, and microtubules are thought to be a primary target of $CH_3HgCl$ and TMS, mercury in all its forms is considered non-specific and can interact directly with sulfhydryl (-SH) groups on many membrane and intracellular targets in addition to membrane receptors, PKC, microtubules or other cellular components postulated to be specific targets of mercury. Even if initially acting through these pathways, mercury may therefore produce effects distinct from those seen with agonist ligands or target-specific chemicals.

In $HgCl_2$-treated YAC-1 cells, inhibition of responses to polarized stimuli preceded the loss of microtubules and the onset of cell death, as hypothesized. Effects on polarized stimuli were in turn preceded by a transient $Ca^{2+}$ signal, with $[Ca^{2+}]_i$; however, this $Ca^{2+}$ signal appeared abortive, accompanied not by an increase, but by a paradoxic decrease in PTyr-P and only partial down-regulation of CD3 receptors. Failure of $HgCl_2$-treated YAC-1 cells to respond to polarized stimuli did therefore not appear to be simply a function of reduced CD3 binding sites following $HgCl_2$ exposure, but may have nonetheless been related to disruption of polarization responses by the abortive signal in some as yet undetermined fashion, given that only a very brief exposure to $HgCl_2$ was necessary to induce complete loss of viability. Given that $Hg^{2+}$ is a potent inhibitor of microtubule polymerization and inhibition of polarization is seen prior to extensive loss of microtubule staining, the effects appear to involve mechanisms that precede significant entry of free $Hg^{2+}$ in the cytosol. In addition, $HgCl_2$ exposure was followed rapidly by necrotic cell death, rather than apoptotic cell death as might be presumed to follow activation of receptor pathways.

Similarly, *p*-CMB-treated YAC-1 cells failed to respond to polarized stimuli before effects on microtubules or loss of viability. Effects on many assays were delayed as compared to $HgCl_2$, which may reflect delayed diffusion into the cell interior due to ionization; however, a transient $Ca^{2+}$ signal and progressive loss of F-actin preceded effects in all other assays and may account for loss of polarized responses. In B lymphocytes the strength of activation signals is thought to be related to the degree of actin deploymerization (Hao and August, 2005). As such, the different effects on actin produced by $HgCl_2$ and *p*-CMB may therefore represent different 'interpretations' of the

overall signaling alterations produced by the two compounds, in addition to the possibility of different specific targets.

Nonetheless it was $CH_3HgCl$ and TMS that produced immediate and profound effects on CD3 receptor expression, $[Ca^{2+}]_i$ and PTyr-P, with concurrent loss of microtubules and polarized signaling responses. Unfortunately the rapid onset of $CH_3HgCl$ and TMS effects made it difficult to identify their sequence; however, sustained PTyr-P is generally considered to be required to maintain increased $[Ca^{2+}]_i$. In addition, microtubule deaggregation was accompanied by complete inhibition of tubulin synthesis. These changes seemed to indicate a general loss of cellular homeostasis not seen in $HgCl_2$- and *p*-CMB-treated cells, which did not necessarily produce simultaneous loss of viability, as TMS-treated cells remained viable for 30 min while $CH_3HgCl$-treated cells became apoptotic within 1 min. Nonetheless, the YAC-1 cells proceeded to cell death more slowly, remaining early apoptotic after 4 hr, when almost all $HgCl_2$- and *p*-CMB-treated cells were necrotic. Unexpectedly, both compounds also produced approximately 50% down-regulation of CD3 receptors at 4 hr, a finding that may be considered consistent with protein kinase C activation and not receptor-mediated PTyr-P, although effects on the cytoskeleton may have prevented complete down-regulation. Nonetheless, for all mercury treatments, YAC-1 cell responses to polarized stimuli were reduced at time points when CD3 receptors were not down-regulated.

### 7.7 Responses to Polarized Stimuli and Cytoskeletal Changes

The inhibitory effects of the four mercury compounds on conjugation, morphologic and cytoskeletal reorientation responses were consistent with their relative

cytotoxicities in the MTT assay and at 4 hr in the dye exclusion assay. As seen in other assays, two patterns of mercury effects emerged.

The reduction in bead binding in $HgCl_2$-treated cells is difficult to explain. Loss of bead-binding responses was expected be due to down-regulation of CD3 receptors after aberrant triggering via cross-linking of –SH groups by divalent $Hg^{2+}$ (a mechanism not thought to be operative for monovalent organomercurial compounds). However, CD3 expression was only marginally reduced, along with pTyr-P, and only at 5 min when bead-binding responses were unaffected. At 30 min, when all bead-binding responses were reduced, CD3 expression and pTyr-P had returned to baseline levels; F-actin levels were however somewhat reduced, although not the extent seen in *p*-CMB-treated cells. At 30 min, β-tubulin staining in $HgCl_2$-treated cells was reduced to levels similar to those associated with inhibition of bead binding responses at 5 min in $CH_3HgCl$- and TMS-treated cells. As such, the entire time-course of mercury effects may simply be delayed for $HgCl_2$; however, distinct differences in the time-course of effects on β-tubulin synthesis and $[Ca^{2+}]_i$, and the magnitude and direction of effects on CD3 expression and pTyr-P would indicate that such a phenomenon is unlikely. $HgCl_2$-treated YAC-1 cells may nonetheless have been 'paralysed' by a global membrane-mediated $Hg^{2+}$ stimulus, but further investigations are required to determine if receptor desensitization, prevention of normal receptor movement and recycling through membranes, global recruitment of cytoskeletal components or some other mechanism may have been responsible. Regardless, the lack of effects on microtubules at time points when CD3 expression, pTyr-P and $[Ca^{2+}]_i$ were all affected is suggestive that, whatever the mechanism, YAC-1 cells are affected by $Hg^{2+}$ prior to significant accumulation of free $Hg^{2+}$ in the cytosol.

As actin is critical to shape changes, motility and the MTOC reorientation response (Dustin and Cooper, 2000), the loss of bead-binding responses would appear to be specifically related to loss of F-actin in *p*-CMB-treated cells, but whether due to solely to loss of F-actin or somehow secondary to the small increase in $[Ca^{2+}]_i$ is not known. However, it should be noted that $HgCl_2$ induced a similar early increase in $[Ca^{2+}]_i$, but did not affect F-actin to the same degree as *p*-CMB at early time points. The relatively greater loss of F-actin in *p*-CMB-treated cells may nonetheless explain the greater frequency of cells with no identifiable MTOC and randomly or peripherally located microtubules, as the cytoskeletal fibres are closely interlinked (Burn et al., 1988; Das et al., 2002; Faure et al., 2004; Kupfer et al., 1990).

For $CH_3HgCl$, inhibition of bead-binding responses was preceded by, or coincident with, alterations in dye uptake, microtubule integrity and signaling components, but prior to down-regulation of CD3 receptors. As such, the loss of viability can be considered responsible for the loss of polarized signaling responses. However, although TMS produced very similar overall effects on bead-binding responses, microtubule integrity and disruption of signaling cascades, the effects preceded dye uptake. TMS-related loss of polarized signaling responses would therefore appear to be secondary to profound disturbances in the intracellular environment, indicating that viability alone does not determine whether cells can respond to a polarized stimulus.

The cytoskeletal polarization response may involve multiple signaling components, from ligation and activation of cell surface receptors, to the formation of stable signaling scaffolds within the cell and creation of gradients of intracellular calcium across the cytosol – all of which may be influenced by mercury treatment. However,

given the complexity of the formation of the immunological synapse, multiple mechanisms may underlie the inhibition of lymphocyte polarization by each of the four mercury compounds. The results presented here indicate that each of the four mercury compounds may initially influence those pathways in unique ways. Nonetheless, perhaps the most striking finding is that overall, two general patterns of effects produced by $HgCl_2$ and *p*-CMB, and by $CH_3HgCl$ and TMS, emerged in almost all the assays.

## 7.8 Conclusions

The toxicity of $HgCl_2$ and $CH_3HgCl$ are known to differ with respect to events related to apoptosis, including cytochrome C release and expression of the anti-apoptotic protein bcl-2 (Shenker et al., 2000). The two patterns of effects on receptor expression, protein tyrosine phosphorylation, intracellular calcium, microtubules, and progression through apoptosis seen here may represent still more manifestations of these fundamental differences in mechanisms preceding the onset of cell death following mercury exposure.

Together, these findings indicate the two groups of mercury compounds may alter responses to polarized stimuli and induce cell death by distinct pathways, one related to an apparently abortive signal and the other mediated by much more profound disruption of cellular homeostasis. Within the larger patterns there are further differences between the effects produced by each Hg compound, likely reflecting the combined influence of pharmaco–kinetic and –dynamic factors governing access to and interactions with different cellular targets leading to cell death. These distinct targets may in turn be reflected in the different immune effects produced by these compounds *in vivo*, including both immune stimulation and inhibition.

## 8.0 REFERENCES


Abal, M., Andreu, J.M. and Barasoain, I., 2003. Taxanes: microtubule and centrosome targets, and cell cycle dependent mechanisms of action. Curr. Cancer Drug Targets 3, 193-203.

Abedi Valugerdi, M. and Moller, G., 2000. Contribution of H-2 and non-H-2 genes in the control of mercury-induced autoimmunity. Int. Immunol. 12, 1425-1430.

Akhand, A.A., Kato, M., Suzuki, H., Miyata, T. and Nakashima, I., 1998. Level of HgCl2-mediated phosphorylation of intracellular proteins determines death of thymic T-lymphocytes with or without DNA fragmentation. J. Cell. Biochem. 71, 243-253.

Al-Alwan, M.M., Rowden, G., Lee, T.D. and West, K.A., 2001. The dendritic cell cytoskeleton is critical for the formation of the immunological synapse. J. Immunol. 166, 1452-1456.

Alexandre, H., Delsinne, V., Goval, J.J. and Van Cauwenberge, A., 2003. Effect of taxol and okadaic acid on microtubule dynamics in thimerosal-arrested primary mouse oocytes: a confocal study. Biol. Cell 95, 407-414.

Allenspach, E.J., Cullinan, P., Tong, J., Tang, Q., Tesciuba, A.G., Cannon, J.L., Takahashi, S.M., Morgan, R., Burkhardt, J.K. and Sperling, A.I., 2001. ERM-dependent movement of CD43 defines a novel protein complex distal to the immunological synapse. Immunity 15, 739-750.

al-Sabti, K., 1994. Micronuclei induced by selenium, mercury, methylmercury and their mixtures in binucleated blocked fish erythrocyte cells. Mutat. Res. 320, 157-163.

Altman, A., Isakov, N. and Baier, G., 2000. Protein kinase Ctheta: a new essential superstar on the T-cell stage. Immunol. Today 21, 567-573.

Altman, A. and Villalba, M., 2002. Protein kinase C-theta (PKC theta): a key enzyme in T cell life and death. J. Biochem. (Tokyo) 132, 841-846.

Anner, B.M., 1997. Transposing results from an artificial minicell to a real cell. Experimental evidence for a working hypothesis linking Na,K-ATPase permeability states to specific alterations of cell life. Ann. N,Y. Acad. Sci. 834, 367-371.

Anton van der Merwe, P., Davis, S.J., Shaw, A.S. and Dustin, M.L., 2000. Cytoskeletal polarization and redistribution of cell-surface molecules during T cell antigen recognition. Semin. Immunol. 12, 5-21.

Aronson, S.M., 1998. A tale of Danbury hatters, detectives and Dartmouth chemists. Med. Health R I 81, 114-115.

Aten, J., Prigent, P., Poncet, P., Blanpied, C., Claessen, N., Druet, P. and Hirsch, F., 1995. Mercuric chloride-induced programmed cell death of a murine T cell hybridoma. I. Effect of the proto-oncogene Bcl-2. Cell. Immunol. 161, 98-106.

Bachmann, M.F., Oxenius, A., Speiser, D.E., Mariathasan, S., Hengartner, H., Zinkernagel, R.M. and Ohashi, P.S., 1997. Peptide-induced T cell receptor down-regulation on naive T cells predicts agonist/partial agonist properties and strictly correlates with T cell activation. Eur. J. Immunol. 27, 2195-2203.

Badou, A., Savignac, M., Moreau, M., Leclerc, C., Pasquier, R., Druet, P. and Pelletier, L., 1997. HgCl2-induced interleukin-4 gene expression in T cells involves a protein kinase C-dependent calcium influx through L-type calcium channels. J. Biol. Chem. 272, 32411-32418.

Bagenstose, L.M., Salgame, P. and Monestier, M., 1998a. IL-12 down-regulates autoantibody production in mercury-induced autoimmunity. J. Immunol. 160, 1612-1617.

Bagenstose, L.M., Salgame, P. and Monestier, M., 1998b. Mercury-induced autoimmunity in the absence of IL-4. Clin. Exp. Immunol. 114, 9-12.

Ball, L.K., Ball, R. and Pratt, R.D., 2001. An assessment of thimerosal use in childhood vaccines. Pediatrics 107, 1147-1154.

Ballatori, N., 2002. Transport of toxic metals by molecular mimicry. Env. Health Persp. 110, 689-694.

Ballatori, N. and Boyer, J.L., 1996. Disruption of cell volume regulation by mercuric chloride is mediated by an increase in sodium permeability and inhibition of an osmolyte channel in skate hepatocytes. Toxicol. Appl. Pharmacol. 140, 404-410.

Ballatori, N., Lieberman, M.W. and Wang, W., 1998. N-acetylcysteine as an antidote in methylmercury poisoning. Env. Health Persp. 106, 267-271.

Ballatori, N., Shi, C. and Boyer, J.L., 1988. Altered plasma membrane ion permeability in mercury-induced cell injury: studies in hepatocytes of elasmobranch Raja erinacea. Toxicol. Appl. Pharmacol. 95, 279-291.

Barregard, L., Sallsten, G. and Conradi, N., 1999a. Tissue levels of mercury determined in a deceased worker after occupational exposure. Int. Arch. Occup. Environ. Health 72, 169-173.

Barregard, L., Svalander, C., Schutz, A., Westberg, G., Sallsten, G., Blohme, I., Molne, J., Attman, P.O. and Haglind, P., 1999b. Cadmium, mercury, and lead in kidney cortex of the general Swedish population: a study of biopsies from living kidney donors. Environ. Health Perspect. 107, 867-871.

Barregeard, L., Enestreom, S., Ljunghusen, O., Wieslander, J. and Hultman, P., 1997. A study of autoantibodies and circulating immune complexes in mercury-exposed chloralkali workers. Int. Arch. Occup. Environ Healt.h 70, 101-106.

Bates, M.N., Fawcett, J., Garrett, N., Cutress, T. and Kjellstrom, T., 2004. Health effects of dental amalgam exposure: a retrospective cohort study. Int. J. Epidemiol. 33, 894-902.

Bernaudin, J.F., Druet, E., Belair, M.F., Pinchon, M.C., Sapin, C. and Druet, P., 1979. Extrarenal immune complex type deposits induced by mercuric chloride in the Brown Norway rat. Clin. Exp. Immunol. 38, 265-273.

Berridge, M.J., 1997a. Elementary and global aspects of calcium signalling. J. Exp. Biol. 200 Pt 2, 315-319.

Berridge, M.J., 1997b. Lymphocyte activation in health and disease. Crit. Rev. Immunol. 17, 155-178.

Blakley, B.R., 1984. Enhancement of urethan-induced adenoma formation in Swiss mice exposed to methylmercury. Can. J. Comp. Med. 48, 299-302.

Blakley, B.R., Sisodia, C.S. and Mukkur, T.K., 1980. The effect of methylmercury, tetraethyl lead, and sodium arsenite on the humoral immune response in mice. Toxicol. Appl. Pharmacol. 52, 245-254.

Blanchard, N. and Hivroz, C., 2002. The immunological synapse: the more you look the less you know. Biol. Cell 94, 345-354.

Bowman, C., Mason, D.W., Pusey, C.D. and Lockwood, C.M., 1984. Autoregulation of autoantibody synthesis in mercuric chloride nephritis in the Brown Norway rat. I. A role for T suppressor cells. Eur. J. Immunol. 14, 464-470.

Brawer, J.R., McCarthy, G.F., Gornitsky, M., Frankel, D., Mehindate, K. and Schipper, H.M., 1998. Mercuric chloride induces a stress response in cultured astrocytes characterized by mitochondrial uptake of iron. Neurotoxicology 19, 767-776.

Bromley, S.K., Iaboni, A., Davis, S.J., Whitty, A., Green, J.M., Shaw, A.S., Weiss, A. and Dustin, M.L., 2001. The immunological synapse and CD28-CD80 interactions. Nat. Immunol. 2, 1159-1166.

Brown, D.L., Reuhl, K.R., Bormann, S. and Little, J.E., 1988. Effects of methyl mercury on the microtubule system of mouse lymphocytes. Toxicol. Appl. Pharm. 94, 66-75.

Brunner, M., Albertini, S. and Wurgler, F.E., 1991. Effects of 10 known or suspected spindle poisons in the in vitro porcine brain tubulin assembly assay. Mutagenesis 6, 65-70.

Burn, P., Kupfer, A. and Singer, S.J., 1988. Dynamic membrane-cytoskeletal interactions: specific association of integrin and talin arises in vivo after phorbol ester treatment of peripheral blood lymphocytes. Proc. Natl. Acad. Sci. U.S.A. 85, 497-501.

Busselberg, D., 1995. Calcium channels as target sites of heavy metals. Toxicol. Lett. 82-83, 255-261.

Buttgereit, F., Burmester, G.R. and Brand, M.D., 2000. Bioenergetics of immune functions: fundamental and therapeutic aspects. Immunol. Today 21, 192-199.

Bygrave, F.L., Karjalainen, A. and Altin, J.G., 1989. Passive calcium influx by plasma membrane vesicles isolated from rat liver. Cell Calcium 10, 235-240.

Cadrin, M., Wasteneys, G.O., Jones-Villeneuve, E.M., Brown, D.L. and Reuhl, K.R., 1988. Effects of methylmercury on retinoic acid-induced neuroectodermal derivatives of embryonal carcinoma cells. Cell Biol. Toxicol. 4, 61-80.

Cai, F., Backman, H.A. and Baines, M.G., 1988. Thimerosal: an ophthalmic preservative which acts as a hapten to elicit specific antibodies and cell mediated immunity. Curr. Eye Res. 7, 341-351.

Cantrell, D.A., Davies, A.A. and Crumpton, M.J., 1985. Activators of protein kinase C down-regulate and phosphorylate the T3/T-cell antigen receptor complex of human T lymphocytes. Proc. Natl. Acad. Sci. U.S.A. 82, 8158-8162.

Caplan, S. and Baniyash, M., 1996. Normal T cells express two T cell antigen receptor populations, one of which is linked to the cytoskeleton via zeta chain and displays a unique activation-dependent phosphorylation pattern. J. Biol. Chem. 271, 20705-20712.

Caron, J., Jones, A. and Kirschner, M., 1985. Autoregulation of tubulin synthesis in hepatocytes and fibroblasts. J. Cell Biol. 101, 1763-1772.

Carranza-Rosales, P., Said-Fernandez, S., Sepulveda-Saavedra, J., Cruz-Vega, D.E. and Gandolfi, A.J., 2005. Morphologic and functional alterations induced by low doses of

mercuric chloride in the kidney OK cell line: ultrastructural evidence for an apoptotic mechanism of damage. Toxicology 210, 111-121.

Castedo, M., Pelletier, L., Pasquier, R. and Druet, P., 1994. Improvement of TH1 functions during the regulation phase of mercury disease in brown Norway rats. Scand. J. Immunol. 39, 144-150.

Castoldi, A.F., Barni, S., Turin, I., Gandini, C. and Manzo, L., 2000. Early acute necrosis, delayed apoptosis and cytoskeletal breakdown in cultured cerebellar granule neurons exposed to methylmercury. J. Neurosci. Res. 59, 775-787.

Chanez, C., Flexor, M.A. and Bourre, J.M., 1989. Effect of organic and inorganic mercuric salts on Na+K+ATPase in different cerebral fractions in control and intrauterine growth-retarded rats: alterations induced by serotonin. Neurotoxicology 10, 699-706.

Chen, Y.Z., Lai, Z.F., Nishi, K. and Nishimura, Y., 1998. Modulation of calcium responses by altered peptide ligands in a human T cell clone. Eur. J. Immunol. 28, 3929-3939.

Chien, Y.H. and Davis, M.M., 1993. How alpha beta T-cell receptors 'see' peptide/MHC complexes. Immunol. Today 14, 597-602.

Clarkson, T.W., 1987. Metal toxicity in the central nervous system. Env. Health Persp. 75, 59-64.

Clements, C.J., 2004. The evidence for the safety of thiomersal in newborn and infant vaccines. Vaccine 22, 1854-1861.

Colombo, M., Hamelin, C., Kouassi, E., Fournier, M. and Bernier, J., 2004. Differential effects of mercury, lead, and cadmium on IL-2 production by Jurkat T cells. Clin. Immunol. 111, 311-322.

Contrino, J., Marucha, P., Ribaudo, R., Ference, R., Bigazzi, P.E. and Kreutzer, D.L., 1988. Effects of mercury on human polymorphonuclear leukocyte function in vitro. Am. J. Pathol. 132, 110-118.

Cooper, J.A., 1987. Effects of cytochalasin and phalloidin on actin. J. Cell Biol. 105, 1473-1478.

Corbin, S.B. and Kohn, W.G., 1994. The benefits and risks of dental amalgam: current findings reviewed. J. Am. Dent. Assoc. 125, 381-388.

Counter, S.A. and Buchanan, L.H., 2004. Mercury exposure in children: a review. Toxicol. Appl. Pharmacol. 198, 209-230.

Cullinan, P., Sperling, A.I. and Burkhardt, J.K., 2002. The distal pole complex: a novel membrane domain distal to the immunological synapse. Immunol. Rev. 189, 111-122.

Dantas, D.C. and Queiroz, M.L., 1997. Immunoglobulin E and autoantibodies in mercury-exposed workers. Immunopharmacol. Immunotoxicol. 19, 383-392.

Das, V., Nal, B., Dujeancourt, A., Thoulouze, M.I., Galli, T., Roux, P., Dautry-Varsat, A. and Alcover, A., 2004. Activation-induced polarized recycling targets T cell antigen receptors to the immunological synapse; involvement of SNARE complexes. Immunity 20, 577-588.

Das, V., Nal, B., Roumier, A., Meas-Yedid, V., Zimmer, C., Olivo-Marin, J.C., Roux, P., Ferrier, P., Dautry-Varsat, A. and Alcover, A., 2002. Membrane-cytoskeleton interactions during the formation of the immunological synapse and subsequent T-cell activation. Immunol. Rev. 189, 123-135.

Delfraissy, J.F., Galanaud, P., Balavoine, J.F., Wallon, C. and Dormont, J., 1984. Captopril and immune regulation. Kidney Int. 25, 925-929.

Delnomdedieu, M. and Allis, J.W., 1993. Interaction of inorganic mercury salts with model and red cell membranes: importance of lipid binding sites. Chemico-Biological Interactions 88, 71-87.

Delon, J., Kaibuchi, K. and Germain, R.N., 2001. Exclusion of CD43 from the immunological synapse is mediated by phosphorylation-regulated relocation of the cytoskeletal adaptor moesin. Immunity 15, 691-701.

Diaz-Flores, E., Siliceo, M., Martinez, A.C. and Merida, I., 2003. Membrane translocation of protein kinase Ctheta during T lymphocyte activation requires phospholipase C-gamma-generated diacylglycerol. J. Biol. Chem. 278, 29208-29215.

Dieter, M.P., Luster, M.I., Boorman, G.A., Jameson, C.W., Dean, J.H. and Cox, J.W., 1983. Immunological and biochemical responses in mice treated with mercuric chloride. Toxicol. Appl. Pharm. 68, 218-228.

Dietrich, J., Menne, C., Lauritsen, J.P., von Essen, M., Rasmussen, A.B., Odum, N. and Geisler, C., 2002. Ligand-induced TCR down-regulation is not dependent on constitutive TCR cycling. J. Immunol. 168, 5434-5440.

Dodes, J.E., 2001. The amalgam controversy. An evidence-based analysis. J. Am. Dent. Assoc. 132, 348-356.

Donnadieu, E., Cefai, D., Tan, Y.P., Paresys, G., Bismuth, G. and Trautmann, A., 1992. Imaging early steps of human T cell activation by antigen-presenting cells. J. Immunol. 148, 2643-2653.

D'Oro, U., Vacchio, M.S., Weissman, A.M. and Ashwell, J.D., 1997. Activation of the Lck tyrosine kinase targets cell surface T cell antigen receptors for lysosomal degradation. Immunity 7, 619-628.

Druet, E., Fournie, G., Mandet, C., Sapin, C., Geunther, E. and Druet, P., 1979a. Genetic control of susceptibility to immune complex type nephritis induced by HgCl2 in rats. Transplant. Proc. 11, 1600-1603.

Druet, P., Ayed, K., Bariety, J., Bernaudin, J.F., Druet, E., Girard, J.F., Hinglais, N. and Sapin, C., 1979b. Experimental immune glomerulonephritis induced in the rat by mercuric chloride. Adv. Nephrol. Necker Hosp. 8, 321-342.

Druet, P., Druet, E., Potdevin, F. and Sapin, C., 1978. Immune type glomerulonephritis induced by HgCl2 in the Brown Norway rat. Ann. D Immunologie 129 C, 777-792.

Dubey, D., Kuhn, J., Vial, M.C., Druet, P. and Bellon, B., 1993. Anti-interleukin-2 receptor monoclonal antibody therapy supports a role for Th1-like cells in HgCl2-induced autoimmunity in rats. Scand. J. Immunol. 37, 406-412.

Dustin, M.L., 2002. The immunological synapse. Arthr. Res. 4 Suppl 3, S119-125.

Dustin, M.L., 2003. Coordination of T cell activation and migration through formation of the immunological synapse. Ann. N.Y. Acad. Sci. 987, 51-59.

Dustin, M.L. and Cooper, J.A., 2000. The immunological synapse and the actin cytoskeleton: molecular hardware for T cell signaling. Nat. Immunol. 1, 23-29.

Egen, J.G. and Allison, J.P., 2002. Cytotoxic T lymphocyte antigen-4 accumulation in the immunological synapse is regulated by TCR signal strength. Immunity 16, 23-35.

Ehrlich, L.I., Ebert, P.J., Krummel, M.F., Weiss, A. and Davis, M.M., 2002. Dynamics of p56lck translocation to the T cell immunological synapse following agonist and antagonist stimulation. Immunity 17, 809-822.

Ekstrand, J., Bjorkman, L., Edlund, C. and Sandborgh-Englund, G., 1998. Toxicological aspects on the release and systemic uptake of mercury from dental amalgam. Eur. J. Oral Sci. 106, 678-686.

Endo, T., Kimura, O., Sakata, M. and Shaikh, Z.A., 1997. Mercury uptake by LLC-PK1 cells: dependence on temperature and membrane potential. Toxicol. Appl. Pharmacol. 146, 294-298.

Endo, T., Sakata, M. and Shaikh, Z.A., 1995a. Mercury uptake by primary cultures of rat renal cortical epithelial cells. I. Effects of cell density, temperature, and metabolic inhibitors. Toxicol. Appl .Pharmacol. 132, 36-43.

Endo, T., Sakata, M. and Shaikh, Z.A., 1995b. Mercury uptake by primary cultures of rat renal cortical epithelial cells. II. Effects of pH, halide ions, and alkali metal ions. Toxicol. Appl. Pharmacol. 134, 321-325.

Eto, K., 1997. Pathology of Minamata disease. Toxicol. Pathol. 25, 614-623.

Eto, K., 2000. Minamata disease. Neuropathology 20 Suppl, S14-19.

Eto, K., Takizawa, Y., Akagi, H., Haraguchi, K., Asano, S., Takahata, N. and Tokunaga, H., 1999. Differential diagnosis between organic and inorganic mercury poisoning in human cases--the pathologic point of view. Toxicol. Pathol. 27, 664-671.

Etter, E.F., Minta, A., Poenie, M. and Fay, F.S., 1996. Near-membrane [Ca2+] transients resolved using the Ca2+ indicator FFP18. Proc. Natl. Acad. Sci. U.S.A. 93, 5368-5373.

Evers, D., Kaplan, J., Meyer, M., Reaman, P., Braselton, W., Major, A., Burgess, N. and Scheuhammer, A., 1998. Geographic trend in mercury measured in common loon feathers and blood. Env. Toxicol. Chem. 17, 173-183.

Fan, P.L., Arenholt-Bindslev, D., Schmalz, G., Halbach, S. and Berendsen, H., 1997. Environmental issues in dentistry--mercury. FDI Commission. Int. Dent. J. 47, 105-109.

Far, D.F., Peyron, J.F., Imbert, V. and Rossi, B., 1994. Immunofluorescent quantification of tyrosine phosphorylation of cellular proteins in whole cells by flow cytometry. Cytometry 15, 327-334.

Farber, D.L., Acuto, O. and Bottomly, K., 1997. Differential T cell receptor-mediated signaling in naive and memory CD4 T cells. Eur. J. Immunol. 27, 2094-2101.

Faroudi, M., Utzny, C., Salio, M., Cerundolo, V., Guiraud, M., Muller, S. and Valitutti, S., 2003. Lytic versus stimulatory synapse in cytotoxic T lymphocyte/target cell interaction: manifestation of a dual activation threshold. Proc. Natl. Acad. Sci. U.S.A. 100, 14145-14150.

Faure, S., Salazar-Fontana, L.I., Semichon, M., Tybulewicz, V.L., Bismuth, G., Trautmann, A., Germain, R.N. and Delon, J., 2004. ERM proteins regulate cytoskeleton relaxation promoting T cell-APC conjugation. Nat. Immunol. 5, 272-279.

Favier, B., Burroughs, N.J., Wedderburn, L. and Valitutti, S., 2001. TCR dynamics on the surface of living T cells. Int. Immunol. 13, 1525-1532.

Fernando, Q., 1995. Metal speciation in environmental and biological systems. Environ. Health Perspect. 103 Suppl. 1, 13-16.

Fitzgerald, W., 1995. Is mercury increasing in the atmosphere? The need for an atmospheric mercury network (AMNET). Water Air Soil Poll. 80, 245-254.

Foa, C., Mege, J.L., Capo, C., Benoliel, A.M., Galindo, J.R. and Bongrand, P., 1988. T-cell-mediated cytolysis: analysis of killer and target cell deformability and deformation during conjugate formation. J. Cell Sci. 89 ( Pt 4), 561-573.

Foulkes, E.C., 1974. Excretion and retention of Cd, Zn, and Hg by the rabbit kidney. Am J. Physiol. 227, 1356–1360.

Foulkes, E.C., 1988. On the mechanism of transfer of heavy metals across cell membranes. Toxicology 52, 263-272.

Foulkes, E.C., 1991. Nature of Cd and Hg effects on epithelial amino acid transport in vivo and role of chelators. Toxicology 69, 177-185.

Foulkes, E.C., 2000. Transport of toxic heavy metals across cell membranes. Proc. Soc. Exp. Biol. Med. 223, 234-240.

Freiberg, B.A., Kupfer, H., Maslanik, W., Delli, J., Kappler, J., Zaller, D.M. and Kupfer, A., 2002. Staging and resetting T cell activation in SMACs. Nat. Immunol. 3, 911-917.

Gardner, P., 1989. Calcium and T lymphocyte activation. Cell 59, 15-20.

Geisler, C., 2004. TCR trafficking in resting and stimulated T cells. Crit. Rev. Immunol. 24, 67-86.

Girardi, G. and Elaias, M.M., 1998. Verapamil protection against mercuric chloride-induced renal glomerular injury in rats. Toxicol. Appl. Pharm. 152, 360-365.

Girardi, G., Saball, D.E., Salvarrey, M.S. and Elias, M.M., 1996. Glomerular compromise in mercuric chloride-induced nephrotoxicity. J. Biochem. Toxicol. 11, 189-196.

Girault, L., Boudou, A. and Drfourc, E.J., 1997. Methyl mercury interactions with phospholipid membranes as reported by fluorescence, 31P and 199Hg NMR. Biochim. Biophys. Acta 1325, 250-262.

Girault, L., Lemaire, P., Boudou, A., Debouzy, J.C. and Dufourc, E.J., 1996. Interactions of inorganic mercury with phospholipid micelles and model membranes. A 31*P*-NMR study. Eur. Biophys. J. 24, 413-421.

Graeme, K.A. and Pollack, C.V., Jr., 1998. Heavy metal toxicity, Part I: arsenic and mercury. J. Emerg. Med. 16, 45-56.

Grakoui, A., Bromley, S.K., Sumen, C., Davis, M.M., Shaw, A.S., Allen, P.M. and Dustin, M.L., 1999a. The immunological synapse: a molecular machine controlling T cell activation. Science 285, 221-227.

Grakoui, A., Donermeyer, D.L., Kanagawa, O., Murphy, K.M. and Allen, P.M., 1999b. TCR-independent pathways mediate the effects of antigen dose and altered peptide ligands on Th cell polarization. J. Immunol. 162, 1923-1930.

Grakoui, A., VanDyk, L.F., Dowdy, S.F. and Allen, P.M., 1998. Molecular basis for the lack of T cell proliferation induced by an altered peptide ligand. Int. Immunol. 10, 969-979.

Gray, L.S., Gnarra, J.R., Sullivan, J.A., Mandell, G.L. and Engelhard, V.H., 1988. Spatial and temporal characteristics of the increase in intracellular Ca2+ induced in cytotoxic T lymphocytes by cellular antigen. J. Immunol. 141, 2424-2430.

Gremm, D. and Wegner, A., 2000. Gelsolin as a calcium-regulated actin filament-capping protein. Eur. J. Biochem. 267, 4339-4345.

Griem, P., Scholz, E., Turfeld, M., Zander, D., Wiesner, U., Dunemann, L. and Gleichmann, E., 1997. Strain differences in tissue concentrations of mercury in inbred mice treated with mercuric chloride. Toxicol. Appl. Pharm. 144, 163-170.

Gukovskaya, A.S., Trepakova, E.S., Zinchenko, V.P., Korystov, Y.N. and Bezuglov, V.V., 1992. Effect of the sulfhydryl reagent thimerosal on cytosolic free Ca2+ and membrane potential of thymocytes. Biochim. Biophys. Acta 1111, 65-74.

Gutknecht, J., 1981. Inorganic mercury (Hg2+) transport through lipid bilayer membranes. J. Memb. Biol. 61, 61-66.

Hansen, J.C. and Danscher, G., 1997. Organic mercury: an environmental threat to the health of dietary-exposed societies? Rev. Environ. Health 12, 107-116.

Hao, S. and August, A., 2005. Actin depolymerization transduces the strength of B-cell receptor stimulation. Mol. Biol. Cell 16, 2275-2284.

Hashemi, B.B., Slattery, J.P., Holowka, D. and Baird, B., 1996. Sustained T cell receptor-mediated Ca2+ responses rely on dynamic engagement of receptors. J. Immunol. 156, 3660-3667.

Havarinasab, S., Lambertsson, L., Qvarnstrom, J., Hultman, P., Frech, W., Haggqvist, B., Nielsen, J.B. and Hansson-Georgiadis, H., 2004. Dose-response study of thimerosal-induced murine systemic autoimmunity. Toxicol. Appl. Pharmacol. 194, 169-179.

Heo, Y., Lee, W.T. and Lawrence, D.A., 1997. In vivo the environmental pollutants lead and mercury induce oligoclonal T cell responses skewed toward type-2 reactivities. Cell. Immunol. 179, 185-195.

Hill, G.S., 1986. Drug-associated glomerulopathies. Toxicol Pathol 14, 37-44.

Hinkle, P.M., Kinsella, P.A. and Osterhoudt, K.C., 1987. Cadmium uptake and toxicity via voltage-sensitive calcium channels. J. Biol. Chem. 262, 16333-16337.

Hodes, R.J. and Singer, A., 1984. MHC restriction in T cell/B cell interaction: role of B-cell subpopulations and B-cell activation state. Ann. D Immunologie 135D, 91-95.

Holdorf, A.D., Lee, K.H., Burack, W.R., Allen, P.M. and Shaw, A.S., 2002. Regulation of Lck activity by CD4 and CD28 in the immunological synapse. Nat. Immunol. 3, 259-264.

Holmes, A.S., Blaxill, M.F. and Haley, B.E., 2003. Reduced levels of mercury in first baby haircuts of autistic children. Int. J. Toxicol. 22, 277-285.

Hoorntje, S.J., Kallenberg, C.G., Weening, J.J., Donker, A.J., The, T.H. and Hoedemaeker, P.J., 1980. Immune-complex glomerulopathy in patients treated with captopril. Lancet 1, 1212-1215.

Howard, T.H. and Meyer, W.H., 1984. Chemotactic peptide modulation of actin assembly and locomotion in neutrophils. J. Cell Biol. 98, 1265-1271.

Hu, H., Meoller, G. and Abedi-Valugerdi, M., 1999. Mechanism of mercury-induced autoimmunity: both T helper 1- and T helper 2-type responses are involved. Immunology 96, 348-357.

Hu, H., Moller, G. and Abedi-Valugerdi, M., 1997. Thiol compounds inhibit mercury-induced immunological and immunopathological alterations in susceptible mice. Clin. Exp. Immunol. 107, 68-75.

Hua, J., Pelletier, L., Berlin, M. and Druet, P., 1993. Autoimmune glomerulonephritis induced by mercury vapour exposure in the Brown Norway rat. Toxicology 79, 119-129.

Hultman, P., Bell, L.J., Enestreom, S. and Pollard, K.M., 1992. Murine susceptibility to mercury. I. Autoantibody profiles and systemic immune deposits in inbred, congenic, and intra-H-2 recombinant strains. Clin. Immunol. Immunopath. 65, 98-109.

Hultman, P. and Enestrom, S., 1992. Dose-response studies in murine mercury-induced autoimmunity and immune-complex disease. Toxicol. Appl. Pharmacol. 113, 199-208.

Hultman, P. and Hansson-Georgiadis, H., 1999. Methyl mercury-induced autoimmunity in mice. Toxicol. Appl. Pharm. 154, 203-211.

Hultman, P., Lindh, U. and Horsted-Bindslev, P., 1998. Activation of the immune system and systemic immune-complex deposits in Brown Norway rats with dental amalgam restorations. J. Dent. Res. 77, 1415-1425.

Hultman, P. and Nielsen, J.B., 1998. The effect of toxicokinetics on murine mercury-induced autoimmunity. Environ. Res. 77, 141-148.

Hultman, P. and Nielsen, J.B., 2001. The effect of dose, gender, and non-H-2 genes in murine mercury-induced autoimmunity. J. Autoimmun. 17, 27-37.

Hultman, P., Skogh, T. and Enestreom, S., 1989. Circulating and tissue immune complexes in mercury-treated mice. J. Clin. Lab. Immunol. 29, 175-183.

Idziorek, T., Estaquier, J., De Bels, F. and Ameisen, J.C., 1995. YOPRO-1 permits cytofluorometric analysis of programmed cell death (apoptosis) without interfering with cell viability. J. Immunol. Meth. 185, 249-258.

Iezzi, G., Karjalainen, K. and Lanzavecchia, A., 1998. The duration of antigenic stimulation determines the fate of naive and effector T cells. Immunity 8, 89-95.

Imura, N., Miura, K., Inokawa, M. and Nakada, S., 1980. Mechanism of methylmercury cytotoxicity: by biochemical and morphological experiments using cultured cells. Toxicology 17, 241-254.

Inoue, Y., Saijoh, K. and Sumino, K., 1988. Action of mercurials on activity of partially purified soluble protein kinase C from mice brain. Pharmacol. Toxicol. 62, 278-281.

InSug, O., Datar, S., Koch, C.J., Shapiro, I.M. and Shenker, B.J., 1997. Mercuric compounds inhibit human monocyte function by inducing apoptosis: evidence for formation of reactive oxygen species, development of mitochondrial membrane permeability transition and loss of reductive reserve. Toxicology 124, 211-224.

Irvine, D.J., Purbhoo, M.A., Krogsgaard, M. and Davis, M.M., 2002. Direct observation of ligand recognition by T cells. Nature 419, 845-849.

Isakov, N. and Altman, A., 2002. Protein kinase C(theta) in T cell activation. Annu. Rev. Immunol. 20, 761-794.

Jiang, Y. and Moller, G., 1995. In vitro effects of HgCl2 on murine lymphocytes. I. Preferable activation of CD4+ T cells in a responder strain. J. Immunol. 154, 3138-3146.

Jiang, Y. and Moller, G., 1996. In vitro effects of HgCl2 on murine lymphocytes. II. Selective activation of T cells expressing certain V beta TCR. Int. Immunol. 8, 1729-1736.

Johansson, B.R. and Nannmark, U., 1996. Ultrastructure of interactions between activated murine natural killer cells and melanoma cells in an extracellular matrix (Matrigel) environment. Nat. Immun. 15, 98-106.

Johansson, U., Hansson-Georgiadis, H. and Hultman, P., 1998. The genotype determines the B cell response in mercury-treated mice. Intl. Arch. Aller. Immunol. 116, 295-305.

Johansson, U., Sander, B. and Hultman, P., 1997. Effects of the murine genotype on T cell activation and cytokine production in murine mercury-induced autoimmunity. J. Autoimmun. 10, 347-355.

Jordan, M.A., 2002. Mechanism of action of antitumor drugs that interact with microtubules and tubulin. Curr. Med. Chem. Anti-Canc. Agents 2, 1-17.

Kaiser, J., 1998. Toxicologists shed new light on old poisons. Science 279, 1850-1851.

Kanluen, S. and Gottlieb, C.A., 1991. A clinical pathologic study of four adult cases of acute mercury inhalation toxicity. Arch. Path. Lab. Med. 115, 56-60.

Kaplan, J.H. and Mone, M.D., 1985. Modified cation activation of the (Na+K)-ATPase following treatment with thimerosal. Arch. Biochem. Biophys. 237, 386-395.

Karr, T.L., Kristofferson, D. and Purich, D.L., 1980. Calcium ion induces endwise depolymerization of bovine brain microtubules. J. Biol. Chem. 255, 11853-11856.

Kastrup, J., Lauritsen, J.P., Menne, C., Dietrich, J. and Geisler, C., 2000. The phosphatase domains of CD45 are required for ligand induced T-cell receptor downregulation. Scand. J. Immunol. 51, 491-496.

Katano, Y., Pu, M.Y., Akhand, A.A., Hamaguchi, M., Koga, Y., Isobe, K., Fukuda, Y., Hayakawa, T. and Nakashima, I., 1995. Evidence of redox-linked signaling for producing a giant signal complex. J. Cell. Biochem. 57, 432-439.

Kauppinen, R.A., Komulainen, H. and Taipale, H., 1989. Cellular mechanisms underlying the increase in cytosolic free calcium concentration induced by methylmercury in cerebrocortical synaptosomes from guinea pig. J. Pharmacol. Exp. Ther. 248, 1248-1254.

Kazantzis, G., 2002. Mercury exposure and early effects: an overview. Med. Lav. 93, 139-147.

Kazantzis, G., Schiller, K.F., Asscher, A.W. and Drew, R.G., 1962. Albuminuria and the nephrotic syndrome following exposure to mercury and its compounds. Q. J. Med. 31, 403-418.

Keates, R.A. and Yott, B., 1984. Inhibition of microtubule polymerization by micromolar concentrations of mercury (II). Can. J. Biochem. Cell Biol. 62, 814-818.

Kerper, L.E., Ballatori, N. and Clarkson, T.W., 1992. Methylmercury transport across the blood-brain barrier by an amino acid carrier. Am. J. Physiol. 262, R761-765.

Kerper, L.E. and Hinkle, P.M., 1997. Lead uptake in brain capillary endothelial cells: activation by calcium store depletion. Toxicol. Appl. Pharm. 146, 127-133.

Kerper, L.E., Mokrzan, E.M., Clarkson, T.W. and Ballatori, N., 1996. Methylmercury efflux from brain capillary endothelial cells is modulated by intracellular glutathione but not ATP. Toxicol. Appl. Pharmacol. 141, 526-531.

Kiely, P.D., Gillespie, K.M. and Oliveira, D.B., 1995. Oxpentifylline inhibits tumor necrosis factor-alpha mRNA transcription and protects against arthritis in mercuric chloride-treated brown Norway rats. Eur. J. Immunol. 25, 2899-2906.

Kim, E., Kim, J.H., Kim, H.S., Ryu, S.H. and Suh, P.G., 2002. Thimerosal stimulates focal adhesion kinase and cytoskeletal changes by redox modulation. Biochim. Biophys. Acta 1593, 9-15.

Knox, J.D., Mitchel, R.E. and Brown, D.L., 1993. Effects of taxol and taxol/hyperthermia treatments on the functional polarization of cytotoxic T lymphocytes. Cell Motil. Cytoskeleton 24, 129-138.

Komulainen, H. and Bondy, S.C., 1987. Increased free intrasynaptosomal Ca2+ by neurotoxic organometals: distinctive mechanisms. Toxicol. Appl. Pharm. 88, 77-86.

Kono, D.H., Balomenos, D., Pearson, D.L., Park, M.S., Hildebrandt, B., Hultman, P. and Pollard, K.M., 1998. The prototypic Th2 autoimmunity induced by mercury is dependent on IFN-gamma and not Th1/Th2 imbalance. J. Immunol. 161, 234-240.

Koropatnick, J. and Zalups, R.K., 1997. Effect of non-toxic mercury, zinc or cadmium pretreatment on the capacity of human monocytes to undergo lipopolysaccharide-induced activation. Br. . Pharmacol. 120, 797-806.

Kosuda, L.L., Hannigan, M.O., Bigazzi, P.E., Leif, J.H. and Greiner, D.L., 1996. Thymus atrophy and changes in thymocyte subpopulations of BN rats with mercury-induced renal autoimmune disease. Autoimmunity 23, 77-89.

Kulig, K., 1998. A tragic reminder about organic mercury. N. Engl. J. Med. 338, 1692-1694.

Kupfer, A., Burn, P. and Singer, S.J., 1990. The PMA-induced specific association of LFA-1 and talin in intact cloned T helper cells. J. Mol. Cell. Immunology 4, 317-325.

Kupfer, A. and Dennert, G., 1984. Reorientation of the microtubule-organizing center and the Golgi apparatus in cloned cytotoxic lymphocytes triggered by binding to lysable target cells. J. Immunol. 133, 2762-2766.

Kupfer, A., Dennert, G. and Singer, S.J., 1983. Polarization of the Golgi apparatus and the microtubule-organizing center within cloned natural killer cells bound to their targets. Proc. Natl. Acad. Sci. U.S.A. 80, 7224-7228.

Kupfer, A., Dennert, G. and Singer, S.J., 1985. The reorientation of the Golgi apparatus and the microtubule-organizing center in the cytotoxic effector cell is a prerequisite in the lysis of bound target cells. J. Mol. Cell. Immunol. 2, 37-49.

Kupfer, A., Louvard, D. and Singer, S.J., 1982. Polarization of the Golgi apparatus and the microtubule-organizing center in cultured fibroblasts at the edge of an experimental wound. Proc. Natl. Acad. Sci. U.S.A. 79, 2603-2607.

Kupfer, A., Mosmann, T.R. and Kupfer, H., 1991. Polarized expression of cytokines in cell conjugates of helper T cells and splenic B cells. Proc. Natl. Acad. Sci. U.S.A. 88, 775-779.

Kupfer, A. and Singer, S.J., 1989a. Cell biology of cytotoxic and helper T cell functions: immunofluorescence microscopic studies of single cells and cell couples. Ann. Rev. Immunol. 7, 309-337.

Kupfer, A. and Singer, S.J., 1989b. The specific interaction of helper T cells and antigen-presenting B cells. IV. Membrane and cytoskeletal reorganizations in the bound T cell as a function of antigen dose. J. Exp. Med. 170, 1697-1713.

Kupfer, A., Singer, S.J. and Dennert, G., 1986a. On the mechanism of unidirectional killing in mixtures of two cytotoxic T lymphocytes. Unidirectional polarization of cytoplasmic organelles and the membrane-associated cytoskeleton in the effector cell. J. Exp. Med. 163, 489-498.

Kupfer, A., Singer, S.J., Janeway, C.A., Jr. and Swain, S.L., 1987a. Coclustering of CD4 (L3T4) molecule with the T-cell receptor is induced by specific direct interaction of helper T cells and antigen-presenting cells. Proc. Natl. Acad. Sci. U.S.A. 84, 5888-5892.

Kupfer, A., Swain, S.L., Janeway, C.A., Jr. and Singer, S.J., 1986b. The specific direct interaction of helper T cells and antigen-presenting B cells. Proc. Natl. Acad. Sci. U.S.A. 83, 6080-6083.

Kupfer, A., Swain, S.L. and Singer, S.J., 1987b. The specific direct interaction of helper T cells and antigen-presenting B cells. II. Reorientation of the microtubule organizing center and reorganization of the membrane-associated cytoskeleton inside the bound helper T cells. J. Exp. Med. 165, 1565-1580.

Kupfer, H., Monks, C.R. and Kupfer, A., 1994. Small splenic B cells that bind to antigen-specific T helper (Th) cells and face the site of cytokine production in the Th cells selectively proliferate: immunofluorescence microscopic studies of Th-B antigen-presenting cell interactions. J. Exp. Med. 179, 1507-1515.

Kwan Lim, G.E., McNeill, L., Whitley, K., Becker, D.L. and Zamoyska, R., 1998. Co-capping studies reveal CD8/TCR interactions after capping CD8 beta polypeptides and intracellular associations of CD8 with p56 lck. Eur. J. Immunol. 28, 745-754.

Lander, H.M., Levine, D.M. and Novogrodsky, A., 1992. Stress stimuli-induced lymphocyte activation. Cell. Immunol. 145, 146-155.

Lanzavecchia, A. and Sallusto, F., 2001. Antigen decoding by T lymphocytes: from synapses to fate determination. Nat. Immunol. 2, 487-492.

Lash, L.H. and Zalups, R.K., 1996. Alterations in renal cellular glutathione metabolism after in vivo administration of a subtoxic dose of mercuric chloride. J. Biochem. Toxicol. 11, 1-9.

Lauritsen, J.P., Christensen, M.D., Dietrich, J., Kastrup, J., Odum, N. and Geisler, C., 1998. Two distinct pathways exist for down-regulation of the TCR. J Immunol 161, 260-267.

Lauritsen, J.P., Menne, C., Kastrup, J., Dietrich, J. and Geisler, C., 2001. Protein phosphatase 2A isotypes regulate cell surface expression of the T cell receptor. Exp. Clin. Immunogenet. 18, 24-33.

Lee, K.H., Dinner, A.R., Tu, C., Campi, G., Raychaudhuri, S., Varma, R., Sims, T.N., Burack, W.R., Wu, H., Wang, J., Kanagawa, O., Markiewicz, M., Allen, P.M., Dustin, M.L., Chakraborty, A.K. and Shaw, A.S., 2003. The immunological synapse balances T cell receptor signaling and degradation. Science 302, 1218-1222.

Lewis, R.N. and Bowler, K., 1983. Rat brain (Na+-K+)ATPase: modulation of its ouabain-sensitive K+-PNPPase activity by thimerosal. Int. J. Biochem. 15, 5-7.

Lewis, R.S. and Cahalan, M.D., 1995. Potassium and calcium channels in lymphocytes. Ann. Rev. Immunol. 13, 623-653.

Lindow, S.W., Knight, R., Batty, J. and Haswell, S.J., 2003. Maternal and neonatal hair mercury concentrations: the effect of dental amalgam. Bjog 110, 287-291.

Lindvall, M., Eriksson, H., Hedlund, G. and Sjogren, H.O., 1997. Selective cytotoxicity of two rodent T cell lymphomas to rat yolk sac tumours involves a retroviral envelope protein expressed by the lymphoma. Scand. J. Immunol. 46, 479-487.

Liu, H., Rhodes, M., Wiest, D.L. and Vignali, D.A., 2000. On the dynamics of TCR:CD3 complex cell surface expression and downmodulation. Immunity 13, 665-675.

Loftenius, A., Ekstrand, J. and Meoller, E., 1997. In vitro effects of mercuric chloride HgCl2 on human mononuclear cells. Clin. Exp. Immunol. 110, 418-422.

Lowin Kropf, B., Shapiro, V.S. and Weiss, A., 1998. Cytoskeletal polarization of T cells is regulated by an immunoreceptor tyrosine-based activation motif-dependent mechanism. J. Cell Biol. 140, 861-871.

MacDougal, K.C., Johnson, M.D. and Burnett, K.G., 1996. Exposure to mercury alters early activation events in fish leukocytes. Env. Health Persp. 104, 1102-1106.

Magos, L., 2001. Review on the toxicity of ethylmercury, including its presence as a preservative in biological and pharmaceutical products. J. Appl. Toxicol. 21, 1-5.

Makani, S., Gollapudi, S., Yel, L., Chiplunkar, S. and Gupta, S., 2002. Biochemical and molecular basis of thimerosal-induced apoptosis in T cells: a major role of mitochondrial pathway. Genes Immun. 3, 270-278.

Maltsev, V.A., Wolff, B., Hess, J. and Werner, G., 1994. Calcium signalling in individual T-cells measured by confocal microscopy. Immunology Letters 42, 41-47.

Marchi, B., Burlando, B., Panfoli, I. and Viarengo, A., 2000. Interference of heavy metal cations with fluorescent Ca2+ probes does not affect Ca2+ measurements in living cells. Cell Calcium 28, 225-231.

Marwali, M.R., MacLeod, M.A., Muzia, D.N. and Takei, F., 2004. Lipid rafts mediate association of LFA-1 and CD3 and formation of the immunological synapse of CTL. J. Immunol. 173, 2960-2967.

Mason, H.J., Hindell, P. and Williams, N.R., 2001. Biological monitoring and exposure to mercury. Occup. Med. (Lond) 51, 2-11.

Mathieson, P.W., Stapleton, K.J., Oliveira, D.B. and Lockwood, C.M., 1991. Immunoregulation of mercuric chloride-induced autoimmunity in Brown Norway rats: a role for CD8+ T cells revealed by in vivo depletion studies. Eur. J. Immunol. 21, 2105-2109.

Mathieson, P.W., Thiru, S. and Oliveira, D.B., 1992. Mercuric chloride-treated brown Norway rats develop widespread tissue injury including necrotizing vasculitis. Lab. Invest. 67, 121-129.

Matsuda, M., Maeda, Y., Shirakawa, C., Morita, S., Koyama, A., Horiuchi, F., Hamazaki, H., Irimajiri, K. and Horiuchi, A., 1994. Possible involvement of protein kinase C activation in down-regulation of CD3 antigen on adult T cell leukaemia cells. Br. J. Haematol. 86, 399-401.

Matsuoka, M., Wispriyono, B., Iryo, Y. and Igisu, H., 2000. Mercury chloride activates c-Jun N-terminal kinase and induces c-jun expression in LLC-PK1 cells. Toxicol. Sci. 53, 361-368.

Mattingly, R.R., Felczak, A., Chen, C.C., McCabe, M.J., Jr. and Rosenspire, A.J., 2001. Low concentrations of inorganic mercury inhibit Ras activation during T cell receptor-mediated signal transduction. Toxicol. Appl. Pharmacol. 176, 162-168.

McCabe, M.J., Jr., Eckles, K.G., Langdon, M., Clarkson, T.W., Whitekus, M.J. and Rosenspire, A.J., 2005. Attenuation of CD95-induced apoptosis by inorganic mercury: caspase-3 is not a direct target of low levels of Hg2+. Toxicol. Lett. 155, 161-170.

McCabe, M.J., Jr., Santini, R.P. and Rosenspire, A.J., 1999. Low and nontoxic levels of ionic mercury interfere with the regulation of cell growth in the WEHI-231 B-cell lymphoma. Scand. J. Immunol. 50, 233-241.

McCloskey, M.A. and Poo, M.M., 1986. Contact-induced redistribution of specific membrane components: local accumulation and development of adhesion. J. Cell Biol. 102, 2185-2196.

McNulty, T.J. and Taylor, C.W., 1999. Extracellular heavy-metal ions stimulate Ca2+ mobilization in hepatocytes. Biochem. J. 339, 555-561.

Menne, C., Moller Sorensen, T., Siersma, V., von Essen, M., Odum, N. and Geisler, C., 2002. Endo- and exocytic rate constants for spontaneous and protein kinase C-activated T cell receptor cycling. Eur. J. Immunol. 32, 616-626.

Miceli, M.C., Moran, M., Chung, C.D., Patel, V.P., Low, T. and Zinnanti, W., 2001. Co-stimulation and counter-stimulation: lipid raft clustering controls TCR signaling and functional outcomes. Semin. Immun. 13, 115-128.

Miura, K., Inokawa, M. and Imura, N., 1984. Effects of methylmercury and some metal ions on microtubule networks in mouse glioma cells and in vitro tubulin polymerization. Toxicol. Appl. Pharm. 73, 218-231.

Miura, K., Kobayashi, K., Toyoda, H. and Imura, N., 1998. Methylmercury-induced microtubule depolymerization leads to inhibition of tubulin synthesis. J. Toxicol. Sci. 23, 379-388.

Miura, K., Koide, N., Himeno, S., Nakagawa, I. and Imura, N., 1999. The involvement of microtubular disruption in methylmercury-induced apoptosis in neuronal and nonneuronal cell lines. Toxicol. Appl. Pharmacol. 160, 279-288.

Mizuno, M. and Singer, S.J., 1993. A soluble secretory protein is first concentrated in the endoplasmic reticulum before transfer to the Golgi apparatus. Proc. Natl. Acad. Sci. U.S.A. 90, 5732-5736.

Mollinedo, F. and Gajate, C., 2003. Microtubules, microtubule-interfering agents and apoptosis. Apoptosis 8, 413-450.

Monks, C.R., Freiberg, B.A., Kupfer, H., Sciaky, N. and Kupfer, A., 1998. Three-dimensional segregation of supramolecular activation clusters in T cells. Nature 395, 82-86.

Monks, C.R., Kupfer, H., Tamir, I., Barlow, A. and Kupfer, A., 1997. Selective modulation of protein kinase C-theta during T-cell activation. Nature 385, 83-86.

Montoya, M.C., Sancho, D., Vicente-Manzanares, M. and Sanchez-Madrid, F., 2002. Cell adhesion and polarity during immune interactions. Immunol. Rev. 186, 68-82.

Moskalewski, S. and Thyberg, J., 1990. Disorganization and reorganization of the Golgi complex and the lysosomal system in association with mitosis. J. Submicrosc. Cyt. Path. 22, 159-171.

Mosmann, T., 1983. Rapid colorimetric assay for cellular growth and survival: application to proliferation and cytotoxicity assays. J. Immunol. Meth. 65, 55-63.

Moss, W.C., Irvine, D.J., Davis, M.M. and Krummel, M.F., 2002. Quantifying signaling-induced reorientation of T cell receptors during immunological synapse formation. Proc. Natl. Acad. Sci. U.S.A. 99, 15024-15029.

Moszczyanski, P., Rutowski, J., S±owianski, S. and Bem, S., 1998. Immunological effects of occupational exposure to metallic mercury in the population of T-cells and NK-cells. Analyst 123, 99-103.

Muller, S., Demotz, S., Bulliard, C. and Valitutti, S., 1999. Kinetics and extent of protein tyrosine kinase activation in individual T cells upon antigenic stimulation. Immunology 97, 287-293.

Naganuma, A., Anderson, M.E. and Meister, A., 1990. Cellular glutathione as a determinant of sensitivity to mercuric chloride toxicity. Prevention of toxicity by giving glutathione monoester. Biochem. Pharmacol. 40, 693-697.

Nakada, S. and Imura, N., 1982. Uptake of methylmercury and inorganic mercury by mouse glioma and mouse neuroblastoma cells. Neurotoxicology 3, 249-258.

Nakashima, I., Pu, M.Y., Nishizaki, A., Rosila, I., Ma, L., Katano, Y., Ohkusu, K., Rahman, S.M., Isobe, K., Hamaguchi, M. and et al., 1994. Redox mechanism as alternative to ligand binding for receptor activation delivering disregulated cellular signals. J. Immunol. 152, 1064-1071.

Nakatsuru, S., Oohashi, J., Nozaki, H., Nakada, S. and Imura, N., 1985. Effect of mercurials on lymphocyte functions in vitro. Toxicology 36, 297-305.

Nath, K.A., Croatt, A.J., Likely, S., Behrens, T.W. and Warden, D., 1996. Renal oxidant injury and oxidant response induced by mercury. Kidney Int. 50, 1032-1043.

Nathanson, M.H., Mariwalla, K., Ballatori, N. and Boyer, J.L., 1995. Effects of Hg2+ on cytosolic Ca2+ in isolated skate hepatocytes. Cell Calcium 18, 429-439.

Nesic, D., Henderson, S. and Vukmanovic, S., 1998. Prevention of antigen-induced microtubule organizing center reorientation in cytotoxic T cells by modulation of protein kinase C activity. Int. Immunol. 10, 1741-1746.

Nielsen, J.B. and Hultman, P., 2002. Mercury-induced autoimmunity in mice. Environ. Health Perspect. 110 Suppl. 5, 877-881.

Nierenberg, D.W., Nordgren, R.E., Chang, M.B., Siegler, R.W., Blayney, M.B., Hochberg, F., Toribara, T.Y., Cernichiari, E. and Clarkson, T., 1998. Delayed cerebellar disease and death after accidental exposure to dimethylmercury. N. Engl. J. Med. 338, 1672-1676.

Nordlind, K., 1985. Binding and uptake of mercuric chloride in human lymphoid cells. Int. Arch. Allergy Appl. Immunol. 77, 405-408.

O'Brien, E.T., Salmon, E.D. and Erickson, H.P., 1997. How calcium causes microtubule depolymerization. Cell Motil. Cytoskeleton 36, 125-135.

O'Keefe, J.P., Blaine, K., Alegre, M.L. and Gajewski, T.F., 2004. Formation of a central supramolecular activation cluster is not required for activation of naive CD8+ T cells. Proc. Natl. Acad. Sci. U.S.A. 101, 9351-9356.

Ostrov, D.A., Shi, W., Schwartz, J.C., Almo, S.C. and Nathenson, S.G., 2000. Structure of murine CTLA-4 and its role in modulating T cell responsiveness. Science 290, 816-819.

Palmer, R.F., Blanchard, S., Stein, Z., Mandell, D. and Miller, C., Environmental mercury release, special education rates, and autism disorder: an ecological study of Texas. Health & Place In Press, Corrected Proof,

Park, S.H., Araki, S., Nakata, A., Kim, Y.H., Park, J.A., Tanigawa, T., Yokoyama, K. and Sato, H., 2000. Effects of occupational metallic mercury vapour exposure on suppressor-inducer (CD4+CD45RA+) T lymphocytes and CD57+CD16+ natural killer cells. Int. Arch. Occup. Environ. Health 73, 537-542.

Pelassy, C., Breittmayer, J.P., Ticchioni, M. and Aussel, C., 1994. Effect of thimerosal on cytosolic calcium and phosphatidylserine synthesis in Jurkat T cells. Int. J. Biochem. 26, 93-96.

Pelletier, L., Pasquier, R., Guettier, C., Vial, M.C., Mandet, C., Nochy, D., Bazin, H. and Druet, P., 1988. HgC12 induces T and B cells to proliferate and differentiate in BN rats. Clin. Exp. Immunol. 71, 336-342.

Pelletier, L., Pasquier, R., Rossert, J. and Druet, P., 1987a. HgCl2 induces nonspecific immunosuppression in Lewis rats. Eur. J. Immunol. 17, 49-54.

Pelletier, L., Pasquier, R., Vial, M.C., Mandet, C., Moutier, R., Salomon, J.C. and Druet, P., 1987b. Mercury-induced autoimmune glomerulonephritis: requirement for T-cells. Nephrology, Dialysis, Transplantation 1, 211-218.

Pintado, E., Baquero-Leonis, D., Conde, M. and Sobrino, F., 1995. Effect of thimerosal and other sulfhydryl reagents on calcium permeability in thymus lymphocytes. Biochem. Pharmacol. 49, 227-232.

Pirker, C., Moslinger, T., Wantke, F., Gotz, M. and Jarisch, R., 1993. Ethylmercuric chloride: the responsible agent in thimerosal hypersensitivity. Contact Dermatitis 29, 152-154.

Pizzo, P., Giurisato, E., Bigsten, A., Tassi, M., Tavano, R., Shaw, A. and Viola, A., 2004. Physiological T cell activation starts and propagates in lipid rafts. Immunol. Lett. 91, 3-9.

Pizzo, P. and Viola, A., 2004. Lipid rafts in lymphocyte activation. Microbes Infect. 6, 686-692.

Podack, E.R. and Kupfer, A., 1991. T-cell effector functions: mechanisms for delivery of cytotoxicity and help. Annu. Rev. Cell Biol. 7, 479-504.

Poenie, M., Tsien, R.Y. and Schmitt-Verhulst, A.M., 1987. Sequential activation and lethal hit measured by [Ca2+]i in individual cytolytic T cells and targets. EMBO J. 6, 2223-2232.

Ponce, R.A., Kavanagh, T.J., Mottet, N.K., Whittaker, S.G. and Faustman, E.M., 1994. Effects of methyl mercury on the cell cycle of primary rat CNS cells in vitro. Toxicol. Appl. Pharm. 127, 83-90.

Poo, W.J., Conrad, L. and Janeway, C.A., Jr., 1988. Receptor-directed focusing of lymphokine release by helper T cells. Nature 332, 378-380.

Potter, T.A., Grebe, K., Freiberg, B. and Kupfer, A., 2001. Formation of supramolecular activation clusters on fresh ex vivo CD8+ T cells after engagement of the T cell antigen receptor and CD8 by antigen-presenting cells. Proc. Natl. Acad. Sci. U.S.A. 98, 12624-12629.

Prigent, P., Poncet, P., Aten, J., Blanpied, C., Chand, A., Faevrier, M., Druet, P. and Hirsch, F., 1995. Mercuric chloride-induced programmed cell death of a murine T cell hybridoma. II. Opposite effect of interleukin-2 and interleukin-4. Cell. Immunol. 161, 107-111.

Pu, M., Ma, L., Ohkusu, K., Isobe, K., Taguchi, R., Ikezawa, H., Hamaguchi, M. and Nakashima, I., 1995. Direct evidence of involvement of glycosylphosphatidylinositol-anchored proteins in the heavy metal-mediated signal delivery into T lymphocytes. FEBS Lett. 361, 295-298.

Pu, M.Y., Akhand, A.A., Kato, M., Koike, T., Hamaguchi, M., Suzuki, H. and Nakashima, I., 1996. Mercuric chloride mediates a protein sulfhydryl modification-based pathway of signal transduction for activating Src kinase which is independent of the phosphorylation/dephosphorylation of a carboxyl terminal tyrosine. J. Cell. Biochem. 63, 104-114.

Purbhoo, M.A., Irvine, D.J., Huppa, J.B. and Davis, M.M., 2004. T cell killing does not require the formation of a stable mature immunological synapse. Nat. Immunol. 5, 524-530.

Qi, S.Y., Groves, J.T. and Chakraborty, A.K., 2001. Synaptic pattern formation during cellular recognition. Proc. Natl. Acad. Sci. U.S.A 98, 6548-6553.

Queiroz, M.L. and Dantas, D.C., 1997a. B lymphocytes in mercury-exposed workers. Pharmacol. Toxicol. 81, 130-133.

Queiroz, M.L. and Dantas, D.C., 1997b. T lymphocytes in mercury-exposed workers. Immunopharmacol. Immunotoxicol. 19, 499-510.

Queiroz, M.L., Perlingeiro, R.C., Bincoletto, C., Almeida, M., Cardoso, M.P. and Dantas, D.C., 1994a. Immunoglobulin levels and cellular immune function in lead exposed workers. Immunopharmacol. Immunotoxicol. 16, 115-128.

Queiroz, M.L., Perlingeiro, R.C., Dantas, D.C., Bizzacchi, J.M. and De Capitani, E.M., 1994b. Immunoglobulin levels in workers exposed to inorganic mercury. Pharmacol. Toxicol. 74, 72-75.

Rahman, S.M., Pu, M.Y., Hamaguchi, M., Iwamoto, T., Isobe, K. and Nakashima, I., 1993. Redox-linked ligand-independent cell surface triggering for extensive protein tyrosine phosphorylation. FEBS Lett. 317, 35-38.

Rios, R.M. and Bornens, M., 2003. The Golgi apparatus at the cell centre. Curr. Opin. Cell Biol. 15, 60-66.

Risher, J.F., Murray, H.E. and Prince, G.R., 2002. Organic mercury compounds: human exposure and its relevance to public health. Toxicol Ind. Health 18, 109-160.

Ritchie, K.A., Burke, F.J., Gilmour, W.H., Macdonald, E.B., Dale, I.M., Hamilton, R.M., McGowan, D.A., Binnie, V., Collington, D. and Hammersley, R., 2004. Mercury vapour levels in dental practices and body mercury levels of dentists and controls. Br. Dent. J. 197, 625-632; discussion 621.

Ritchie, K.A., Gilmour, W.H., Macdonald, E.B., Burke, F.J., McGowan, D.A., Dale, I.M., Hammersley, R., Hamilton, R.M., Binnie, V. and Collington, D., 2002. Health and neuropsychological functioning of dentists exposed to mercury. Occup. Environ. Med. 59, 287-293.

Robbins, E. and Gonatas, N.K., 1964. Histochemical and Ultrastructural Studies on Hela Cell Cultures Exposed to Spindle Inhibitors with Special Reference to the Interphase Cell. J. Histochem. Cytochem. 12, 704-711.

Robey, E. and Allison, J.P., 1995. T-cell activation: integration of signals from the antigen receptor and costimulatory molecules. Immunol. Today 16, 306-310.

Robinson, C.J., Balazs, T. and Egorov, I.K., 1986. Mercuric chloride-, gold sodium thiomalate-, and D-penicillamine-induced antinuclear antibodies in mice. Toxicol. Appl. Pharmacol. 86, 159-169.

Roda Navarro, P., Mittelbrunn, M., Ortega, M., Howie, D., Terhorst, C., Sanchez-Madrid, F. and Fernandez-Ruiz, E., 2004. Dynamic redistribution of the activating 2B4/SAP complex at the cytotoxic NK cell immune synapse. J. Immunol. 173, 3640-3646.

Rogalski, A.A. and Singer, S.J., 1984. Associations of elements of the Golgi apparatus with microtubules. J. Cell Biol. 99, 1092-1100.

Roos, A., Claessen, N., Schilder-Tol, E.J., Chand, M.A., Weening, J.J. and Aten, J., 1997. Thiol levels in CD134-defined subsets of rat T lymphocytes: possible implications for HgCl2-induced immune dysregulation. Biochem. Biophys. Res. Commun. 240, 452-457.

Rosenspire, A.J., Bodepudi, S., Mathews, M. and McCabe, M.J., Jr., 1998. Low levels of ionic mercury modulate protein tyrosine phosphorylation in lymphocytes. Int. J. Immunopharmacol. 20, 697-707.

Rothoeft, T., Gonschorek, A., Bartz, H., Anhenn, O. and Schauer, U., 2003. Antigen dose, type of antigen-presenting cell and time of differentiation contribute to the T helper 1/T helper 2 polarization of naive T cells. Immunology 110, 430-439.

Rothstein, A. (1972) Mercaptans, the biological target for mercurials. In: M. Miller and T. Clarkson (Eds), Mercury, Mercurials and Mercaptans, Charles C Thomas, Springfield, IL, pp. 68-93.

Rowat, S.C., 1998. Integrated defense system overlaps as a disease model: with examples for multiple chemical sensitivity. Env. Health Persp. 106 Suppl 1, 85-109.

Sager, P.R., 1988. Selectivity of methyl mercury effects on cytoskeleton and mitotic progression in cultured cells. Toxicol. Appl. Pharm. 94, 473-486.

Sager, P.R., Doherty, R.A. and Olmsted, J.B., 1983. Interaction of methylmercury with microtubules in cultured cells and in vitro. Exp. Cell Res. 146, 127-137.

Sakihama, T., Smolyar, A. and Reinherz, E.L., 1995. Molecular recognition of antigen involves lattice formation between CD4, MHC class II and TCR molecules. Immunol. Today 16, 581-587.

Salio, M., Valitutti, S. and Lanzavecchia, A., 1997. Agonist-induced T cell receptor down-regulation: molecular requirements and dissociation from T cell activation. Eur. J. Immunol. 27, 1769-1773.

Sanchez-Lockhart, M., Marin, E., Graf, B., Abe, R., Harada, Y., Sedwick, C.E. and Miller, J., 2004. Cutting Edge: CD28-mediated transcriptional and posttranscriptional regulation of IL-2 expression are controlled through different signaling pathways. J. Immunol. 173, 7120-7124.

Sanders, V.M., Fernandez-Botran, R., Coffman, R.L., Mosmann, T.R. and Vitetta, E.S., 1988. A single antigen-specific B cell can conjugate to either a type 1 or a type 2 helper T cell. Proc. Natl. Acad. Sci. U.S.A 85, 7724-7728.

Santucci, B., Cannistraci, C., Cristaudo, A., Camera, E. and Picardo, M., 1998. Thimerosal positivities: the role of organomercury alkyl compounds. Contact Dermatitis 38, 325-328.

Sapin, C., Druet, E. and Druet, P., 1977. Induction of anti-glomerular basement membrane antibodies in the Brown-Norway rat by mercuric chloride. Clin. Exp. Immunol. 28, 173-179.

Sapin, C., Mandet, C., Druet, E., Gunther, E. and Druet, P., 1982. Immune complex type disease induced by HgCl2 in Brown-Norway rats: genetic control of susceptibility. Clin. Exp. Immunol. 48, 700-704.

Schaefer, B.C., Kappler, J.W., Kupfer, A. and Marrack, P., 2004. Complex and dynamic redistribution of NF-kappaB signaling intermediates in response to T cell receptor stimulation. Proc. Natl. Acad. Sci. U.S.A 101, 1004-1009.

Schmitz, M.L., Bacher, S. and Dienz, O., 2003. NF-kappaB activation pathways induced by T cell costimulation. FASEB J. 17, 2187-2193.

Sechi, A.S. and Wehland, J., 2004. Interplay between TCR signalling and actin cytoskeleton dynamics. Trends Immunol. 25, 257-265.

Sedwick, C.E., Morgan, M.M., Jusino, L., Cannon, J.L., Miller, J. and Burkhardt, J.K., 1999. TCR, LFA-1, and CD28 play unique and complementary roles in signaling T cell cytoskeletal reorganization. J. Immunol. 162, 1367-1375.

Shenker, B.J., Berthold, P., Decker, S., Mayro, J., Rooney, C., Vitale, L. and Shapiro, I.M., 1992a. Immunotoxic effects of mercuric compounds on human lymphocytes and monocytes. II. Alterations in cell viability. Immunopharmacol. Immunotoxicol. 14, 555-577.

Shenker, B.J., Berthold, P., Rooney, C., Vitale, L., DeBolt, K. and Shapiro, I.M., 1993a. Immunotoxic effects of mercuric compounds on human lymphocytes and monocytes. III. Alterations in B-cell function and viability. Immunopharmacol. Immunotoxicol. 15, 87-112.

Shenker, B.J., Datar, S., Mansfield, K. and Shapiro, I.M., 1997. Induction of apoptosis in human T-cells by organomercuric compounds: a flow cytometric analysis. Toxicol. Appl. Pharmacol. 143, 397-406.

Shenker, B.J., Guo, T.L., O, I. and Shapiro, I.M., 1999. Induction of apoptosis in human T-cells by methyl mercury: temporal relationship between mitochondrial dysfunction and loss of reductive reserve. Toxicol. Appl. Pharmacol. 157, 23-35.

Shenker, B.J., Guo, T.L. and Shapiro, I.M., 1998. Low-level methylmercury exposure causes human T-cells to undergo apoptosis: evidence of mitochondrial dysfunction. Environ. Res. 77, 149-159.

Shenker, B.J., Guo, T.L. and Shapiro, I.M., 2000. Mercury-induced apoptosis in human lymphoid cells: evidence that the apoptotic pathway is mercurial species dependent. Environ. Res. 84, 89-99.

Shenker, B.J., Mayro, J.S., Rooney, C., Vitale, L. and Shapiro, I.M., 1993b. Immunotoxic effects of mercuric compounds on human lymphocytes and monocytes. IV. Alterations in cellular glutathione content. Immunopharmacol. Immunotoxicol. 15, 273-290.

Shenker, B.J., Pankoski, L., Zekavat, A. and Shapiro, I.M., 2002. Mercury-induced apoptosis in human lymphocytes: caspase activation is linked to redox status. Antioxid. Redox Signal 4, 379-389.

Shenker, B.J., Rooney, C., Vitale, L. and Shapiro, I.M., 1992b. Immunotoxic effects of mercuric compounds on human lymphocytes and monocytes. I. Suppression of T-cell activation. Immunopharmacol. Immunotoxicol. 14, 539-553.

Siegler, R.W., Nierenberg, D.W. and Hickey, W.F., 1999. Fatal poisoning from liquid dimethylmercury: a neuropathologic study. Hum. Pathol. 30, 720-723.

Silbergeld, E.K., Sacci, J.B., Jr. and Azad, A.F., 2000. Mercury exposure and murine response to Plasmodium yoelii infection and immunization. Immunopharmacol. Immunotoxicol. 22, 685-695.

Silva, I., Nyland, J., Gorman, A., Perisse, A., Ventura, A., Santos, E., de Souza, J., Burek, C., Rose, N. and Silbergeld, E., 2004. Mercury exposure, malaria, and serum antinuclear/antinucleolar antibodies in amazon populations in Brazil: a cross-sectional study. Environ. Health 3, 11.

Singer, S.J., 1992. Intercellular communication and cell-cell adhesion. Science 255, 1671-1677.

Sirois, J.E. and Atchison, W.D., 1996. Effects of mercurials on ligand- and voltage-gated ion channels: a review. Neurotoxicology 17, 63-84.

Sirois, J.E. and Atchison, W.D., 2000. Methylmercury affects multiple subtypes of calcium channels in rat cerebellar granule cells. Toxicol. Appl. Pharmacol. 167, 1-11.

Slemr, F. and Langer, E., 1992. Increase in global atmospheric concentrations of mercury inferred from measurements over the Atlantic Ocean. Nature 355, 434 - 437.

Sloan Lancaster, J., Evavold, B.D. and Allen, P.M., 1994a. Th2 cell clonal anergy as a consequence of partial activation. J. Exp. Med. 180, 1195-1205.

Sloan Lancaster, J., Shaw, A.S., Rothbard, J.B. and Allen, P.M., 1994b. Partial T cell signaling: altered phospho-zeta and lack of zap70 recruitment in APL-induced T cell anergy [see comments]. Cell 79, 913-922.

Smith, M.W., Ambudkar, I.S., Phelps, P.C., Regec, A.L. and Trump, B.F., 1987. HgCl2-induced changes in cytosolic Ca2+ of cultured rabbit renal tubular cells. Biochim. Biophys. Acta 931, 130-142.

Soleo, L., Vacca, A., Vimercati, L., Bruno, S., Di Loreto, M., Zocchetti, C., Di Stefano, R., Candilio, G., Lasorsa, G., Franco, G. and Foa, V., 1997. Minimal immunological effects on workers with prolonged low exposure to inorganic mercury. Occupational and Environ. Med. 54, 437-442.

Somersalo, K., Anikeeva, N., Sims, T.N., Thomas, V.K., Strong, R.K., Spies, T., Lebedeva, T., Sykulev, Y. and Dustin, M.L., 2004. Cytotoxic T lymphocytes form an antigen-independent ring junction. J. Clin. Invest. 113, 49-57.

Sommer, F., Bischof, S., Rollinghoff, M. and Lohoff, M., 1994. Demonstration of organic anion transport in T lymphocytes. L-lactate and fluo-3 are target molecules. J. Immunol. 153, 3523-3532.

Speizer, L.A., Watson, M.J., Kanter, J.R. and Brunton, L.L., 1989. Inhibition of phorbol ester binding and protein kinase C activity by heavy metals. J. Biol. Chem. 264, 5581-5585.

Sperling, A.I., Sedy, J.R., Manjunath, N., Kupfer, A., Ardman, B. and Burkhardt, J.K., 1998. TCR signaling induces selective exclusion of CD43 from the T cell-antigen-presenting cell contact site. J. Immunol. 161, 6459-6462.

Standeven, L.J., Carlin, L.M., Borszcz, P., Davis, D.M. and Burshtyn, D.N., 2004. The actin cytoskeleton controls the efficiency of killer Ig-like receptor accumulation at inhibitory NK cell immune synapses. J. Immunol. 173, 5617-5625.

Stejskal, V.D., Danersund, A., Lindvall, A., Hudecek, R., Nordman, V., Yaqob, A., Mayer, W., Bieger, W. and Lindh, U., 1999. Metal-specific lymphocytes: biomarkers of sensitivity in man. Neuroendocrinol. Lett. 20, 289-298.

Stejskal, V.D., Forsbeck, M., Cederbrant, K.E. and Asteman, O., 1996. Mercury-specific lymphocytes: an indication of mercury allergy in man. J. Clin. Immunol. 16, 31-40.

Stinchcombe, J.C., Bossi, G., Booth, S. and Griffiths, G.M., 2001. The immunological synapse of CTL contains a secretory domain and membrane bridges. Immunity 15, 751-761.

Suda, T., Okazaki, T., Naito, Y., Yokota, T., Arai, N., Ozaki, S., Nakao, K. and Nagata, S., 1995. Expression of the Fas ligand in cells of T cell lineage. J. Immunol. 154, 3806-3813.

Sumen, C., Dustin, M.L. and Davis, M.M., 2004. T cell receptor antagonism interferes with MHC clustering and integrin patterning during immunological synapse formation. J. Cell Biol. 166, 579-590.

Takahashi, N., 1982. Cytotoxicity of mercurial preservatives in cell culture. Ophthalm. Res. 14, 63-69.

Tan, X.X., Tang, C., Castoldi, A.F., Manzo, L. and Costa, L.G., 1993. Effects of inorganic and organic mercury on intracellular calcium levels in rat T lymphocytes. J. Toxicol. Env. Health 38, 159-170.

Thebault, S. and Ochoa-Garay, J., 2004. Characterization of TCR-induced phosphorylation of PKCtheta in primary murine lymphocytes. Mol. Immunol. 40, 931-942.

Tomas, E.M., Chau, T.A. and Madrenas, J., 2002. Clustering of a lipid-raft associated pool of ERM proteins at the immunological synapse upon T cell receptor or CD28 ligation. Immunol. Lett. 83, 143-147.

Tomsig, J.L. and Suszkiw, J.B., 1991. Permeation of Pb2+ through calcium channels: fura-2 measurements of voltage- and dihydropyridine-sensitive Pb2+ entry in isolated bovine chromaffin cells. Biochim. Biophys. Acta 1069, 197-200.

Tsien, R.W. and Tsien, R.Y., 1990. Calcium channels, stores, and oscillations. Annu. Rev. Cell Biol. 6, 715-760.

Tubbs, R.R., Gephardt, G.N., McMahon, J.T., Pohl, M.C., Vidt, D.G., Barenberg, S.A. and Valenzuela, R., 1982. Membranous glomerulonephritis associated with industrial mercury exposure. Study of pathogenetic mechanisms. Am. J. Clin. Pathol. 77, 409-413.

Ucker, D.S., Hebshi, L.D., Blomquist, J.F. and Torbett, B.E., 1994. Physiological T-cell death: susceptibility is modulated by activation, aging, and transformation, but the mechanism is constant. Immunol. Rev. 142, 273-299.

Unal-Cevik, I., Kilinc, M., Can, A., Gursoy-Ozdemir, Y. and Dalkara, T., 2004. Apoptotic and necrotic death mechanisms are concomitantly activated in the same cell after cerebral ischemia. Stroke 35, 2189-2194.

Valitutti, S., Dessing, M., Aktories, K., Gallati, H. and Lanzavecchia, A., 1995. Sustained signaling leading to T cell activation results from prolonged T cell receptor occupancy. Role of T cell actin cytoskeleton. J. Exp. Med. 181, 577-584.

Valitutti, S. and Lanzavecchia, A., 1997. Serial triggering of TCRs: a basis for the sensitivity and specificity of antigen recognition. Immunol. Today 18, 299-304.

Valitutti, S., Meuller, S., Salio, M. and Lanzavecchia, A., 1997. Degradation of T cell receptor TCR -CD3-zeta complexes after antigenic stimulation [see comments]. J. Exp. Med. 185, 1859-1864.

Van Horn, D.L., Edelhauser, H.F., Prodanovich, G., Eiferman, R. and Pederson, H.F., 1977. Effect of the ophthalmic preservative thimerosal on rabbit and human corneal endothelium. Invest. Ophthalmol. Vis. Sci 16, 273-280.

Van Seventer, G.A., Bonvini, E., Yamada, H., Conti, A., Stringfellow, S., June, C.H. and Shaw, S., 1992. Costimulation of T cell receptor/CD3-mediated activation of resting human CD4+ T cells by leukocyte function-associated antigen-1 ligand intercellular cell adhesion molecule-1 involves prolonged inositol phospholipid hydrolysis and sustained increase of intracellular Ca2+ levels. J Immunol. 149, 3872-3880.

vanLoon, G. and Duffy, S. (2000) 13.3 Three metals--their behaviour in the hydrosphere 13.3.3 Mercury. Environmental Chemistry: A global perspective, Oxford University Press, New York, pp. 272-275.

Vassallo, D.V., Moreira, C.M., Oliveira, E.M., Bertollo, D.M. and Veloso, T.C., 1999. Effects of mercury on the isolated heart muscle are prevented by DTT and cysteine. Toxicol. Appl. Pharm. 156, 113-118.

Verburg-Van Kemenade, B.M., Saeij, J.P., Flik, G. and Willems, P.H., 1998. Ca2+ signals during early lymphocyte activation in carp Cyprinus carpio L. J. Exp. Biol. 201, 591-598.

Verstraeten, T., Davis, R.L., DeStefano, F., Lieu, T.A., Rhodes, P.H., Black, S.B., Shinefield, H. and Chen, R.T., 2003. Safety of thimerosal-containing vaccines: a two-phased study of computerized health maintenance organization databases. Pediatrics 112, 1039-1048.

Vettori, M.V., Alinovi, R., Belletti, S., Goldoni, M., Franchini, I. and Mutti, A., 2003. [In vitro models for the evaluation of the neurotoxicity of methylmercury. Current state of knowledge]. Med. Lav. 94, 183-191.

Viola, A. and Lanzavecchia, A., 1996. T cell activation determined by T cell receptor number and tunable thresholds [see comments]. Science 273, 104-106.

Viola, A., Linkert, S. and Lanzavecchia, A., 1997a. A T cell receptor TCR antagonist competitively inhibits serial TCR triggering by low-affinity ligands, but does not affect triggering by high-affinity anti-CD3 antibodies. Eur. J. Immunol. 27, 3080-3083.

Viola, A., Salio, M., Tuosto, L., Linkert, S., Acuto, O. and Lanzavecchia, A., 1997b. Quantitative contribution of CD4 and CD8 to T cell antigen receptor serial triggering. J. Exp. Med. 186, 1775-1779.

Vogel, D.G., Margolis, R.L. and Mottet, N.K., 1985. The effects of methyl mercury binding to microtubules. Toxicol. Appl. Pharm. 80, 473-486.

Vojdani, A., Pangborn, J.B., Vojdani, E. and Cooper, E.L., 2003. Infections, toxic chemicals and dietary peptides binding to lymphocyte receptors and tissue enzymes are major instigators of autoimmunity in autism. Int. J. Immunopathol. Pharmacol. 16, 189-199.

Volareviac, S., Burns, C.M., Sussman, J.J. and Ashwell, J.D., 1990. Intimate association of Thy-1 and the T-cell antigen receptor with the CD45 tyrosine phosphatase. Proc. Natl. Acad. Sci. U.S.A. 87, 7085-7089.

Volareviac, S., Niklinska, B.B., Burns, C.M., June, C.H., Weissman, A.M. and Ashwell, J.D., 1993. Regulation of TCR signaling by CD45 lacking transmembrane and extracellular domains. Science 260, 541-544.

Volareviac, S., Niklinska, B.B., Burns, C.M., Yamada, H., June, C.H., Dumont, F.J. and Ashwell, J.D., 1992. The CD45 tyrosine phosphatase regulates phosphotyrosine homeostasis and its loss reveals a novel pattern of late T cell receptor-induced Ca2+ oscillations. J. Exp. Med. 176, 835-844.

Volbracht, C., Leist, M. and Nicotera, P., 1999. ATP controls neuronal apoptosis triggered by microtubule breakdown or potassium deprivation. Mol. Med. 5, 477-489.

Voutsinas, G., Zarani, F.E. and Kappas, A., 1997. The effect of environmental aneuploidy-inducing agents on the microtubule architecture of mitotic meristematic root cells in Hordeum vulgare. Cell. Biol. Int. 21, 411-418.

Vyas, Y.M., Maniar, H. and Dupont, B., 2002. Visualization of signaling pathways and cortical cytoskeleton in cytolytic and noncytolytic natural killer cell immune synapses. Immunol. Rev. 189, 161-178.

Wallin, M. and Hartley-Asp, B., 1993. Effects of potential aneuploidy inducing agents on microtubule assembly in vitro. Mutat. Res. 287, 17-22.

Warfvinge, K., Hansson, H. and Hultman, P., 1995. Systemic autoimmunity due to mercury vapor exposure in genetically susceptible mice: dose-response studies. Toxicol. Appl. Pharmacol. 132, 299-309.

Wasteneys, G.O., Cadrin, M., Reuhl, K.R. and Brown, D.L., 1988. The effects of methylmercury on the cytoskeleton of murine embryonal carcinoma cells. Cell Biol. Toxicol. 4, 41-60.

Watson, A.R. and Lee, W.T., 2004. Differences in signaling molecule organization between naive and memory CD4+ T lymphocytes. J. Immunol. 173, 33-41.

Westphal, G. and Hallier, E., 2003. Mercury in infants given vaccines containing thiomersal. Lancet 361, 699; author reply 699.

Whitekus, M.J., Santini, R.P., Rosenspire, A.J. and McCabe, M.J., Jr., 1999. Protection against CD95-mediated apoptosis by inorganic mercury in Jurkat T cells. J. Immunol. 162, 7162-7170.

Wooley, P.H., Griffin, J., Panayi, G.S., Batchelor, J.R., Welsh, K.I. and Gibson, T.J., 1980. HLA-DR antigens and toxic reaction to sodium aurothiomalate and D-penicillamine in patients with rheumatoid arthritis. N. Engl. J. Med. 303, 300-302.

Worth, R.G., Esper, R.M., Warra, N.S., Kindzelskii, A.L., Rosenspire, A.L., Todd, R.F., 3rd and Petty, H.R., 2001. Mercury inhibition of neutrophil activity: evidence of aberrant cellular signalling and incoherent cellular metabolism. Scand. J. Immunol. 53, 49-55.

Wu, G., 1995. Screening of potential transport systems for methyl mercury uptake in rat erythrocytes at 5 degrees by use of inhibitors and substrates. Pharmacol. Toxicol. 77, 169-176.

Wulfing, C. and Davis, M.M., 1998. A receptor/cytoskeletal movement triggered by costimulation during T cell activation. Science 282, 2266-2269.

Wulfing, C., Rabinowitz, J.D., Beeson, C., Sjaastad, M.D., McConnell, H.M. and Davis, M.M., 1997. Kinetics and extent of T cell activation as measured with the calcium signal. J. Exp. Med. 185, 1815-1825.

Wulfing, C., Sjaastad, M.D. and Davis, M.M., 1998. Visualizing the dynamics of T cell activation: intracellular adhesion molecule 1 migrates rapidly to the T cell/B cell interface and acts to sustain calcium levels. Proc. Natl. Acad. Sci. U.S.A. 95, 6302-6307.

Wulfing, C., Sumen, C., Sjaastad, M.D., Wu, L.C., Dustin, M.L. and Davis, M.M., 2002. Costimulation and endogenous MHC ligands contribute to T cell recognition. Nat. Immunol. 3, 42-47.

Zagury, D., Bernard, J., Jeannesson, P., Thiernesse, N. and Cerottini, J.C., 1979. Studies on the mechanism of T cell-mediated lysis at the single effector cell level. I. Kinetic analysis of lethal hits and target cell lysis in multicellular conjugates. J. Immunol. 123, 1604-1609.